Title
Introducing Multifunctionality into Polypeptide Vesicles for Biomedical Applications

Author
Rodriguez, April Rose

Publication Date
2013

Peer reviewed|Thesis/dissertation

UNIVERSITY OF CALIFORNIA

Los Angeles

Introducing Multifunctionality into Polypeptide Vesicles for Biomedical Applications

A dissertation submitted in partial satisfaction of the
requirements for the degree Doctor of Philosophy
in Biomedical Engineering

by

April Rose Rodriguez

2013

ABSTRACT OF THE DISSERTATION

Introducing Multifunctionality into Polypeptide Vesicles for Biomedical Applications

by

April Rose Rodriguez
Doctor of Philosophy in Biomedical Engineering
University of California, Los Angeles, 2013
Professor Timothy J. Deming, Chair

The delivery of naked drugs, DNA, RNA and proteins within living organisms is a challenging endeavor where renal clearance, liver accumulation, solubility issues, enzymatic and proteolytic degradation may reduce the effectiveness of the drug. Researchers are developing drug carriers such as liposomes, micelles, emulsions and vesicles to overcome these obstacles. Such carriers are used to encapsulate drugs and protect them from degradation, and more importantly to protect the patient from toxic side effects. Polypeptide vesicles are of interest because they are made up of long chains of amino acids and may be advantageous for *in vivo* applications since they can degrade to non-toxic metabolites. Natural and unnatural amino acids can be used as building blocks allowing a variety of functionality and tuning of physical properties. Polypeptides are also advantageous in that they can form secondary structures (i.e., α-helices, β-sheets) stabilized by hydrogen bonding, which help to direct their self-assembly. Our group had developed polypeptide vesicles containing polyarginine hydrophilic segments of the

general structure: poly(L-arginine)$_{60}$-*block*-poly(L-leucine)$_{20}$, $R_{60}L_{20}$. The $R_{60}L_{20}$ vesicles were able to encapsulate Texas Red labeled dextran and were taken up by T84, HeLa, and HULEC-5A cell lines, indicating that polyarginine segments are useful for intracellular delivery. While these polypeptide vesicles ($R_{60}L_{20}$) have shown promise for intracellular delivery there are issues that remain to be addressed, such as cytotoxicity and cargo release. In my research, I have focused on addressing these issues by optimizing the hydrophobic segment and introducing multifunctionality into polypeptide vesicles, creating improved drug delivery vehicle candidates.

In order to optimize vesicle self-assembly and the ability to obtain diameters in the nanoscale range, the hydrophobic domain length and composition was varied. Fine-tuning the length of the poly(L-leucine) domain to 20 residues led to stable vesicular assemblies that had reduced cytotoxicity. To reduce the rigidity of the vesicle membrane a statistical copolypeptide was incorporated in the hydrophobic domain to disrupt the crystallinity of the poly(L-leucine)$_{20}$. The incorporation of L-alanine and L-phenylalanine residues allowed vesicle diameters to be manipulated below 200 nanometers with a 1 to 1 ratio of L-leucine to L-phenylalanine resulting in narrow polydispersities.

Replacing the cationically charged hydrophilic domains with neutral segments led to reduced cytotoxicity of block copolypeptide vesicles. It was found that incorporating neutrally charged segments, containing disordered chain conformations, provides the optimal conditions for obtaining minimally toxic vesicles with the ability be extruded to sizes below 200 nanometers in diameter. Glycosylated block copolypeptides not only provided a neutral non-toxic vesicle suspension, but also provide a method for incorporating biofunctionality, with the ability to bind to lectins.

Recent advances in the purification of α-amino acid N-carboxyanhydrides (NCAs) led to the use of L-methionine NCA, which has not been polymerized incorporated into block copolypeptides before. The unique sulfur chemistry of methionine provided a quick alternative to introducing new functionalities into polypeptide vesicles. Oxidation of poly(L-methionine) segments provided polypeptide vesicles with the ability to release its cargo within an environment containing either reducing chemicals or reductase enzymes found in human, animal and plant cells.

The dissertation of April Rose Rodriguez is approved.

Daniel T. Kamei

Gerard C. L. Wong

Christopher Denny

Timothy J. Deming, Committee Chair

University of California, Los Angeles

2013

Table of Contents

List of Figures

List of Tables

ACKNOWLEDGEMENTS

The culmination of my thesis work cannot truly be complete without the recognition of those who provided me with strength, encouragement, and inspiration. Throughout my graduate career and entire life, my grandparents have helped me overcome many adversities. Serving as my pillars of strength and inspiration, my goals would not have been accomplished without them. Their infinite love, selflessness, and wisdom taught me to be kind in all areas of life. For this, and so many other reasons, I dedicate my thesis in its entirety to Enrique and Librada Rodriguez.

My thesis work would not be possible without the guidance and support I received from Professor Timothy Deming. It is hard to put into the words the amount of gratitude I have for someone who not only took a chance on me, but ultimately believed in my capabilities as a researcher. While it may not have been completely obvious at times, Tim's high expectations and consistent feedback and suggestions are what allowed me to reach my full potential. I ultimately realized that these nuances are what set me up for success and a sense of accomplishment in regards to my work. I will always appreciate and admire Tim's intelligence, and take all of the skills and knowledge he as bestowed upon me for future avenues that I take.

The collaborative work I did with Professor Daniel Kamei and Mike (Uh-Joo) Choe greatly contributed to the overall depth and success of my research. I feel so fortunate to have worked closely with Dan, who often reminded me that it was still possible to laugh, even during the most stressful of times. Thank you for your support, and allowing me to feel welcome in your lab. I thoroughly enjoyed growing as a scientist, while working alongside Mike. Thank you for putting up with my demands, and being such a wonderful colleague. You truly deserve all of

the achievement and success that I know will follow you. I would also like to thank my dissertation committee members, Professor Gerard Wong and Dr. Christopher Denny.

The support of my family cannot go unnoticed, because their love and appreciation for my desire to push my boundaries, test my strengths and try new things never subsided. While they may not be able to personally relate to my academic career, they took great pride in my work, and for that I am eternally grateful. I hope they know that I am equally proud of them. I would not be the person I am today without them, but especially my mother. I'd like to think that I am following in her footsteps as a strong, independent woman.

From the Deming Group, I want to recognize my labmates who accompanied me on this journey. To Dr. Jarrod Hanson, thank you for your patience and providing me with the foundation to begin my thesis work. To Jessica, thank you for all the help and the collaborative work we accomplished together. To Allie, thank you for all the shared experiences and support along the way. To Ilya, thank you for your constant optimism and allowing me to turn to you for any questions and struggles I had. You were not only my labmate, but a gym buddy, my coffee buddy, my roommate and most importantly my friend. I will always remember procrast-o-grams, our quote board, and the laugher we shared.

Last but not least, I want to recognize others who helped me in many ways get through the obstacles of graduate school and helped me feel at home here in Los Angeles. To all my rugby teammates on the UCLA and Santa Monica teams, who made me feel welcome and provided me with an outlet for the stresses of research. To Eddy, thank you for all the adventures and I look forward to many more. To the friends I made along the way, thank you for all the love and support. To Whitney Vance, there are no words to express how grateful I am for all the love

and support through this journey of finishing up my thesis work. You provided so much stability during those days when I felt like I would never reach the end and wanted to give up.

Chapter 2 is a version of Choe, U. J.; Rodriguez, A. R.; Li, Z.; Boyarskiy, S.; Deming, T. J.; Kamei, D. T. *Macromol. Chem. Phys.* DOI: 10.1002/macp.2012000591. Rodriguez and Li performed chemical synthesis and characterization of block copolypeptides, vesicle formation and imaging by TEM. Choe and Boyarskiy were responsible for cytotoxicity studies, vesicle purification and quantification. Chapter 3 is a version of Rodriguez, A. R.; Choe, U. J.; Kamei, D. T.; Deming, T. J. *Macromol. Biosci.* 2012, 12, 805-811. Rodriguez performed chemical synthesis and characterization of block copolypeptides, self-assembling material processing, vesicle extrusion, DLS, and structure imaging by DIC, LCSM and TEM. Choe was responsible for cytotoxicity studies and cell uptake studies. Chapter 4 is a version of Kramer, J. R.; Rodriguez, A. R.; Choe, U. J.; Kamei, D. T.; Deming, T. J. *Soft Matter*. 2013, 9, 3389-3395. Kramer performed all chemical synthesis and characterization, CD, and lectin binding studies. Both Kramer and Rodriguez were responsible for experimental self-assembling material processing, DLS, and structure imaging by DIC. Rodriguez was responsible for vesicle extrusion, and imaging by TEM and LSCM. Choe performed cytotoxicity studies.

VITA

2007	B.S. Chemistry, *summa cum laude* University of Texas at El Paso
2007	National Science Foundation Alliances for Graduate Education and the Professoriate Summer Research Scholars University of California, Los Angeles
2007-2011	Eugene V. Cota-Robles Graduate Fellowship University of California, Los Angeles
2009	Teaching Assistant Department of Bioengineering University of California, Los Angeles
2009	M.S. Biomedical Engineering University of California, Los Angeles
2010	International Center for Materials Research Summer School on Preparative Strategies in Solid State and Materials Chemistry University of California, Santa Barbara
2010-2011	Graduate Research Mentorship Program University of California, Los Angeles

PUBLICATIONS

1. Mishra, A.; Lai, G. H.; Schmidt, N. W.; Sun, V. Z.; Rodriguez, A. R.; Tong, R.; Tang, L.; Cheng, J.; Deming, T. J.; Kamei, D. T.; Wong, G. C. L. Translocation of HIV TAT peptide and analogues induced by multiplexed membrane and cytoskeletal interactions. *PNAS.* **2011**, 108, 16883-16888.

2. Rodriguez, A. R.; Choe, U. J.; Kamei, D. T.; Deming, T. J. Fine Tuning of Vesicle Assembly and Properties using Dual Hydrophilic Triblock Copolypeptides. *Macromol. Biosci.* **2012**, 12, 805- 811.

3. Sun, V. Z.; Choe, U. J.; Rodriguez, A. R.; Dai, H.; Deming, T. J.; Kamei, D. T. Transfection of mammalian cells using block copolypeptide vesicles. *Macromol. Biosci.* **2013**, Advance online publication, DOI: 10.1002/mabi.201200383.

4. Choe, U. J.; Rodriguez, A. R.; Li, Z.; Boyarskiy, S.; Deming, T. J.; Kamei, D. T. Characterization and minimization of block copolypeptide vesicle cytotoxicity using different hydrophobic chain lengths. *Macromol. Chem. Phys*. DOI: 10.1002/macp.2012000591.

5. Kramer, J.; Rodriguez, A. R.; Choe, U. J.; Kamei, D. T.; Deming, T. J. Glycopolypeptide conformations in bioactive block copolymer assemblies influence their nanoscale morphology. *Soft Matter*, **2013**, 9, 3389- 3395.

PRESENTATIONS

1. Rodriguez, A. R.; Hanson, J.; Li, Z.; Deming, T. J. Adding functionality to polypeptide vesicles: Nanoscale membranes for biomedical applications. Poster presentation. SACNAS National Conference, Salt Lake City, UT, United States, October 2008.

2. Rodriguez, A. R.; Hanson, J.; Li, Z.; Deming, T. J. Adding functionality to polypeptide vesicles: Nanoscale membranes for biomedical applications. Poster presentation. The Annual UCLA Engineering Technology Forum, Los Angeles, CA, February 2010.

3. Rodriguez, A. R.; Choe, U. J.; Kamei, D. T.; Deming, T. J. Polypeptide Vesicles: Chain Length Studies. Poster presentation. 239th ACS National Meeting, San Francisco, CA, United States, March 21-25, 2010.

4. Rodriguez, A. R.; Choe, U. J.; Kamei, D. T.; Deming, T. J. Polypeptide Vesicle: Nanoscale membranes for biomedical applications. Poster presentation. The 2nd Annual UCLA ISPE Research Networking Fair, Los Angeles, California, March 2012

CHAPTER ONE

Introduction

1.1 Introduction

Delivery of naked drugs, DNA, RNA and proteins within biological systems is a challenging endeavor where renal clearance, liver accumulation, solubility issues, enzymatic and proteolytic degradation may reduce the effectiveness of the drug.[1,2] Only 10% of drugs that enter clinical trials receive FDA approval, the majority fail due to poor pharmokinetics, adverse side effects, and toxicity.[3] To overcome these obstacles, researchers have developed drug carriers such as liposomes,[4,5] nanoparticles,[6,7] dendrimers,[8,9] emulsions,[10] micelles[11] and vesicles[2,12-14] (**Figure 1.1**). These carriers are used to encapsulate a drug to protect it from degradation, and more importantly to protect the patient from toxic side effects. These drug delivery systems also allow targeted delivery, increased circulation times, controlled release and enhanced cellular uptake.[1] As of 2008, 24 small-molecule therapeutics formulated into delivery vehicles were approved by the FDA.[15]

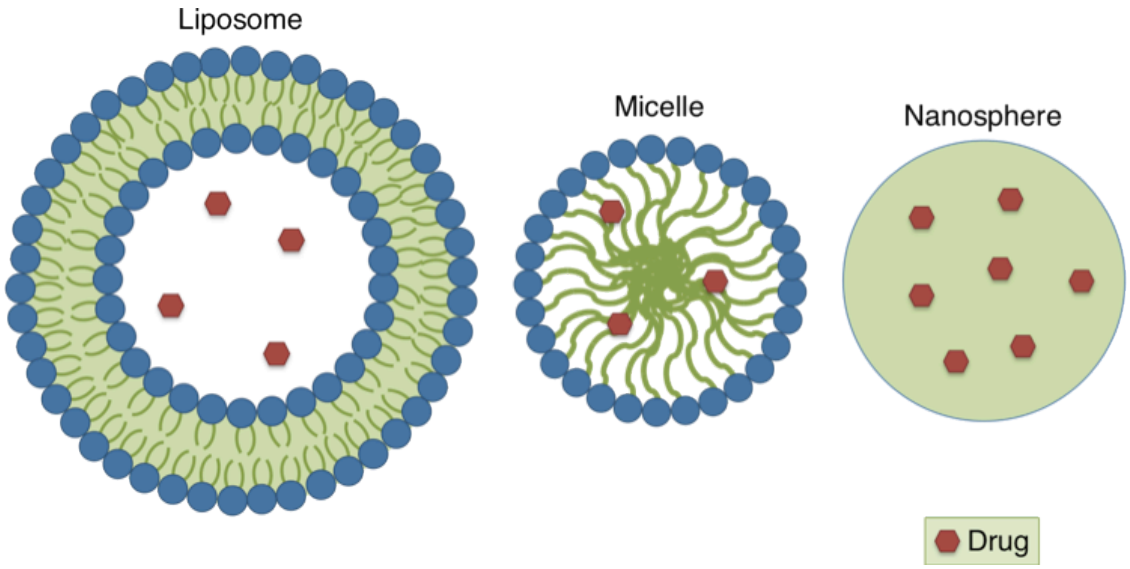

Figure 1.1 Various nanocarriers for drug delivery.

1.2 Obstacles of Free Drug Delivery

There are many methods and modes of delivering drugs and therapeutics to biological systems. There have been many advances in genetic and biological therapeutics, such as the development of DNA,[16,17] RNA,[18] antibodies[19] and other peptidic[20] compounds. However, oral administrations of these types of therapeutics fail, due to the harsh denaturing conditions of the digestive system, poor absorption and degradation.[3,21,22] For the purposes of this dissertation, intravenous drug administration will be the focus for drug delivery mode.[2,23]

Drug injection is the most prominent method of delivering drugs. This method is the administration of therapeutics directly into the circulatory system *via* veins.[1] The cardiovascular system is an intricate network and has access to all areas of a human body. The circulatory system is responsible for transport of blood, nutrients, hormones, gases, and electrolytes to and from cells. It is also responsible in removing metabolic waste from cells and eventually out of the body.[24] It helps to fight disease, maintain temperature, and pH providing the optimal conditions to thrive.[24]

By injecting drugs directly into the circulatory system, under ideal conditions, the drugs will circulate until they find the desired destination and will then only interact with the targeted tissues and cells. However, this is not the case for the delivery of conventional free drugs with poor pharmacokinetics, biodistribution, toxicity and clearance problems. For example, the drugs that are intended to target and kill cancer cells have the ability to harm normal cells and tissues resulting in adverse side effects such as nausea, loss of hair, loss of appetite and fatigue.[25,26]

Another problem that must be addressed is the solubility of certain drugs or possible drug candidates. Many drug candidates that show the potential to kill cancer cells or target a certain disease during *in vitro* studies or small animal *in vivo* studies usually do not continue to FDA approval if the drug is not soluble in aqueous media, because organic solvents are very harmful and many are immiscible with water making them impossible to use.

1.3 Advances in Drug Delivery

In order to overcome these obstacles faced by conventional free drug delivery, many researchers have focused on the development of drug delivery systems. These drug delivery systems are composed of the therapeutics and a particulate carrier, usually composed of lipids and polymers. These carriers have the ability to alter the pharmacokinetics, biodistribution, circulation times, and solubility in the circulatory system.[1] These vehicles can serve as a barrier to protect certain therapeutics (i.e., DNA/siRNA, antibodies) from degradation and interaction in the blood, but also serve as protection to normal cells and tissues to reduce toxicity and adverse side effects.

1.4 Nano-Carriers

There are many approaches to developing nano-carriers and vehicles for transporting drugs. Some researchers will simply attach the drug to a large polymer to increase the particulate size to increase circulation times. Genetic therapeutics such as DNA and siRNA are negatively charged and can be condensed with polymers that are positively charged to help with transport across cell membranes, which is necessary for DNA and siRNA to enter cells to have a therapeutic effect.[27,28] Other advanced systems require the assembly of the carrier around the drug, encapsulating it, such as liposomes, emulsion droplets, micelles and vesicles.

There are such carriers already found in nature and this development of compartmentalization is what separates prokaryotes from eukaryotes.[29-31] Within eukaryotic cells there are many vehicles and subunits known as vesicles and more complex structures known has organelles. These vesicles are enclosed by a lipid bilayer, which also is a major component of cell walls. The inner cavity of a vesicle is isolated from the external environment. Within the cell, these vesicles are involved in the storage of enzymes and proteins, have roles in metabolism, and are responsible for transport of molecules between organelles. Other vesicles act as chemical reaction chambers known as endosomes and lysosmes that can reduce the pH within the cavity by pumping in protons and can digest and discard waste from the cells. With inspiration from nature, researchers have developed similar synthetic carriers.

1.5 Liposomes

Liposomes are the most heavily studied drug delivery system.[32] They were first discovered in 1961 when Bangham and R. W. Horne imaged phospholipid vesicles using

electron microscopy.[33] The first proposal of liposomes as a drug carrier was by Gregoriadis et al. in 1971.[34]

Liposomes are produced by the self-assembly of phospholipids into a bilayer membrane that encloses an inner aqueous compartment.[35] This reservoir can encapsulate water-soluble compounds, protecting them from the outside environment. Phospholipids are amphiphilic molecules that contain small hydrophobic tails covalently attached to a polar hydrophilic head group (**Figure 1.2**). These small amphiphilic molecules have critical aggregation concentrations (CAC) in the millimolar range. The critical aggregation concentration is the minimal concentration at which the amphiphilic molecules will begin to self-assemble into stable aggregates. Below this concentration the aggregates will not be stable in solution and will disperse.

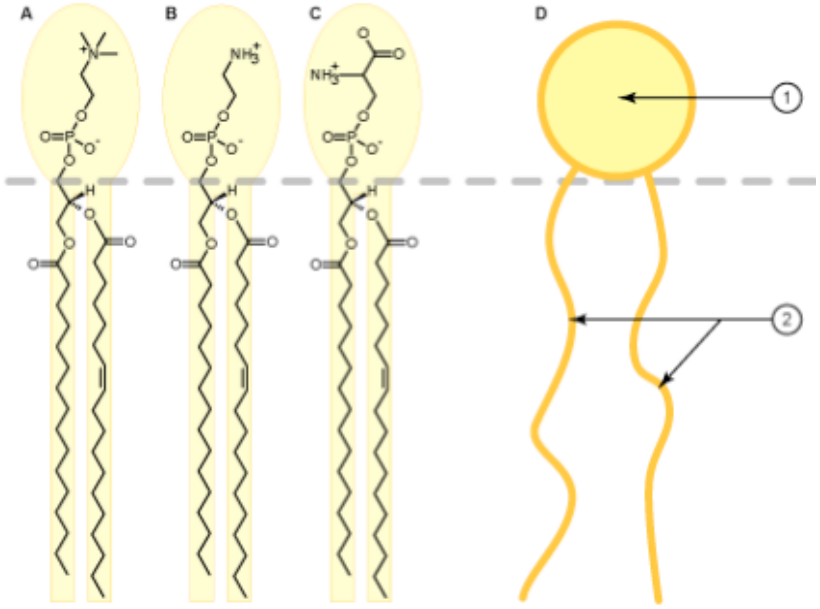

Figure 1.2 Sample lipids with (A) phosphatidylcholine, (B) phosphatidylethanolamine, (C) phosphatidylserine head groups. (D) Schematic representation of a phospholipid with a (1) hydrophilic head group and (2) hydrophobic tails.[36]

When assembled, these amphiphilic molecules can form thin highly dynamic membranes allowing easy processing and extrudability. However, this can potentially lead to problems when used for *in vivo* applications due to membrane instability and degradation.[13] Researchers have tried many approaches to overcome these issues by varying the length and degree of saturation of the hydrophobic tails, incorporating crosslinkable units,[37] and adding large amounts of cholesterol[32] to increase rigidity and stability of liposomal membranes.

Another obstacle faced by liposomes (and other drug delivery systems) during *in vivo* application is the rapid clearance from the body caused by phagocytic cells of the reticuloendothelial system (RES). Studies have shown that altering the composition of the surface of the liposome[32,38] (PEG modified liposomes) and reducing the size of liposomes to a diameter of 100 to 200 nm,[32,39] gave increased circulation times. It was found that size could dictate the biodistribution and fate of drug delivery systems by allowing them to circulate and go undetected by the RES.

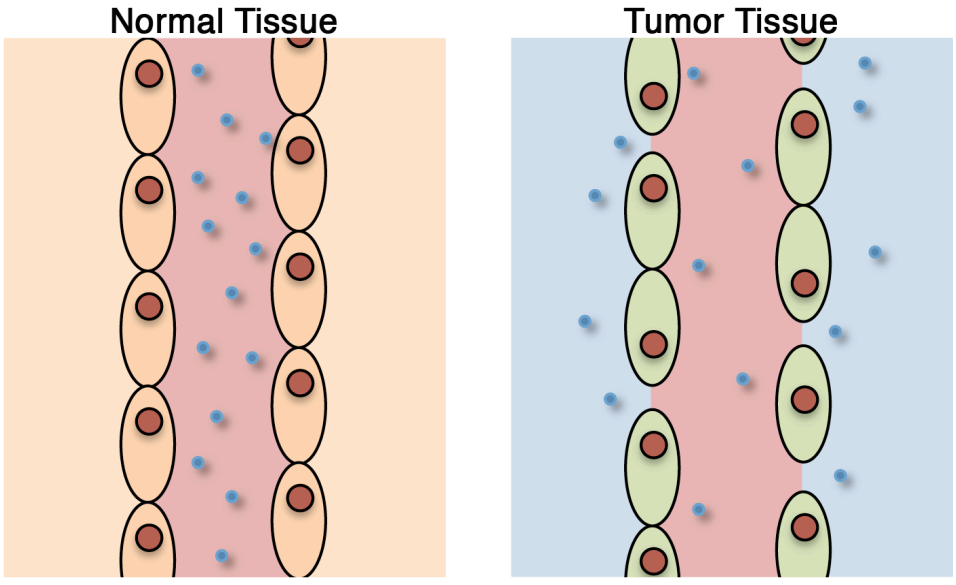

Figure 1.3 Representation of the leaky vasculature in tumor tissue and extravasation of polymer therapeutics by the enhanced permeation and retention (EPR) effect.

The size of a drug carrier is not only important for avoiding the RES but also for its accumulation in tumors by the enhanced permeability and retention (EPR) effect.[7] Studies have shown that as tumors grow they require additional blood supply and release growth factors to stimulate angiogenesis. This promotes the formation of abnormal blood vessels that are leaky due to poor alignment of the endothelial cells (**Figure 1.3**). The leaky vasculature allows for infiltration of molecules of a certain size (i.e., liposomes with diameters of 100 nm) and has been used successfully to accumulate liposomes and other nanoscale carriers in tumors.

1.6 Block Copolymer Vesicles, Polymersomes

Polymersomes[12] are similar to liposomes, but are composed of amphiphilic polymer chains that are larger than lipids. A wide range of structures have been incorporated to create block copolymers containing polyethylene oxide, polystyrene, polylactide, polyethylethylene and polybutadiene segments, which broadens the range of vesicle properties.[12,13,40] In addition, the higher molecular weights of the polymers increase membrane thickness and stability. This is supported by their overall much lower CACs. Although polymersomes show greater promise for use as drug encapsulants, some of these polymers could potentially be toxic long term and their degradation pathways are unknown.

1.7 Polypeptides

Proteins are large biomacromolecules found in nature and serve a vast number of important functions within living organisms. Proteins can be made from one or more chains of amino acids, which contain specific amino acid sequences that dictate the folding of the protein

into a specific three-dimensional shape. The three-dimensional shape is very important in that it directs the activity of the protein. Denaturing the structure of a protein can result in loss of activity and possible loss of solubility. There are vast number of proteins and only 20 standard amino acids (α-amino acids) (**Figure 1.4**).

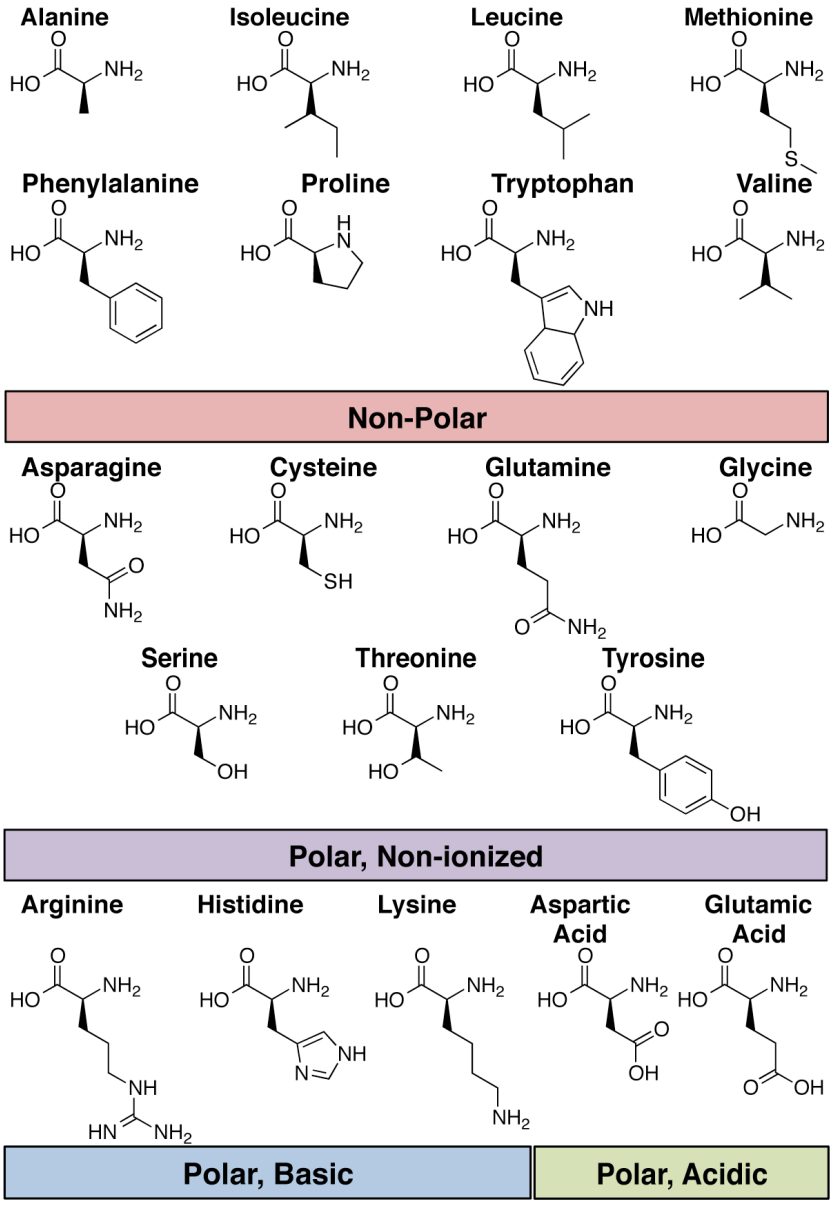

Figure 1.4 A list of the 20 natural amino acids, grouped based on side chain functionality.

The difference between each amino acid is based solely on its side chain structure and functionality, which also determines its polarity. Based on these features, each of these amino acids has a preferred secondary structure (**Figure 1.5**) that it can adopt when polymerized as homopolypeptide chains. In a protein, when amino acids preferring the same secondary structure are grouped together will give rise to that structure within a protein.

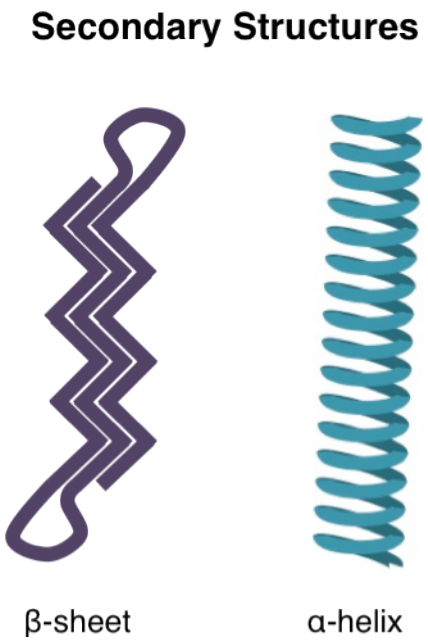

Figure 1.5 Secondary structures found in proteins.

There has been an increasing interest in developing materials that have the ability to self-assemble into complex, highly ordered structures, which has led to an interest in synthesizing designed polypeptides. These synthetic materials can be used for a variety of applications in biomaterials, diagnostics, tissue engineering and drug delivery.

Synthetic polypeptides are long chains of amino acids that may be advantageous for *in vivo* applications since they can degrade to non-toxic metabolites. Natural and unnatural amino

acids can be used as building blocks allowing a variety of functionality and physical properties. Polypeptides are also advantageous in that they can form secondary structures (i.e., α-helices, β-sheets) stabilized by hydrogen bonding.[41]

1.7.1 Synthetic Approaches to Polypeptides

There are two main strategies to preparing polypeptides that can incorporate both natural and unnatural amino acids. Solid phase peptide synthesis (SPPS) is a method used to create a peptide, usually less than 30 to 50 residues, with a specific amino acid sequence and length (**Figure 1.6**).[42] This method has a step-by-step procedure to ensure one amino acid is added at one time, requiring the addition and removal of many protecting groups (i.e., *tert*-butyloxcarbonyl (BOC), carbobenzyloxy (Cbz), 9-fluoroenylmethoxycarbonyl (FMOC)) to limit the number of functional groups present during each step. The peptide is bound to a solid, insoluble resin that allows for easy isolation and purification between each step. The disadvantage to this procedure is the efficiency of conjugation chemistry, limiting the length of the peptides. It is very difficult to synthesize large polypeptides. However, this is a very useful procedure for the synthesis of small peptides with defined sequences.

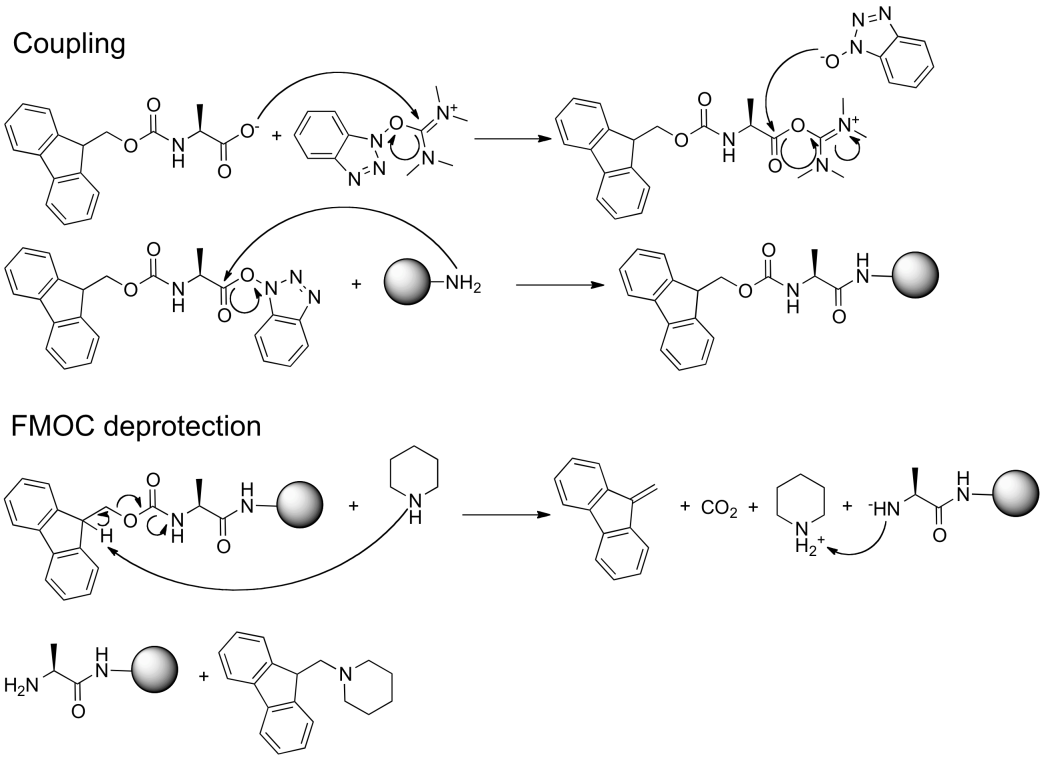

Figure 1.6 SPPS synthetic scheme.

A facile route to preparing polypeptides is the ring-opening polymerization (ROP) of α-amino acid *N*-carboxyanhydrides (NCAs). The polymerization of NCAs dates back to the early part of the 20th century when Hermann Leuchs discovered NCAs while heating *N*-ethoxycarbonyl and *N*-methoxycarbonyl α-amino acid chlorides.[43] When the corresponding NCAs were exposed to water, an insoluble mass was observed. Within the last 20 years, there have been significant advances to preparing and polymerizing NCAs, with enhanced control of molecular weight, composition, and low polydispersities.

There are two primary methods to preparing NCAs to high-purity. The Leuchs method requires an alkyl or aryl carbamate on the α-amine and a chlorinating reagent to activate the carboxylic acid to an acyl chloride for cyclization.[43] The second and most common method is the

Fuchs-Farthing method, which prepares NCAs through the use of phosgene (triphosgene) as the cyclizing agent.

The conventional method for polymerizing NCAs is the use of nucleophiles and bases, such as primary amines, tertiary amines, alkoxide and hydroxide ions. The use of these initiators can result in two mechanisms, the amine mechanism (AM) or activated monomer mechanism (AMM). The AM pathway requires a highly nucleophilic initiator to initiate the ring-opening polymerization by attacking the C_5 carbon of the NCA (**Figure 1.7**). The following step involves release of carbon dioxide (CO_2) unmasking the amine, which may then attack another NCA. Primary amines are generally good initiators for the polymerization of NCA monomers through AM pathway. More basic initiators can result in AMM route (**Figure 1.8**); however, a system may switch between mechanisms during polymerization. The AM polymerization tends to be slow and can result in many side reactions inhibiting the ability to control composition and the polymerization of large molecular weight polypeptides.

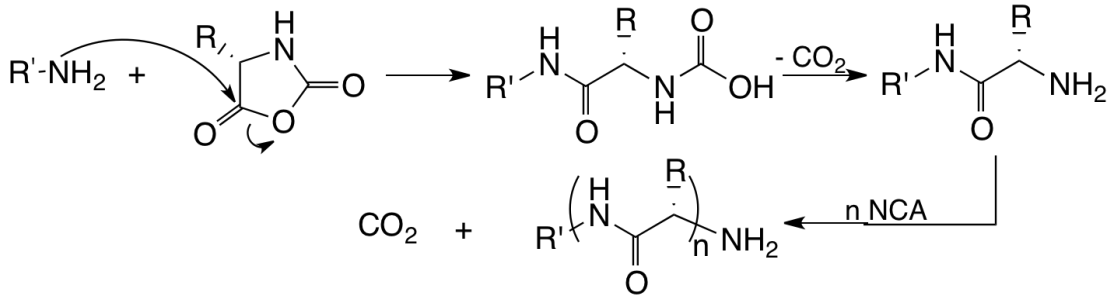

Figure 1.7 Polymerization of NCAs via the amine mechanism.

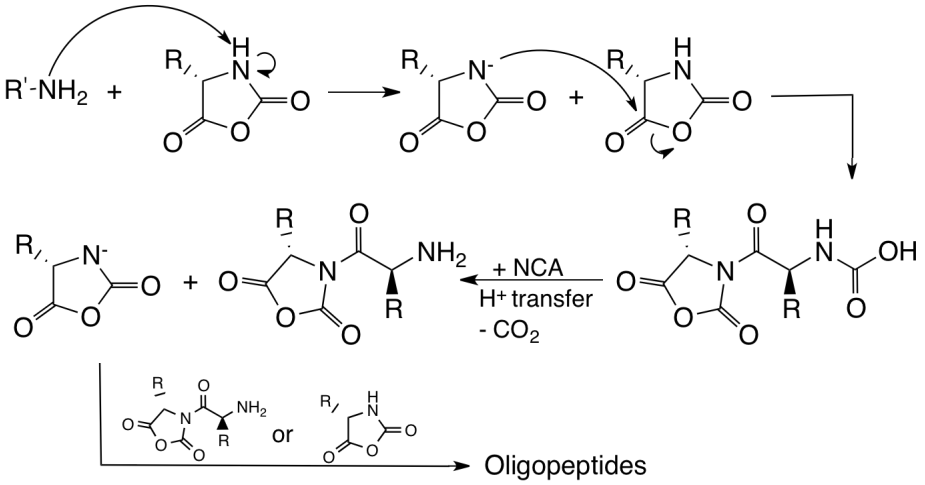

Figure 1.8 Polymerization of NCAs via the activated monomer mechanism.

1.7.2 Transition Metal-Mediated ROP of NCAs

The conventional methods of polymerizing NCAs has been plagued with side reactions due to limited control over the reactivity of the growing polypeptide chains. This can result in high polydispersities, impurities of homopolymers when attempting to synthesize more complex block copolypeptides, and limited control of polypeptide lengths. In search of better initiators for control of the chain end reactivity, researchers turned to the use of transition-metal complexes as end groups to control each NCA addition.[43] It has been proven that the use of transition metals in organic and polymer synthesis can lead to increased selectivity and efficiency during reactions. Early research focused on metal alkoxides, which primarily act as strong bases resulting in polymerizations with low efficiency and molecular weight control similar to conventional methods.

Research in the Deming lab focused on finding a means for living polymerization of NCAs using zerovalent transition metal initiators (**Figure 1.9** and **Figure 1.10**). Zerovalent

nickel and cobalt initiators were developed (i.e., bpyNi(COD) and $(PMe_3)_4Co$) providing access to living polymerization of NCAs to high molecular weight polypeptides with control of both length and composition with narrow polydispersities (M_w/M_n = 1.05-1.3).[44-49]

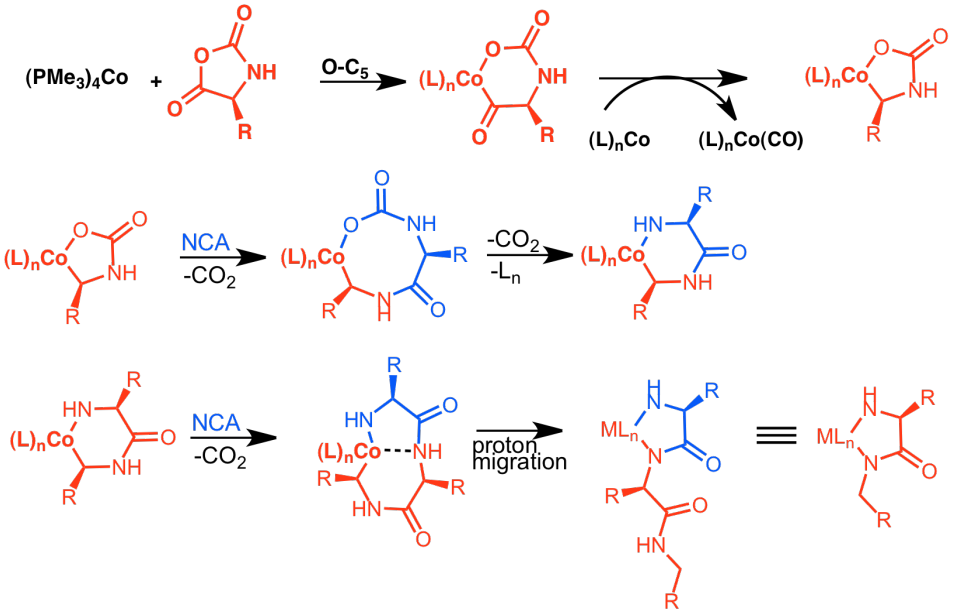

Figure 1.9 Initiation of NCA polymerization with zerovalent cobalt.

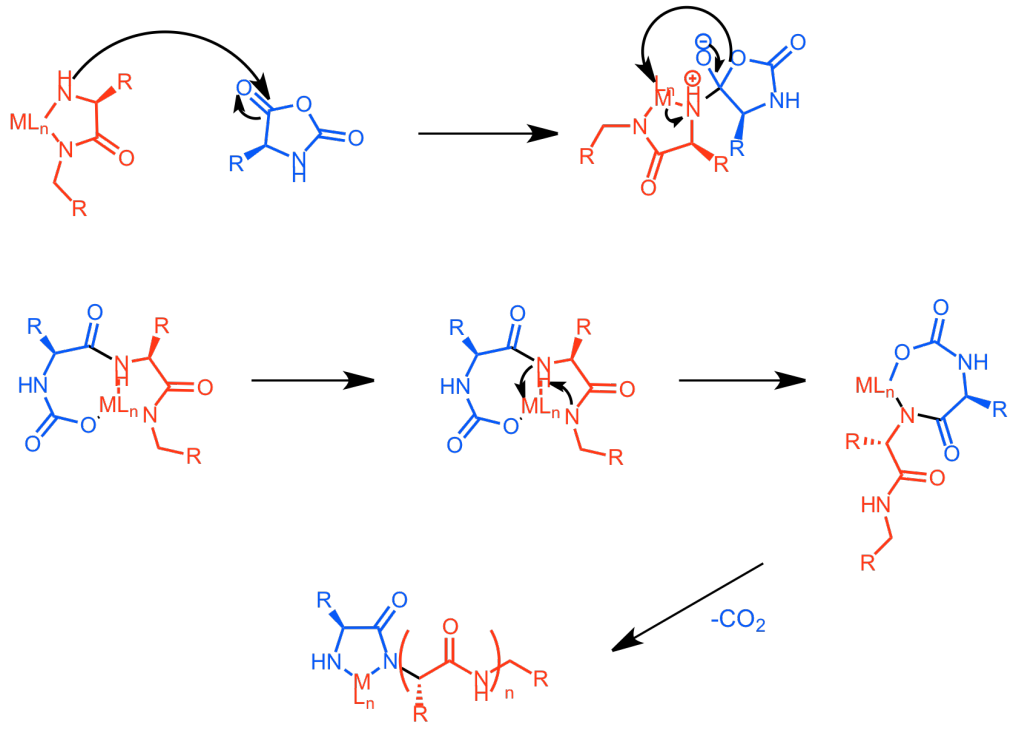

Figure 1.10 Propagation of polypeptide chain via amido-amidate metallacycle.

1.8 Block Copolypeptides

In the Deming lab, the use of zerovalent nickel and cobalt initiators for NCA polymerization has allowed the synthesis of well-defined block copolypeptides. With many natural and unnatural amino acids to choose from and the development of new methods for purification of NCAs, the synthesis of complex block copolypeptides is endless. The development of amphiphilic block copolypeptides have led to a number of different self-assembling materials such as micelles,[50] emulsions,[10] hydrogels[51-53] and vesicles.[54-56] The use of polypeptides can provide materials that are biodegradable, bioresorbable and possibly biocompatible and biological active.

1.9 Block Copolypeptide Vesicles

Amphiphilic block copolymers have the ability to self-assemble into a variety of structures (i.e., micelles,[57,58] emulsion droplets,[10,59,60] hydrogels,[52,61-64] vesicles,[13,65] and cylindrical micelles[66,67]) and have been the focus of research for applications in drug delivery, biosensors, and biomaterials. More interest has been placed on developing peptide-based block copolymers. Lecommandoux et al. reported the self-assembly of micelles and vesicles with a polymer-polypeptide hybrid block copolymer, poly(butadiene)-*block*-poly(L-glutamic acid).[54] The poly(butadiene) polymer was end-capped with an amine that was used to initiate amine mechanism polymerization of γ-benzyl-L-glutamate *N*-carboxyanhydride (Bn-Glu NCA). Many other reports have combined polypeptide blocks with polymer blocks (i.e., polyisoprene,[68] poly(ε-caprolactone),[69] polybutadiene[54,70]) to increase control of function and structure of self-assemblies.

Vesicles can also be formed from the self-assembly of amphiphilic block copolypeptides. Recently, Lecommandoux et al. reported the self-assembly of poly(L-glutamic acid)$_{15}$-*block*-poly(L-lysine)$_{15}$, or $E_{15}K_{15}$, into vesicles.[71] The self-assembly was controlled by the selective protonation and deprotonation of the individual polypeptide segments. In another report, Shantz et al. synthesized inorganic nanoparticles (silica and silver bromide) with the help of block copolypeptide vesicles using, poly(L-lysine)$_x$-*block*-poly(L-phenylalanine)$_y$ (x:y = 12:4, 23:23, 32:5, 150:15) and poly(L-lysine)$_x$-*block*-poly(DL-phenylalanine)$_y$ (x:y = 24:4, 80:10).[72]

In the Deming lab, we developed a procedure for the living ring-opening polymerization of α-amino acid-*N*-carboxyanhydrides (NCAs) using transition metal initiators, such as $(PMe_3)_4Co$.[44,73,74] Our system provides direct control of molecular weight, composition and the ability to form block copolymers having low polydispersities (M_w/M_n <1.3). Using this

procedure, the Deming group has created two families of block copolypeptide amphiphiles that form vesicles.

1.10 Neutral Diblock Copolypeptides

The first family is composed of a nonionic hydrophilic diethylene glycol modified lysine domain and a hydrophobic leucine domain of the general structure: poly(N_ε-2-(2-(2-methoxyethoxy)ethoxy)acetyl-L-lysine)$_x$-*block*-poly(L-leucine)$_y$, or $K^P{}_xL_y$ (x = 60 to 200, y = 10 to 40).[55] Both domains adopt α-helical conformations leading to rod-like chains that self-assemble into unilamellar membranes due to the alignment of the helical axes. The $K^P{}_xL_y$ membranes are very robust and rigid, which prevents extrusion of micron-sized vesicles through small pore polycarbonate (PC) filters to obtain nanoscale vesicles (**Figure 1.11**). The inability to obtain vesicles with diameters in the nanoscale range makes these materials unsuitable for drug delivery applications.

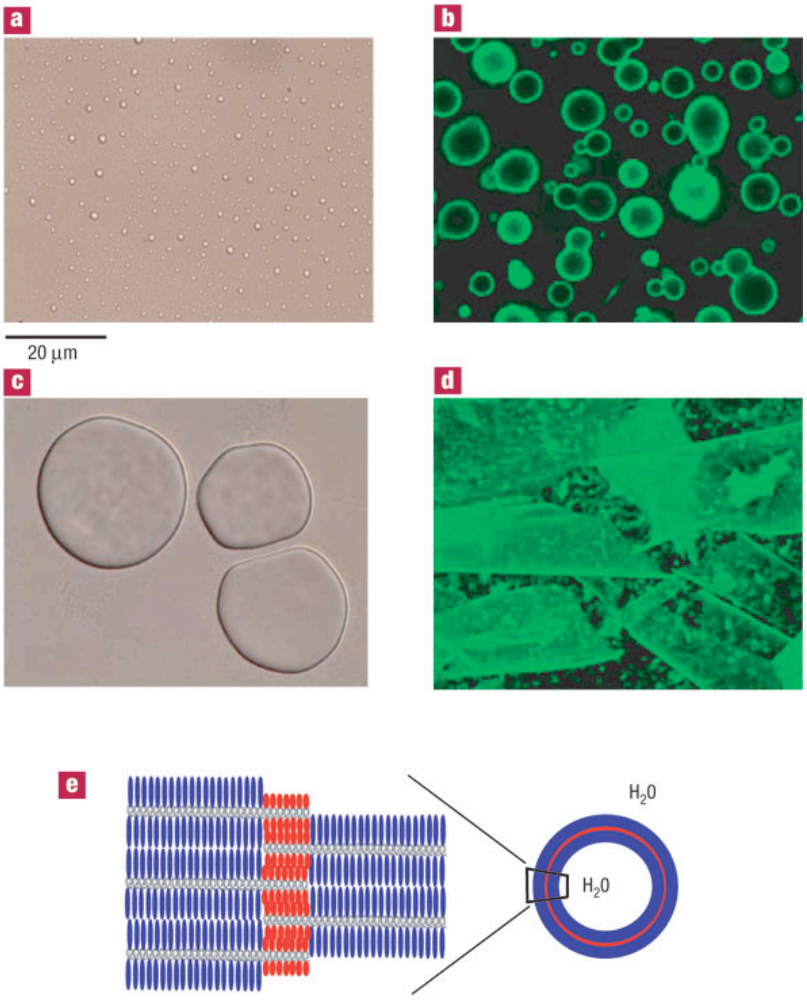

Figure 1.11 Images of different $K^P_xL_y$ samples.[55]

1.11 Charged Diblock Copolypeptides

The second family contains highly charged polyelectrolyte segments (i.e., poly(L-lysine), or poly(L-glutamate)) as the hydrophilic domain, while also containing oligoleucine hydrophobic domains.[56,75] Holowka et al. varied both chain lengths of the hydrophilic and hydrophobic domains of poly(L-lysine)$_x$-*block*-poly(L-leucine)$_y$, K_xL_y, from x = 20 to 80 residues and y = 10

to 30 residues. Poly(L-lysine)$_{60}$-*block*-poly(L-leucine)$_{20}$, $K_{60}L_{20}$, gave the optimal composition for vesicle self-assembly (**Figure 1.12**).

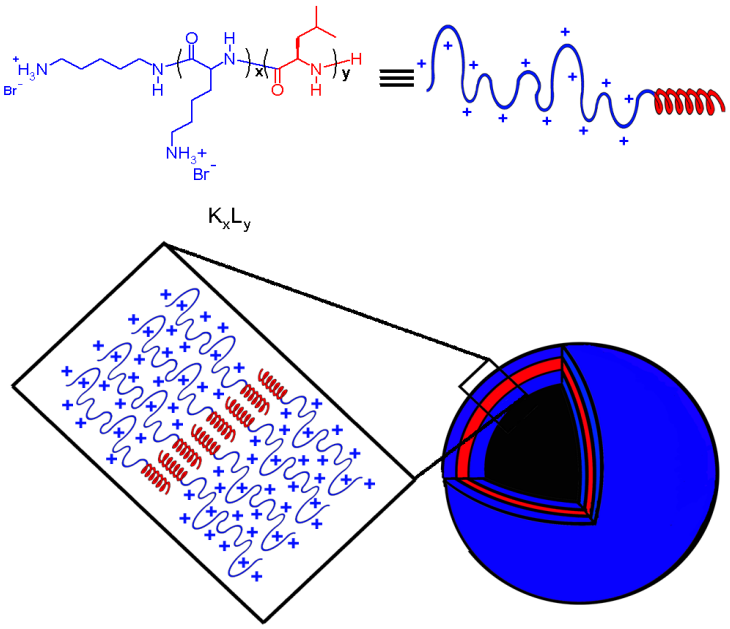

Figure 1.12 Polylysine-*block*-polyleucine vesicle representation.[56]

The highly charged polyelectrolyte segment imparts solubility and flexibility within the polypeptide chains allowing more fluidity of the vesicle membranes. Indeed, our $K_{60}L_{20}$ vesicles are easily processed down to nanoscale sizes and can encapsulate solutes (i.e., Texas Red labeled dextran) during extrusion. However, the reproducibility of extruding these vesicles below 200 nm, desirable for drug delivery applications, has been a challenge. Cytotoxicity studies of $K_{60}L_{20}$ vesicle suspension have revealed an increase in toxicity with an increase in polypeptide concentrations, which is typical of highly cationic polymers.[76,77] However, studies of the negatively charged $E_{60}L_{20}$ vesicles have shown results of little to no toxicity at concentrations up to 100 μg/mL. This result may be due to limited interaction with the negatively charged surfaces of cells.

1.12 Cellular Uptake of Charged Diblock Copolypeptides

Arginine-rich segments are found on protein-transduction domains (PTDs) including the well-studied transactivator of transcription for HIV-1 Tat.[78-83] We found that $K_{60}L_{20}$ vesicles do not readily enter cells and require additional functionality for cell uptake. Our group developed polypeptide vesicles with polyarginine hydrophilic segments of the general structure: poly(L-arginine)$_{60}$-*block*-poly(L-leucine)$_{20}$, $R_{60}L_{20}$.[75] The $R_{60}L_{20}$ vesicles were able to encapsulate Texas Red labeled dextran and were taken up by T84 and HULEC-5A cell lines, indicating that polyarginine segments are critical for intracellular delivery.

While these polypeptide vesicles ($R_{60}L_{20}$) have shown promise for intracellular delivery there are issues that remain to be addressed. Previous studies have shown that cytotoxicity increases with the concentration of the polypeptide vesicles. For *in vivo* applications it would be beneficial to eliminate or reduce vesicle toxicity allowing for increased dose administration. Intracellular trafficking studies have shown that $R_{60}L_{20}$ vesicles enter the cell by a macropinocytosis pathway and are routed to early endosomes and then recycled back to the cell surface.[84] In order to deliver therapeutics, it would be beneficial for the vesicles to have endosome-disrupting ability.

1.13 Obstacles Faced by Current Diblock Copolypeptides Vesicles

There has been a huge effort to develop polypeptide vesicles in the Deming Lab and previous results have presented guidelines for amphiphilic polypeptide compositions and functionalities. Previous research revealed that a hydrophobic domain adopting a α-helical structure helps to drive the vesicle self-assembly under aqueous conditions. However, there is

room for optimizing the length of the α-helical domain and testing the stability of the vesicles and its effect on *in vitro* studies. The development of an optimal hydrophobic domain for vesicle self-assembly is important for increasing stability and minimizing toxicity of the polypeptide vesicles. Finally the hydrophobic domain length and composition may be tuned to provide fluidity to vesicle membranes for reproducible extrusion to more desirable diameters and lower critical aggregation concentrations.

Cytotoxicity of polypeptide vesicles is another obstacle that has been faced and an important one to overcome. Toxicity of the drug carrier may cause undesirable side effects when used *in vivo*, and will limit the amount that can be administered. Previous results have shown that vesicle surface charges play a role in the cytotoxicity, with cationic materials being more toxic[76] than negatively charged domains. However, the cationic arginine segments have shown promise with enhancing cellular uptake. Finding a balance of charges on the vesicle surface while retaining cellular uptake may help reduce the cytotoxicity of the polypeptide vesicles.

Advances have been made recently in developing smart drug delivery systems, which incorporates a material that is stimuli responsive to environmental conditions.[85-88] Recently Bellomo et al., incorporated the amino side chain functionality of lysine into the hydrophobic domain by copolymerizing with hydrophobic leucine residues to give the polymer, poly(N_ε-2-(2-(2-methoxyethoxy)ethoxy)acetyl-L-lysine)$_{160}$-*block*-poly(L-leucine$_{0.3}$-*co*-L-lysine$_{0.7}$)$_{40}$, $K^P{}_{160}(L_{0.2}/K_{0.7})_{40}$.[55] At a high pH, poly(L-lysine) is uncharged and adopts an α-helical conformation, contributing to the secondary structure of the hydrophobic domain allowing the formation of vesicles. Below pH 9, the amino group becomes charged and destabilizes the vesicles releasing it cargo. This example shows a proof of concept of adding stimuli responsiveness to vesicles, however, for *in vivo* application it may not be suitable for

physiological pH. Mabrouk et al. recently developed polymersomes that incorporated a liquid-crystalline polymer that is responsive to light. Upon exposure to UV light, the azobenzene functional group of this polymer undergoes a trans-to-cis configuration transition causing a change in the conformation of the polymer inducing polymersome rupture. Incorporating a polypeptide domain that may respond to environmental conditions would be desirable for having triggered release of encapsulated cargoes. This may ensure that once the vesicle has reached its targeted location it may open and release the drugs to provide their therapeutic effects.

1.14 References

(1) Allen, T. M.; Cullis, P. R. *Science* **2004**, *303*, 1818.

(2) Langer, R. *Science* **1990**, *249*, 1527.

(3) Saltzman, M. W. *Drug Delivery: Engineering Principles for Drug Therapy*; Oxford University Press, 2001.

(4) Allen, T. M. *Current Opinion in Colloid & Interface Science* **1996**, *1*, 645.

(5) Cao, Z.; Tong, R.; Mishra, A.; Xu, W.; Wong, G. C. L.; Cheng, J.; Lu, Y. *Angewandte Chemie International Edition* **2009**, *48*, 6494.

(6) Cho, K.; Wang, X.; Nie, S.; Chen, Z.; Shin, D. M. *Clinical Cancer Research* **2008**, *14*, 1310.

(7) Davis, M. E.; Chen, Z.; Shin, D. M. *Nat Rev Drug Discov* **2008**, *7*, 771.

(8) Frechet, J. M. J. *Proceedings of the National Academy of Sciences of the United States of America* **2002**, *99*, 4782.

(9) Gillies, E. R.; FrÈchet, J. M. J. *Drug Discovery Today* **2005**, *10*, 35.

(10) Hanson, J. A.; Chang, C. B.; Graves, S. M.; Li, Z.; Mason, T. G.; Deming, T. J. *Nature* **2008**, *455*, 85.

(11) Kataoka, K.; Harada, A.; Nagasaki, Y. *Advanced Drug Delivery Reviews* **2001**, *47*, 113.

(12) Discher, B. M.; Won, Y.-Y.; Ege, D. S.; Lee, J. C.-M.; Bates, F. S.; Discher, D. E.; Hammer, D. A. *Science* **1999**, *284*, 1143.

(13) Discher, D. E.; Eisenberg, A. *Science* **2002**, *297*, 967.

(14) Kukula, H.; Schlaad, H.; Antonietti, M.; Forster, S. *Journal of the American Chemical Society* **2002**, *124*, 1658.

(15) Zhang, L.; Gu, F. X.; Chan, J. M.; Wang, A. Z.; Langer, R. S.; Farokhzad, O. C. *Clin Pharmacol Ther* **2007**, *83*, 761.

(16) Stull, R.; Szoka, J. F. *Pharmaceutical Research* **1995**, *12*, 465.

(17) Lowrie, D. B.; Tascon, R. E.; Bonato, V. L. D.; Lima, V. M. F.; Faccioli, L. H.; Stavropoulos, E.; Colston, M. J.; Hewinson, R. G.; Moelling, K.; Silva, C. L. *Nature* **1999**, *400*, 269.

(18) Whitehead, K. A.; Langer, R.; Anderson, D. G. *Nat Rev Drug Discov* **2009**, *8*, 129.

(19) Chapman, A. P.; Antoniw, P.; Spitali, M.; West, S.; Stephens, S.; King, D. J. *Nat Biotech* **1999**, *17*, 780.

(20) Offner, H.; Hashim, G. A.; Vandenbark, A. A. *Science* **1991**, *251*, 430.

(21) Van Breemen, R. B.; Bartlett, M. G.; Tsou, Y. H.; Culver, C.; Swaisgood, H.; Unger, S. E. *Drug Metabolism and Disposition* **1991**, *19*, 683.

(22) Sinha, V. R.; Trehan, A. *Journal of Controlled Release* **2003**, *90*, 261.

(23) Yalkowsky, S. H.; Krzyzaniak, J. F.; Ward, G. H. *Journal of Pharmaceutical Sciences* **1998**, *87*, 787.

(24) Iaizzo, P. In *Handbook of Cardiac Anatomy, Physiology, and Devices*; Iaizzo, P. A., Ed.; Humana Press: 2009, p 3.

(25) Burish, T. G.; Tope, D. M. *Journal of Pain and Symptom Management* **1992**, *7*, 287.

(26) Komarov, P. G.; Komarova, E. A.; Kondratov, R. V.; Christov-Tselkov, K.; Coon, J. S.; Chernov, M. V.; Gudkov, A. V. *Science* **1999**, *285*, 1733.

(27) Lynn, D. M.; Langer, R. *Journal of the American Chemical Society* **2000**, *122*, 10761.

(28) Choi, J. S.; Joo, D. K.; Kim, C. H.; Kim, K.; Park, J. S. *Journal of the American Chemical Society* **2000**, *122*, 474.

(29) Bogorad, L. *Science* **1975**, *188*, 891.

(30) Herrmann, R. G.; Maier, R. M.; Schmitz-Linneweber, C. *Philosophical Transactions: Biological Sciences* **2003**, *358*, 87.

(31) Vellai, T.; Vida, G. *Proceedings: Biological Sciences* **1999**, *266*, 1571.

(32) Lian, T.; Ho, R. J. Y. *Journal of Pharmaceutical Sciences* **2001**, *90*, 667.

(33) Bangham, A. D.; Horne, R. W. *Journal of Molecular Biology* **1964**, *8*, 660.

(34) Gregoriadis, G.; Ryman, B. E. *Biochemical Journal* **1971**, *124*, 58P.

(35) Szoka, F.; Papahadjopoulos, D. *Annual Review of Biophysics and Bioengineering* **1980**, *9*, 467.

(36) Foobar In *Foobar*; representation.png, P. s., Ed. 2006; Vol. 25 KB, p Schematic representation of phosphoacylglycerols.

(37) Ruysschaert, T.; Germain, M.; da Silva Gomes, J. F. P.; Fournier, D.; Sukhorukov, G. B.; Meier, W.; Winterhalter, M. *NanoBioscience, IEEE Transactions on* **2004**, *3*, 49.

(38) Zasadzinski, J. A. *Current Opinion in Solid State and Materials Science* **1997**, *2*, 345.

(39) Nagayasu, A.; Uchiyama, K.; Kiwada, H. *Advanced Drug Delivery Reviews* **1999**, *40*, 75.

(40) Discher, D. E.; Ahmed, F. *Annual Review of Biomedical Engineering* **2006**, *8*, 323.

(41) Deming, T. J. *Advanced Materials* **1997**, *9*, 299.

(42) Merrifield, R. B. *Journal of the American Chemical Society* **1963**, *85*, 2149.

(43) Kricheldorf, H. R. *Angewandte Chemie International Edition* **2006**, *45*, 5752.

(44) Deming, T. J. *Nature* **1997**, *390*, 386.

(45) Deming, T. J. *Journal of the American Chemical Society* **1998**, *120*, 4240.

(46) Deming, T. J. *Macromolecules* **1999**, *32*, 4500.

(47) Deming, T. J. *Abstracts of Papers of the American Chemical Society* **2000**, *219*, 5.

(48) Deming, T. J. *Journal of Polymer Science Part a-Polymer Chemistry* **2000**, *38*, 3011.

(49) Goodwin, A. A.; Bu, X. H.; Deming, T. J. *Journal of Organometallic Chemistry* **1999**, *589*, 111.

(50) Hanson, J. A.; Li, Z.; Deming, T. J. *Macromolecules* **2010**, *43*, 6268.

(51) Breedveld, V.; Nowak, A. P.; Sato, J.; Deming, T. J.; Pine, D. J. *Macromolecules* **2004**, *37*, 3943.

(52) Chu-Ya, Y.; Bingbing, S.; Yan, A.; Nowak, A. P.; Abelowitz, R. B.; Korsak, R. A.; Havton, L. A.; Deming, T. J.; Sofroniew, M. V. *Biomater.* **2009**, *30*, 2881.

(53) Deming, T. J. *Soft Matter* **2005**, *1*, 28.

(54) Chécot, F.; Lecommandoux, S.; Gnanou, Y.; Klok, H.-A. *Angewandte Chemie International Edition* **2002**, *41*, 1339.

(55) Bellomo, E. G.; Wyrsta, M. D.; Pakstis, L.; Pochan, D. J.; Deming, T. J. *Nat Mater* **2004**, *3*, 244.

(56) Holowka, E. P.; Pochan, D. J.; Deming, T. J. *Journal of the American Chemical Society* **2005**, *127*, 12423.

(57) Shuai, X.; Ai, H.; Nasongkla, N.; Kim, S.; Gao, J. *Journal of Controlled Release* **2004**, *98*, 415.

(58) Jones, M.-C.; Leroux, J.-C. *European Journal of Pharmaceutics and Biopharmaceutics* **1999**, *48*, 101.

(59) Utada, A. S.; Lorenceau, E.; Link, D. R.; Kaplan, P. D.; Stone, H. A.; Weitz, D. A. *Science* **2005**, *308*, 537.

(60) Riess, G.; Nervo, J.; Rogez, D. *Polymer Engineering & Science* **1977**, *17*, 634.

(61) Hoare, T. R.; Kohane, D. S. *Polymer* **2008**, *49*, 1993.

(62) Yu, L.; Ding, J. *Chemical Society Reviews* **2008**, *37*, 1473.

(63) Nowak, A. P.; Breedveld, V.; Pakstis, L.; Ozbas, B.; Pine, D. J.; Pochan, D.; Deming, T. J. *Nature* **2002**, *417*, 424.

(64) Nowak, A. P.; Sato, J.; Breedveld, V.; Deming, T. J. *Supramolecular Chemistry* **2006**, *18*, 423.

(65) Luo, L.; Eisenberg, A. *Langmuir* **2001**, *17*, 6804.

(66) Wang, H.; Wang, H. H.; Urban, V. S.; Littrell, K. C.; Thiyagarajan, P.; Yu, L. *Journal of the American Chemical Society* **2000**, *122*, 6855.

(67) Rodríguez-Hernández, J.; Chécot, F.; Gnanou, Y.; Lecommandoux, S. *Progress in Polymer Science* **2005**, *30*, 691.

(68) Babin, J.; Rodriguez-Hernandez, J.; Lecommandoux, S.; Klok, H.-A.; Achard, M.-F. *Faraday Discussions* **2005**, *128*, 179.

(69) Rong, G.; Deng, M.; Deng, C.; Tang, Z.; Piao, L.; Chen, X.; Jing, X. *Biomacromolecules* **2003**, *4*, 1800.

(70) Gervais, M.; Douy, A.; Gallot, B.; Erre, R. *Polymer* **1988**, *29*, 1779.

(71) Rodriguez-Hernandez, J.; Lecommandoux, S. *Journal of the American Chemical Society* **2005**, *127*, 2026.

(72) Jan, J.-S.; Lee, S.; Carr, C. S.; Shantz, D. F. *Chemistry of Materials* **2005**, *17*, 4310.

(73) Deming, T. J. *Journal of Polymer Science Part A: Polymer Chemistry* **2000**, *38*, 3011.

(74) Deming, T. J.; Curtin, S. A. *Journal of the American Chemical Society* **2000**, *122*, 5710.

(75) Holowka, E. P.; Sun, V. Z.; Kamei, D. T.; Deming, T. J. *Nat Mater* **2007**, *6*, 52.

(76) Lv, H.; Zhang, S.; Wang, B.; Cui, S.; Yan, J. *Journal of Controlled Release* **2006**, *114*, 100.

(77) Merdan, T.; Kopecˇek, J.; Kissel, T. *Advanced Drug Delivery Reviews* **2002**, *54*, 715.

(78) Mitchell, D. J.; Steinman, L.; Kim, D. T.; Fathman, C. G.; Rothbard, J. B. *The Journal of Peptide Research* **2000**, *56*, 318.

(79) Brooks, H.; Lebleu, B.; VivËs, E. *Advanced Drug Delivery Reviews* **2005**, *57*, 559.

(80) Futaki, S. *Peptide Science* **2006**, *84*, 241.

(81) Mishra, A.; Gordon, V. D.; Yang, L.; Coridan, R.; Wong, G. C. L. *Angewandte Chemie International Edition* **2008**, *47*, 2986.

(82) Mishra, A.; Lai, G. H.; Schmidt, N. W.; Sun, V. Z.; Rodriguez, A. R.; Tong, R.; Tang, L.; Cheng, J.; Deming, T. J.; Kamei, D. T.; Wong, G. C. L. *Proceedings of the National Academy of Sciences* **2011**, *108*, 16883.

(83) Wadia, J. S.; Dowdy, S. F. *Advanced Drug Delivery Reviews* **2005**, *57*, 579.

(84) Sun, V. Z.; Li, Z.; Deming, T. J.; Kamei, D. T. *Biomacromolecules* **2010**, *12*, 10.

(85) Alarcon, C. d. l. H.; Pennadam, S.; Alexander, C. *Chemical Society Reviews* **2005**, *34*, 276.

(86) Schmaljohann, D. *Advanced Drug Delivery Reviews* **2006**, *58*, 1655.

(87) Li, M.-H.; Keller, P. *Soft Matter* **2009**, *5*, 927.

(88) Stuart, M. A. C.; Huck, W. T. S.; Genzer, J.; Muller, M.; Ober, C.; Stamm, M.; Sukhorukov, G. B.; Szleifer, I.; Tsukruk, V. V.; Urban, M.; Winnik, F.; Zauscher, S.; Luzinov, I.; Minko, S. *Nat Mater* **2010**, *9*, 101.

CHAPTER TWO

Optimization of Block Copolypeptide Vesicles by Modification of Hydrophobic Domain Length and Composition

2.1 Abstract

Previously the amphiphilic block copolypeptide, poly(L-lysine)$_{60}$-*block*-poly(L-leucine)$_{20}$ ($K_{60}L_{20}$), was shown to self assemble into vesicles and could be manipulated to different sizes by extrusion.[1] However, we have found the ability to obtain vesicles in the lower nanometer range to be difficult. Previous work on varying the length of the hydrophobic domain showed that shorter lengths of leucine resulted in reduced helical conformation, confirmed by circular dichroism.[1] The effect of the length on vesicle stability and cytotoxicity has not been investigated. This study is to expand upon the role of the hydrophobic domain by varying the length of the hydrophobic segment to optimize the vesicles so that they are monodisperse and low in toxicity. Polypeptide vesicles with longer oligoleucine segments were found to exhibit lower toxicity than vesicles self-assembled from polypeptides with shorter oligoleucine segments. Based on transmission electron microscopy and dynamic light scattering, this increase in toxicity was attributed to the formation of toxic micelles, small aggregates and unstable vesicles formed from shorter leucine segments. Long oligoleucine segments, however, result in very rigid hydrophobic helix that form rigid vesicle membranes that prevent the processing and extrusion of monodisperse population in the lower nanometer range (< 200 nm) making them less suitable as drug delivery vehicles. To overcome the formation of highly rigid vesicle membranes, the hydrophobic domain composition was altered by copolymerization of

phenylalanine NCAs with leucine NCAs forming a domain that still favors an α-helical conformation and the self-assembly of polypeptide vesicles. Extrusion of vesicles resulted in diameters in the lower nanometer range (< 200 nm) with low polydispersities.

2.2 Background

The hydrophobic domain of amphiphilic polymers provides the driving force of self-assembly under aqueous conditions. The use of amphiphilic polypeptides over synthetic conventional polymers is the ability of polypeptides to adopt secondary structures dependent on the amino acid side chains. The most common secondary structures, the alpha helix and beta sheet, are found in proteins and help drive the self-assembly of the protein tertiary structures. Poly(L-leucine) homopolypeptide is very hydrophobic and favors the alpha helical conformation. In nature, L-leucine amino acids in alpha helical domains can drive the alignment and formation of helix-helix assembles along their axes, resulting in tight interaction know as leucine zippers (**Figure 2.1**).[2] Helices wanting to align along their axes result in unilamellar membranes that can be used to self-assemble vesicles.

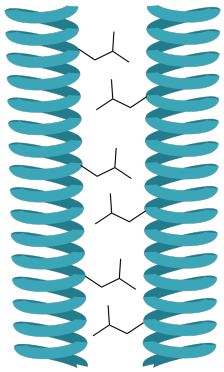

Figure 2.1 Formation of leucine zippers by interaction and stacking of the hydrophobic leucine side chains.

2.3 Introduction

In the drug delivery field, block copolypeptides represent an emerging class of materials that has gained interest recently.[3-5] Synthetic polypeptides comprised of natural amino acid residues show promise of chemical diversity, possible improved biocompatibility and hierarchical assembly by incorporation of secondary structures. The previous development of the block copolypeptide, poly(L-lysine)$_{60}$-*block*-poly(L-leucine)$_{20}$ ($K_{60}L_{20}$), showed the self-assembly of versatile vesicles that could be extruded to different sizes and the ability to encapsulate hydrophilic cargo.[1]

This chapter summarized efforts to further understand and optimize these vesicle structures as potential drug delivery vesicles by studying the role of the hydrophobic domain. The first step in identifying the optimal vesicle former is to vary the hydrophilic/hydrophobic ratio by fine-tuning the length of the hydrophobic segment, while keeping the hydrophilic segment constant. By changing the ratio of the hydrophobic segment to hydrophilic segment the geometry of the polymer in solution is altered[6,7] and by varying the length of the hydrophobic segment, helical content of the polypeptide chain is varied. Both of these properties can affect the self-assembly of the supramolecular structure formed and its stability. In a previous paper, it was found as the hydrophobic oligoleucine segment becomes shorter, the alpha-helix becomes less stable, resulting in a more disordered structure.[1] The shorter hydrophobic oligoleucine segment built in the block copolypeptides are expected to assume a conical shape that favors the self-assembly into spherical micelles and non-vesicular aggregates (**Figure 2.2**). In contrast, polypeptide with longer leucine segments are predicted to adopt a truncated-cone shape that aids the self-assembly into bilayered vesicles.

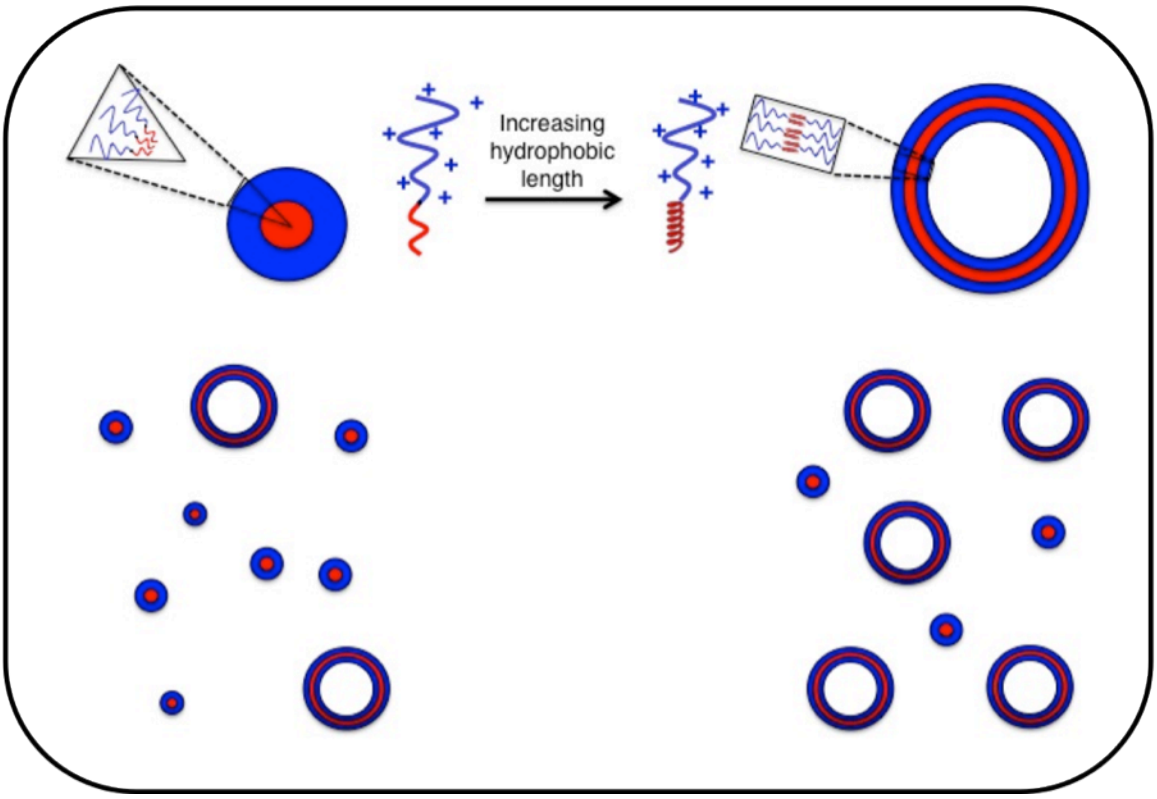

Figure 2.2 Effect of the hydrophobic chain length on the self-assembly of block copolypeptides. Block copolypeptides with shorter oligoleucine segments are expected to give rise to disordered segments that could favor the formation of micelles or non-vesicular aggregates.

By fine-tuning the length of the hydrophobic segment, we expect to alter the polypeptide's ability to form vesicles in solution. The rise of different supramolecular structures, such as micelles, aggregates and vesicles, in the suspension population can result in different levels of toxicity. In addition, the length of the hydrophobic domain may affect the ability to extrude the vesicles suspension into a monodisperse population, as different lengths may affect the stability and rigidity of the bilayer membranes. In the first part of this chapter, we explored how the length of the hydrophobic domain affects the formation, cytotoxicity, extrudability and stability of the vesicles by preparing block copolypeptides of varying hydrophobic chain length.

The last part of this chapter focuses on maintaining the length of the hydrophobic segment, while varying the composition and exploring the effects on vesicle formation and extrudability. As previously described, the leucine domain provides a rigid hydrophobic domain that can act as leucine zippers found in nature. The rigidity of the leucine helices may limit the vesicle membrane fluidity making it difficult to extrude these highly charged diblock copolypeptide vesicles to monodisperse populations below 200 nanometers. It is believed that incorporating other hydrophobic amino acids that favor helical formation can reduce the rigidity and crystallinity of the leucine domain (**Figure 2.3**).

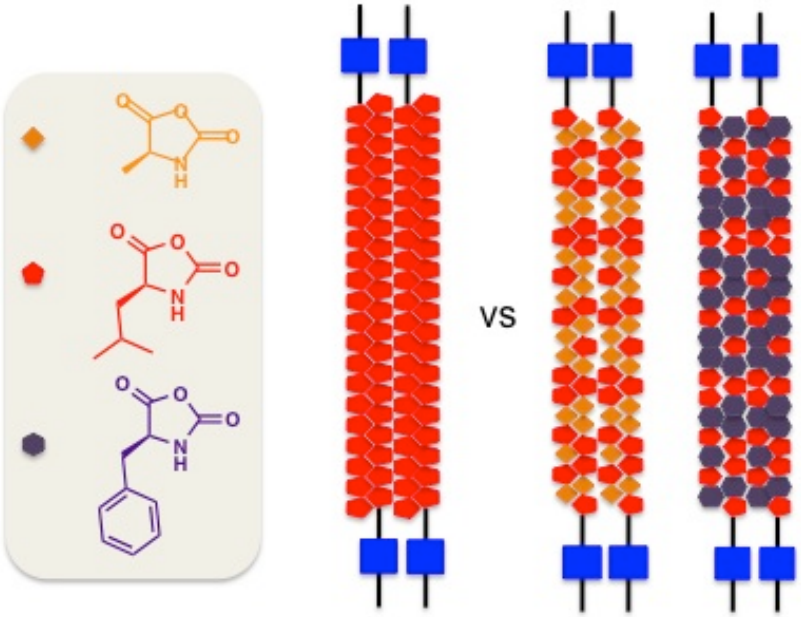

Figure 2.3 Disruption of poly(L-leucine) crystallinity by copolymerization of other hydrophobic residues.

For these studies phenylalanine and alanine were copolymerized with leucine in the hydrophobic domain. Phenylalanine is more hydrophobic and more bulky that leucine and can result in a decrease of the critical aggregation concentration. Alanine is less hydrophobic and small in comparison to leucine and can result in an increase in the critical aggregation

concentration. By fine-tuning the composition of the hydrophobic segment, we expect to alter the vesicle self-assembly and extrudability for more desired diameters for drug delivery.

2.4 Role of Hydrophobic Length on Self-Assembled Nanostructures

Four diblock copolypeptides with different leucine lengths were synthesized ($K_{60}L_{10}$, $K_{60}L_{15}$, $K_{60}L_{20}$, and $K_{60}L_{25}$) and processed into vesicles to investigate the effects of the hydrophobic length on the aggregation properties of the polypeptides. Differential interference contrast (DIC) microscopy was used to image the self-assembled vesicle suspensions of the different block copolypeptides (**Figure 2.4**). Within the range of the hydrophobic segments investigated, all block copolypeptides formed vesicles in the micron-scale range with smaller assemblies not visible my DIC.

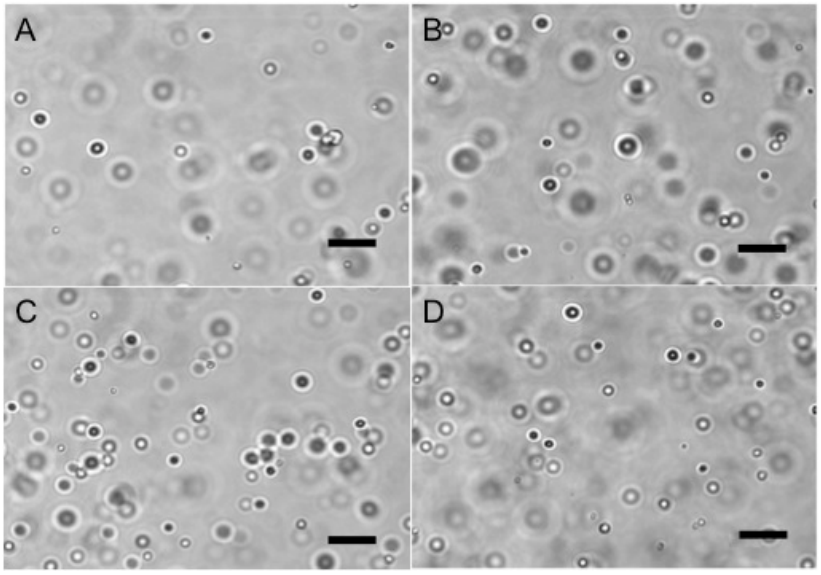

Figure 2.4 DIC images of the processed suspensions of (A) $K_{60}L_{10}$, (B) $K_{60}L_{15}$, (C) $K_{60}L_{20}$, and (D) $K_{60}L_{25}$ (Scale bar = 10 μm).

Images from DIC confirmed the presence of vesicles for both $K_{60}L_{10}$ and $K_{60}L_{20}$. Although we previously found that the $K_{60}L_{10}$ polypeptide predominantly forms micelles, we have found that our improved processing method of using a THF to water ratio of 3:1 leads to the formation of vesicles along with other smaller aggregates. These micelles and small aggregates were present at a much higher concentration in the $K_{60}L_{10}$ suspension than in $K_{60}L_{20}$, as indicated by high magnification TEM images (**Figure 2.5**).

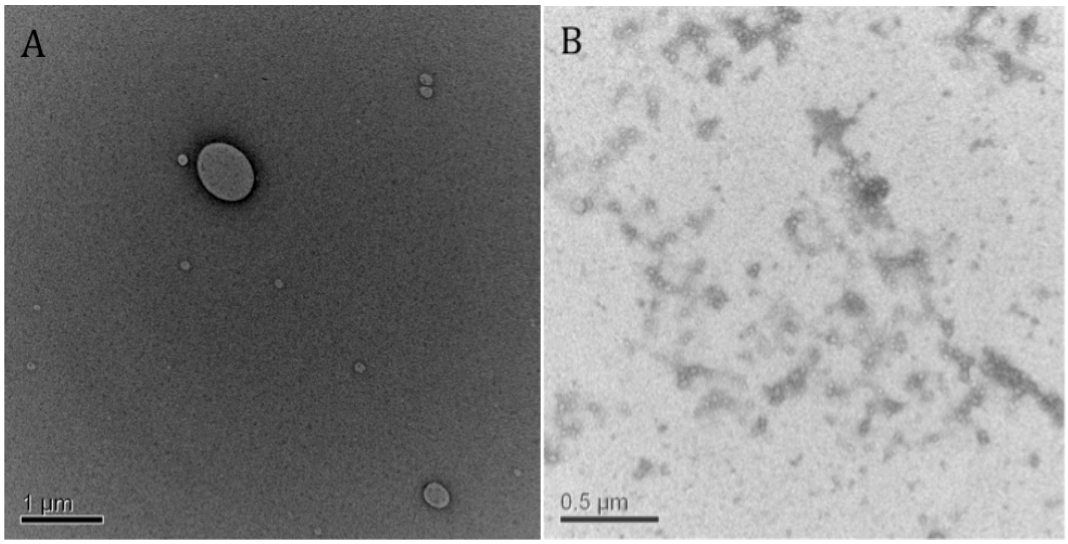

Figure 2.5 TEM images of the processed suspensions of (A) $K_{60}L_{20}$, and (B) $K_{60}L_{10}$.

2.5 Cytotoxicity as a Function of Hydrophobic Length

The effect of the hydrophobic domain length on toxicity was investigated. An increase in cell viability was seen as the length increased from 10 to 20 residues, with a viability plateaus at $K_{60}L_{20}$ for processed suspensions. These results are consistent with our previous report of the poly(L-leucine) α-helix becoming stable at approximately 20 residues.[2] The $K_{60}L_{20}$ and $K_{60}L_{25}$ vesicles were subsequently passed through 1.0, 0.4 and 0.2 µm track-etched polycarbonate (PC)

membranes to compare their sizes after extrusion. A more monodisperse population was yielded by the extrusion of $K_{60}L_{20}$ vesicles, with average diameters closer in size to the final pore size, suggesting that the polyleucine segment of $K_{60}L_{25}$ may be too long and rigid to form small vesicles (**Figure 2.6**).

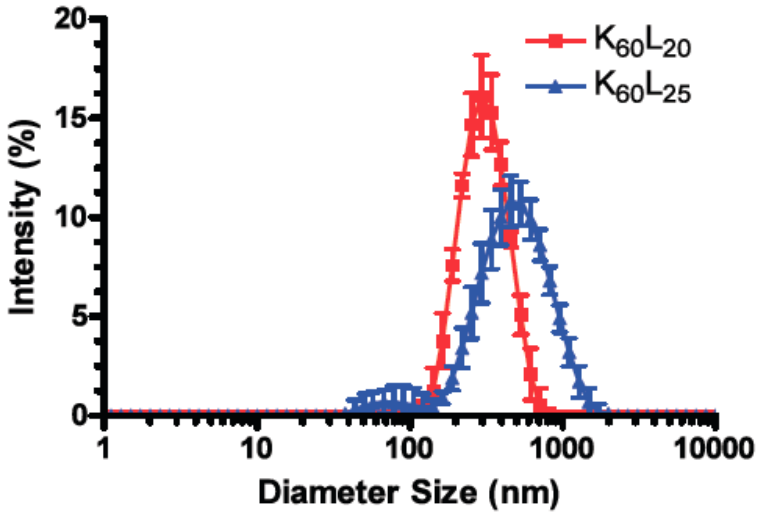

Figure 2.6 Size distributions of the $K_{60}L_{20}$ and $K_{60}L_{25}$ vesicle samples after serial extrusion through PC membranes with 1.0, 0.4, and 0.2 μm pores. Error bars represent the standard deviation from an average of three measurements.

In collaboration, it was found that the hydrophobic chain length does have an impact on cytotoxicity, with vesicles formed from block copolypeptides with shorter hydrophobic blocks being more toxic (**Figure 2.7**). It was hypothesized that the additional cytotoxicity of the shorter hydrophobic blocks is attributed to the presence of micelles and smaller aggregates at higher concentrations within these suspensions.

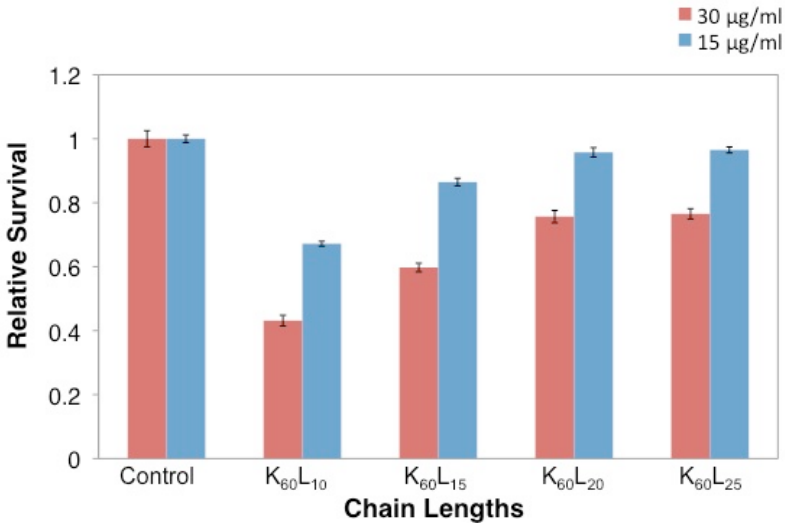

Figure 2.7 5 hr cytotoxicity results of processed vesicle suspensions where the length of the hydrophobic block was varied. Error bars represent the standard deviation from an average of three measurements.

To determine if there were micelles and smaller aggregates present at higher concentrations in processed suspensions, dialysis was performed to separate micelles and small aggregates from the larger vesicle assemblies. After dialysis, concentrations were determined to calculate loss of material attributed to the removal of micelles and smaller aggregates and cytotoxicity was then reexamined for each suspension. The preformed vesicle suspensions were added to a 1,000,000 MWCO dialysis membrane (estimated pore size = 80 nm) and dialyzed in a system where the vesicles were retained in the membrane, while the micelles or small aggregates less than 80 nm in diameter were dialyzed away (**Figure 2.8**).

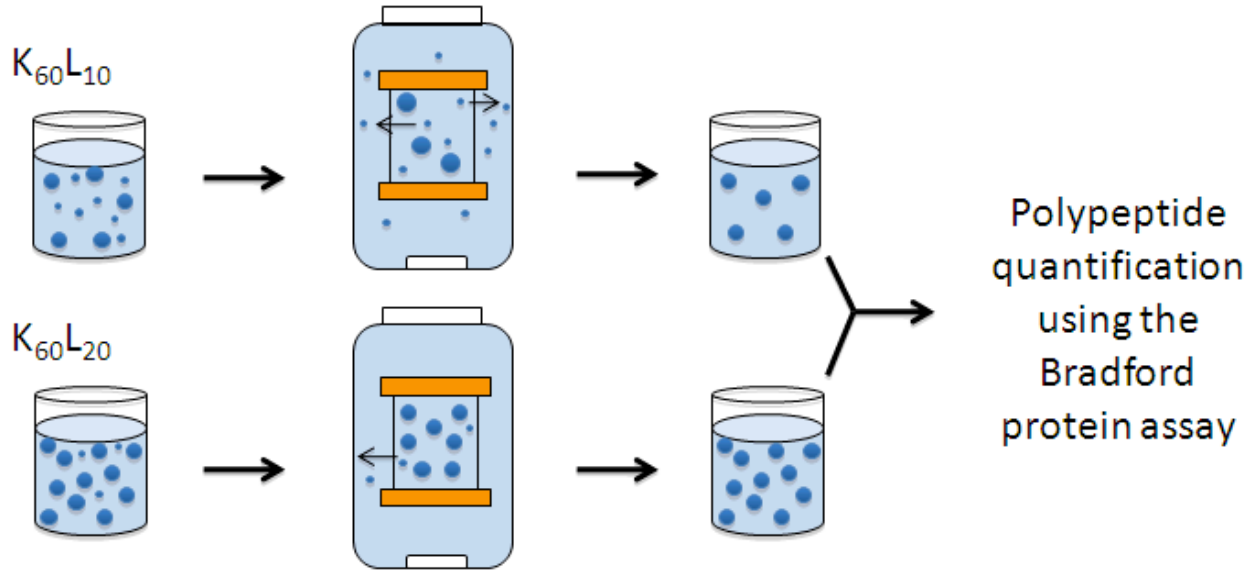

Figure 2.8 Schematic diagram of the purification process for the polypeptide vesicles, followed by quantification using the Bradford protein assay. A 1,000 kDa MWCO membrane was used to dialyze away spherical micelles and small aggregates from the vesicles.

For this experiment, we investigated $K_{60}L_{10}$, the most toxic polypeptide suspension, and $K_{60}L_{20}$, the least toxic polypeptide suspension. The amount of polypeptide was determined before and after the dialysis treatment. The Bradford assay revealed a decrease in the overall amount of polypeptide for both $K_{60}L_{10}$ and $K_{60}L_{20}$, verifying the existence of micelles and small aggregates (<80 nm) in both samples prior to dialysis (**Figure 2.9**a). Furthermore, less polypeptide was retained for the $K_{60}L_{10}$ suspension after dialysis, which correlates with the observations from the TEM images that the $K_{60}L_{10}$ had more micelles within the population. The toxicities were then investigated with the dialyzed samples to see if the removal of micelles and smaller aggregates decreased the toxicity. As shown in **Figure 2.9**b, $K_{60}L_{20}$ vesicle suspension, which had the micelles and aggregates removed by dialysis, demonstrated a lower toxicity than the $K_{60}L_{20}$ vesicle solution that did not undergo dialysis purification. This result implies that the vesicles are

less toxic than micelles and smaller aggregates of the same polypeptide sample. For the case of $K_{60}L_{10}$, the effect of the dialysis treatment was not apparent.

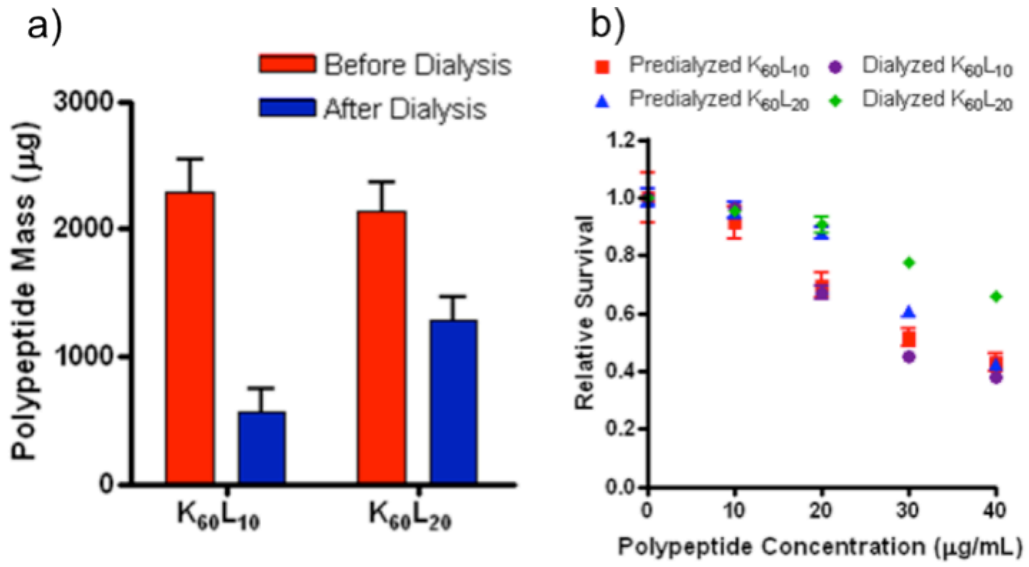

Figure 2.9 Purification of processed vesicle solutions with dialysis using a 1,000 kDa MWCO membrane. (a) Amount of copolypeptide in each sample after dialysis. (b) 5 hr cytotoxicity of dialyzed and predialyzed vesicles. Error bars represent the standard deviation from an average of three measurements.

2.6 Vesicle Self-Assembly and With Varied Hydrophobic Composition

The composition of the hydrophobic domain was varied by the copolymerization of different NCA residues to test affects on vesicle self-assembly, stability and extrudability. The resulting amphiphilic block copolypeptides were synthesized, poly(L-lysine)$_{60}$-*block*-poly(L-leucine$_{0.5}$-*co*-L-alanine$_{0.5}$)$_{20}$ and poly(L-lysine)$_{60}$-*block*-poly(L-leucine$_{0.5}$-*co*-L-phenylalanine$_{0.5}$)$_{20}$, $K_{60}(L_{0.5}/A_{0.5})_{20}$ and $K_{60}(L_{0.5}/F_{0.5})_{20}$ respectively (**Figure 2.10**).

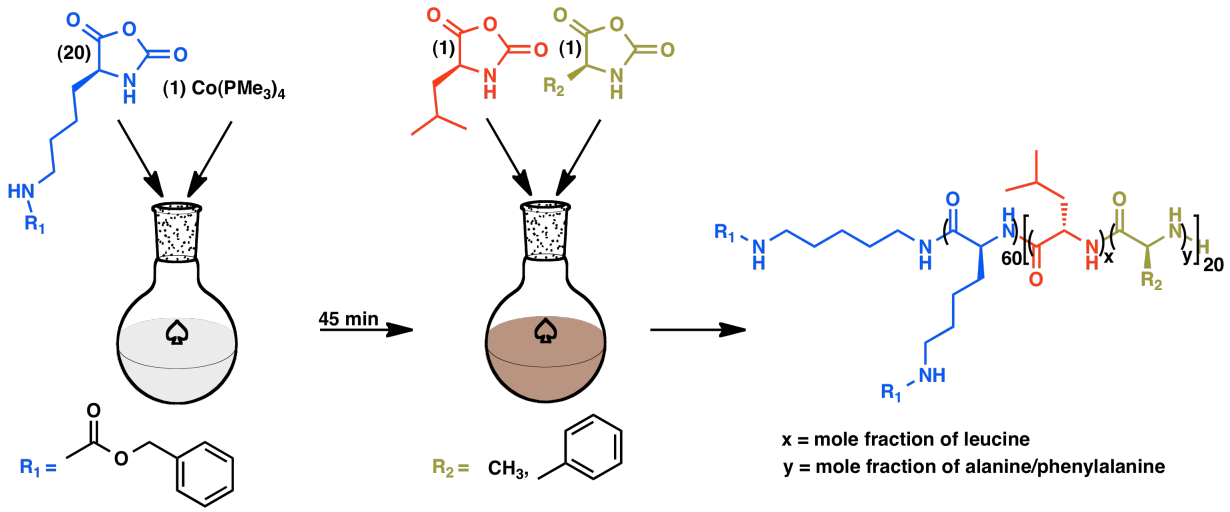

Figure 2.10 Schematic diagram of copolymerization of the hydrophobic domain.

After preparation of the block copolypeptides, the critical aggregation concentration (CAC) was determined using pyrene fluorescence. It was believed that the CAC would decrease with the incorporation of the more hydrophobic phenylalanine but it showed a slight increase. Overall, varying the composition of the hydrophobic domain did not drastically change the CAC.

Table 2.1 Characterization of $K_{60}L_{20}$, $K_{60}(L_{0.5}/F_{0.5})_{20}$, and $K_{60}(L_{0.5}/A_{0.5})_{20}$ diblock copolypeptides

Block Copolypeptide	M_n[a]	M_w/M_n[a]	Found Composition[b]	CAC (M)[c]
$(Z)K_{60}L_{20}$	15,710	1.18	$(Z)K_{60}L_{20}$	6.7×10^{-7}
$(Z)K_{60}(L_{0.5}/F_{0.5})_{20}$	17,690	1.09	$(Z)K_{67}(L_{0.4}/F_{0.6})_{18}$	9.5×10^{-7}
$(Z)K_{60}(L_{0.5}/A_{0.5})_{20}$	17,690	1.09	$(Z)K_{67}(L_{0.45}/A_{0.55})_{20}$	6.8×10^{-7}

[a]Hydrophilic segment lengths (average number molecular weight, M_n, for (Z)K segments) and polydispersities (M_w/M_n) determined using gel permeation chromatography. [b]Calculated using ^{1}H NMR. [c]Critical aggregation concentration (CAC) values were determined using pyrene fluorescence at 20 °C.

The polypeptides were processed and the suspensions were extruded through 200 nm pore size, nuclear track etched PC filters to test the extrudability of the vesicles. The extruded suspensions were analyzed by DLS to determine average assembly diameters (**Table 2.2** and **Figure 2.11**). Validating the design of the hydrophobic domain, both polypeptide vesicle suspensions, $K_{60}(L_{0.5}/F_{0.5})_{20}$ and $K_{60}(L_{0.5}/A_{0.5})_{20}$, were extruded to sizes below 200 nm in diameter. The copolymerization in the hydrophobic domain greatly enhances vesicle membrane flexibility and extrudability. Likewise, it is also notable that these samples could be extruded using much less pressure compared to $K_{60}L_{20}$ based vesicles.

Table 2.2 Characterization of $K_{60}L_{20}$, $K_{60}(L_{0.5}/F_{0.5})_{20}$, and $K_{60}(L_{0.5}/A_{0.5})_{20}$ diblock copolypeptides

Block Copolypeptide	**Size**[a]	**Pdi**[a]
$K_{60}(L_{0.5}/F_{0.5})_{20}$	180	0.213
$K_{60}(L_{0.5}/A_{0.5})_{20}$	137	0.253

[a]Size and Pdi determined by dynamic light scattering using Malvern Zetasizer Nano. Size = Z-average (d.nm).

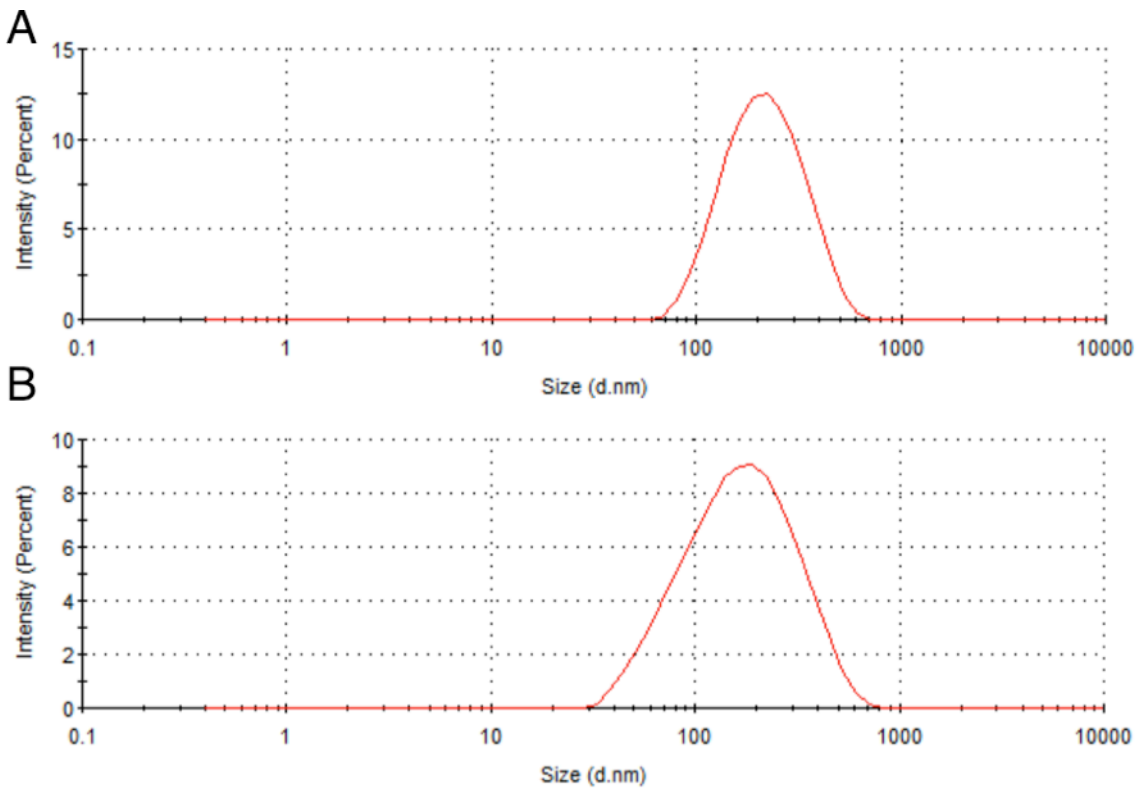

Figure 2.11 DLS data of (A) $K_{60}(L_{0.5}/F_{0.5})_{20}$ and (B) $K_{60}(L_{0.5}/A_{0.5})_{20}$ vesicle suspensions extruded.

2.7 Conclusion

It was found that varying the hydrophilic/hydrophobic ratio of the lysine-leucine block copolypeptides affects the polypeptide's ability to form nontoxic vesicles with controllable sizes. Polypeptides containing longer leucine segments formed vesicles that were less toxic than vesicles formed from polypeptides with shorter leucine segments. Purification of vesicle suspensions, DLS and TEM revealed the presence of more toxic micelles and small aggregates formed by polypeptides with shorter hydrophobic domains. The presence of micelles is attributed to the unstable α-helical structure of the short leucine segments.

Although longer hydrophobic segments of leucine formed stable vesicles that have reduced toxicity, the ability to consistently extrude the samples below 200 nm has been a challenge. The copolymerization of phenylalanine and alanine (both favoring α-helical conformations) with leucine allowed the preparation of vesicles that were extruded below 200 nm with low polydispersities. These studies have shown that by fine-tuning the hydrophilic/hydrophobic ratio and varying the hydrophobic composition, vesicles can be obtained with more suitable properties for drug delivery applications.

2.8 Experimental

2.8.1 General Methods and Materials:

Dry tetrahydrofuran (THF), hexane and diethyl ether were prepared by passage through alumina columns, and oxygen was removed by purging with nitrogen prior to use.[8] Perkin Elmer RX1 FTIR Spectrophotometer was used for recording infrared spectra. ^{1}H NMR spectra were recorded on a Bruker AVANCE 400 MHz spectrometer. Ultrapure (18 MΩ) water was obtained from a Millipore Milli-Q Biocel A10 purification unit. HeLa cell lines were obtained from the American Type Culture Collection (Manassas, Virginia). Minimum essential medium (MEM) with Earl's balanced salt solution, penicillin-streptomycin, sodium pyruvate, phosphate-buffered saline (PBS), and 0.25% trypsin with ethylenediaminetetraacetic acid (EDTA) were purchased from Invitrogen (Carlsbad, California). Fetal bovine serum (FBS) was obtained from Hyclone (Waltham, Massachusetts). The MTS cell proliferation assay kit was purchased from Promega (Madison, Wisconsin). The Bradford reagent was obtained from Bio-Rad (Hercules, California). Dialysis membranes were purchased from Spectrum Laboratories, Inc (Rancho Dominguez,

California). All other tissue culture reagents and chemicals were purchased from Sigma-Aldrich (St. Louis, Missouri).

2.8.2 Synthesis:

All α-amino acid-*N*-carboxyanhydride (NCA) monomers were synthesized using previously described protocols.[9,10] L-Phenylalanine, L-leucine, L-alanine and N_ε-carboxybenzyl-L-lysine *N*-carboxyanhydrides were synthesized by phosgenation in dry THF under inert atmosphere at 40 °C and purified by recrystallization within a glovebox to remove HCl and other impurities.

2.8.3 Synthesis of Poly(N_ε-benzyloxycarbonyl-L-lysine)$_{60}$-*block*-Poly(L-leucine)$_{20,}$ (Z)$K_{60}L_y$ (y = 10, 15, 20, 25):

$K_{60}L_y$ block copolypeptides were synthesized maintaining the lysine domain at 60 residues, while varying the size of the leucine domain (y) from 10 to 25 residues in increments of 5. Under nitrogen atmosphere, N_ε-carboxybenzyl-L-lysine-N-carboxyanhydride (Z-Lys NCA) (1.0 g, 3.3 mmol) was dissolved in THF (20 mL) in a 100 mL round bottom flask with a stir bar. A $(PMe_3)_4Co$ initiator solution (2.6 mL of a 55 mM solution in THF) was then added to the flask via syringe. The flask was sealed and allowed to stir in for 45 minutes at 25 °C. After 45 minutes, an aliquot (50 μL) was removed and analyzed by FTIR to confirm that all the Z-lys NCA was consumed. The aliquot was diluted to a concentration of 5 mg/mL in DMF containing 0.1 M LiBr for GPC/LS analysis (M_n =15,710; M_w/M_n = 1.18). The living poly(N_ε-Z-L-lysine) reaction mixture was divided into four equivalent aliquots and the respective amounts of L-leucine-N-carboxyanhydrides (Leu-NCA) (430 μL, 640 μL, 855 μL, 1070 μL of 320 mM solution in THF) was added to give the desired diblock copolypeptide amphiphiles $K_{60}L_{10}$,

$K_{60}L_{15}$, $K_{60}L_{20}$, $K_{60}L_{25}$. The number of the leucine residues was checked using ^{1}H NMR and GC (Actual compositions $K_{60}L_9$, $K_{60}L_{13}$, $K_{60}L_{18}$, $K_{60}L_{25}$).

Table 2.3 Properties of the $K_{60}L_y$ block copolypeptides.

Copolypeptide	Actual Composition[a]
$K_{60}L_{10}$	$K_{60}L_9$
$K_{60}L_{15}$	$K_{60}L_{13}$
$K_{60}L_{20}$	$K_{60}L_{18}$
$K_{60}L_{25}$	$K_{60}L_{25}$

[a]Determined by integration of proton peaks using ^{1}H NMR.

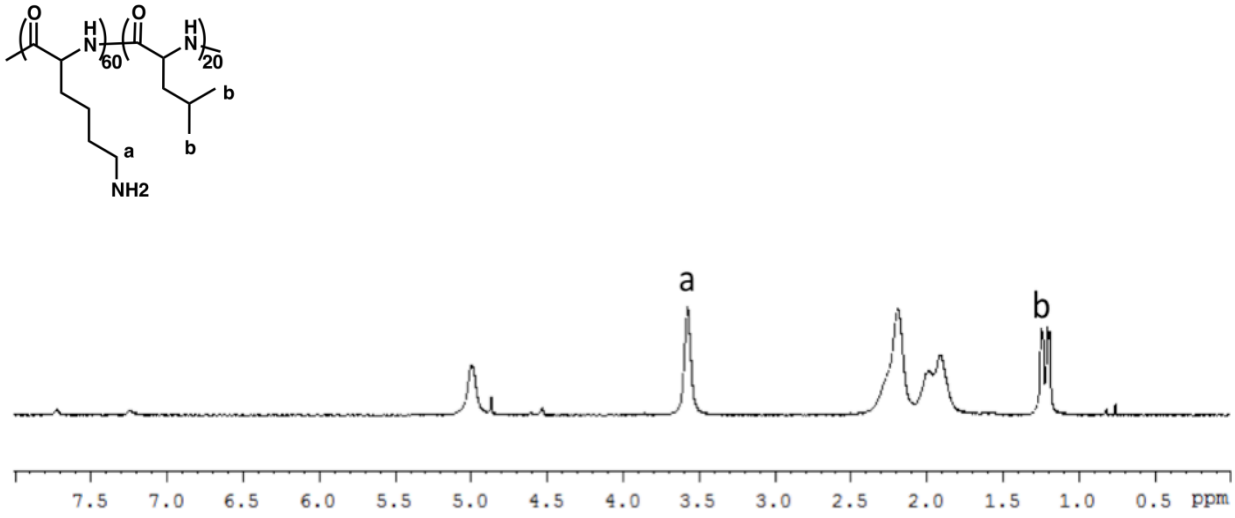

Figure 2.12 ^{1}H NMR spectrum of $K_{60}L_{20}$ dissolved in deuterated trifluoroacetic acid (*d*-TFA). (a) lysine methylene resonance, and (b) leucine methyl resonances.

2.8.4 Poly(L-lysine-HCl)$_{60}$-*block*-Poly(L-leucine)$_y$, $K_{60}L_y$ (y = 10, 15, 20, 25):

A 100 mL round-bottom flask was charged with (Z)$K_{60}L_y$ (y = 10, 15, 20, 25) (250 mg) and TFA (10 mL) and a stir bar. The flask was placed in an ice bath and allowed to stir until polymer was completely dissolved and the flask was cooled to 0 °C. At this point, HBr (800 μL of 33 %

solution in HOAc, 5 equivalents to (Z)-Lysine) was added to the solution and was allowed to stir in the ice bath for 1 hour. Diethyl ether (30 mL) was added to precipitate the polymer. The product was isolated by centrifugation and was washed with ether twice more before resuspending in water. The solution was placed in a dialysis bag (MWCO = 2000 Da) and dialyzed against aqueous disodium EDTA (3 mM, 2 days), then aqueous HCl and NaCl (10 mM, 10 mM, 2 days), followed by water (2 days) before lyophilization to give a fluffy white powder.

2.8.5 Synthesis of Poly(N_ε-benzyloxycarbonyl-L-lysine)$_{60}$-*block*-Poly(L-leucine$_{0.5}$-*co*-L-alanine$_{0.5}$)$_{20}$ and Poly(N_ε-benzyloxycarbonyl-L-lysine)$_{60}$-*block*-Poly(L-leucine$_{0.5}$-*co*-L-phenylalanine$_{0.5}$)$_{20}$, (Z)K$_{60}$(L$_{0.5}$/A$_{0.5}$)$_{20}$ and (Z)K$_{60}$(L$_{0.5}$/F$_{0.5}$)$_{20}$:

Under nitrogen atmosphere, N_ε-benzyloxycarbonyl-L-lysine-N-carboxyanhydride (Z-Lys NCA) (500 mg, 1.6 mmol) was dissolved in THF (10 mL) in a 20 mL scintillation. A $Co(PMe_3)_4$ initiator solution (1.5 mL of a 52 mM solution in THF) was then added to the vial via syringe. The vial was sealed and allowed to stir in for 45 minutes at 25 °C. After 45 minutes, an aliquot (50 μL) was removed and analyzed by FTIR to confirm that all the Z-lys NCA was consumed. The aliquot was diluted to a concentration of 5 mg/mL in DMF containing 0.1 M LiBr for GPC/LS analysis (Mn =17,690; M_w/M_n = 1.09). The living poly(N_ε-Z-L-lysine) reaction mixture was divided into two equivalent amounts in two 20 mL scintillation vials and the respective mixtures, L-leucine-N-carboxyanhydrides (Leu-NCAs) and L-alanine-N-carboxyanhydrides (Ala-NCAs) (20 mg, 0.13 mmol Leu NCA and 15 mg, 0.13 mmol Ala NCA dissolved in 700 μL of THF) and L-leucine-N-carboxyanhydrides (Leu-NCAs) and L-phenylalanine-N-carboxyanhydrides (Phe-NCAs) (20 mg, 0.13 mmol Leu NCA and 25 mg, 0.13 mmol Phe NCA

dissolved in 900 μL of THF) were added to give the desired diblock copolypeptide amphiphiles, $(Z)K_{67}(L_{0.45}/A_{0.55})_{20}$ and $(Z)K_{67}(L_{0.4}/F_{0.6})_{18}$.

2.8.6 Poly(L-lysine-HCl)$_{60}$-*block*-Poly(L-leucine$_{0.5}$-*co*-L-alanine$_{0.5}$)$_{20}$ and Poly(L-lysine-HCl)$_{60}$-*block*-Poly(L-leucine$_{0.5}$-*co*-L-phenylalanine$_{0.5}$)$_{20}$, $K_{60}(L_{0.5}/A_{0.5})_{20}$ and $K_{60}(L_{0.5}/F_{0.5})_{20}$:

A 20 mL scintillation vial was charged with $(Z)K_{60}(L_{0.5}/A_{0.5})_{20}$ or $(Z)K_{60}(L_{0.5}/F_{0.5})_{20}$ (250 mg) and TFA (8 mL) and a stir bar. The vial was placed in an ice bath and allowed to stir until polymer was completely dissolved and the flask was cooled to 0 °C. At this point, HBr (720 μL of 33 % solution in HOAc, 5 equivalents to (Z)-Lysine) was added to the solution and was allowed to stir in the ice bath for 1 hour. Diethyl ether (30 mL) was added to precipitate the polymer. The product was isolated by centrifugation and was washed with ether twice more before resuspending in water. The solution was placed in a dialysis bag (MWCO = 2000 Da) and dialyzed against aqueous disodium EDTA (3 mM, 2 days), then aqueous HCl and NaCl (10 mM, 10 mM, 2 days), followed by water (2 days) before lyophilization to give a fluffy white powder.

2.8.7 Preparation of Diblock Copolypeptide Assemblies in Water:

Solid copolypeptide powder ($K_{60}L_y$ (y = 10, 15, 20, and 25), $K_{60}(L_{0.5}/A_{0.5})_{20}$, or $K_{60}(L_{0.5}/F_{0.5})_{20}$) was dispersed in THF to give a 4 % (w/v) suspension, which was then placed in a bath sonicator for 30 minutes until the copolypeptides were evenly dispersed. An equal volume of Millipore water was added to the suspension and place in a bath sonicator for 30 minutes. An equal volume of THF was then added to the suspension in four equivalent aliquots with vortexing in between each addition to give a final concentration of 1 % (w/v) copolypeptides suspension in 3:1 ratio of THF to water. The suspension was placed in a dialysis bag (MWCO = 2000 Da) and dialyzed against Millipore water for 24 hours. The water was changed every hour for the first 4 hours. The

next day, the suspension was collected and imaged using the Zeiss Axiovert 200 DIC/Fluorescence Inverted Optical Microscope (Carl Zeiss Inc., Thornwood, New York) to confirm the formation of the vesicles.

2.8.8 Extrusion of Vesicles Suspensions:

Aqueous vesicles suspensions of $K_{60}L_y$ (y = 10, 15, 20, and 25), $K_{60}(L_{0.5}/A_{0.5})_{20}$, or $K_{60}(L_{0.5}/F_{0.5})_{20}$ samples, 0.2 % (w/v), were extruded using an Avanti Mini-Extruder. Extrusions were performed using different pore size Whatman Nucleopore Track-Etched polycarbonate (PC) membranes (1.0 μm, 0.8 μm, 0.4 μm, 0.2 μm). The PC membranes and support membranes were soaked in Millipore water for 10 minutes prior to extrusion.

2.8.9 Transmission Electron Microscopy (TEM):

$K_{60}L_{10}$ and $K_{60}L_{20}$ copolypeptide suspensions (0.1 % w/v) were processed into vesicles as described above. One drop of each respective sample was placed on a sheet of parafilm, and a carbon coated copper grid was placed on the droplet and allowed to sit for 90 seconds. Filter paper was then used to remove the residual sample and liquid. One drop of 2 % w/v uranyl acetate (negative stain) was then placed on parafilm, and the grid was placed on the droplet and allowed to stand for 30 seconds. Excess liquid was removed by wicking away with filter paper. The resulting samples were imaged using a JEM1200-EX transmission electron microscope (JOEL, Tokyo) at 80 keV and ambient temperature.

2.8.10 Cell Culture:

The HeLa cell line is a human cervical cancer cell line widely used in scientific research. These cells were maintained in MEM supplemented with 26.2 mM sodium bicarbonate, 10 % v/v FBS,

100 units mL^{-1} penicillin, 100 μg mL^{-1} streptomycin, and 1 mM sodium pyruvate at a pH of 7.4 in a 37ºC humidified atmosphere with 5 % CO_2.

2.8.11 Toxicity Assay:

MTS cell proliferation assay was performed according to the manufacture-supplied instructions. Briefly, HeLa cells were seeded onto a 48-well tissue culture plate at 40,000 cells/cm^{-2} and incubated overnight in a 37 ºC humidified atmosphere with 5 % Co_2. The next day the media was aspirated off for each well, and the cells were incubated with 250 μL of fresh media containing different concentrations of vesicles for 5 hours. Afterwards, the media was aspirated, followed by an addition of 250 μL of media and 50 μL of MTS reagent to each well. The cells were then place a 37 °C air incubator for 1 hour and absorbance of each well was measured with an Infinite F200 plate reader (Tecan Systems Inc., San Jose, California) at 490 nm (A_{490}). The background absorbance was also read at 700 nm (A_{700}) and subtracted from A_{490}. The relative survival of cells relative to the control was calculated by taking the ratio of the ($A_{490}B - A_{700}$) values.

2.8.12 Vesicle Purification and Quantification:

Vesicle suspensions of either $K_{60}L_{10}$ or $K_{60}L_{20}$ were dialyzed against sterile Milli-Q water using a MWCO = 1,000 kDa membrane (estimated pore diameter = 80 nm)[11] in order to purify the vesicles from the micelles and small aggregates (Figure 2). The dialysis was conducted overnight with four water changes using sterile Milli-Q water, and the contents inside the dialysis bag were collected the next day. After dialysis, the concentration of polypeptide in each dialysis bag was quantified using the Bradford protein assay, according to the manufacture-supplied instructions, using the pre-dialyzed vesicles as the standard.

2.8.13 Vesicle Stability Assay:

The stability of the $K_{60}L_{10}$ and $K_{60}L_{20}$ vesicles was assessed in the presence of ethanol. Vesicle suspensions (0.2 % w/v) were subjected to an equal volume of ethanol, and the resulting samples were allowed to stand for 30 min. The mixtures were then examined using differential interference contrast (DIC) optical microscopy.

2.9 Spectral Data:

^{1}H-NMR spectra of polypeptides in *d*-TFA

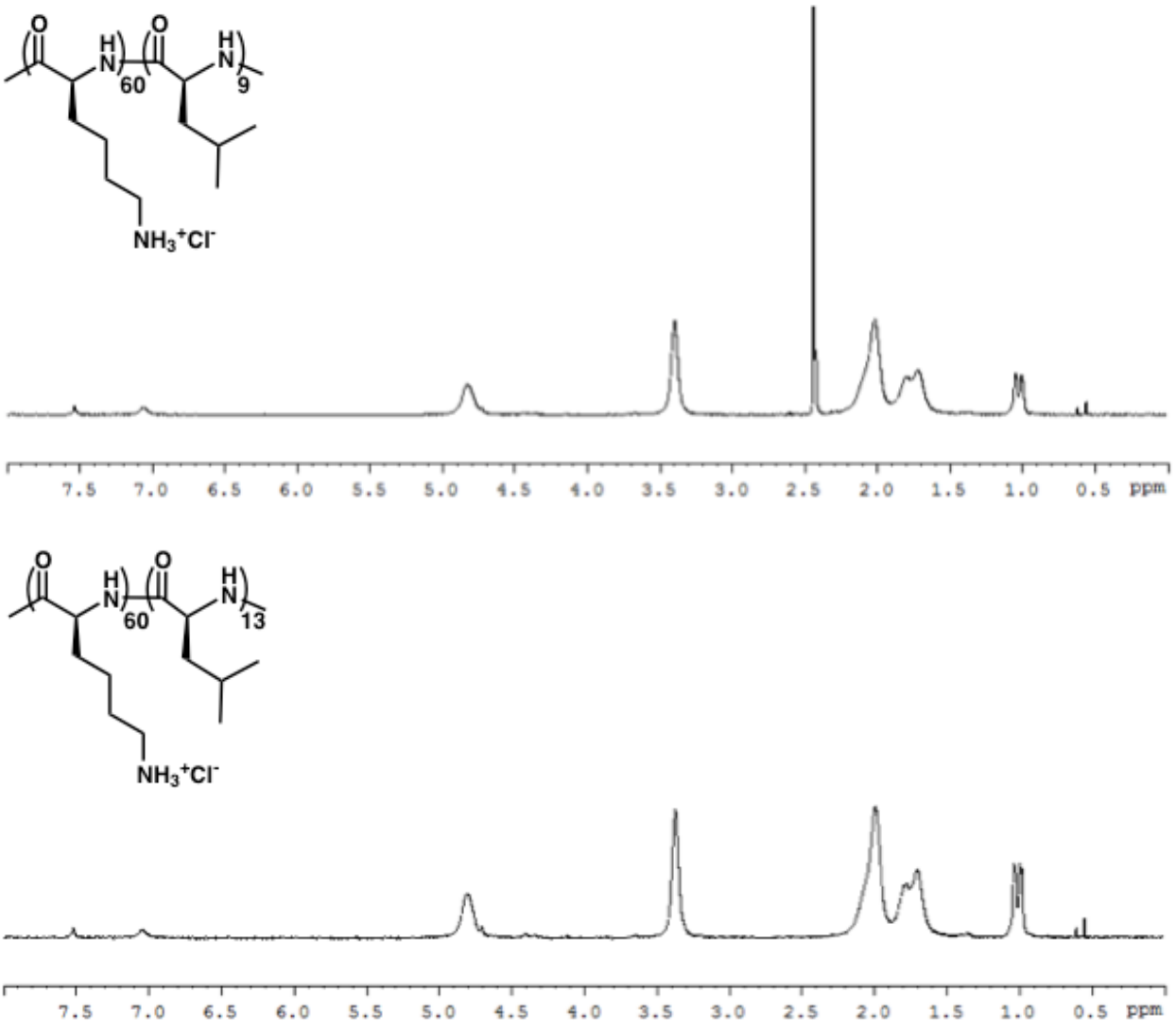

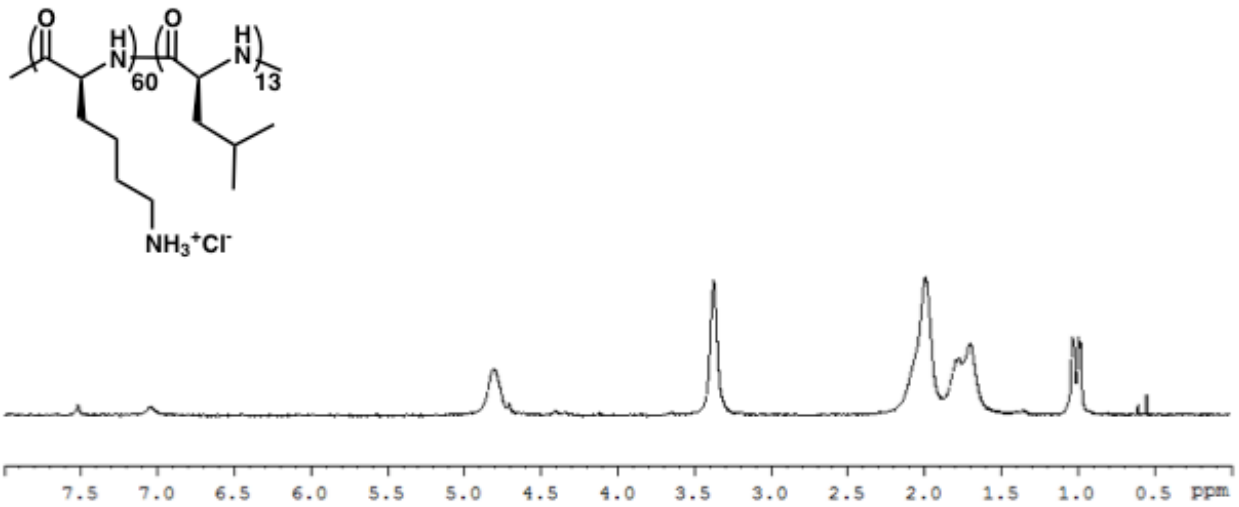
O
H
N
60
O
H
N
13
NH3+Cl-
7.5 7.0 6.5 6.0 5.5 5.0 4.5 4.0 3.5 3.0 2.5 2.0 1.5 1.0 0.5 ppm

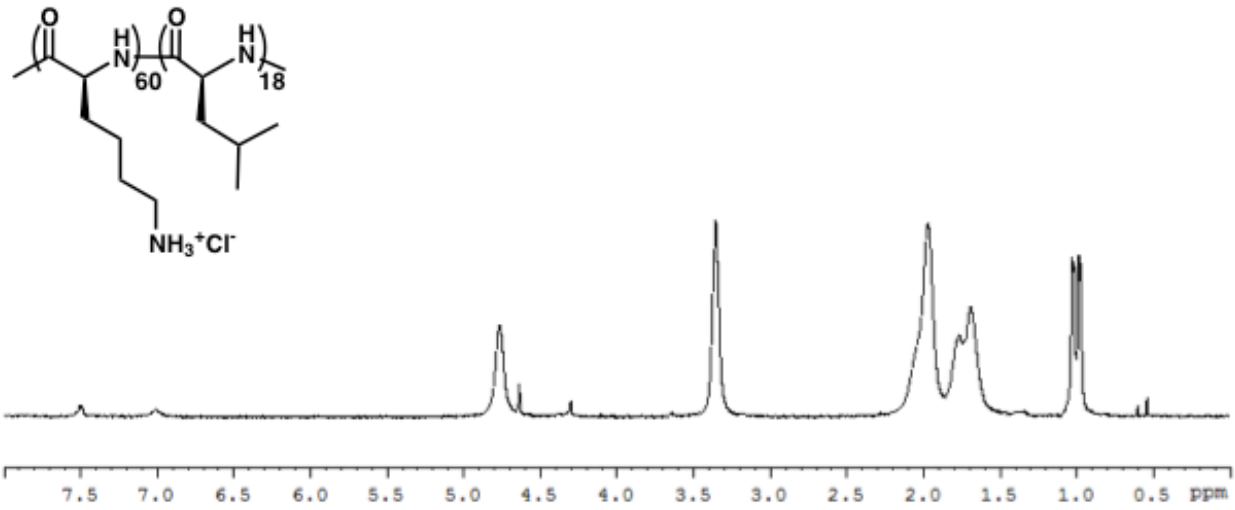
O
H
N
60
O
H
N
18
NH3+Cl-
7.5 7.0 6.5 6.0 5.5 5.0 4.5 4.0 3.5 3.0 2.5 2.0 1.5 1.0 0.5 ppm

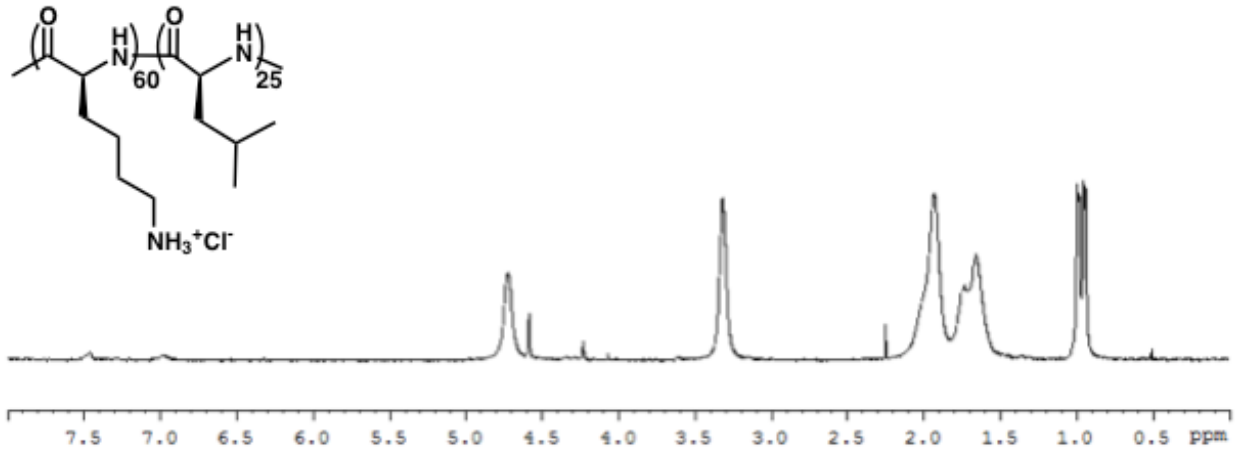
O
H
N
60
O
H
N
25
NH3+Cl-
7.5 7.0 6.5 6.0 5.5 5.0 4.5 4.0 3.5 3.0 2.5 2.0 1.5 1.0 0.5 ppm

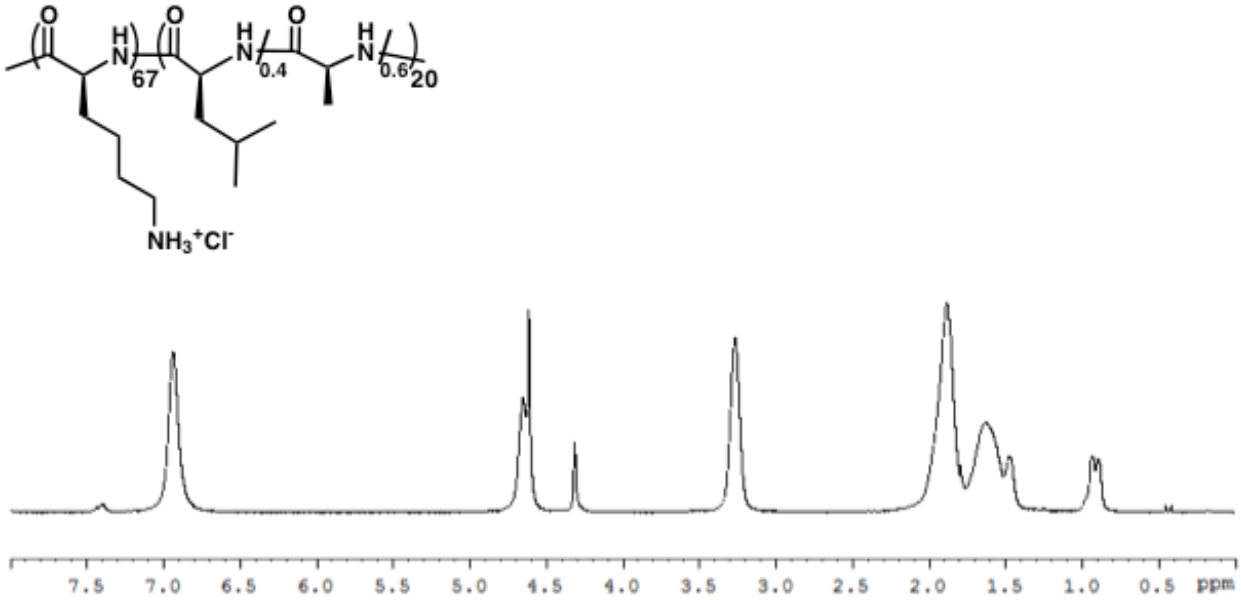

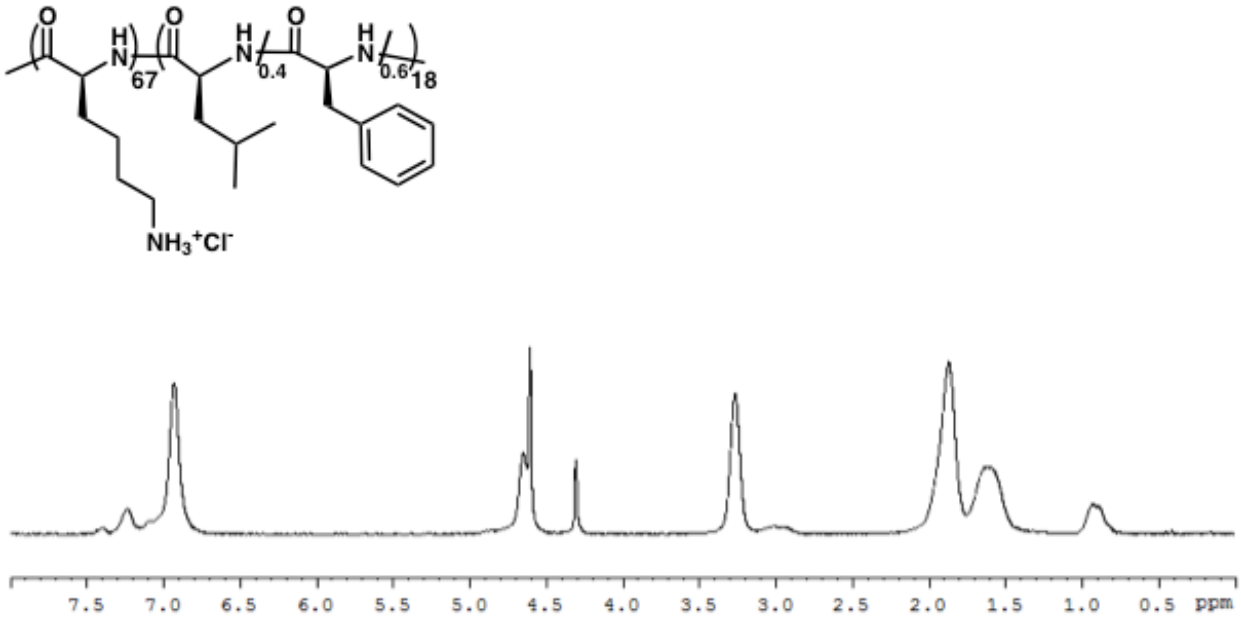

2.10 References

(1) Holowka, E. P.; Pochan, D. J.; Deming, T. J. *Journal of the American Chemical Society* **2005**, *127*, 12423.

(2) O'Shea, E. K.; Rutkowski, R.; Kim, P. S. *Science* **1989**, *243*, 538.

(3) Deming, T. J. *Advanced Materials* **1997**, *9*, 299.

(4) Deming, T. J. *Advanced Drug Delivery Reviews* **2002**, *54*, 1145.

(5) Kricheldorf, H. R. *Angewandte Chemie International Edition* **2006**, *45*, 5752.

(6) Discher, B. M.; Won, Y.-Y.; Ege, D. S.; Lee, J. C.-M.; Bates, F. S.; Discher, D. E.; Hammer, D. A. *Science* **1999**, *284*, 1143.

(7) Discher, D. E.; Eisenberg, A. *Science* **2002**, *297*, 967.

(8) Pangborn, A. B.; Giardello, M. A.; Grubbs, R. H.; Rosen, R. K.; Timmers, F. J. *Organometallics* **1996**, *15*, 1518.

(9) Breedveld, V.; Nowak, A. P.; Sato, J.; Deming, T. J.; Pine, D. J. *Macromolecules* **2004**, *37*, 3943.

(10) Fuller, W. D.; Verlander, M. S.; Goodman, M. *Biopolymers* **1976**, *15*, 1869.

(11) Porter, M. C. *Handbook of industrial membrane technology*; Noyes Publications: Park Ridge, N.J., U.S.A., 1990.

CHAPTER THREE

Fine Tuning of Vesicle Assembly and Properties Using Dual Hydrophilic Triblock

3.1 Abstract

Block copolymer vesicles are being developed as carriers for therapeutic drugs and diagnostic molecules. Here, we report the design, synthesis and self-assembly of the first dual hydrophilic triblock copolypeptide vesicles, $R^{H}_{m}E_{n}L_{o}$ and $K^{P}_{m}R^{H}_{n}L_{o}$. In these materials, variation of the two distinct hydrophilic domains was used to optimize cellular interactions while maintaining self-assembly properties. The self-assembly of these block copolypeptides in water was studied, and their structures determined using optical microscopy and dynamic light scattering. Cell culture studies were used to evaluate cytotoxicity as well as intracellular uptake of the vesicles. The ability of polypeptides to incorporate ordered chain conformations that guide self-assembly, as well as the ability to readily prepare functional, multiblock copolypeptide sequences of defined lengths allowed the preparation of vesicles with a promising combination of decreased cytotoxicity and retention of cell uptake ability that makes them attractive for development as drug carriers.

3.2 Introduction

There has been an abundance of research in recent years on polymeric vesicles as drug carriers.[1,2] These materials can exhibit greater stability and incorporate additional levels of

functionality compared to conventional lipid or surfactant based carriers, and thus show great promise for encapsulation and delivery applications. Incorporation of functionality can be challenging since many vesicle forming systems have limited capability for modification, and once functionalized, finely balanced self assembly properties may be significantly altered or impaired.[1,2] Hence, there is a need for amphiphilic polymers that can be readily prepared with tunable chemical composition and structure, using building blocks that are biocompatible and readily functionalized. We have been studying polypeptide amphiphiles since these materials are reproducibly prepared metal and pyrogen free in large quantities, chain lengths and compositions are easily controlled, they allow facile incorporation of bioactive functionality in amino acid monomers, and, most importantly, their chain conformations can be used to guide assembly into vesicles independent of many other parameters.[3-5] Here, we report the use of dual hydrophilic segments in triblock copolymers to tune the cytotoxicity and cellular uptake of polypeptide vesicles.

Previously, we and others reported that diblock copolypeptides containing hydrophilic and α-helical hydrophobic segments assemble in water to form spherical, unilamellar vesicles ranging in diameter from tens of nanometers to tens of microns.[3-8] While nonionic, purely α-helical copolypeptides, e.g. poly(N_ε-2-(2-(2-methoxyethoxy)ethoxy)acetyl-L-lysine)$_{100}$-*block*-poly(L-leucine)$_{20}$ ($K^P_{100}L_{20}$), gave micron sized vesicles with rigid membranes,[5] samples with charged hydrophilic domains, e.g. poly(L-lysine-HCl)$_{60}$-*block*-poly(L-leucine)$_{20}$ ($K_{60}L_{20}$) or poly(L-glutamate-Na)$_{60}$-*block*-poly(L-leucine)$_{20}$ ($E_{60}L_{20}$), gave vesicles with flexible membranes that could be extruded to diameters down to *ca*. 100 nm.[4] Vesicles of this size are potentially useful for drug delivery via the blood circulation, where they can take advantage of the enhanced permeability and retention (EPR) effect for passive targeting to tumors.[9] Functionality for cell

uptake was introduced into these charged vesicles by using poly(L-arginine), R, or poly(L-homoarginine), R^H, in place of the lysine or glutamate segments, i.e. $R_{60}L_{20}$ or $R^H_{60}L_{20}$ respectively.[3] These polyguanidinium segments served as hydrophilic domains to promote vesicle formation, and also added functionality to bind to cell surfaces and promote non-specific cellular uptake similar to the cell penetrating ability found in the HIV TAT peptide sequence.[10]

While the $R_{60}L_{20}$ and $R^H_{60}L_{20}$ vesicles are promising for drug delivery applications, their highly cationic nature can make them cytotoxic at higher concentrations,[3] which limits the doses that could potentially be administered. Consequently, we wanted to redesign these copolypeptides to reduce their cytotoxicity while retaining the polyguanidinium functionality for cell uptake. We had observed that cytotoxicity of polypeptide vehicles can be essentially eliminated by simply replacing cationic polyguanidinium with anionic poly-L-glutamate, E, or uncharged pegylated poly-L-lysine, K^P, segments.[11] However, complete replacement of the polyguanidinium segments in the vesicles also removes their ability to be taken up by cells.[3] In order to retain some guanidinium residues for cell uptake, yet make the majority of the hydrophilic domain anionic or uncharged to minimize cytotoxicity, we prepared triblock copolypeptides containing two distinct hydrophilic segments. Other "dual hydrophilic" triblock copolymer vesicles have been prepared previously,[12-14] but differ from our strategy by having each hydrophilic segment on opposite sides of the hydrophobic domain. Here, we have prepared the first dual hydrophilic triblock copolypeptide vesicles, where both hydrophilic segments are on the same sides of the membranes. Since it is known that individual polyguanidine segments of *ca*. 6 to 9 residues in length are sufficient to promote cellular uptake,[10] we designed the triblock copolypeptides poly(L-homoarginine·HCl)$_m$-*block*-poly(L-glutamate·Na)$_n$-*block*-poly(L-leucine)$_{20}$ ($R^H_mE_nL_{20}$), where m = 5 or 10 and n = 70 or 85, to minimize the cationic and

maximize the anionic domains (**Figure 3.1**). Since oppositely charged polypeptide segments typically form strong polyion complexes that are water insoluble,[15] we designed the charged segments to be greatly different in length to maintain aqueous solubility of the vesicles.

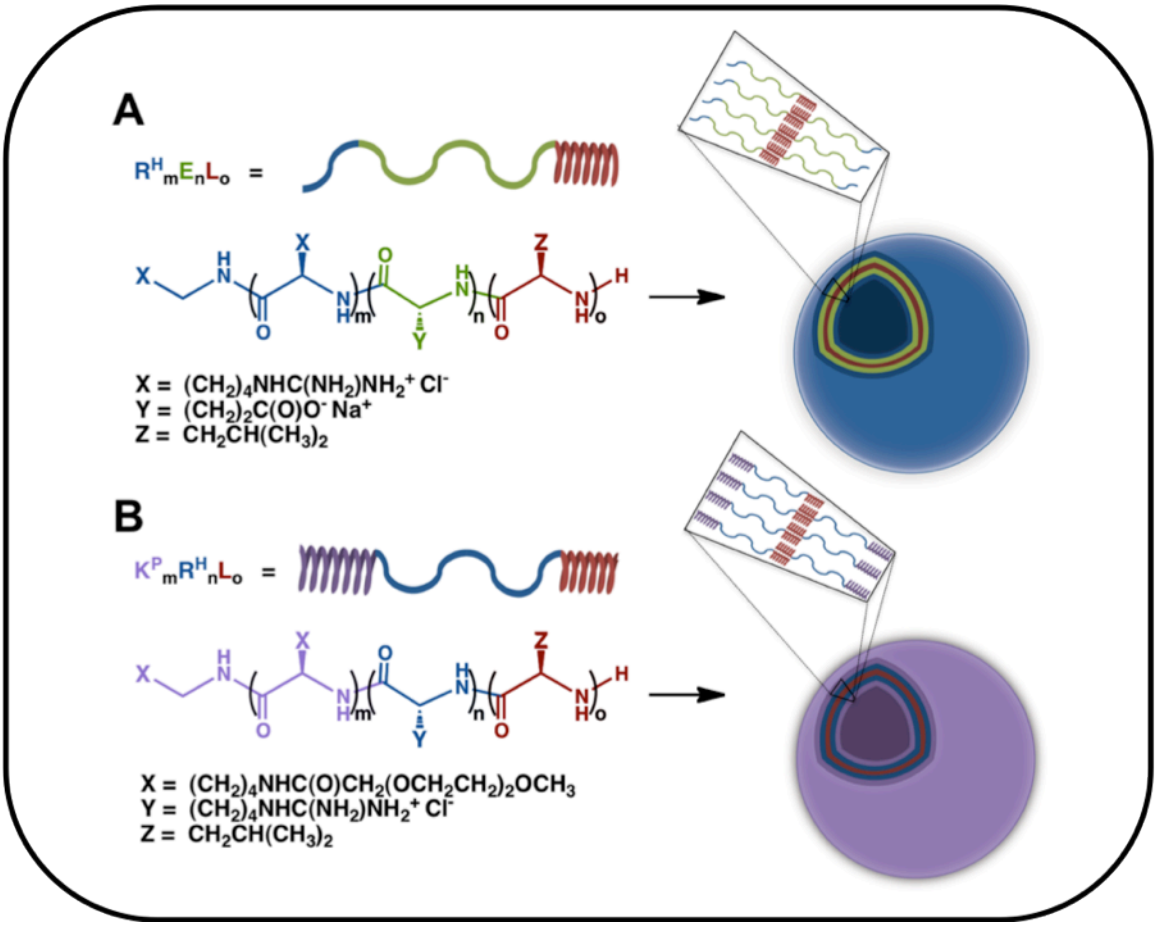

Figure 3.1 Structures and schematic drawings of triblock copolypeptides and their proposed self-assembly into vesicles. (A) $R^H_mE_nL_o$ samples and (B) $K^P_mR^H_nL_o$ samples.

3.3 Cationic-Anionic-Hydrophobic Triblock Copolypeptide Amphiphiles, $R^H_mE_nL_{20}$

The $R^H_mE_nL_{20}$ triblock copolypeptides were synthesized using cobalt initiated sequential living polymerization of α-amino acid-N-carboxyanhydride (NCA) monomers.[16] The copolymers were prepared with short K segments that were subsequently converted to R^H segments after

removal of protecting groups. It has previously been shown that both R^H and R can be used as hydrophilic segments in block copolypeptide vesicles and give indistinguishable properties.[3] The length of the lysine domain was chosen based on the minimum amount of guanidinium groups necessary for cellular uptake. Literature shows that individual polyguanidine segments of ca. 6-9 residues in length are sufficient to promote cellular uptake,[17] triblock copolypeptides were designed with the composition poly(L-homoarginine-HCl)$_m$-*block*-poly(L-glutamate-Na)$_n$-*block*-poly(L-leucine)$_{20}$, $R^H{}_mE_nL_{20}$, where m = 5 or 10 and n = 70 or 85, to minimize the cationic and maximize the anionic domains (**Table 3.1**). Since oppositely charged polypeptide segments typically form strong poly-ion complexes that are water-insoluble, the charged segments are designed to be greatly different in length to maintain aqueous solubility of the vesicles. Studies on poly-ion complexes have shown that if one of the segments is short (i.e. less than 15 charged residues) then complexation is dynamic and there can be fast exchange of chains between the complexes and free chains in solution.[18] Hence, our triblock copolymers were designed to allow formation of vesicles with good water solubility since the charge imbalance is large and the excess of anionic charges should lower toxicity by minimizing adverse interactions with cell surfaces. The R^H and E segments will likely interact with each other, yet the short R^H lengths may allow them to be transiently available to interact with cell surfaces and promote vesicle uptake.[18]

Table 3.1 Characterization and properties of $R^H_mE_nL_o$ triblock copolypeptides and diblock copolypeptides.

Block Copolypeptide	M_n (x 10^3)[a]	M_w/M_n[a]	Found Composition[b]	Yield[c] (%)	Self-Assembled Structure[d]
$K_5E_{70}L_{20}$	17	1.2	$K_6E_{68}L_{15}$	85	V,A
$K_{10}E_{70}L_{20}$	19	1.2	$K_{12}E_{73}L_{24}$	88	V,A,P
$K_5E_{85}L_{20}$	21	1.3	$K_7E_{84}L_{22}$	79	V
$K_{10}E_{85}L_{20}$	23	1.2	$K_{12}E_{88}L_{21}$	88	V,A
$E_{55}L_{20}$	12	1.3	$E_{53}L_{19}$	89	V
$K_{55}L_{20}$	14	1.1	$K_{54}L_{18}$	93	V

[a]Hydrophilic segment lengths (number average molecular weight, M_n, includes (Z)K, and (Bn)E segments) and polydispersities (M_w/M_n) determined using gel permeation chromatography; [b]Calculated using M_n values from gel permeation chromatography and ^{1}H NMR integrations; [c]Isolated yields of pure block copolypeptides; [d]Structure determined visually from DIC microscopy images (V = vesicle, A = irregular aggregate, P = plate).

3.4 Vesicle Self-Assembly and Stability of $K_xE_{70}L_{20}$ and $R^H_xE_{70}L_{20}$ (x = 5, 10)

Initially, the triblock copolypeptides with the compositions of $R^H_5E_{70}L_{20}$ and $R^H_5E_{70}L_{20}$ were prepared, since hydrophilic segments of *ca*. 50 to 70 residues, as in $E_{60}L_{20}$, were known to promote vesicle formation.[4] Using the same protocol for self-assembly of $K_{60}L_{20}$ in water, $R^H_5E_{70}L_{20}$ and $R^H_{10}E_{70}L_{20}$ were processed into aqueous suspensions and analyzed by DIC. Vesicles were found to form (**Figure 3.2**A), yet over time (1 to 2 hours after removal from dialysis) material was found to settle out on the bottom of the container (**Figure 3.2**B).

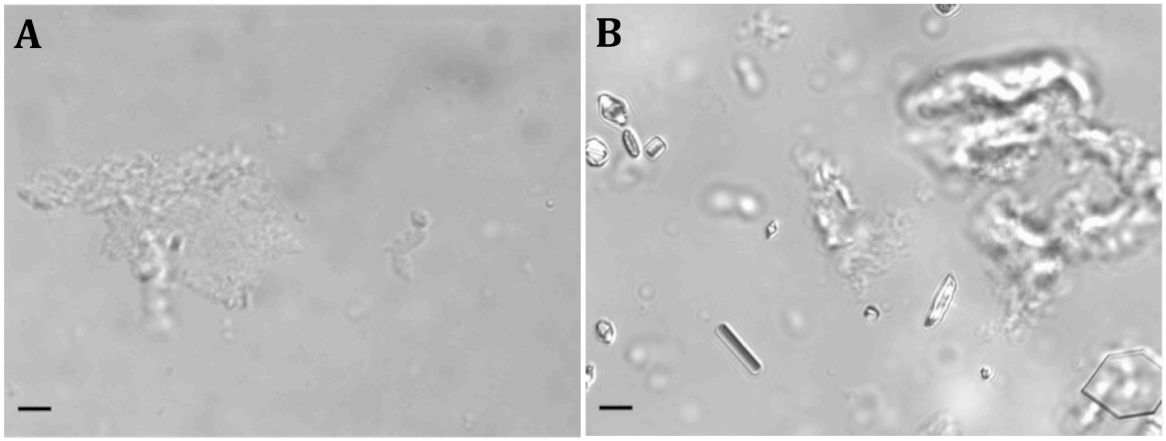

Figure 3.2 Differential interference contrast (DIC) images of 1 % (w/v) aqueous suspensions of $R^{H}_{m}E_{n}L_{o}$ triblock copolypeptides. (A) $R^{H}_{5}E_{70}L_{20}$ (aggregates/vesicles), and (B) $R^{H}_{10}E_{70}L_{20}$ (vesicles/aggregates/plates). Bars = 5 μm.

The results from imaging both suspensions showed that the triblock copolypeptides have the ability to form vesicles but there are also other irregular structures formed. To weaken the poly-ion complexation of the amino and carboxylic acid groups on the copolypeptides, the samples were processed into vesicles in the presence of 150 mM aqueous NaCl. However, the use of ionic media did not significantly improve vesicle formation.

3.5 Vesicle Self-Assembly and Stability of $K_{10}E_{85}L_{20}$ and $R^{H}_{10}E_{85}L_{20}$

The copolymers were then redesigned to incorporate longer anionic segments, i.e. $R^{H}_{10}E_{85}L_{20}$, to compensate for poly-ion complexation and improve aqueous solubility. Improved vesicle formation was seen, however disordered aggregates were still present (**Figure 3.3**).

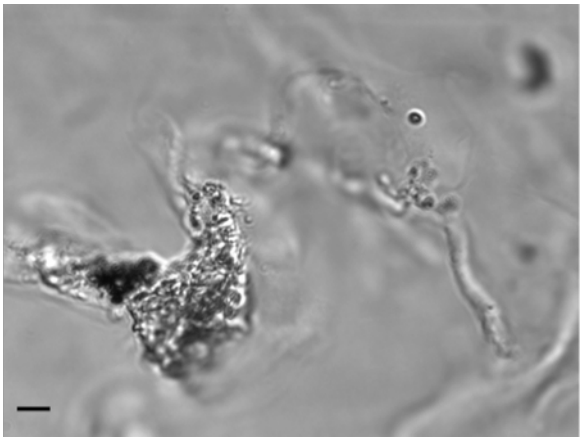

Figure 3.3 Differential interference contrast (DIC) images of 1 % (w/v) aqueous suspensions of $R^{H}_{10}E_{85}L_{20}$ (vesicles/aggregates/plates). Bars = 5 μm.

In order to reduce the amount of electrostatic complexation, the triblock with a longer E segment, $K_{10}E_{85}L_{20}$, was mixed during vesicle formation with the purely anionic sample, $E_{60}L_{20}$. The triblock with the longer E block was used in hopes of placing the lysine block (or guanylated form) away from the vesicle surface. In a previous report of mixtures of polypeptide amphiphiles it was found that vesicle assemblies could be stabilized with different hydrophilic lengths as long as the hydrophobic α-helix segment remained the same (e.g. $K_{80}L_{20}$:$K_{60}L_{20}$, $K_{40}L_{20}$:$K_{60}L_{20}$, $K_{100}L_{20}$:$K_{60}L_{20}$).[19] $K_{100}L_{20}$, $K_{80}L_{20}$, and $K_{40}L_{20}$ polypeptides did not form vesicles without mixing with $K_{60}L_{20}$.

The mixtures are prepared by combining the corresponding amounts of polypeptide and following the same processing protocol with adjustments made depending on sample. The ratio of 3:7 (triblock:diblock) showed optimal vesicle self-assembly with minimal sediment. We wanted to maximize the amount of triblock that can be used in these mixtures to increase the amount of guanidinium groups on the surface of the vesicle, but with increased triblock amounts, more aggregation and sediment could be seen. Vesicle self-assembly was seen for both the lysine and guanylated versions of the triblock (**Figure 3.4**).

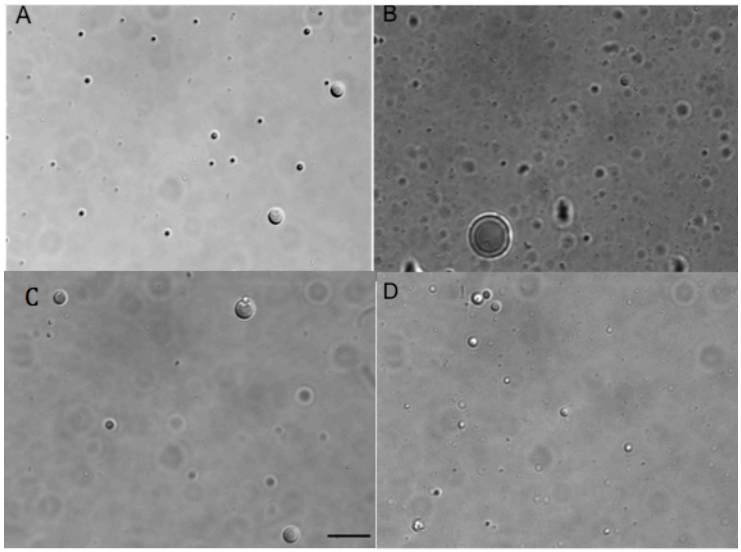

Figure 3.4 DIC images of 0.2 % (w/v) aqueous triblock: diblock suspensions. (A) 30 % $K_{10}E_{85}L_{20}$: 70 % $E_{60}L_{20}$ evaporated, (B) 30 % $R^{H}_{10}E_{85}L_{20}$: 70 % $E_{60}L_{20}$ evaporated, (C) 30 % $K_{10}E_{85}L_{20}$: 70 % $E_{60}L_{20}$ dialyzed against 150 mM NaCl, and (D) 30 % $R^{H}_{10}E_{85}L_{20}$: 70 % $E_{60}L_{20}$ dialyzed against 150 mM NaCl. Scale bar = 10 μm.

To check that the $K_{10}E_{85}L_{20}$ polypeptide was contributing to vesicle self-assembly and not just $E_{60}L_{20}$, the triblock copolypeptide was fluorescently tagged (before mixing) and imaged with fluorescent microscopy (**Figure 3.5**). The images revealed fluorescent vesicular assemblies, confirming the presence of triblock copolypeptides contributing to the vesicle formation.

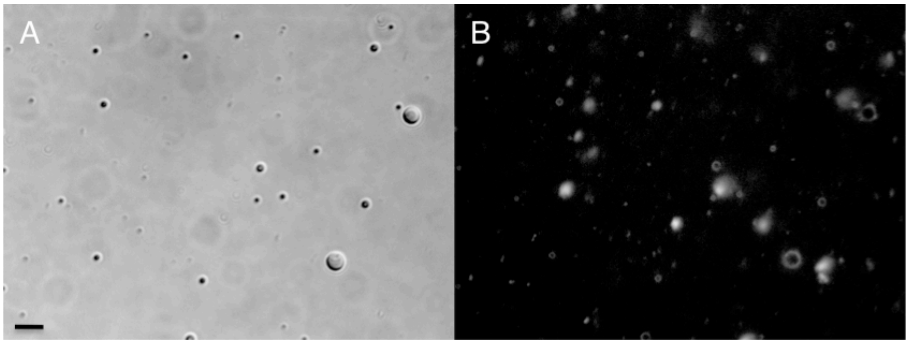

Figure 3.5 Images of 1 % (w/v) aqueous 30 % Fitc-$K_{10}E_{85}L_{20}$:70 % $E_{60}L_{20}$suspensions. (A) DIC image and (B) fluorescent image. Scale bar = 5 μm.

3.6 Cytotoxicity of 30 % $K_{10}E_{85}L_{20}$: 70 % $E_{60}L_{20}$ and 30 % $R^{H}_{10}E_{85}L_{20}$: 70 % $E_{60}L_{20}$ Vesicles

The triblock:diblock copolypeptide vesicles were tested for cytotoxicty. These vesicles were reduced in size by extrusion through nuclear track-etched PC membranes with well-defined pore sizes (down to 200 nm), which we previously had shown gives vesicles with average diameters of ca. 200 nm. Cytotoxicity of the unextruded and extruded 30 % $K_{10}E_{85}L_{20}$: 70 % $E_{60}L_{20}$ and 30 % $R^{H}_{10}E_{85}L_{20}$: 70 % $E_{60}L_{20}$ copolymer vesicles were measured by MTS assay in HeLa cells, which were found to be highly viable up to copolymer concentrations of 40 μg/mL (**Figure 3.6**). This result indicates that even though cationic homoarginine is still present on the vesicles, the abundance of anionic glutamic acid helps reduce the toxicity.

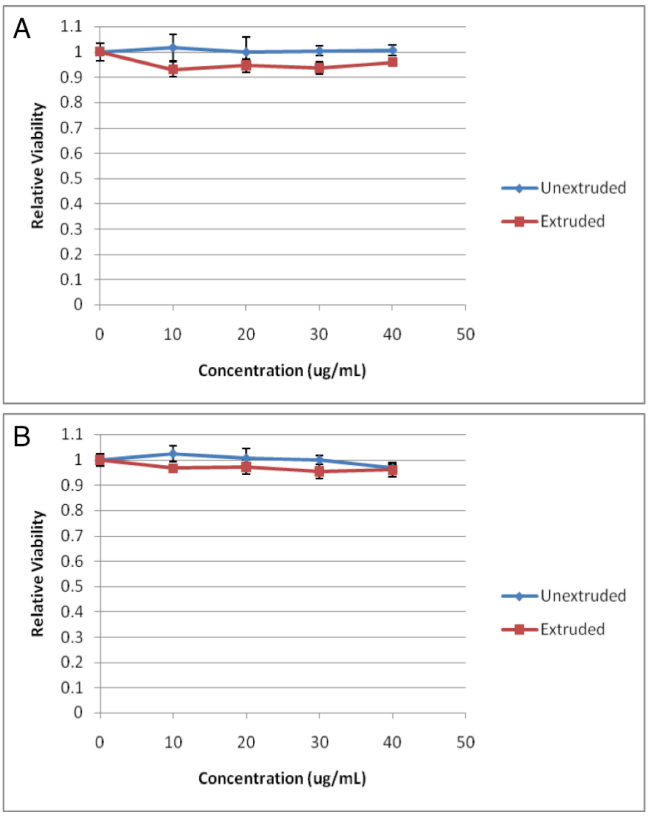

Figure 3.6 MTS cell survival data after 5 hours for HeLa cells incubated with medium containing either extruded or unextruded copolypeptide suspensions. (A) 30 % $K_{10}E_{85}L_{20}$: 70 % $E_{60}L_{20}$ and **(B)** 30 % $R^{H}_{10}E_{85}L_{20}$: 70 % $E_{60}L_{20}$ copolypeptide vesicle suspensions.

3.7 Cellular Uptake of 30 % $R^{H}_{10}E_{85}L_{20}$: 70 % $E_{60}L_{20}$ Vesicles

The triblock copolymer, $R^{H}_{10}E_{80}L_{20}$, was able to self-assemble into vesicles when mixed with $E_{60}L_{20}$. This result shows that there is freedom to mix polypeptides of different hydrophilic composition and make more complex polypeptides without losing the ability to form vesicles. In this case, the cytotoxicity of the vesicles was reduced but at the cost of decreased intracellular uptake (**Figure 3.7**). Fluorescein labeled vesicles incubated with HeLa cells showed minimal intracellular uptake.

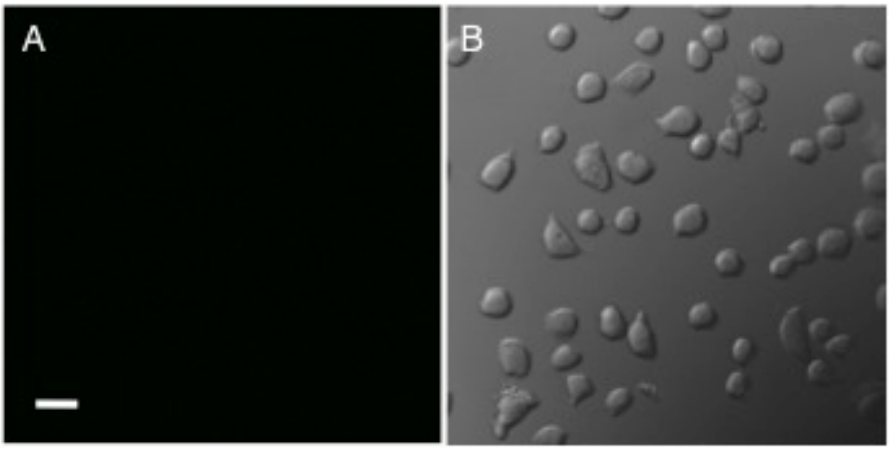

Figure 3.7 Images of HeLa cells incubated with 30 % FITC-$R^{H}_{10}E_{80}L_{20}$: 70 % $E_{60}L_{20}$ vesicles for 5 hr at 37° C. (A) Fluorescence microscopy image and (B) DIC image. Scale bar = 25 μm.

3.8 Vesicle Self-Assembly and Stability of $R^{H}_{5}E_{85}L_{20}$

To simplify the preparation of vesicles, the triblock was redesigned to incorporate a shorter cationic segment, $R^{H}_{5}E_{85}L_{20}$, to reduce the poly-ion complexation and increase water solubility. When processed in the presence of 150 mM NaCl only vesicle assemblies were observed by DIC (**Figure 3.8**A).

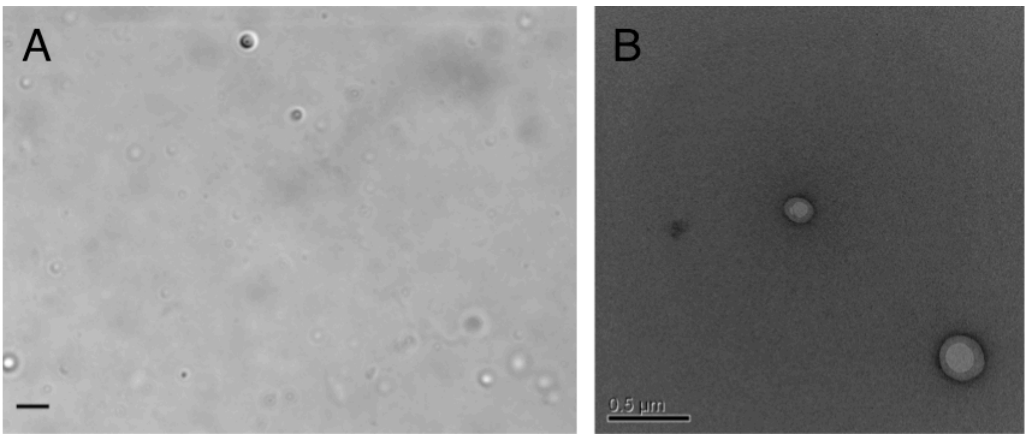

Figure 3.8 Differential interference contrast (DIC) image and transmission electron micrograph of aqueous suspensions of $R^{H}_{5}E_{85}L_{20}$, (A) and (B) respectively. (A) scale bar = 5 μm. (B) scale bar = 0.5 μm.

Similar to our previously reported $R^{H}_{60}L_{20}$ and $E_{60}L_{20}$ samples,[3,4] $R^{H}_{5}E_{85}L_{20}$ formed polydisperse vesicles with diameters ranging from a few hundred nanometers to a few microns, as seen by optical microscopy and transmission electron microscopy (TEM) (**Figure 3.8**B). These vesicles gave stable suspensions that did not aggregate or precipitate over time in DI water, and possessed an overall negative charge determined by zeta potential measurements (-57.4 mV). This optimized composition of $R^{H}_{5}E_{85}L_{20}$ was utilized for further studies.

3.9 Cytotoxicity of $R^{H}_{5}E_{85}L_{20}$ Vesicles

For use in cell studies, the $R^{H}_{5}E_{85}L_{20}$vesicles were reduced in size by extrusion to average diameters of ca. 200 nm. Cytotoxicity of the extruded vesicles, as well as $E_{55}L_{20}$ and $R^{H}_{55}L_{20}$ control samples, were measured using the MTS metabolic assay with LAPC-4 cells, prostate cancer cell line. As expected the $E_{55}L_{20}$ sample showed negligible toxicity, while the $R^{H}_{55}L_{20}$ vesicles were highly toxic at elevated concentrations. The $R^{H}_{5}E_{85}L_{20}$ vesicles were also found to

be negligibly toxic, showing that the excess of anionic residues was able to negate the toxic effects of the terminal cationic segments (**Figure 3.9**).

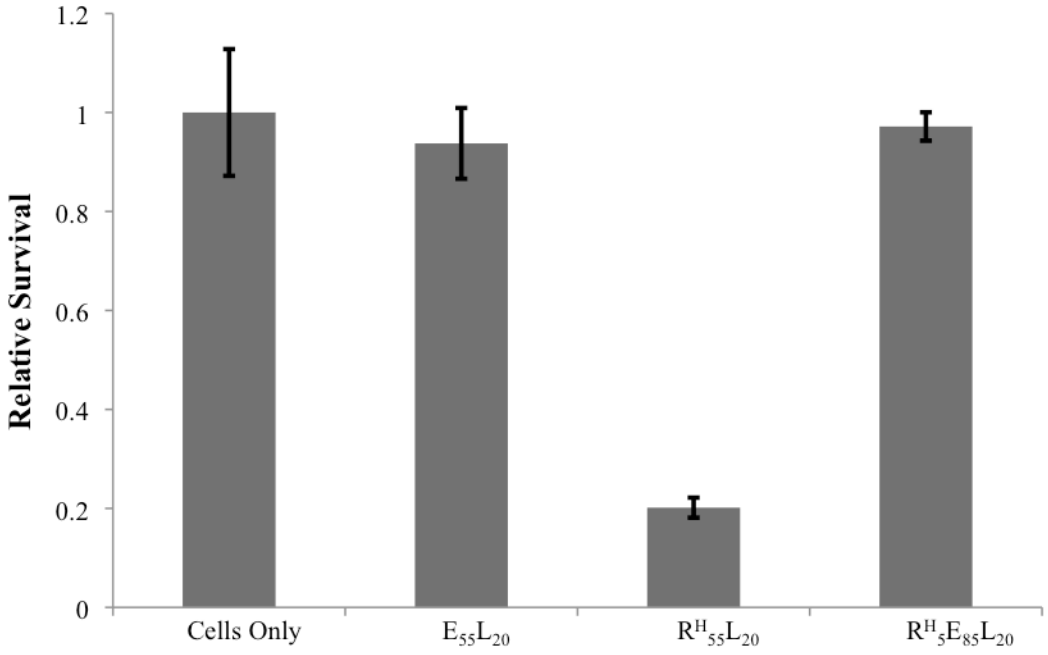

Figure 3.9 MTS cell survival data after 5 hours for LAPC-4 cells separately incubated with medium containing 30 μg/mL of each different extruded copolypeptide vesicle suspension.

3.10 Cellular Uptake of $R^H_5E_{85}L_{20}$ Vesicles

The incorporation of the long anionic domain reduced the cytotoxicity of polypeptide vesicles. The next step was to test the cellular uptake of these triblock polypeptides to see if the R^H segment could enhance cellular uptake of these highly anionic vesicles. Cell uptake studies revealed the fluorescein labeled $R^H_5E_{85}L_{20}$ vesicles were not efficiently taken up by LAPC-4 cells as compared to $R^H_{55}L_{20}$, suggesting that the R^H segments in the triblock vesicles were unavailable for cell binding. In these samples, it appears the cationic R^H segments are bound too tightly to the E segments, which diminishes their ability to promote cellular uptake.

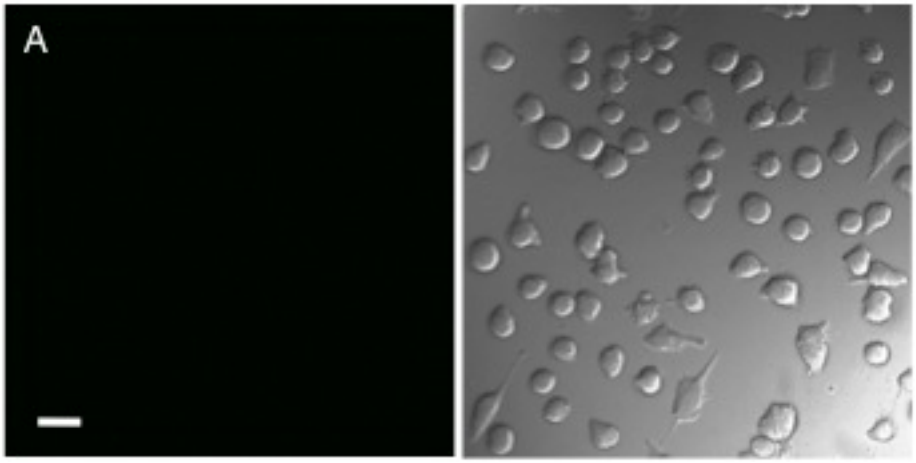

Figure 3.10 Images of LAPC-4 cells incubated with FITC- $R^{H}_{5}E_{85}L_{20}$vesicles for 5 hr at 37° C. (A) Fluorescence microscopy image and (B) DIC image. Scale bar = 25 μm.

3.11 Nonionic-Cationic-Hydrophobic Triblock Copolypeptides Amphiphiles, $K^{P}_{m}R^{H}_{n}L_{20}$

To avoid the issues caused by poly-ion complexation, we redesigned the triblock copolypeptides to contain cationic R^{H} segments and non-ionic, α-helical K^{P} segments of the formula $K^{P}_{m}R^{H}_{n}L_{20}$. Block copolypeptides of the composition $K^{P}_{m}L_{20}$ are known to give only large, μm sized vesicles with rigid membranes and for this reason was not used as a middle segment. Instead, the K^{P} segments were placed at the outer surface to provide a non-ionic, non-interacting sheath that should lower vesicle cytotoxicity, and also not interfere with polycationic R^{H} interior segments that may be revealed upon interaction with cells. Adding this polycationic interior segment, which contains a random coiled conformation could potential provide more fluidity to the membrane making them less rigid in order to achieve polypeptide vesicles of nanometer sizes. To vary the hydrophilic segment lengths, triblock copolypeptides with the compositions $K^{P}_{10}R^{H}_{50}L_{20}$ and $K^{P}_{30}R^{H}_{80}L_{20}$ where prepared (**Table 3.2**).

Table 3.2 Characterization and properties of $K^P_mR^H_nL_o$ triblock copolypeptides and diblock copolypeptides.

Block Copolypeptide	M_n (x 10^3)[a]	M_w/M_n[a]	Found Composition[b]	Yield[c] (%)	Self-Assembled Structure[d]
$K^P_{10}K_{50}L_{20}$	14	1.1	$K^P_8K_{47}L_{18}$	90	V
$K^P_{30}K_{80}L_{20}$	29	1.2	$K^P_{28}K_{79}L_{22}$	92	V

[a]Hydrophilic segment lengths (number average molecular weight, M_n, for K^P, and (Z)K segments) and polydispersities (M_w/M_n) determined using gel permeation chromatography; [b]Calculated using M_n values from gel permeation chromatography and ^{1}H NMR integrations; [c]Isolated yields of pure block copolypeptides; [d]Structure determined visually from DIC microscopy images (V = vesicle).

3.12 Vesicle Self-Assembly and Stability of $K^P_mR^H_nL_{20}$

Upon mixed solvent annealing, both of these samples formed only vesicles, with diameters ranging from ca. 700 nm to a few μms, as determined by optical microscopy (**Figure 3.11**A, B and D). The vesicle morphology of $K^P_{30}R^H_{80}L_{20}$ assemblies was confirmed by labeling their hydrophilic domain with fluorescein and imaging thin slices through suspensions of the sample using laser scanning confocal microscopy (LSCM), which revealed their membrane structure and hydrophilic interior (**Figure 3.11**C).

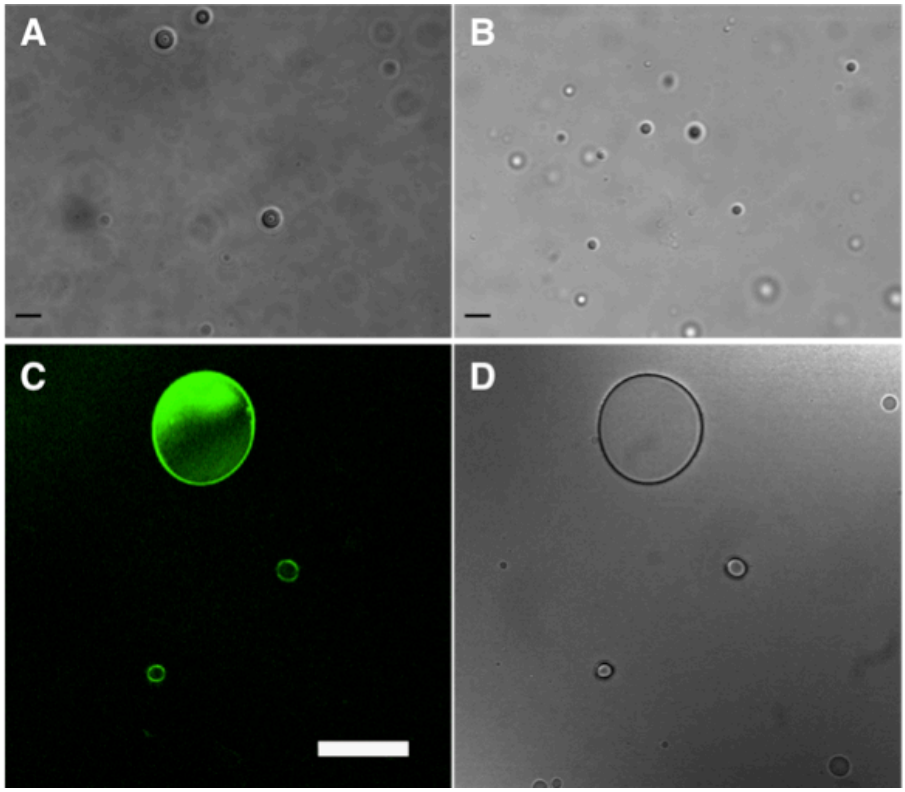

Figure 3.11 Differential interference contrast (DIC) images $K^{P}_{m}R^{H}_{n}L_{20}$ vesicle suspensions. (A) $K^{P}_{10}R^{H}_{50}L_{20}$ and (B) $K^{P}_{30}R^{H}_{80}L_{20}$ (Scale bars = 5 μm). LSCM image of an unextruded, FITC-labeled $K^{P}_{30}R^{H}_{80}L_{20}$ vesicle suspension. (C) Fluorescent image and (D) DIC image (scale bar = 30 μm).

Negative stain transmission electron microscopy was also used to visualize the spherical morphologies (**Figure 3.12**). Vesicle could be seen with diameters in micron range with 2 % uranyl acetate stain (**Figure 3.12**C and D). Vesicular morphologies were also visualized with diameters ranging from the 100 to 500 nanometers.

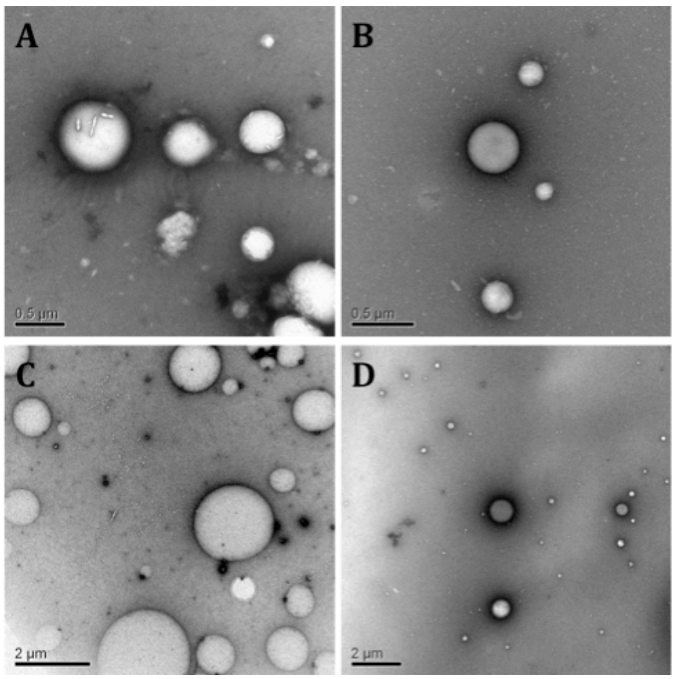

Figure 3.12 Transmission electron micrographs of vesicle suspensions of (A and C) $K^{P}_{10}R^{H}_{50}L_{20}$ and (B and D) $K^{P}_{30}R^{H}_{80}L_{20}$ respectively. (A and B) Scale bar = 0.5 μm. (C and D) Scale bar = 2 μm.

The ability of these vesicles to encapsulate hydrophilic cargoes was also shown by their retention of Texas Red labeled dextran (M_n = 3000 Da) after removal of unencapsulated cargo by dialysis (**Figure 3.13**).

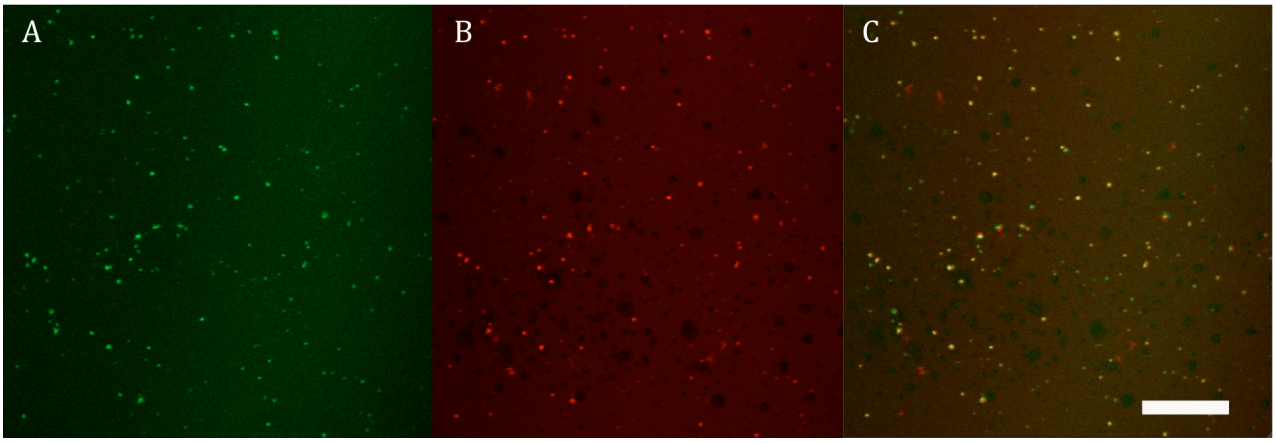

Figure 3.13 LCSM of FITC-labeled $K^{P}_{30}R^{H}_{80}L_{20}$ vesicle suspension encapsulating Texas Red-labeled Dextran. (A) FITC-labeled $K^{P}_{30}R^{H}_{80}L_{20}$ vesicle suspension, (B) Texas red-labeled Dextran, and (C) overlay. (scale bar = 10 μm).

Although the vesicles contains neutral K^{P} segments on the surface the vesicles possessed overall positive surface charge similar to $K_{55}L_{20}$ as determined by zeta potential measurements (**Table 3.3**).

Table 3.3 Zeta potential values of 0.01 % (w/v) aqueous vesicle suspension in Millipore water measured at 25 °C.

Vesicle Suspension	Zeta Potential (mV)
$K_{55}L_{20}$	45.8
$K^{P}_{10}K_{50}L_{20}$	69
$K^{P}_{30}K_{80}L_{20}$	77.5

Extrusion of these aqueous vesicle suspensions through PC membranes was able to reduce their average diameters to ca. 410 nm. Extrusion of these samples was more difficult compared to $R^{H}_{5}E_{85}L_{20}$ vesicles, likely due to the rigidity of the α-helical K^{P} segments, but was a significant improvement compared to the unextrudable $K^{P}_{m}L_{20}$ samples. The helical conformation

of the K^P segments in $K^P_{30}R^H_{80}L_{20}$ was confirmed in circular dichroism spectra, which showed a significant increase in α-helical content compared to the $R^H_{55}L_{20}$ polymer (**Figure 3.14**).

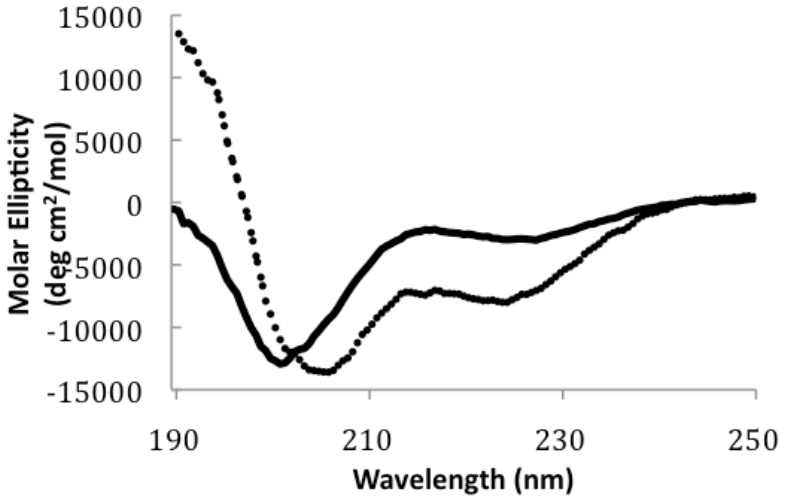

Figure 3.14 Circular dichorism spectrum of 0.25 mg/mL samples of (solid line) $R^H_{55}L_{20}$ and (dotted line) $K^P_{30}R^H_{80}L_{20}$ in deionized water.

3.13 Cytotoxicity of $K^P_mR^H_nL_{20}$ Vesicles

Validating our design, MTS assays using LAPC-4 cells showed that both $K^P_{10}R^H_{50}L_{20}$ and $K^P_{30}R^H_{80}L_{20}$ vesicles were significantly less toxic than $R^H_{55}L_{20}$ (**Figure 3.15**). It appears the hydrophilic K^P segments in these samples provide enough surface coverage on the vesicles to mask the cytotoxicity of the R^H segments.

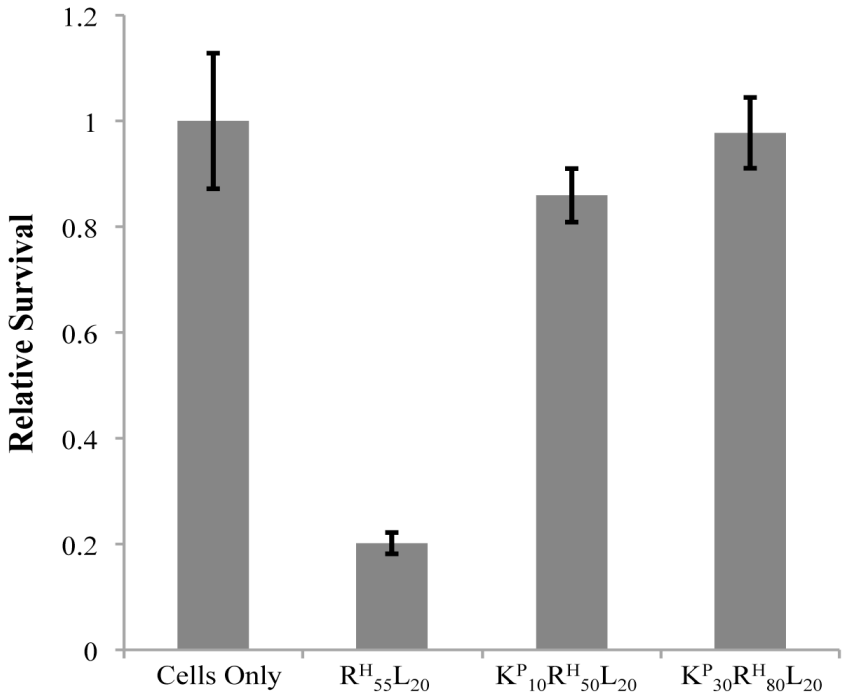

Figure 3.15 MTS cell survival data after 5 hours for LAPC-4 cells separately incubated with medium containing 30 μg/mL of each different extruded copolypeptide vesicle suspensions, $R^H_{55}L_{20}$, $K^P_{10}R^H_{50}L_{20}$, and $K^P_{30}R^H_{80}L_{20}$ with LAPC-4 cell lines.

3.14 Cellular Uptake of $K^P_mR^H_nL_{20}$ Vesicles

To test if the K^P segments are detrimental by potentially masking the ability of the R^H segments to promote cell uptake, fluorescein labeled $K^P_{30}R^H_{80}L_{20}$ vesicles were incubated with LAPC-4 cells. It was found that they were taken up with efficiency comparable to the $R^H_{55}L_{20}$ samples, indicating that the middle R^H segments in these triblock vesicles were able to interact with cell surfaces (**Figure 3.16**).

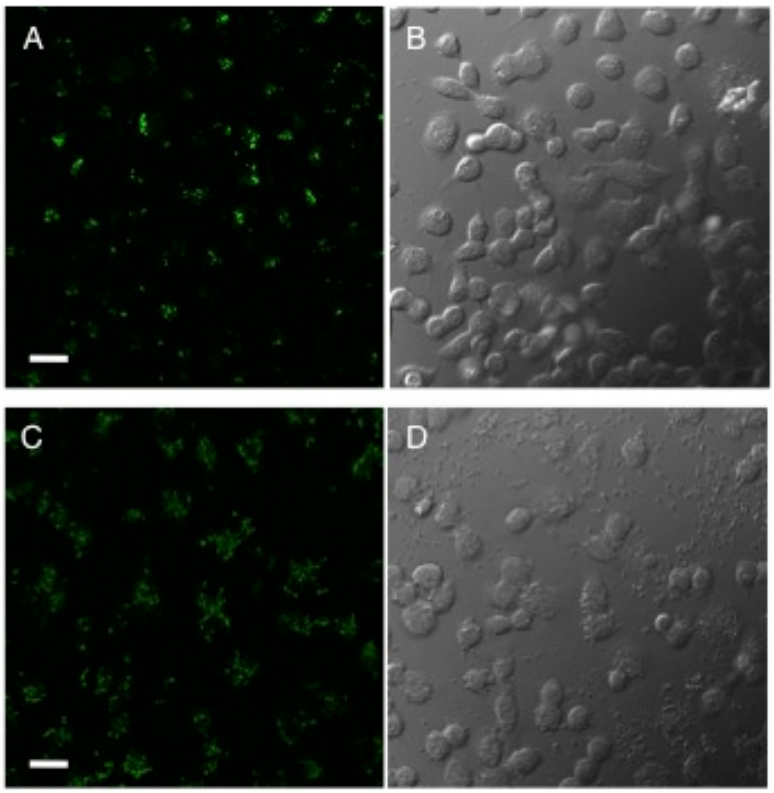

Figure 3.16 Fluorescence microscopy and DIC images of LAPC-4 cells incubated with (A and B, respectively) $R^{H}_{55}L_{20}$ vesicles (10 μg/mL) and $K^{P}_{30}R^{H}_{80}L_{20}$ vesicles (10 μg/mL) for 5 hr at 37 °C. Scale bar = 25 μm.

3.15 Conclusion

The $K^{P}_{10}R^{H}_{50}L_{20}$ and $K^{P}_{30}R^{H}_{80}L_{20}$ vesicles show the potential advantages of using dual hydrophilic segments to optimize polymer vesicle properties, namely allowing a promising combination of lowered cytotoxicity and retention of cell uptake ability that makes them attractive for development as drug carriers. Optimization of vesicles was possible due to the ability of polypeptides to incorporate ordered α-helical conformations that direct self-assembly, as well as the ability to readily prepare functional, multiblock copolypeptide sequences of defined lengths without the need for a combination of different synthetic methods.

3.16 Experimental

3.16.1 Materials and Methods:

Unless stated otherwise, reactions were conducted in oven-dried glassware under an atmosphere of nitrogen using anhydrous solvents. Hexanes, THF, and diethyl ether were purified by first purging with dry nitrogen, followed by passage through columns of activated alumina. All commercially obtained reagents were used as received without further purification unless otherwise stated. The $E_{55}L_{20}$ and $R_{55}L_{20}$ copolypeptides, whose cell uptake and cytotoxicity properties are indistinguishable from $E_{60}L_{20}$ and $R_{60}L_{20}$ samples, were synthesized by transition metal-initiated α-amino acid N-carboxyanhydride polymerization using $(PMe_3)_4Co$ as previously described.[3,4] The polymers were deprotected and then dialyzed exhaustively against DI water to remove any contaminants under pyrogen free conditions. $(PMe_3)_4Co$ was prepared according to literature procedures.[20] Reaction temperatures were controlled using an IKA magnetic temperature modulator, and unless stated otherwise, reactions were performed at room temperature (RT, approximately 23 °C). NMR spectra were recorded on Bruker spectrometers at 400 MHz for ^1H NMR. Fourier Transform Infrared spectroscopy (FTIR) samples were prepared as thin films on NaCl plates and spectra were recorded on a Perkin Elmer RX1 FTIR spectrometer. Tandem gel permeation chromatography/light scattering (GPC/LS) was performed on a SSI Accuflow Series III liquid chromatograph pump equipped with a Wyatt DAWN EOS light scattering detector and Wyatt Optilab rEX refractive index (RI) detectors. Separations were achieved using 10^5, 10^4, and 10^3 Å Phenomenex Phenogel 5 mm columns using 0.10 M LiBr in DMF as the eluent at 60 °C. All GPC/LS samples were prepared at concentrations of 5 mg/mL. Millipore water was obtained from a Millipore Milli-Q Biocel A10 purification unit.

Iscove's Modified Dulbecco's Medium (IMDM), penicillin-streptomycin, and phosphate-buffered saline (PBS) were purchased from Invitrogen (Carlsbad, CA). Fetal bovine serum (FBS) was obtained from Thermo Fisher Scientific (Waltham, MA), and all other tissue culture reagents and chemicals were purchased from Sigma-Aldrich (St. Louis, MO) unless otherwise noted. LAPC-4 cells were generously donated by Prof. Lily Wu (Molecular Pharmacology, UCLA). The 48-well tissue culture plates and 8-well chambered coverglass units were purchased from Corning (Lowell, MA) and Lab-Tek (Rochester, NY), respectively. The MTS cell proliferation assay kit was purchased from Promega (Madison, WI).

3.16.2 Triblock Copolypeptide Synthesis:

The α-amino acid-N-carboxyanhydride NCA monomers were synthesized using previously published protocols.[3-5] All of the triblock copolypeptides were prepared using the $(PMe_3)_4Co$ initiator, with representative examples given below. The resulting copolypeptides were characterized using GPC, ^1H NMR and IR spectroscopy. The compositions of the copolymers were determined by analysis of the integration values from ^1H NMR spectra recorded in *d*-TFA. The lysine (K) residues in all copolymers were converted to homoarginine (R^H) residues following the procedure described below.

3.16.3 Poly(N_ε-benzyloxycarbonyl-L-lysine)$_5$-*block*-poly(γ-benzyl-L-glutamate)$_{70}$-*block*-poly(L-leucine)$_{20}$, (Z)K_5(Bn)$E_{70}L_{20}$:

In a nitrogen filled glove box, N_ε-benzyloxycarbonyl-L-lysine-N-carboxyanhydride (Z-Lys NCA) (100 mg, 0.38 mmol) was dissolved in THF (2 mL) and placed in a 20 mL scintillation vial containing a stir bar. To the vial, $(PMe_3)_4Co$ initiator solution (4 mL of a 20 mg/mL solution in THF) was added via syringe. The vial was sealed and allowed to stir in the glove box for 45

minutes. An aliquot (20 μL) was removed and analyzed by FTIR to confirm that all Z-Lys NCA was consumed. In the glove box, γ-benzyl-L-glutamate-N-carboxyanhydride (Bn-Glu NCA) (1.05 g, 4.00 mmol) was dissolved in THF (11 mL) and was added to the polymerization solutions. The vial was sealed and allowed to stir in the glove box for 45 minutes. An aliquot (50 μL) was removed from the polymerization solution for GPC/LS analysis (M_n = 17,000 g/mol, M_w/M_n = 1.26) and analysis by FTIR to confirm that all Bn-Glu NCA was consumed. L-Leucine-N-carboxyanhydride (L-Leu NCA) (209 mg, 1.32 mmol) was dissolved in THF (4.2mL), added to the polymerization solution, and let stir for 1 hour to give the triblock copolypeptide $(Z)K_5(Bn)E_{70}L_{20}$. Outside of the dry box, the copolypeptide was isolated by evaporating off all volatiles, and was then used directly for the deprotection reaction. The average composition of the copolymer as determined by GPC and NMR integrations was $(Z)K_6(Bn)E_{68}L_{15}$.

3.16.4 Poly(L-lysine-HCl)$_5$-*block*-poly(L-glutamate-Na)$_{70}$-*block*- poly(L-leucine)$_{20}$, $K_5E_{70}L_{20}$:

In a nitrogen filled glove box, a 100 mL round-bottom flask was charged with $(Z)K_5(Bn)E_{70}L_{20}$ (from the previous reaction), CH_2Cl_2 (88 mL), and a stir bar. To the flask, TMSI (3.1 mL, 5 equivalents per protecting group) was added and the flask quickly capped and removed from the glove box. The flask was then attached to a reflux condenser under positive nitrogen flow on a Schlenk line. The mixture was allowed to reflux in a silicone oil bath at 40 °C for 24 hours. The flask was allowed to cool and the polymer was then precipitated by addition of diethyl ether and isolated by centrifugation. Precipitation using ether was repeated twice before suspending the sample in Millipore water containing NaOH (pH was raised to between 8 and 9). The suspension was transferred to a dialysis bag (MWCO = 2000 Da) and dialyzed against Millipore water containing sodium bisulfite (10 mM, 2 days) and disodium EDTA (3 mM, 2 days), aqueous

NaOH (pH 8, 2 days), NaCl (10 mM, 2 days) and water (2 days) before lyophilizing to give a white fluffy powder (670 mg, 85 % overall yield for synthesis and deprotection).

3.16.5 Poly(N_ε-benzyloxycarbonyl-L-lysine)$_{10}$-*block*-poly(γ-benzyl-L-glutamate)$_{70}$-*block*-poly(L-leucine)$_{20}$, (Z)K_{10}(Bn)$E_{70}L_{20}$:

In a nitrogen filled glove box, N_ε-benzyloxycarbonyl-L-lysine-N-carboxyanhydride (Z-Lys NCA) (100 mg, 0.33 mmol) was dissolved in THF (2 mL) and placed in a 20 mL scintillation vial containing a stir bar. To the vial, $(PMe_3)_4Co$ initiator solution (0.9 mL of a 40 mg/mL solution in THF) was added via syringe. The vial was sealed and allowed to stir in the glove box for 45 minutes. An aliquot (20 μL) was removed and analyzed by FTIR to confirm that all Z-Lys NCA was consumed. In a separate vial, γ-benzyl-L-glutamate-N-carboxyanhydride (Bn-Glu NCA) (515 mg, 1.96 mmol) was dissolved in THF (8.5 mL) and was added to the polymerization solutions. The vial was sealed and allowed to stir in the glove box for 45 minutes. An aliquot (50 μL) was removed from the polymerization solution for GPC/LS analysis (M_n = 19,000 g/mol, M_w/M_n = 1.27) and analysis by FTIR to confirm that all Bn-Glu NCA was consumed. L-Leucine-N-carboxyanhydride (L-Leu NCA) (100 mg, 0.64 mmol) was dissolved in THF (2 mL), added to the polymerization solution, and let stir for 1 hour to give the triblock copolypeptide (Z)K_{10}(Bn)$E_{70}L_{20}$. Outside of the dry box, the copolypeptide was isolated by evaporating off all volatiles, and was then used directly for the deprotection reaction. The average composition of the copolymer as determined by GPC and ^{1}H NMR integrations was (Z)K_{12}(Bn)$E_{73}L_{24}$.

3.16.6 Poly(L-lysine-HCl)$_{10}$-*block*-poly(L-glutamate-Na)$_{70}$-*block*-poly(L-leucine)$_{20}$, $K_{10}E_{70}L_{20}$:

In a nitrogen filled glove box, a 100 mL round-bottom flask was charged with (Z)K_{10}(Bn)$E_{70}L_{20}$ (from the previous reaction), CH_2Cl_2 (65 mL), and a stir bar. To the flask, TMSI (2.1 mL, 5 equivalents per protecting group) was added and the flask quickly capped and removed from the glove box. The flask was then attached to a reflux condenser under positive nitrogen flow on a Schlenk line. The mixture was allowed to reflux in a silicone oil bath at 40 °C for 24 hours. The flask was allowed to cool and the polymer was then precipitated by addition of ether and isolated by centrifugation. Precipitation using ether was repeated twice before suspending the sample in Millipore water containing NaOH (pH was raised to between 8 and 9). The suspension was transferred to a dialysis bag (MWCO = 2000 Da) and dialyzed against Millipore water containing sodium bisulfite (10 mM, 2 days) and disodium EDTA (3 mM, 2 days), aqueous NaOH (pH 8, 2 days), NaCl (10 mM, 2 days) and water (2 days) before lyophilizing to give a white fluffy powder (420 mg, 88 % overall yield for synthesis and deprotection).

3.16.7 Poly(N_ε-benzyloxycarbonyl-L-lysine)$_{10}$-*block*-Poly(γ-benzyl-L-glutamate)$_{85}$-*block*-Poly(L-leucine)$_{20}$, (Z)K_{10}(Bn)$E_{85}L_{20}$:

In a nitrogen filled glove box, N_ε-benzyloxycarbonyl-L-lysine-N-carboxyanhydride (Z-Lys NCA) (100 mg, 0.33 mmol) was dissolved in THF (2 mL) and placed in a 20 mL scintillation vial containing a stir bar. To the vial, $(PMe_3)_4Co$ initiator solution (0.9 mL of a 40 mg/mL solution in THF) was added quickly via syringe. The vial was sealed and allowed to stir in the glove box for 45 minutes. An aliquot (20 μL) was removed and analyzed by FTIR to confirm that all Z-Lys NCA was consumed. In a separate vial, γ-benzyl-L-glutamate-N-

carboxyanhydride (Bn-Glu NCA) (687 mg, 2.61 mmol) was dissolved in THF (11 mL) and was added to the living polylysine solutions. The vial was sealed and allowed to stir in the glove box for 45 minutes. An aliquot (50 μL) was removed from the polymerization solution for GPC/LS analysis (M_n = 23,000 g/mol, M_w/M_n = 1.27) and analysis by FTIR to confirm that all Bn-Glu NCA was consumed. L-Leucine-N-carboxyanhydride (L-Leu NCA) (100 mg, 0.64 mmol) was dissolved in THF (2 mL), added to the living polymer solution, and let stir for 1 hour to give the triblock copolypeptide $(Z)K_{10}(Bn)E_{85}L_{20}$. Outside of the dry box, the copolypeptide was isolated by evaporating off all volatiles, and was then used directly for the deprotection reaction below. The average composition of the copolymer as determined by GPC and NMR integrations was $(Z)K_{12}(Bn)E_{88}L_{21}$. A similar procedure was used to prepare the other $(Z)K_m(Bn)E_nL_o$ triblock copolypeptides.

3.16.8 Poly(L-lysine-HCl)$_{10}$-*block*-Poly(L-glutamate-Na)$_{85}$-*block*-Poly(L-leucine)$_{20}$, $K_{10}E_{85}L_{20}$:

In a nitrogen filled glove box, a 100 mL round-bottom flask was charged with $(Z)K_{10}(Bn)E_{85}L_{20}$ (from the previous reaction), CH_2Cl_2 (65 mL), and a stir bar. To the flask, TMSI (2.1 mL, 5 equivalents per protecting group) was added and the flask quickly capped and removed from the glove box. The flask was then attached to a reflux condenser under positive nitrogen flow on a Schlenk line. The mixture was allowed to reflux in a silicone oil bath at 40 °C for 24 hours. The flask was allowed to cool and the polymer was then precipitated by addition of ether and isolated by centrifugation. Precipitation using ether was repeated twice before suspending the sample in Millipore water containing NaOH (pH was raised to between 8 and 9). The suspension was transferred to a dialysis bag (MWCO = 2000 Da) and dialyzed against Millipore water containing sodium bisulfite (10 mM, 2 days) and disodium EDTA (3 mM, 2 days), aqueous

NaOH (pH 8, 2 days), NaCl (10 mM, 2 days) and water (2 days) before lyophilizing to give the product as a white fluffy powder (420 mg, 88 % overall yield after both synthesis and deprotection).

3.16.9 Poly(N_ε-benzyloxycarbonyl-L-lysine)$_5$-*block*-poly(γ-benzyl-L-glutamate)$_{85}$-*block*-poly(L-leucine)$_{20}$, (Z)K_5(Bn)$E_{85}L_{20}$:

In a nitrogen filled glove box, N_ε-benzyloxycarbonyl-L-lysine-N-carboxyanhydride (Z-Lys NCA) (40 mg, 0.13 mmol) was dissolved in THF (800 μL) and placed in a 20 mL scintillation vial containing a stir bar. To the vial, $(PMe_3)_4Co$ initiator solution (1.5 mL of a 20 mg/mL solution in THF) was added via syringe. The vial was sealed and allowed to stir in the glove box for 45 minutes. An aliquot (20 μL) was removed and analyzed by FTIR to confirm that all Z-Lys NCA was consumed. In the glove box, γ-benzyl-L-glutamate-N-carboxyanhydride (Bn-Glu NCA) (413 mg, 1.57 mmol) was dissolved in THF (8.3 mL) and was added to one of the polymerization solutions. The vial was sealed and allowed to stir in the glove box for 45 minutes. An aliquot (50 μL) was removed from the polymerization solution for GPC/LS analysis (M_n = 21,000 g/mol, M_w/M_n = 1.32) and analysis by FTIR to confirm that all Bn-Glu NCA was consumed. L-Leucine-N-carboxyanhydride (L-Leu NCA) (82 mg, 0.52 mmol) was dissolved in THF (1.64 mL), added to the polymerization solution, and let stir for 1 hour to give the triblock copolypeptide (Z)K_5(Bn)$E_{85}L_{20}$. Outside of the dry box, the copolypeptide was isolated by evaporating off all volatiles, and was then used directly for the deprotection reaction. The average composition of the copolymer as determined by GPC and NMR integrations was (Z)K_7(Bn)$E_{84}L_{22}$.

3.16.10 Poly(L-lysine-HCl)$_5$-*block*-poly(L-glutamate-Na)$_{85}$-*block*- poly(L-leucine)$_{20}$, $K_5E_{85}L_{20}$:

In a nitrogen filled glove box, a 100 mL round-bottom flask was charged with (Z)K_{10}(Bn)$E_{85}L_{20}$ (from the previous reaction), CH_2Cl_2 (36 mL), and a stir bar. To the flask, TMSI (1.2 mL, 5 equivalents per protecting group) was added and the flask quickly capped and removed from the glove box. The flask was then attached to a reflux condenser under positive nitrogen flow on a Schlenk line. The mixture was allowed to reflux in a silicone oil bath at 40 °C for 24 hours. The flask was allowed to cool and the polymer was then precipitated by addition of ether and isolated by centrifugation. Precipitation using ether was repeated twice before suspending the sample in Millipore water containing NaOH (pH was raised to between 8 and 9). The suspension was transferred to a dialysis bag (MWCO = 2000 Da) and dialyzed against Millipore water containing sodium bisulfite (10 mM, 2 days) and disodium EDTA (3 mM, 2 days), aqueous NaOH (pH 8, 2 days), NaCl (10 mM, 2 days) and water (2 days) before lyophilizing to give a white fluffy powder (420 mg, 88 % overall yield for synthesis and deprotection). ^{1}H NMR and FTIR spectra of this material were similar to literature data for samples of K_mL_n and E_mL_n copolymers.

3.16.11 Poly(N_ε-2-(2-(2-methoxyethoxy)ethoxy)acetyl-L-lysine)$_{10}$-*block*-poly(N_ε-benzyloxycarbonyl-L-lysine)$_{50}$-*block*-poly(L-leucine)$_{20}$, $K^P{}_{10}(Z)K_{50}L_{20}$:

N_ε-2-(2-(2-methoxyethyoxy)ethoxy)acetyl-L-lysine-N-carboxyanhydride (EG_2-Lys NCA) (40 mg, 0.12 mmol) was dissolved in THF (800 μL) and placed in a 20 mL scintillation vial containing a stir bar. To the vial, $(PMe_3)_4Co$ initiator solution (875 μL of a 20 mg/mL solution in THF) was added via syringe. The vial was sealed and allowed to stir in the glove box for 45 minutes. An aliquot (20 μL) was removed and analyzed by FTIR to confirm that all EG_2-Lys

NCA was consumed. In the glove box, Z-Lys NCA (224 mg, 0.73 mmol) was dissolved in THF (4.5 mL) and was added to the polymerization solution. The vial was sealed and allowed to stir in the glove box for 45 minutes. An aliquot (50 μL) was removed from the polymerization solution for GPC/LS analysis (M_n = 14,000 g/mol, M_w/M_n = 1.12) and analysis by FTIR to confirm that all Z-Lys NCA was consumed. Next, L-Leu NCA (47 mg, 0.30 mmol) was dissolved in THF (940 μL), added to the polymerization solution, and let stir for 1 hour to give the triblock copolypeptide $K^P_{10}(Z)K_{50}L_{20}$. Outside of the dry box, the copolypeptide was isolated by evaporating off all volatiles, and was then used directly for the deprotection reaction. The average composition of the copolymer as determined by GPC and NMR integrations was $K^P_8(Z)K_{47}L_{18}$.

3.16.12 Poly(N_ε-2-(2-(2-methoxyethoxy)ethoxy)acetyl-L-lysine)$_{10}$-*block*-poly(L-lysine-HCl)$_{50}$-*block*-poly(L-leucine)$_{20}$, $K^P_{10}K_{50}L_{20}$:

A 100 mL round-bottom flask was charged with $K^P_{10}(Z)K_{50}L_{20}$ (from the previous reaction), TFA (9 mL) and a stir bar. The flask was placed in an ice bath and allowed to stir until all polymer was completely dissolved. At this point, HBr (0.64 mL of 33 % solution in HOAc, 5 equivalents per Z group) was added to the solution, which was allowed to stir in the ice bath for 1 hour. Diethyl ether (30 mL) was then added to precipitate the polymer. The product was isolated by centrifugation and was washed with ether twice more before resuspending in water. The solution was placed in a dialysis bag (MWCO = 2000 Da) and dialyzed against aqueous disodium EDTA (3 mM, 2 days), then aqueous HCl and NaCl(10 mM, 10 mM, 2 days), followed by Millipore water (2 days) before lyophilization to give a fluffy white powder (170 mg, 90 % overall yield for synthesis and deprotection).

3.16.13 Poly(N_ε-2-(2-(2-methoxyethoxy)ethoxy)acetyl-L-lysine)$_{30}$-*block*-Poly(N_ε-benzyloxycarbonyl-L-lysine)$_{80}$-*block*-Poly(L-leucine)$_{20}$, $K^P_{30}(Z)K_{80}L_{20}$:

N_ε-2-(2-(2-methoxyethoxy)ethoxy)acetyl-L-lysine-N-carboxyanhydride (EG_2-Lys NCA) (100 mg, 0.30 mmol) was dissolved in THF (2 mL) and placed in a 20 mL scintillation vial containing a stir bar. To the vial, $(PMe_3)_4Co$ initiator solution (460 μL of a 20 mg/mL solution in THF) was added quickly via syringe. The vial was sealed and allowed to stir in the glove box for 45 minutes. An aliquot (20 μL) was removed and analyzed by FTIR to confirm that all EG_2-Lys NCA was consumed. In the glove box, Z-Lys NCA (270 mg, 0.88 mmol) was dissolved in THF (5.4 mL) and was added to the polymerization solution. The vial was sealed and allowed to stir in the glove box for 45 minutes. An aliquot (50 μL) was removed from the polymerization solution for GPC/LS analysis (M_n = 29,600 g/mol, M_w/M_n = 1.25) and analysis by FTIR to confirm that all Z-Lys NCA was consumed. Next, L-Leu NCA (40 mg, 0.25 mmol) was dissolved in THF (800 μL), added to the polymerization solution, and let stir for 1 hour to give the triblock copolypeptide $K^P_{30}(Z)K_{80}L_{20}$. Outside of the dry box, the copolypeptide was isolated by evaporating off all volatiles, and was then used directly for the deprotection reaction below. The average composition of the copolymer as determined by GPC and NMR integrations was $K^P_{28}(Z)K_{79}L_{22}$.

3.16.14 Poly(N_ε-2-(2-(2-methoxyethoxy)ethoxy)acetyl-L-lysine)$_{30}$-*block*-Poly(L-lysine-HCl)$_{80}$-*block*-Poly(L-leucine)$_{20}$, $K^P_{30}K_{80}L_{20}$:

A 100 mL round-bottom flask was charged with $K^P_{30}(Z)K_{80}L_{20}$ (from the previous reaction), TFA (10 mL) and a stir bar. The flask was placed in an ice bath and allowed to stir until all polymer was completely dissolved. At this point, HBr (0.8 mL of 33 % solution in HOAc, 5 equivalents

per Z group) was added to the solution, which was allowed to stir in the ice bath for 1 hour. Diethyl ether (30 mL) was then added to precipitate the polymer. The product was isolated by centrifugation and was washed with ether twice more before resuspending in water. The solution was placed in a dialysis bag (MWCO = 2000 Da) and dialyzed against aqueous disodium EDTA (3 mM, 2 days), then aqueous HCl and NaCl(10 mM, 10 mM, 2 days), followed by Millipore water (2 days) before lyophilization to give the product as a fluffy white powder (210 mg, 92 % overall yield after both synthesis and deprotection). ^{1}H NMR and FTIR spectra of this material were similar to literature data for samples of K_mL_n and $K^P_mL_n$ copolymers.[3-5]

3.16.15 Guanylation of Lysine Residues on Triblock Copolypeptides:

A triblock copolypeptide sample (20 mg) was dispersed in aqueous NaOH (10 mg/ml, 1 mM) in a plastic 15 mL conical tube. The guanylating reagent, 3,5-dimethylpyrazole-1-carboxamidine nitrate (10 eq per each lysyl amine group), was dissolved in aqueous 1 M NaOH and added to the polypeptide suspension. The reaction mixture was sealed and placed in a bath sonicator for 1 minute and then placed in an oven at 37 °C for 72 hours. After 72 h, the reaction mixture was acidified to pH of 3 with HCl and placed in a dialysis bag (MWCO = 2000 Da) and dialyzed against aqueous NaCl (10 mM, 2 days) and Millipore water (2 days), changing each solution 2 times/day. After dialysis, the white powder product was isolated by freeze-drying the solution. The typical guanylation efficiency is *ca*. 90 %, and isolated yields ranged from 85 to 95%.[21]

3.16.16 Fluorescent Probe Modification of Polypeptide Vesicles:

Fluorescein isothiocyanate (FITC) was conjugated to lysyl amine groups in triblock copolypeptides by mixing 1 % (w/v) polypeptide in sodium bicarbonate buffer at pH 8.0 with a 6:1 molar ratio of polypeptide chains to FITC at room temperature for at least 16 h. The

resulting copolypeptide was purified by dialysis against Millipore water under sterile conditions and then freeze dried to give the solid product.

3.16.17 Preparation of Cationic-Anionic-Hydrophobic Triblock Copolypeptide Assemblies in Water:

These triblock copolypeptide samples were dispersed in THF to give 2.0 % (w/v) suspensions, which were then placed in a bath sonicator for 30 minutes until the copolypeptides were evenly dispersed. An equal volume of Millipore water was added to each sample, which was then placed in a bath sonicator for 30 minutes, and then placed in a dialysis bag (MWCO = 2000 Da) and dialyzed against Millipore water under sterile conditions containing 150 mM NaCl for 24 hours. The 150 mM NaCl solution was changed every hour for the first 4 hours.

3.16.18 Preparation of Cationic-Anionic-Hydrophobic Triblock: Diblock Copolypeptide Assemblies in Water:

Amounts (3:7 mole to mole ratio) of triblock copolypeptide powder ($K_{10}E_{80}L_{20}$ or $R^{H}_{10}E_{80}L_{20}$) and diblock copolypeptide ($E_{60}L_{20}$) were dispersed in THF separately to give 2 % (w/v) suspensions, which are then placed in a bath sonicator for 30 minutes until the copolypeptides were evenly dispersed. An equal volume of Millipore water was added to each suspension. The diblock suspension was combined with the triblock and placed in a bath sonicator for 30 minutes. After sonication, the suspension was placed in a dialysis bag (MWCO = 2000 Da) and dialyzed against Millipore water containing 150 mM NaCl for 24 hours. The 150 mM NaCl solution was changed every hour for the first 4 hours. Triblock assemblies consisting of $K_{10}E_{80}L_{20}$ and $E_{60}L_{20}$ could also be processed into assemblies by solvent evaporation with no added salt solution.

3.16.19 Preparation of Nonionic-Cationic-Hydrophobic Triblock Copolypeptide Assemblies in Water:

These triblock copolypeptide samples were dispersed in THF to give 4 % (w/v) suspensions, which were then placed in a bath sonicator for 30 minutes until the copolypeptides were evenly dispersed. An equal volume of Millipore water was added to each suspension, which was then placed in a bath sonicator for 30 minutes. Four equivalent aliquots of THF were then added in succession to the suspension, with vortexing in between each addition, to give final sample concentrations of 1 % (w/v) and a 3:1 ratio of THF to water. The suspensions were then placed in dialysis bags (MWCO = 2000 Da) and dialyzed against Millipore water under sterile conditions for 24 hours. The water was changed every hour for the first 4 hours.

3.16.20 Encapsulation of Texas Red Dextran with $K^{P}_{30}R^{H}_{80}L_{20}$ Vesicles:

The triblock copolypeptide $K^{P}_{30}R^{H}_{80}L_{20}$ was mixed with THF to give a 2 % (w/v) suspension, which was then placed in a bath sonicator for 30 minutes until the copolypeptide was evenly dispersed. An equal volume of Millipore water containing Texas Red labeled dextran (Molecular Probes, M_n = 3000 Da, 0.25 mg/mL) was added to this suspension, which was then placed in a bath sonicator for 30 minutes. Four equivalent aliquots of THF were then added in succession to the suspension, with vortexing in between each addition, to give a final sample concentration of 0.5 % (w/v) and a 3:1 ratio of THF to water. The suspension was then placed in a dialysis bag (MWCO = 2000 Da) and dialyzed against Millipore water under sterile conditions for 24 hours. The water was changed every hour for the first 4 hours. After 24 hours, the suspension was transferred to a larger pore size dialysis bag (MWCO = 8000 Da) and dialyzed for 24 hours to remove all dextran that was not encapsulated by the vesicles. The water was changed every hour

for the first 4 hours. Samples were then analyzed by LSCM. A control sample to check for uptake or adsorption of dye to intact vesicles was also prepared by adding Texas Red labeled dextran to previously prepared $K^{P}_{30}R^{H}_{80}L_{20}$ vesicle suspension. This sample was allowed to stand for 24 hours and was then placed in a large pore size dialysis bag (MWCO = 8000 Da) to remove unencapsulated and unassociated Texas Red Dextran. Analysis of this sample by LCSM showed negligible Texas Red label, indicating that intact vesicles neither bind nor incorporate Texas Red labeled dextran.

3.16.21 Extrusion of Vesicle Suspensions:

Aqueous vesicle suspensions at 0.2 % (w/v) in Millipore water were extruded using an Avanti Mini-Extruder. Extrusions were performed using different pore size Whatman Nucleopore Track-Etched polycarbonate (PC) membranes, following a protocol of serial extrusion of vesicles through decreasing filter pore sizes: 3 times through a 1.0 μm filter, 3 times through a 0.4 μm filter, and 3 times through a 0.2 μm filter. Only for the $K^{P}_{30}K_{80}L_{20}$ sample, this procedure was followed by one extrusion through a 0.1 μm filter. The PC membranes and support membranes were soaked in Millipore water for 10 minutes prior to extrusion.

3.16.22 Dynamic Light Scattering (DLS):

The sizes and polydispersities of the vesicles were determined using dynamic light scattering (DLS) measurements. A total scattering intensity of approximately 1 x 105 cps was targeted. Extruded vesicle suspensions were analyzed with the Malvern Zetasizer Nano ZS model Zen 3600 (Malvern Instruments Inc, Westborough, MA). The autocorrelation data was fitted using the CONTIN algorithm to determine the diameters of suspended vesicles/assemblies.

3.16.23 Cell Culture:

The LAPC-4 cell line was maintained in IMDM supplemented with 10 % FBS, 100 units/mL penicillin, and 100 μg/mL streptomycin at a pH of 7.4 in a 37 °C humidified atmosphere with 5 % CO_2 using standard tissue culture protocols.

3.16.24 MTS Cell Proliferation Assay (LAPC-4 Cells):

The MTS cell proliferation assay (CellTiter 96® AQ_{ueous} Non-Radioactive Cell Proliferation Assay) was used to quantify any cytotoxic effects of the polypeptide vesicle suspensions. The procedure described above for the vesicle uptake studies was followed with the exception of seeding LAPC-4 cells on a 48-well plate instead of an 8-well chambered cover glass. At the end of the 5 hr incubation period, the medium containing polypeptide vesicles was aspirated. Fresh medium containing 20 % MTS was then added to the cells. The cells were placed back into a CO_2 incubator for 1 hr and then the absorbance at 490 nm (A_{490}) was measured with an Infinite F200 plate reader (Tecan Systems Inc., San Jose, CA). The background absorbance was read at 700 nm (A_{700}) and subtracted from A_{490}. The relative survival of the cells at each polypeptide concentration was quantified by taking the ratio of the ($A_{490} - A_{700}$) values and comparing between the experimental and control cells.

3.16.25 MTS Cell Proliferation Assay (HeLa Cells):

MTS cell proliferation assay was performed according to the manufacture-supplied instructions. Briefly, HeLa cells were seeded onto a 48-well tissue culture plate at 40,000 cells/cm^{-2} and incubated overnight in a 37 ºC humidified atmosphere with 5 % Co_2. The next day the media was aspirated off for each well, and the cells were incubated with 250 μL of fresh media containing different concentrations of vesicles for 5 hours. Afterwards, the media was aspirated, followed

by an addition of 250 μL of media and 50 μL of MTS reagent to each well. The cells were then place a 37 °C air incubator for 1 hour and absorbance of each well was measured at 490 nm (A_{490}). The background absorbance was also read at 700 nm (A_{700}) and subtracted from A_{490}. The relative survival of cells relative to the control was calculated by taking the ratio of the ($A_{490}B - A_{700}$) values.

3.16.26 Cellular Uptake of Polypeptide Vesicles (LAPC-4 Cells):

LAPC-4 cells were seeded at a density of $1x10^5$ cells/cm^2 onto an 8-well chambered cover glass prior to the experiment. At the start of the experiment, the cell culture medium was aspirated, and the cells were incubated in medium containing the polypeptide vesicles for 5 hrs in a 37 °C humidified atmosphere with 5 % CO_2. The incubation medium was the same as the cell culture medium except for the absence of FBS, penicillin, and streptomycin. Following this incubation, this medium was aspirated, and the cells were washed with PBS to remove any excess polypeptide vesicles that were not internalized before the confocal images were taken.

3.16.27 Cellular Uptake of Polypeptide Vesicles (HeLa Cells):

HeLa cells were seeded at a density of $4x10^4$ cells/cm^2 onto an 8-well chambered cover glass at least 12 h before the start of experiment. At the start of the experiment, the cell culture medium was aspirated, and the cells were briefly washed with PBS. The cells were incubated in cell culture medium containing different concentrations of the $R_{60}L_{20}$ polypeptide vesicles for 5 h in a 37°C humidified atmosphere with 5 % CO_2. Following this incubation, this medium was aspirated, and the cells were washed with PBS to remove any free-floating polypeptide vesicles that were not internalized before the confocal images were taken.

3.16.28 Laser Scanning Confocal Microscopy (LSCM):

LSCM images of the vesicles and cells were taken on a Leica Inverted TCS-SP MP Spectral Confocal and Multiphoton Microscope (Heidelberg, Germany) equipped with an argon laser (488 nm blue excitation: JDS Uniphase), a diode laser (DPSS; 561 nm yellow-green excitation: Melles Griot), a helium-neon laser (633 nm red excitation), and a two-photon laser setup consisting of a Spectra-Physics Millenia X 532 nm green diode pump laser and a Tsunami Ti-Sapphire picosecond pulsed infrared laser tuned at 768 nm for UV excitation.

3.17 Spectral Data:

^{1}H-NMR spectra of polypeptides in *d*-TFA

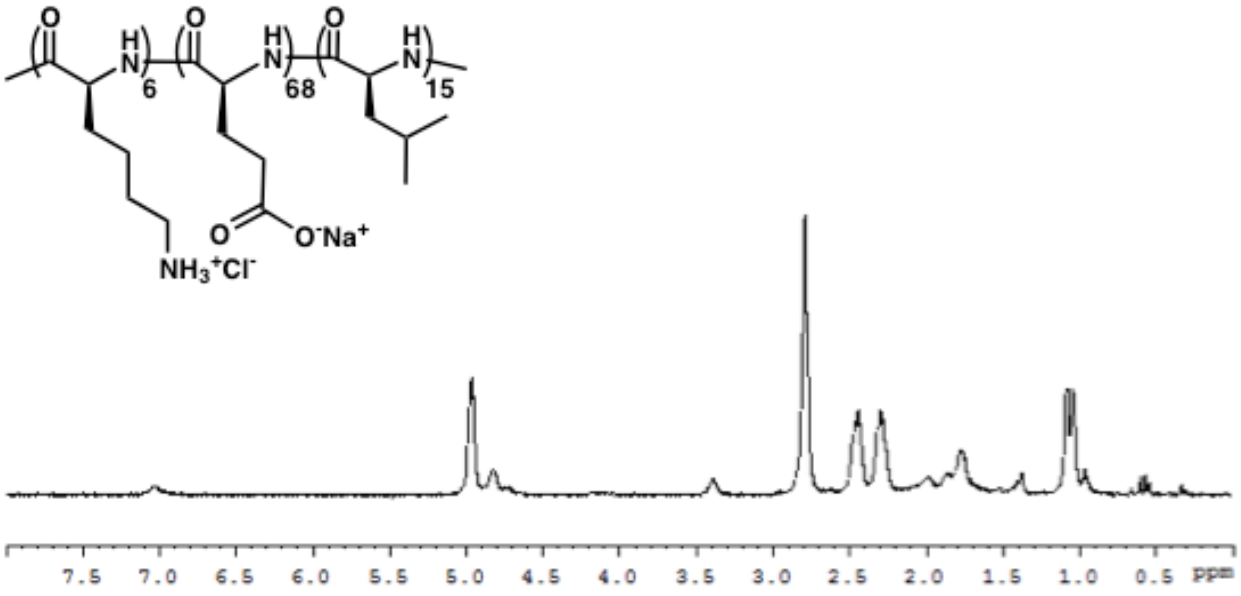

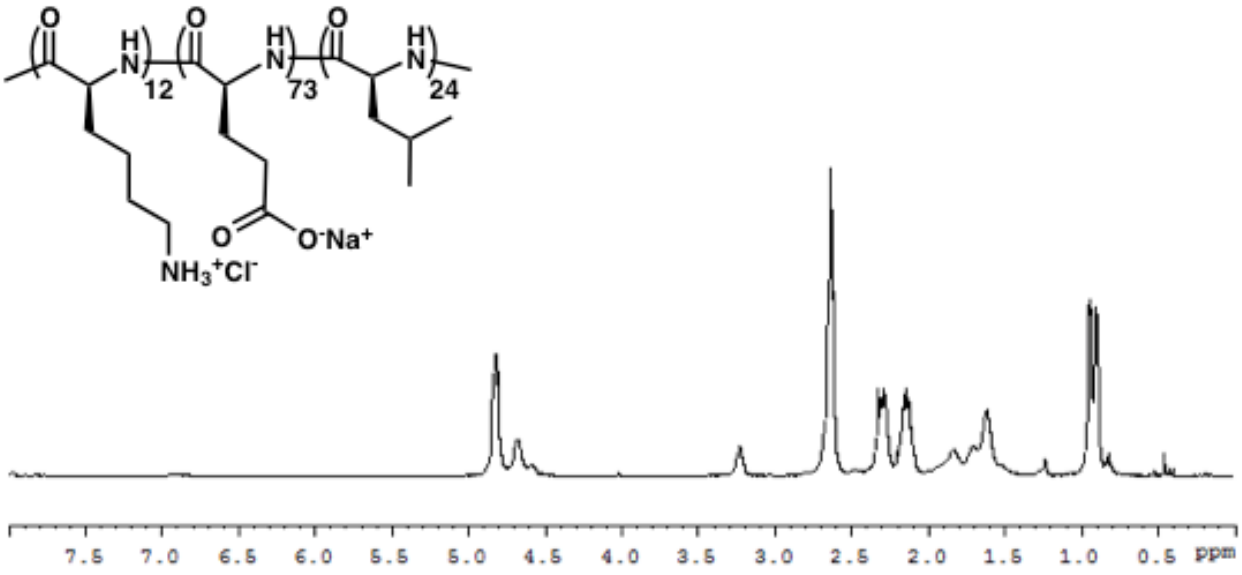
12
73
24
O-Na+
NH3+Cl-
7.5 7.0 6.5 6.0 5.5 5.0 4.5 4.0 3.5 3.0 2.5 2.0 1.5 1.0 0.5 ppm

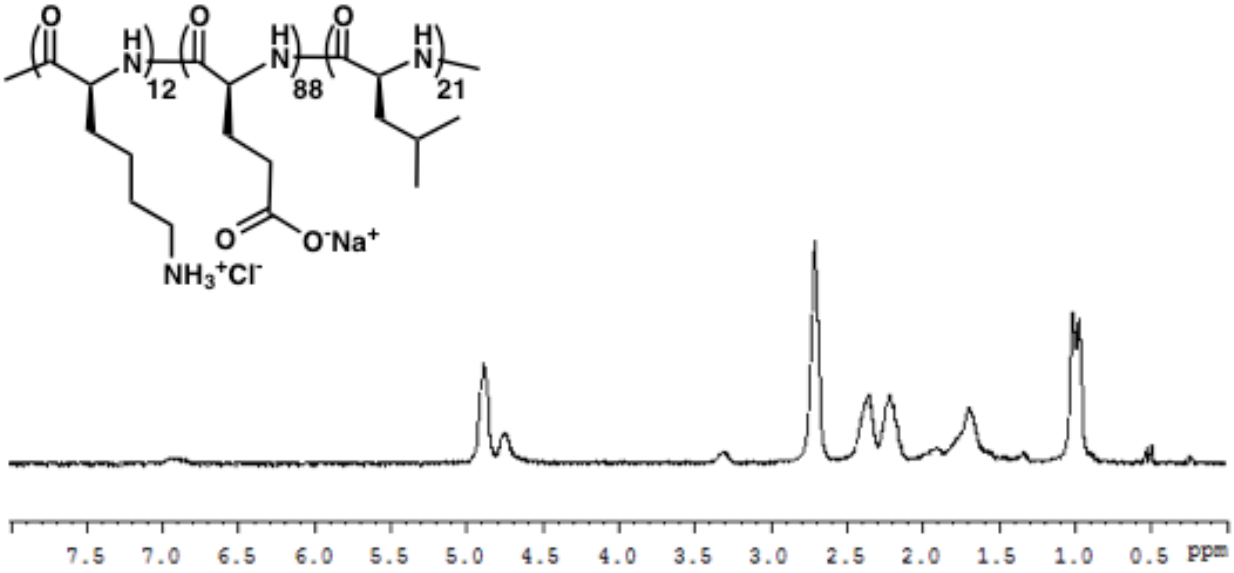
12
88
21
O-Na+
NH3+Cl-
7.5 7.0 6.5 6.0 5.5 5.0 4.5 4.0 3.5 3.0 2.5 2.0 1.5 1.0 0.5 ppm

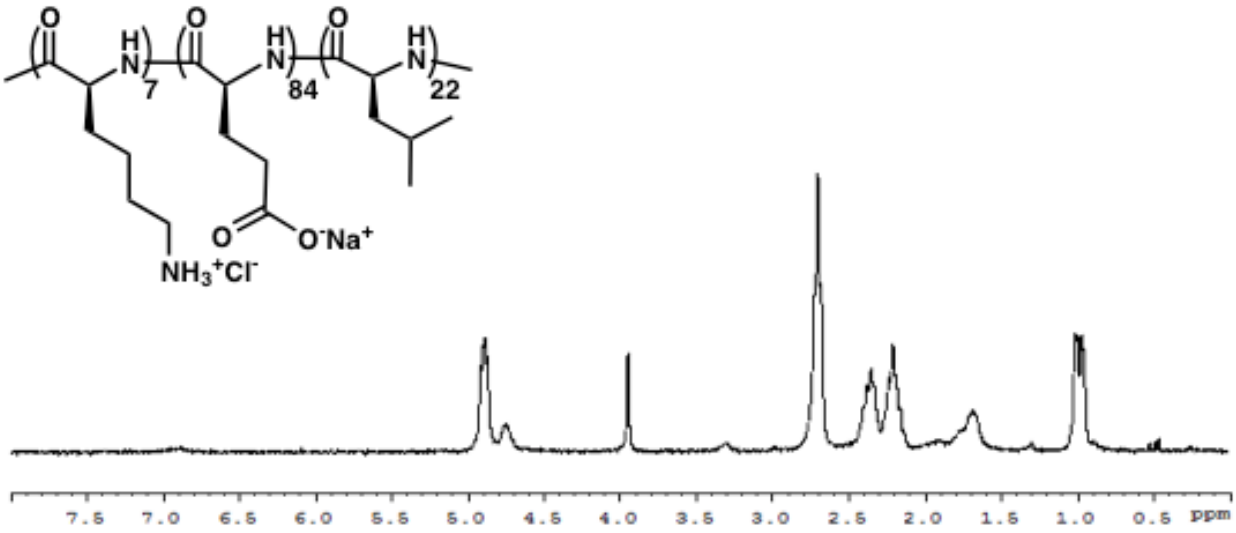
O
H
N
7
84
22
O
O⁻Na⁺
NH₃⁺Cl⁻
7.5 7.0 6.5 6.0 5.5 5.0 4.5 4.0 3.5 3.0 2.5 2.0 1.5 1.0 0.5 ppm

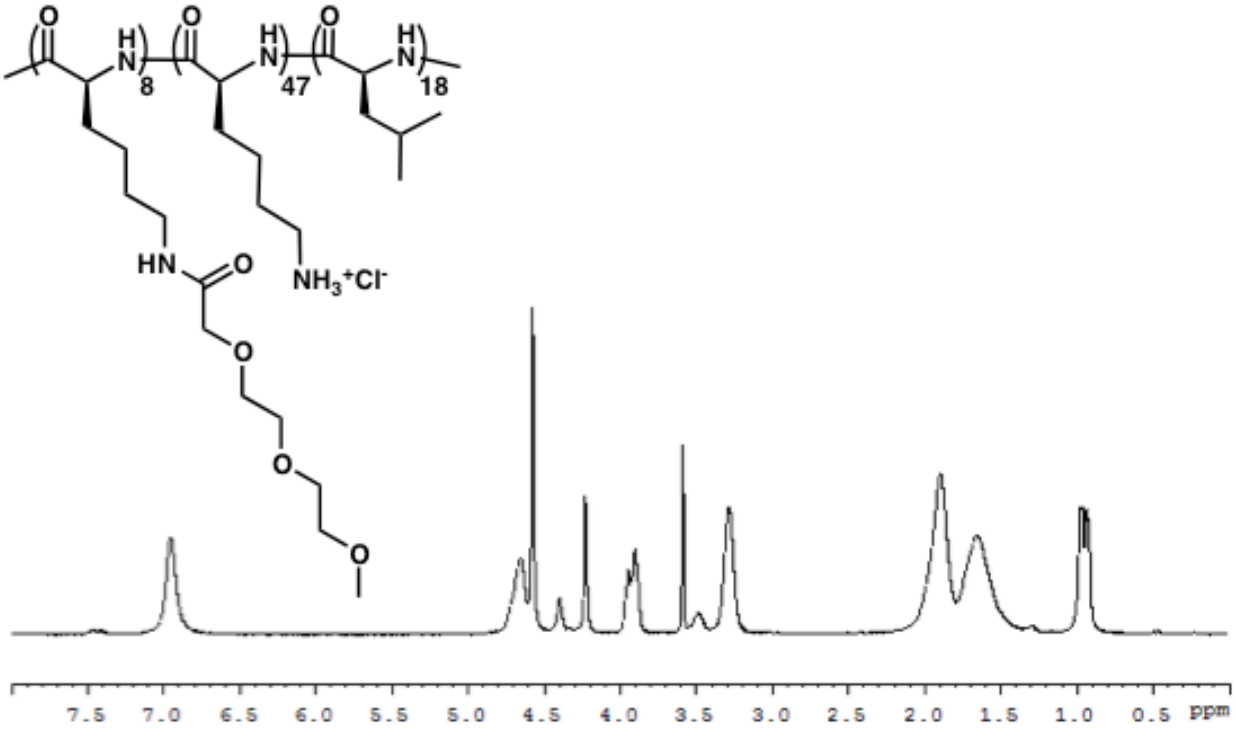
O
H
N
8
47
18
HN
O
NH₃⁺Cl⁻
7.5 7.0 6.5 6.0 5.5 5.0 4.5 4.0 3.5 3.0 2.5 2.0 1.5 1.0 0.5 ppm

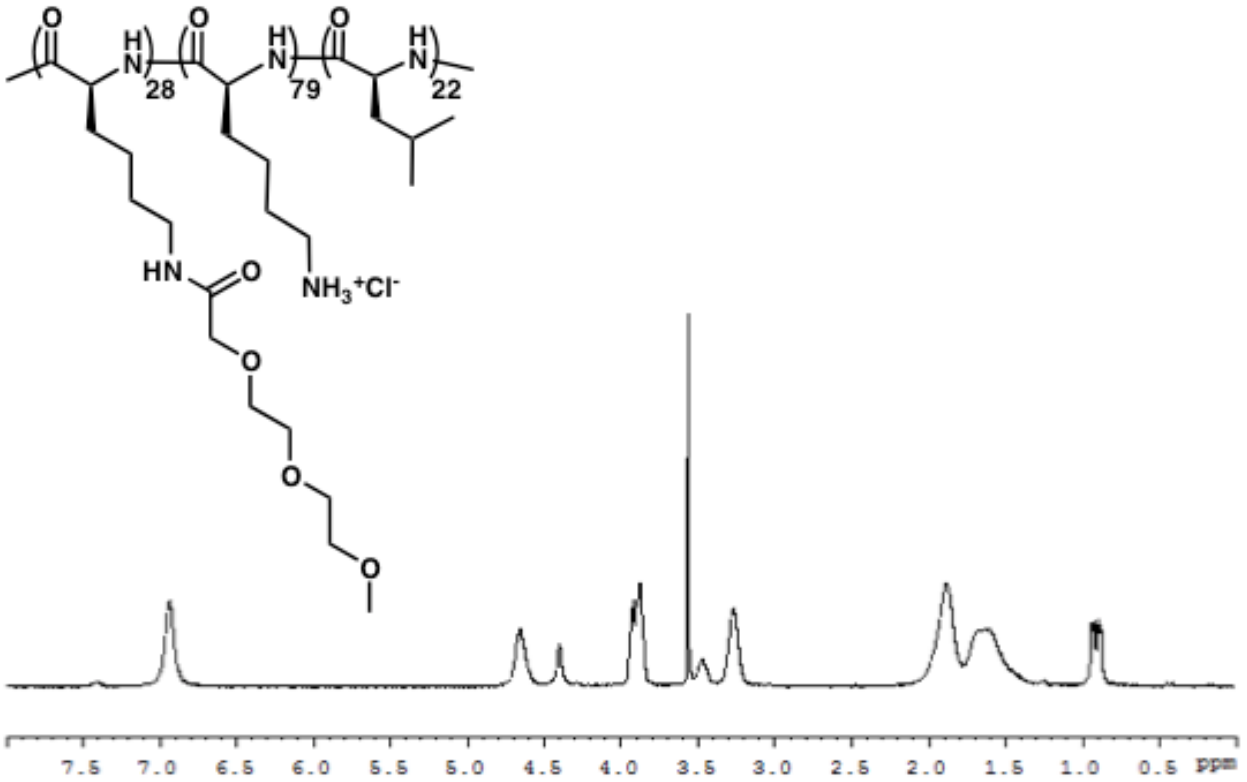

3.18 References

(1) Du, J.; O'Reilly, R. K. *Soft Matter* **2009**, *5*, 3544.

(2) Tanner, P.; Baumann, P.; Enea, R.; Onaca, O.; Palivan, C.; Meier, W. *Accounts of Chemical Research* **2011**, *44*, 1039.

(3) Holowka, E. P.; Sun, V. Z.; Kamei, D. T.; Deming, T. J. *Nat Mater* **2007**, *6*, 52.

(4) Holowka, E. P.; Pochan, D. J.; Deming, T. J. *Journal of the American Chemical Society* **2005**, *127*, 12423.

(5) Bellomo, E. G.; Wyrsta, M. D.; Pakstis, L.; Pochan, D. J.; Deming, T. J. *Nature Materials* **2004**, *3*, 244.

(6) Iatrou, H.; Frielinghaus, H.; Hanski, S.; Ferderigos, N.; Ruokolainen, J.; Ikkala, O.; Richter, D.; Mays, J.; Hadjichristidis, N. *Biomacromolecules* **2007**, *8*, 2173.

(7) Rong, G.; Deng, M.; Deng, C.; Tang, Z.; Piao, L.; Chen, X.; Jing, X. *Biomacromolecules* **2003**, *4*, 1800.

(8) Sun, J.; Chen, X.; Deng, C.; Yu, H.; Xie, Z.; Jing, X. *Langmuir* **2007**, *23*, 8308.

(9) Nagayasu, A.; Uchiyama, K.; Kiwada, H. *Advanced Drug Delivery Reviews* **1999**, *40*, 75.

(10) Brooks, H.; Lebleu, B.; VivËs, E. *Advanced Drug Delivery Reviews* **2005**, *57*, 559.

(11) Sela, M.; Katchalski, E. In *Advances in Protein Chemistry*; C.B. Anfinsen, M. L. A. K. B., John, T. E., Eds.; Academic Press: 1959; Vol. Volume 14, p 391.

(12) Matter, Y.; Enea, R.; Casse, O.; Lee, C. C.; Baryza, J.; Meier, W. *Macromolecular Chemistry and Physics* **2011**, *212*, 937.

(13) Stoenescu, R.; Meier, W. *Chemical Communications* **2002**, *0*, 3016.

(14) Wittemann, A.; Azzam, T.; Eisenberg, A. *Langmuir* **2007**, *23*, 2224.

(15) Idelson, M.; Blout, E. R. *Journal of the American Chemical Society* **1958**, *80*, 2387.

(16) Deming, T. J. *Macromolecules* **1999**, *32*, 4500.

(17) Mitchell, D. J.; Steinman, L.; Kim, D. T.; Fathman, C. G.; Rothbard, J. B. *The Journal of Peptide Research* **2000**, *56*, 318.

(18) Schaffer, D. V.; Fidelman, N. A.; Dan, N.; Lauffenburger, D. A. *Biotechnology and Bioengineering* **2000**, *67*, 598.

(19) Holowka, E. P. Dissertation, University of California Santa Barbara, 2006.

(20) Klein, H. F.; Karsch, H. H. *Inorganic Chemistry* **1975**, *14*, 473.

(21) Yang, C.-Y.; Song, B.; Ao, Y.; Nowak, A. P.; Abelowitz, R. B.; Korsak, R. A.; Havton, L. A.; Deming, T. J.; Sofroniew, M. V. *Biomaterials* **2009**, *30*, 2881.

CHAPTER FOUR

Glycopolypeptide Vesicles

4.1 Abstract

We described the preparation and assembly of glycosylated amphiphilic diblock copolypeptides, where the hydrophilic glycosylated segments adopt either α-helical or disordered conformations. In this study, glycosylated amphiphilic diblock copolypeptides were prepared using poly(L-leucine), poly(L), as the hydrophobic segment, and poly(α-D-galactopyranosyl-L-lysine), poly(α-gal-K), or poly(α-D-galactopyranosyl-L-cysteine sulfone), poly(α-gal-C^{O2}), as the hydrophilic segment. The poly(α-gal-K) and poly(α-gal-C^{O2}) segments are known to be fully α-helical (>90% at 20°C) and fully disordered conformation in water, respectively. We found that block copolypeptides containing galactosylated hydrophilic segments of either α-helical or disordered conformation give different assembly morphologies, where the disordered glycopolypeptide segments favor vesicle formation and also present sugar residues that more effectively bind to biological targets.

4.2 Introduction

There has been considerable recent interest in the development of multifunctional, nanoscale carriers for targeted delivery of therapeutics.[1-3] To precisely control the nanostructured morphology of these delivery vehicles, including shape (e.g. spherical micelles, cylindrical micelles, discs, or vesicles) and internal structure (e.g. spotted, segmented, or core-shell), the

assembly of amphiphilic block copolymers in aqueous solution has been highly useful.[4,5] However, the incorporation of multifunctionality (e.g. for cellular targeting, uptake, or intracellular release of cargos),[6-8] can often perturb the self-assembly process, leading to different morphologies with altered stabilities. We are pursuing the development of block copolypeptide based drug carriers since they are resorbable materials possessing the ordered chain conformations of proteins, which provide an additional means to direct nanostructure independent of many other parameters, such as amino acid composition.[9-11] Here, we describe the preparation and assembly of glycosylated amphiphilic diblock copolypeptides, where the hydrophilic glycosylated segments adopt either α-helical or disordered chain conformations. These distinct glycopolypeptide conformations were found to significantly impact both block copolymer self-assembly as well as the ability of sugar residues in these assemblies to bind to biological targets. These results show how careful choice of polypeptide chain conformations can be used to direct assembly of nanocarriers into desired morphologies and simultaneously enhance their bioactive functionality.

Glycosylation of polymeric drug and gene carriers has been shown to lower cytotoxicity, enhance aqueous solubility, and provide targeting to specific cells and organs.[12,13] It is also well known in biology that the way in which sugar functional groups are presented greatly affects their ability to bind targets and signal cells.[14] We recently reported the preparation of fully glycosylated, high molar mass synthetic polypeptides, which are water soluble and mimic the structures of naturally occurring glycoproteins.[15,16] A key feature of these glycopolymers is that their chain conformations are readily controlled, either by choice of peptide backbone or by selective oxidation of side-chain functional groups, such that fully α-helical or fully disordered chains can be obtained. We have now incorporated these glycopolypeptides as hydrophilic

segments in amphiphilic diblock copolypeptides to study their aqueous self-assembly and evaluate the properties of the resulting nanostructures. While much is known about how different chain conformations of hydrophobic polypeptide segments influence nanoscale morphology, little is known about the corresponding role played by hydrophilic polypeptide conformations in self assembly.[17-20] This has been difficult to study since hydrophilic polypeptide segments presenting similar functionality but differing only in conformation are rare. Here, we have found that block copolypeptides containing galactosylated hydrophilic segments of either α-helical or disordered conformation give different assembly morphologies, where the disordered glycopolypeptide segments favor vesicle formation and present sugar residues that more effectively bind to biological targets.

Previously, we and others reported that amphiphilic diblock copolypeptides containing α-helical hydrophobic segments assemble in water to form spherical, unilamellar vesicles ranging in diameter from tens of nanometers to tens of microns.[18,19,21-25] The rod-like conformations of these hydrophobic segments were found to favor side-by-side packing resulting in lamellar vesicle membranes, while samples with disordered hydrophobic segments were found to pack into spherical micelles,[26,27] similar to other, conformationally disordered, synthetic block copolymers.[5] Block copolypeptides containing hydrophilic segments with either disordered or α-helical conformations in combination with α-helical hydrophobic segments have been found to give vesicular assemblies under certain conditions.[18,19,21-25] However, it has been difficult to unequivocally determine the role of the hydrophilic chain conformation in directing nanostructure, since there have been significant differences between the disordered and α-helical hydrophilic segments in these materials (e.g. ionic vs. nonionic). For example, both nonionic poly(N_ε-2-(2-(2-methoxyethoxy)ethoxy)acetyl-L-lysine)$_{100}$-*block*-poly(L-leucine)$_{20}$ ($K^P_{100}L_{20}$) with

an α-helical hydrophilic segment and ionic poly(L-homoarginine·HCl)$_{60}$-*block*-poly(L-leucine)$_{20}$ ($R^{H}_{60}L_{20}$) with a disordered hydrophilic segment can be assembled into micron sized vesicles in water.[18,19] Some ionic vesicles can be neutralized by adjustment of pH, which results in a transition from disordered to α-helical conformation, but the uncharged, α-helical polypeptide segments are sparingly soluble in water and precipitate above micromolar concentrations.[28,29] Likewise, $K^{P}_{100}L_{20}$ samples with nonionic, disordered hydrophilic segments have been prepared using racemic K^{P} residues, yet inter-chain H-bonding interactions in the resulting disordered segments limit their aqueous solubility as well.[18] Consequently, there remains a need for fully α-helical and disordered hydrophilic polypeptide segments that display similar functionality to determine how hydrophilic chain conformation can be used to direct nanoscale assembly and control presentation of polypeptide functionality.

4.3 Preparation of Glycosylated Amphiphilic Diblock Copolypeptides

In this study, glycosylated amphiphilic diblock copolypeptides were designed to incorporate poly(α-D-galactopyranosyl-L-lysine), poly(α-gal-K),[15] and poly(α-D-galactopyranosyl-L-cysteine sulfone), poly(α-gal-C^{O2}),[16] hydrophilic segments, which are known to be fully α-helical (> 90% at 20 ºC) and fully disordered in water, respectively. The precursor galactosylated amino acid *N*-carboxyanhydride (α-gal-K NCA and α-gal-C NCA) monomers[15,16] were used to prepare diblock copolymers containing galactose bearing hydrophilic segments ca. 65 residues long connected to α-helical hydrophobic oligoleucine segments ca. 20 residues long, i.e. (α-gal-K)$_{65}L_{20}$ and (α-gal-C)$_{65}L_{20}$ (**Figure 4.1**). These chain lengths were chosen to encourage assembly into vesicles, which are desirable nanostructures that can encapsulate both hydrophilic

and hydrophobic cargos,[6-8] and are based on optimized compositions determined for other vesicle forming diblock copolypeptides.[19, 22-25] Synthesis of these copolypeptides using $(PMe_3)_4Co$ initiator in THF yielded samples with narrow chain length distributions and desired compositions,[30] and removal of protecting groups gave the galactosylated amphiphilic block copolymers (**Table 4.1**).[15,16] Since poly(α-gal-C) is partially α-helical in water, we oxidized the thioether linkages in these segments to the corresponding sulfones to produce copolypeptides with fully disordered poly(α-gal-C^{O2}) hydrophilic chains (**Figure 4.1**).[16] Circular dichroism analysis of the block copolymers confirmed that $(\alpha\text{-gal-K})_{65}L_{20}$ is predominantly α-helical in water, and that $(\alpha\text{-gal-C}^{O2})_{65}L_{20}$ is predominantly disordered in water (**Figure 4.2**).

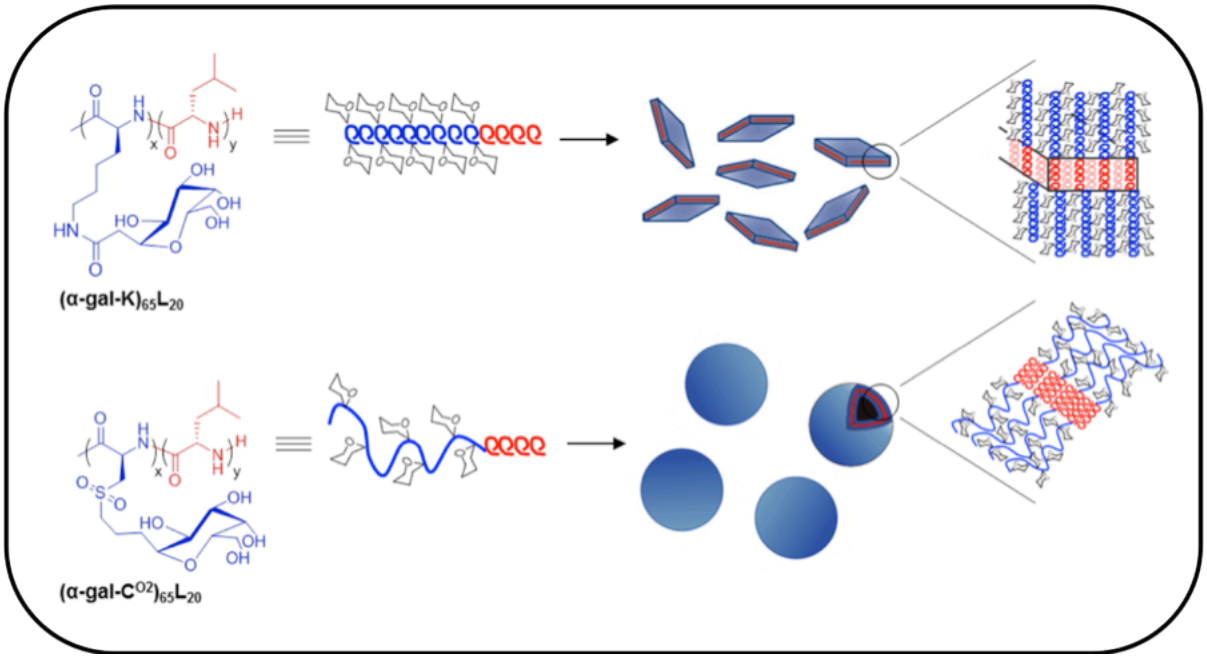

Figure 4.1 Schematic showing structures of amphiphilic glycosylated diblock copolypeptides and observed self-assemblies.

Table 4.1 Characterization and properties of $(\alpha\text{-gal-C})_{65}L_{20}$ and $(\alpha\text{-gal-K})_{65}L_{20}$ diblock copolypeptides.

Block - Copolypeptide	M_n[a]	M_w/M_n[a]	Found Composition[b]	Yield (%)[c]	Self-Assembled Structure[d]
$(\alpha\text{-gal-C})_{65}L_{20}$	30,910	1.09	$(\alpha\text{-gal-C})_{65}L_{22}$	95	V
$(\alpha\text{-gal-K})_{65}L_{20}$	33,130	1.07	$(\alpha\text{-gal-K})_{67}L_{23}$	99	P, A

[a] Hydrophilic segment lengths (number average molecular weight, M_n, for α-gal-K, and α-gal-C segments) and polydispersities (M_w/M_n) determined using gel permeation chromatography and ^{1}H NMR. [b] Calculated using ^{1}H NMR. [c] Total isolated yield of diblock glycopolypeptide. [d] Structures observed visually using optical microscopy (V = vesicle, A = irregular aggregate, P = plate).

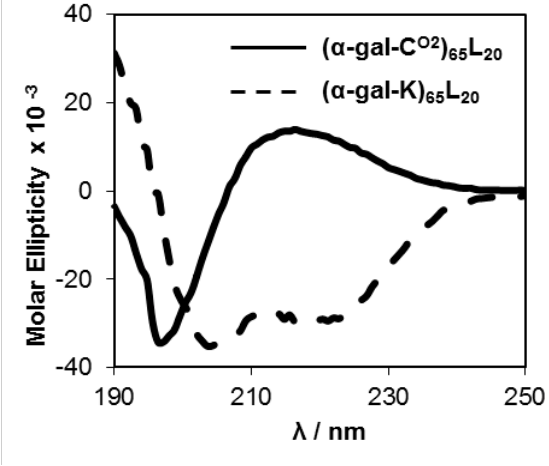

Figure 4.2 Circular dichroism spectra of glycosylated diblock copolypeptides. Samples are $(\alpha\text{-gal-C}^{O2})_{65}L_{20}$ (solid line) and $(\alpha\text{-gal-K})_{65}L_{20}$ (dashed line), 0.2 mg/mL in deionized water. Molar ellipticity is reported in millideg·cm^2·dmol^{-1}.

4.4 Self-assembly of Glycosylated Amphiphilic Diblock Copolypeptides

Attempts were made to assemble vesicles from the galactose containing copolypeptides using mixed solvent annealing, which has been found to assist formation of ordered nanostructures in many other block copolypeptide systems.[18,21] For solvent annealing, two solvent systems were used to self-assemble vesicles, THF to water ratio of 1:1 and DMSO to water ratio of 1:1. The hydrophilic chain conformations of the galactosylated block copolypeptides were found to strongly influence their self assembly in water as visualized by

DIC. The sample with a disordered hydrophilic segment, $(\alpha\text{-gal-C}^{O2})_{65}L_{20}$, gave exclusively vesicles with diameters ranging from hundreds of nanometers to a few microns in diameter in the THF and water cosolvent system (**Figure 4.3**A and F). However in the DMSO and water cosolvent system only aggregates were seen (**Figure 4.3**B).

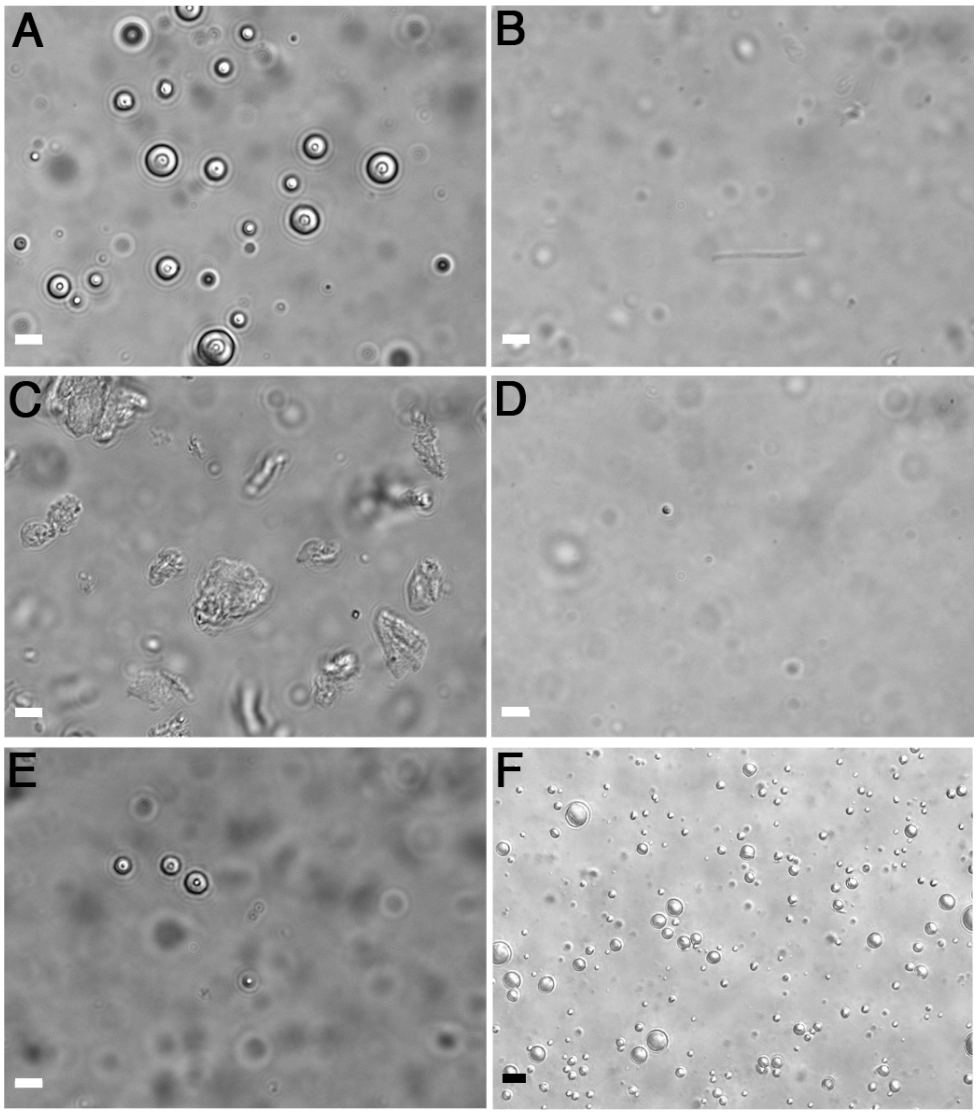

Figure 4.3 Imaging of glycosylated block copolymer self-assemblies. DIC images of (A) $(\alpha\text{-gal-C}^{O2})_{65}L_{20}$ vesicle suspension processed with THF and water, (B) $(\alpha\text{-gal-C}^{O2})_{65}L_{20}$ vesicle suspension processed with DMSO and water, (C) $(\alpha\text{-gal-K})_{65}L_{20}$ plates and aggregates processed with THF and water, (D) $(\alpha\text{-gal-K})_{65}L_{20}$ vesicles and aggregates processed with DMSO and water and (E) $(\alpha\text{-gal-K})_{65}L_{20}$ vesicles and aggregates processed with 3 % (v/v) TFA in THF and water. Whit scale bars = 5 μm. (F) lower magnification of $(\alpha\text{-gal-C}^{O2})_{65}L_{20}$ vesicle suspension processed with THF and water. Black scale bar = 10 μm.

In contrast to the results above, the highly α-helical sample, $(\alpha\text{-gal-K})_{65}L_{20}$ gave nearly no vesicles and instead an abundance of micron sized irregular aggregates and some platelike objects were observed after processing with the THF and water cosolvent system (**Figure 4.3**C). Similar aggregation behavior has been observed previously in block copolypeptides containing either shorter hydrophilic or longer hydrophobic segment lengths, i.e. lower hydrophilic volume fractions.[18,21] Their inability to form vesicles is likely due to the smaller hydrophilic content of these samples not being able to effectively solubilize and stabilize the assemblies against further aggregation. The rod-like nature of the α-helical hydrophilic segments in $(\alpha\text{-gal-K})_{65}L_{20}$ also likely acts to stiffen any membranes formed, leading to rigid sheet-like membranes that lack the flexibility needed to accommodate vesicle curvature.[18] Processing this sample with the DMSO to water cosolvent system allowed the assembly of smaller aggregates to difficult to visualize with DIC (**Figure 4.3**D). A way to overcome the stiffening of the membranes into sheet-like structures with rod-rod polypeptide chains is the use of trifluoroacetic acid (TFA) during processing. This method was previously found to be to help with the self-assembly of vesicle with the rod-rod polypeptide, $K^{P}_{100}L_{20}$.[18] If $(\alpha\text{-gal-K})_{65}L_{20}$ was dispersed in 3 % (v/v) TFA in THF, followed by the addition of an equal volume of water and dialyzed to remove TFA and THF, spherical assemblies and irregular aggregates were observed, with minimal sheet-like structures (**Figure 4.3**E).

The vesicular morphology of the $(\alpha\text{-gal-C}^{O2})_{65}L_{20}$ assemblies was confirmed by labeling their hydrophobic domains with $DiOC_{18}$ dye and imaging thin slices through the suspensions of the samples using laser scanning confocal microscopy (LSCM), which revealed their membrane structure and hydrophilic interior (**Figure 4.4**A). The ability of these vesicles to encapsulate

hydrophilic cargos was also shown by their retention of Texas Red labeled dextran (Mn = 3000 Da) after removal of unencapsulated cargo by dialysis (**Figure 4.4**B).

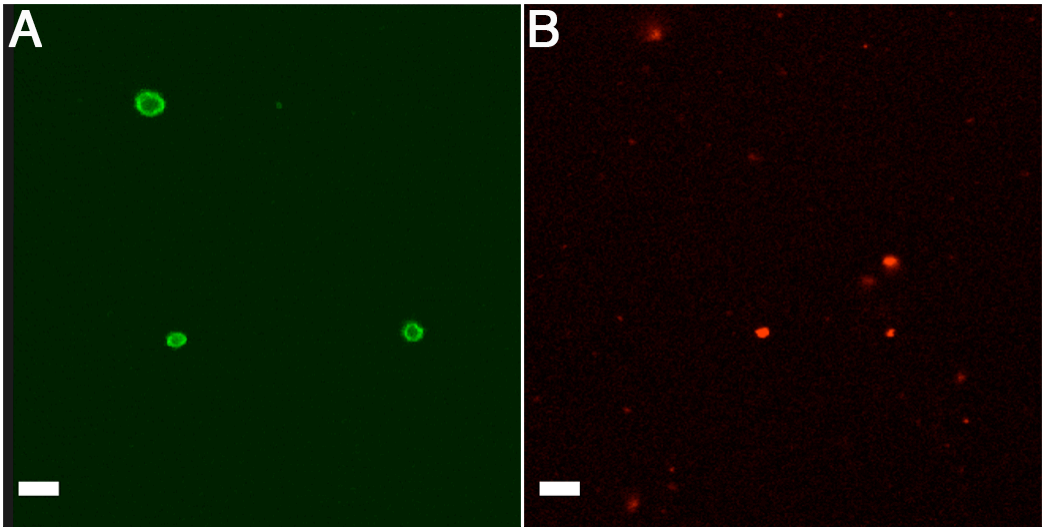

Figure 4.4 Imaging of glycosylated block copolymer self assemblies. LSCM images of (A) (α-gal-C^{O2})$_{65}L_{20}$ vesicles containing $DiOC_{18}$ dye and (B) Texas Red labeled dextran encapsulated within (α-gal-C^{O2})$_{65}L_{20}$ vesicles. White scale bars = 5 μm.

From these solvent annealing methods, we showed the presence of different hydrophilic chain conformations in (α-gal-K)$_{65}L_{20}$ and (α-gal-C^{O2})$_{65}L_{20}$ thus significantly altered their self-assembled morphologies, where the desired vesicle structures were favored by the disordered segments in (α-gal-C^{O2})$_{65}L_{20}$. The flexibility in the poly(α-gal-C^{O2}) segments also allows better mixing with water, essentially increasing their hydrophilicity, compared to the conformationally rigid poly(gal-K) chains. The more open structure of solvated disordered poly(α-gal-C^{O2}) segments should also partially frustrate packing of the rigid hydrophobic oligoleucine segments, making the vesicle membranes themselves more dynamic, flexible and able to accommodate curvature.[21]

4.5 Cytotoxicity of Glycosylated Amphiphilic Diblock Copolypeptide, $(\alpha\text{-gal-C}^{O2})_{65}L_{20}$

Since $(\alpha\text{-gal-C}^{O2})_{65}L_{20}$ self-assembled into vesicles using the THF and water solvent annealing system it was utilized for further studies. The $(\alpha\text{-gal-C}^{O2})_{65}L_{20}$ vesicles were subsequently passed through 1.0, 0.4 and 0.2 μm track-etched polycarbonate (PC) membranes to determine membrane flexibility and stability. The $(\alpha\text{-gal-C}^{O2})_{65}L_{20}$ vesicles could be extruded to obtain low polydispersity nanovesicles with average diameters of 140 nm (PDI = 0.060), which are a desirable size range for use as circulating nanocarriers (**Figure 4.5C**).[6-8] Extruded suspension was imaged with negative stain transmission electron microscopy (TEM) confirming uniform vesicular assemblies with diameter less than 200 nm (**Figure 4.5**A and B).

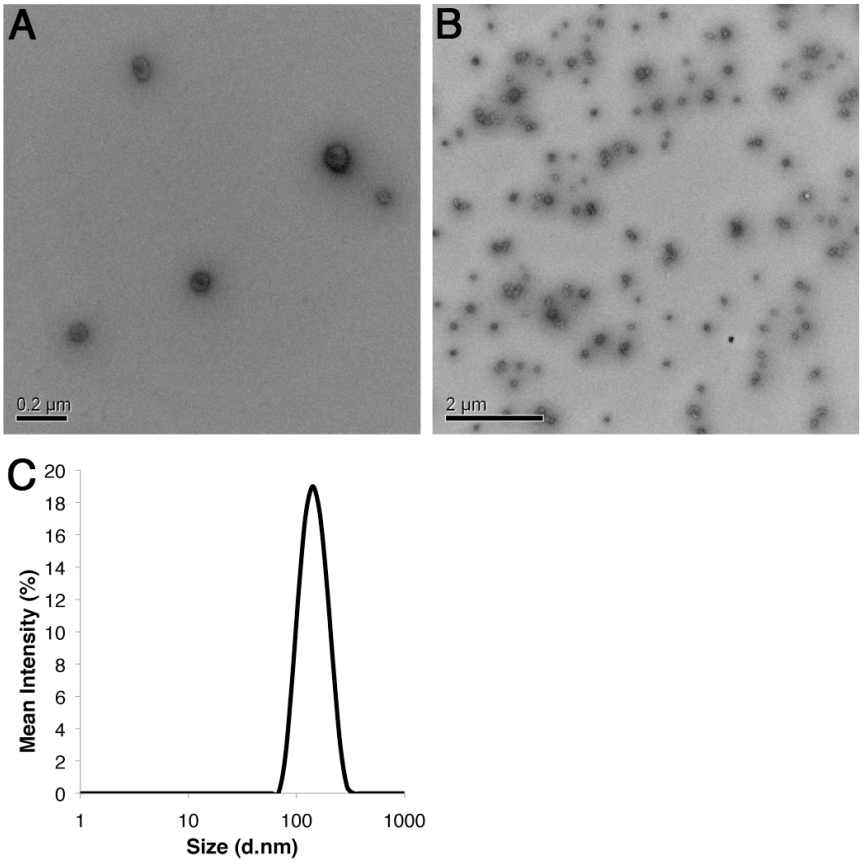

Figure 4.5 Imaging of glycosylated block copolymer self assemblies. (A) TEM image of extruded $(\alpha\text{-gal-C}^{O2})_{65}L_{20}$ vesicles, scale bar = 0.2 μm. (B) TEM image of extruded $(\alpha\text{-gal-C}^{O2})_{65}L_{20}$ vesicles, scale bar = 2.0 μm. (C) DLS of extruded $(\alpha\text{-gal-C}^{O2})_{65}L_{20}$ vesicles.

Cytotoxicity of the extruded (α-gal- C^{O2})$_{65}L_{20}$ vesicles was measured by MTS assay in HeLa Cells, which were found to be highly viable up to polypeptide concentrations of 200 μg/mL (**Figure 4.6**). The (α-gal- C^{O2})$_{65}L_{20}$ vesicles were found to be minimally cytotoxic in comparison to cationic polypeptide vesicles such as $R^{H}_{60}L_{20}$.[19] This low cytotoxicity, even at high concentrations, make these vesicles attractive for development as biofunctional drug carriers with controlled nanostructure.

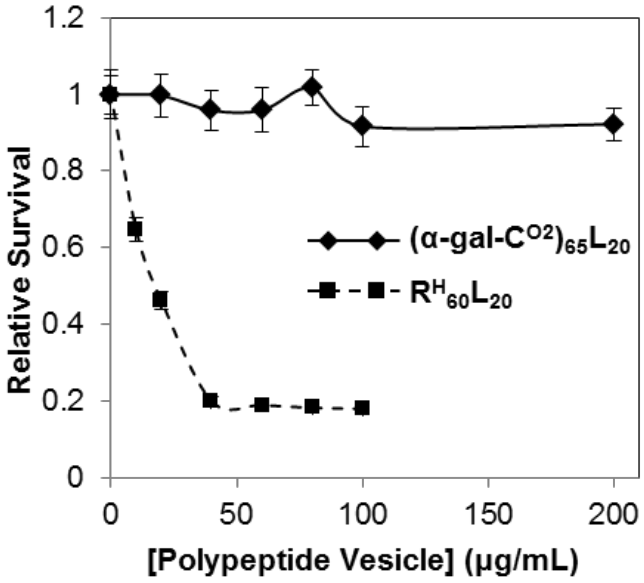

Figure 4.6 Relative survival of HeLa cells incubated for 5 hours with copolypeptide vesicles determined using MTS assay. Samples are (α-gal-C^{O2})$_{65}L_{20}$ (solid line) and $R^{H}_{60}L_{20}$ (dashed line).

4.6 Lectin Binding of Glycosylated Amphiphilic Diblock Copolypeptides

Although (α-gal-K)$_{65}L_{20}$ and (α-gal-C^{O2})$_{65}L_{20}$ self assemble into different structures in water, they were both designed to present the same α-D-galactosyl functionality. To determine how the different glycopolypeptide conformations affect presentation and bioactivity of their pendant galactose units, we separately incubated (α-gal-K)$_{65}$ and (α-gal-C^{O2})$_{65}$ homopolymers

with lectins in a precipitation assay. We chose ricinus communis agglutinin (RCA_{120}) for the polymer binding lectin since it is known to specifically and selectively bind to galactosyl groups, and concanavalin A (Con A) as a control lectin that binds mannosyl and glucosyl, but not galactosyl, groups.[14] When the galactosyl-polypeptides were incubated with RCA_{120}, turbidity of both solutions was found to increase rapidly as expected from aggregation due to lectin binding (**Figure 4.7**).[14] Neither glycopolymer solution became turbid when incubated with Con A, indicating the interactions with RCA_{120} are specific binding interactions between this lectin and the galactosyl groups of the polymers.

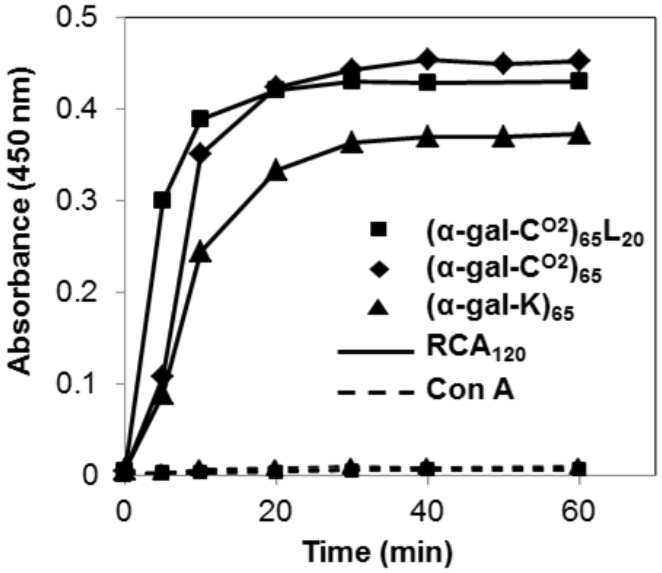

Figure 4.7 Lectin binding of glycopolypeptides versus time. Turbidity (absorbance at 450 nm) of $(\alpha\text{-gal-K})_{65}$ (▲), $(\alpha\text{-gal-C}^{O2})_{65}$ (♦), or $(\alpha\text{-gal-C}^{O2})_{65}L_{20}$ vesicles (■) when mixed with lectin RCA_{120} (solid lines) or Con A (dashed line), in PBS buffer. Glycopeptide concentration = 3.3 mM.

Visible absorbance measurements (450 nm) were used to quantify mixture turbidity, which has been shown to correlate with the concentration of sugar groups available for lectin binding.[31] Notably, at equivalent sugar concentrations, the disordered $(\alpha\text{-gal-C}_{O2})_{65}$ polymer gave

rise to increased turbidity when mixed with RCA_{120} compared to the α-helical $(\alpha\text{-gal-K})_{65}$ polymer, which indicates the disordered $(\alpha\text{-gal-C}^{O2})_{65}$ is more effective at binding to the lectin (**Figure 4.7**). Similarly, $(\alpha\text{-gal-C}^{O2})_{65}L_{20}$ vesicle suspensions mixed with RCA_{120} also became turbid, to roughly the same extent as the $(\alpha\text{-gal-C}^{O2})_{65}$ homopolymer, indicating the disordered glycopolymer segments remain effective in binding biological targets when incorporated into nanoscale vesicles. Comparison of the ability of helical and disordered glycopolymers to bind to lectins has been studied previously, but with mixed results.[32,33] In one study, glycopolymers based on helical polyisocyanide and flexible polyacrylamide backbones were compared.[32] Similar to our findings, the disordered polyacrylamide was found to bind more efficiently to the lectin, but the analysis was complicated by use of different polymer backbones and unknown helical content of the polyisocyanide.[34] Another study compared glycosylated poly(lysines), where the enantiomerically pure (α-helical) and racemic (disordered) polymers were found to bind to lectins with nearly equal affinity.[33] In this study, the α-helical contents of the ordered polymers ranged from 30 to 62%, indicating considerable disorder, which may explain why little difference in lectin binding between samples was observed. Our results here show that a significant difference in lectin binding for α-helical versus disordered polypeptides does exist when using ordered samples with high (>90%) α-helical content, which can pack the sugar residues densely around the chain.

4.7 Conclusion

Overall, we have found that the chain conformation of hydrophilic polypeptide segments can play a significant role in dictating both structure and function in self assembled

nanostructures. The use of hydrophilic segments with disordered conformations in amphiphilic diblock copolypeptides was found to be particularly effective both for formation of vesicular assemblies as well as presentation of functionality in an accessible, active form. The low cytotoxicity, biological targeting capability, and nanoscale size make these vesicles attractive for development as biofunctional drug carriers with controlled nanostructure.

4.8 Experimental

4.8.1 General Methods:

Unless stated otherwise, reactions were conducted in oven-dried glassware under an atmosphere of nitrogen using anhydrous solvents. Hexanes, THF, DCM, and DMF were purified by first purging with dry nitrogen, followed by passage through columns of activated alumina. Deionized water (18 MΩ-cm) was obtaining by passing in-house deionized water through a Millipore Milli-Q Biocel A10 purification unit. All commercially obtained reagents were used as received without further purification unless otherwise stated. Reaction temperatures were controlled using an IKA temperature modulator, and unless stated otherwise, reactions were performed at room temperature (RT, approximately 20 °C). Thin-layer chromatography (TLC) was conducted with EMD gel 60 F254 precoated plates (0.25 mm) and visualized using a combination of UV, anisaldehyde, and phosphomolybdic acid staining. Selecto silica gel 60 (particle size 0.032–0.063 mm) was used for flash column chromatography. ^{1}H NMR spectra were recorded on Bruker spectrometers (at 500 MHz) and are reported relative to deuterated solvent signals. Data for ^{1}H NMR spectra are reported as follows: chemical shift (δ ppm), multiplicity, coupling constant (Hz) and integration. Splitting patterns are designated as follows: s, singlet; d, doublet;

t, triplet; q, quartet; m, multiplet and br, broad. ^{13}C NMR spectra were recorded on Bruker Spectrometers (at 125 MHz). Data for ^{13}C NMR spectra are reported in terms of chemical shift. High-resolution mass spectrometry (HRMS) was performed on a Micromass Quatro-LC Electrospray spectrometer with a pump rate of 20 μL/min using electrospray ionization (ESI). All Fourier Transform Infrared (FTIR) samples were prepared as thin films on NaCl plates, spectra were recorded on a Perkin Elmer RX1 FTIR spectrometer, and are reported in terms of frequency of absorption (cm^{-1}). Tandem gel permeation chromatography/light scattering (GPC/LS) was performed on a SSI Accuflow Series III liquid chromatograph pump equipped with a Wyatt DAWN EOS light scattering (LS) and Optilab rEX refractive index (RI) detectors. Separations were achieved using 10^5, 10^4, and 10^3 Å Phenomenex Phenogel 5 mm columns using 0.10 M LiBr in DMF as the eluent at 60 °C. All GPC/LS samples were prepared at concentrations of 5 mg/mL. The preparation of 2,3,4,6-tetra-*O*-acetyl-α-D-galactopyranosyl-L-lysine-*N*-carboxyanhydride[15] (α-gal-K NCA), 2,3,4,6-tetra-O-acetyl-α-D-galactopyranosyl-L-cysteine-N-carboxyanhydride[16] (α-gal-C NCA), L-leucine N-carboxyanhydride (Leu NCA),[38] and $(PMe_3)_4Co$[39] have been previously reported.

4.8.2 Preparation of Glycosylated Diblock Copolypeptides:

All polymerization reactions were performed in a dinitrogen filled glove box. To a solution of α-gal-K NCA or α-gal-C NCA (1 equiv) in THF (50 mg/mL) was rapidly added, via syringe, a solution of $(PMe_3)_4$ Co in THF (0.05 equiv., 30 mg/mL). The reaction was stirred at RT and polymerization progress was monitored by FTIR. Polymerization reactions were generally complete within 3 hours. Immediately upon polymerization completion, aliquots were removed for GPC/LS and endgroup analysis[36] using 1K MW isocyanate terminated PEG. A solution of

Leu NCA in THF (0.33 equiv., 50 mg/mL) was added and the polymerization was monitored by FTIR. Polymerization reactions were generally complete within 3 hours. After complete consumption of NCA, reactions were removed from the glovebox and precipitated into hexanes. Solids were collected by centrifugation and washed with 2 portions of water at pH 2 (HCl), followed by DI water. The polymers were lyophilized to yield white solids. (95-99% yield).

4.8.3 Molecular Weight Determination:

The degree of polymerization (DP) of the first block, poly(α-gal-C) or poly(α-gal-K), was determined by ^{1}H NMR integrations of the aliquot end-capped with PEG. Integrations were calibrated using the polyethylene glycol chemical shift found at δ 3.64, and the polypeptide DP's were found to be $(\alpha\text{-gal-C})_{65}$ and $(\alpha\text{-gal-K})_{67}$. Polydispersities were determined by GPC/LS, M_w/M_n for $(\alpha\text{-gal-C})_{65}$ = 1.09 and M_w/M_n for $(\alpha\text{-gal-K})_{67}$ =1.07. The DP of the second block was determined by ^{1}H NMR integrations calibrated using the DP of the first block. Final polypeptide compositions were determined to be $(\alpha\text{-gal-C})_{65}L_{22}$ and $(\alpha\text{-gal-K})_{67}L_{23}$.

4.8.4 Poly(2,3,4,6-tetra-*O*-acetyl-α-D-galactopyranosyl-L-cysteine)$_{65}$-*b*-(leucine)$_{22}$:

^{1}H NMR (500 MHz, $CDCl_3$, 25 ºC): δ 5.39 (s, 65H), 5.26-5.17 (m, 128H), 4.27-4.02 (m, 359.5H), 3.16-2.98 (m, 132H), 2.61 (s, 126H), 2.15-1.96 (m, 893H), 1.89-1.52 (m, 882H), 0.97-0.84 (m, 136H). FTIR (thin film, THF): 3568, 3492, 3284, 2966, 2851, 2678, 1955, 1752, 1651, 1524, 1457, 1366 cm^{-1}.

4.8.5 Poly(2,3,4,6-tetra-*O*-acetyl-α-D-galactopyranosyl-L-lysine)$_{67}$-*b*-(leucine)$_{23}$:

^{1}H NMR (500 MHz, $CDCl_3$, 25 ºC): δ 5.42 (s, 67H), 5.34-5.04 (m, 200H), 4.75 (s, 71H), 4.31-3.80 (m, 396H), 3.19 (s, 225H), 2.76-2.36 (m, 257H), 2.2-1.26 (m, 1274H), 0.98-0.84 (m, 137H). FTIR (thin film, THF): 3272, 2966, 2853, 1752, 1654, 1541, 1450, 1365 cm^{-1}.

4.8.6 Glycosylated Diblock Copolypeptide Deprotection Procedure:

To a solution of acetylated (α-gal-C)$_{65}$L$_{22}$ or (α-gal-K)$_{67}$L$_{23}$ in DCM:methanol 1:2 (10 mg/mL) was added hydrazine monohydrate (4 equiv./ OH group). The reactions were stirred overnight at room temperature. The product was observed as a white precipitate. Reactions were quenched by addition of drops of acetone. Et_2O was added and the solids collected by centrifugation (99% yield). The solids were taken up with water and transferred to 2000 molecular weight cutoff dialysis tubing and dialyzed against Millipore water for 3 days, with water changes twice per day. Dialyzed polymers were lyophilized to dryness to yield white fluffy solids. (80% yield after dialysis)

4.8.7 Poly(α-D-galactopyranosyl-L-cysteine)$_{65}$-*b*-(leucine)$_{22}$; (α-gal-C)$_{65}$L$_{22}$:

^{1}H NMR (500 MHz, d-TFA, 25 ºC): δ 4.69 (s, 65H), 4.54-4.05 (m, 308H), 3.21-2.61 (m, 233H), 2.04-1.57 (m, 314H), 1.27 (s, 21H), 0.99-0.89 (m, 150H).

4.8.8 Poly(α-D-galactopyranosyl-L-lysine)$_{67}$-*b*-(leucine)$_{23;}$ (α-gal-K)$_{67}$L$_{23}$:

^{1}H NMR (500 MHz, D_2O, 25 ºC): δ 4.35 (s, 67H), 3.91-3.81 (m, 148H), 3.67 (s, 59H), 3.63-3.43 (m 257H), 3.05 (s, 135H), 2.66-2.38 (m, 153H), 1.88-1.08 (m, 552H), 0.85-0.71 (m, 61H).

4.8.9 Oxidation of $(\alpha\text{-Gal-C})_{65}L_{22}$:

$(\alpha\text{-Gal-C})_{65}L_{22}$ was dissolved in a solution of 5% acetic acid and 10% H_2O_2 in DI water (20 mg/mL), and the reaction was heated to 38 ºC for 16 hours. A few drops of 1M sodium thiosulfate were added, and then the reaction was transferred to 2000 molecular weight cutoff dialysis tubing, and dialyzed against Millipore water for 3 days, with water changes twice per day. Dialyzed copolypeptides were lyophilized to dryness to yield poly(α-D-galactopyranosyl-L-cysteine sulfone)$_{65}$-*b*-(leucine)$_{22}$ ($(\alpha\text{-gal-C}^{O2})_{65}L_{22}$) as a white fluffy solid (80% yield after dialysis). ^{1}H NMR (500 MHz, d-TFA, 25 ºC): δ 4.75 (s, 65H), 4.49 (s, 155H), 4.36-4.06 (m, 242H), 3.49 (s, 133H), 2.39-1.94 (m, 268H), 1.89-1.64 (m, 132H), 1.35 (s, 24H), 1.08-0.92 (m, 153H).

4.8.10 Circular Dichroism of Diblock Glycopolypeptides:

Circular dichroism spectra were recorded on an OLIS RSM CD spectrophotometer running in conventional scanning mode. Spectra (190–250 nm) were recorded in a quartz cuvette of 0.1 cm path length with samples prepared using Millipore deionized water. All spectra were recorded as an average of 3 scans. The spectra are reported in units of molar ellipticity $[\theta]$ (deg·cm^2·dmol^{-1}). The formula used for calculating molar ellipticity, $[\theta]$, was $[\theta] = (\theta \times 100 \times M_W)/(c \times l)$ where θ is the experimental ellipticity in millidegrees, M_W is the average molecular weight of a residue in g/mol, c is the peptide concentration in mg/mL; and l is the cuvette pathlength in cm. The percent a-helical content of the glycopeptides was estimated using the formula % a-helix = $100x(-[\theta]_{222nm} +3000)/39000)$ where $[\theta]_{222nm}$ is the measured molar ellipticity at 222 nm.[37]The calculated helicity of $(\alpha\text{-gal-K})_{67}L_{23}$ was 94%.

4.8.11 Preparation of Diblock Glycopolypeptide Assemblies:

Solid $(\alpha\text{-gal-C}^{O2})_{65}L_{22}$ or $(\alpha\text{-gal-K})_{67}L_{23}$ was dispersed in THF to give a 1% (w/v) suspension. The suspension was placed in a bath sonicator for 30 minutes to evenly disperse the polypeptide and reduce large particulates. An equivalent amount of Millipore water was then added to give a 0.5 % (w/v) suspension. The suspension became clear as the solution was mixed by vortexing. The mixture was then dialyzed (2,000 MWCO membrane) against Millipore water overnight with 3 water changes. Vesicular assemblies were also obtained via slow evaporation of the THF.

4.8.12 Differential Interference Microscopy (DIC):

Assembled copolypeptide suspensions of $(\alpha\text{-gal-C}^{O2})_{65}L_{22}$ or $(\alpha\text{-gal-K})_{67}L_{23}$ (0.5 % (w/v)) were visualized on glass slides with a spacer between the slide and the cover slip (double-sided tape or Secure Seal Imaging Spacer, *Grace Bio-labs*) allowing the structures to be minimally disturbed during focusing. The samples were imaged using a Zeiss Axiovert 200 DIC/Fluorescence Inverted Optical Microscope.

4.8.13 Extrusion of Vesicle Assemblies:

A 0.2 % (w/v) aqueous $(\alpha\text{-gal-C}^{O2})_{65}L_{22}$ vesicle suspension was extruded using an Avanti Mini-Extruder. Serial extrusion of vesicle suspensions were performed through Whatman Nuclepore Track-Etched polycarbonate (PC) membranes with decreasing filter pore sizes: 3 times through a 1.0 μm filter, 3 times through 0.4 μm filter, and 3 times through 0.2 μm filter. The PC membranes and filter supports are soaked in Millipore water for 10 minutes prior to extrusion.

4.8.14 Dynamic Light Scattering (DLS) of Extruded Vesicles:

A 0.2 % (w/v) solution of extruded (α-gal-C^{O2})$_{65}L_{22}$ vesicles was placed in a disposable cuvette and analyzed with the Malvern Zetasizer Nano ZS model Zen 3600 (Malvern Instruments Inc, Westborough, MA). A total scattering intensity of approximately 1 x 10^5 cps was targeted. The autocorrelation data was fitted using the CONTIN algorithm to determine the diameters of suspended assemblies.

4.8.15 Laser Scanning Confocal Microscopy (LSCM) of Fluorescently Labeled Vesicles:

LSCM images of (α-gal-C^{O2})$_{65}L_{22}$ vesicle suspensions were taken on a Leica Inverted TCS-SP1 MP-Inverted Confocal and Multiphoton Microscope equipped with an argon laser (476 and 488 nm blue lines), a diode (DPSS) laser (561 nm yellow-green line), and a helium-neon laser (633 nm far red line). Suspensions of the fluorescently labeled copolypeptides (0.5 % (w/v)) were visualized on glass slides with a spacer between the slide and the cover slip (Secure Seal Imaging Spacer, *Grace Bio-labs*) allowing the self-assembled structures to be minimally disturbed during focusing. Imaging of an xy plane with an optical z-slice showed that the assemblies were water filled, unilamellar vesicles.

4.8.16 Transmission Electron Microscopy (TEM) of Extruded Vesicles:

Extruded (α-gal-C^{O2})$_{65}L_{22}$ vesicle suspensions were diluted to 0.1 % (w/v). Samples (4 μL) were placed on a 300 mesh Formvar/carbon coated copper grid (Ted Pella) and allowed to remain on the grid for 60 seconds. Filter paper was used to remove the residual sample. One drop of 2 % (w/v) uranyl acetate (negative stain) was then placed on the grid for 90 seconds, and subsequently removed by washing with drops of Millipore water and removing the excess liquid

with filter paper. The grids were allowed to dry before imaging with JEM 1200-EX (JEOL) transmission electron microscope at 80 kV.

4.8.17 Encapsulation of Texas Red Labeled Dextran in Vesicles:

Vesicles composed of poly(α-gal-C^{O2})$_{65}$-*b*-(Leu)$_{22}$ were prepared as previously described, except the aqueous phase contained 0.125 mg/mL Texas red- labeled dextran (3000 Da). Vesicle solutions were dialyzed in 8000 MWCO tubing overnight to remove unencapsulated Texas red-labeled dextran. As a control, pre-formed (α-gal-C^{O2})$_{65}$-*b*-(Leu)$_{22}$ vesicles were incubated overnight with a 0.125 mg/mL Texas red-labeled dextran solution and then dialyzed in 8000 MWCO tubing overnight. The samples were then imaged by DIC and confocal microscopes as previously described. No fluorescence was observed in the pre-formed vesicles incubated with Texas red-labeled dextran.

4.8.18 Evaluation of Carbohydrate-Lectin Binding by Turbidity:

Ricinus Communis Agglutinin I (RCA_{120}) was purchased from Vector labs, Conconavalin A (Con A) was purchased from Sigma-Aldrich. Lectin solutions were prepared at a concentration of 2 mg/mL in 10 mM phosphate, 0.15 M NaCl, pH 7.8. Lectin solutions (600 μL) were transferred to cuvettes and baseline measurements were taken. Solutions of poly(α-gal-K)$_{67}$, poly(α-gal-C^{O2})$_{65}$, and poly(α-gal-C^{O2})$_{65}$-*b*-(Leu)$_{22}$ vesicles were prepared at a concentration of 1 mg/mL in DI water, and 60 μL of each solution was added to the cuvettes containing either RCA_{120} or Con A. Final glycopeptide concentrations were 3.3 mM. The solutions were gently mixed and absorbance spectra were recorded at various time points.

4.8.19 MTS Cell Proliferation Assay:

The MTS cell proliferation assay (CellTiter 96 AQ_{ueous} Non-Radioactive Cell Proliferation Assay) was used to quantify any cytotoxic effects of the poly(α-gal-C^{O2})$_{65}$-*b*-(Leu)$_{22}$ vesicle suspensions. HeLa cells were seeded at a density of $4x10^4$ cells per cm^{-2} on a 96-well plate prior to the experiment. At the start of the experiment, the cell culture medium was aspirated, and the cells were incubated in medium containing the polypeptide vesicles for 5 h in a 37 ºC humidified atmosphere with 5% CO_2. The incubation medium was the same as the cell culture medium except for the absence of FBS, penicillin, and streptomycin. Following the 5 h incubation period, the medium containing polypeptide vesicles was aspirated. Fresh medium containing 20% MTS was then added to the cells. The cells were placed back into a CO_2 incubator for 1 h and then the absorbance at 490 nm (A_{490}) was measured with an Infinite F200 plate reader (Tecan Systems Inc., San Jose, CA, USA). The background absorbance was read at 700 nm (A_{700}) and subtracted from A_{490}. The relative survival of the cells at each polypeptide concentration was quantified by taking the ratio of the (A_{490}–A_{700}) values and comparing between the experimental and control cells.

4.9 References

(1) Torchilin, V. P. *Advanced Drug Delivery Reviews* **2006**, *58*, 1532.

(2) Bae, Y.; Fukushima, S.; Harada, A.; Kataoka, K. *Angewandte Chemie, International Edition* **2003**, *42*, 4640.

(3) Bae, Y.; Jang, W-D.; Nishiyama, N.; Fukushima, S.; Kataoka, K. *Molecular BioSystems* **2005**, *1*, 242.

(4) Li, Z.; Hillmyer, M. A., Lodge, T. P. *Nano Letters* **2006**, *6*, 1245.

(5) Moughton, A. O.; Hillmyer, M. A., Lodge, T. P. *Macromolecules* **2012**, *45*, 2.

(6) Du, J.; O'Reilly, R. K. *Soft Matter* **2009**, *5*, 3544.

(7) Brinkhuis, R. P.; Rutjes, F. P. J. T.; van Hest, J. C. M. *Polymer Chemistry* **2011**, *2*, 1449.

(8) Egli, S.; Schlaad, H.; Bruns, N.; Meier, W. *Polymers* **2011**, *3*, 252.

(9) Yang, C-Y.; Song, B.; Ao, Y.; Nowak, A. P.; Abelowitz, R. B.; Korsak, R. A.; Havton, L. A.; Deming, T. J.; Sofroniew, M. V. *Biomaterials* **2009**, *30*, 2881.

(10) Deming, T. J. *Progress in Polymer Science* **2007**, *32*, 858.

(11) Deming, T. J. (Ed.) Peptide-Based Materials. *Topics in Current Chemistry* **2012**, *310*, 1.

(12) Voit, B.; Appelhans, D. *Macromolecular Chemistry Phys*ics **2010**, *211*, 727.

(13) Schatz, C.; Lecommandoux, S. *Macromolecular Rapid Communication* **2010**, *31*, 1664.

(14) Ambrosi, M.; Cameron, N.; Davis, B. G. *Organic and Biomolecular Chemistry* **2005**, *3*, 1593.

(15) Kramer, J. R.; Deming, T. J. *Journal of the American Chemical Society* **2010**, *132*, 15068.

(16) Kramer, J. R.; Deming, T. J. *Journal of the American Chemical Society* **2012**, *134*, 4112.

(17) Nowak, A. P.; Breedveld, V.; Pakstis, L.; Ozbas, B.; Pine, D. J.; Pochan, D.; Deming, T. J. *Nature* **2002**, *417*, 424.

(18) Bellomo, E.; Wyrsta, M. D.; Pakstis, L.; Pochan, D. J.; Deming, T. J. *Nature Materials* **2004**, *3*, 244.

(19) Holowka, E. P.; Sun, V. Z.; Kamei, D. T.; Deming, T. J. *Nature Materials* **2007**, *6*, 52.

(20) Deming, T. J. *Soft Matter* **2005**, *1*, 28.

(21) Holowka, E. P.; Pochan, D. J.; Deming, T. J. *Journal of the American Chemical Society* **2005**, *127*, 12423.

(22) Rodriguez-Hernandez, J.; Lecommandoux, S. *Journal of the American Chemical Society* **2005**, *127*, 2026.

(23) Sun, J.; Chen, X.; Deng, C.; Yu, H.; Xie, Z.; Jing, X. *Langmuir* **2007**, *23*, 8308.

(24) Holowka, E. P.; Deming, T. J. *Macromolecular Bioscience* **2010**, *10*, 496.

(25) Rodriguez, A. R.; Choe, U-J.; Kamei, D. T.; Deming, T. J. *Macromolecular Bioscience* **2012**, *12*, 805.

(26) Hanson, J. A.; Chang, C. B.; Graves, S. M.; Li, Z.; Mason, T. G.; Deming, T. J. *Nature* **2008**, *455*, 85.

(27) Hanson, J. A.; Li, Z.; Deming, T. J. *Macromolecules* **2010**, *43*, 6268.

(28) Checot, F.; Lecommandoux, S.; Gnanou, Y.; Klok, H-A. *Angewandte Chemie, International Edition* **2002**, *41*, 1340.

(29) Kukula, H.; Schlaad, H.; Antonietti, M. Forster, S. *Journal of the American Chemical Society* **2002**, *124*, 1658.

(30) Deming, T. J. *Macromolecules* **1999**, *32*, 4500.

(31) Huang, J.; Bonduelle, C.; Thevenot, J.; Lecommandoux, S.; Heise, A. *Journal of the American Chemical Society* **2012**, *134*, 119.

(32) Hasegawa, T.; Kondoh, S.; Matsuura, K.; Kobayashi, K. *Macromolecules* **1999**, *32*, 6595.

(33) Pati, D.; Shaikh, A. Y.; Das, S.; Nareddy, P. K.; Swamy, M. J.; Hotha, S.; Gupta, S. S. *Biomacromolecules* **2012**, *13*, 1287.

(34) Green, M. M.; Gross, R. A.; Schilling, F. C.; Zero, K.; Crosby III, C. *Macromolecules* **1988**, *21*, 1839.

(35) Fuller, W. D.; Verlander, M. S.; Goodman, M. A. *Biopolymers* **1976**, *15*, 1869.

(36) Brzezinska, K. R.; Curtin, S. A.; Deming, T. J. *Macromolecules* **2002**, *35*, 2970.

(37) Morrow, J. A.; Segal, M. L.; Lund-Katz, S.; Philips, M. C.; Knapp, M.; Rupp, B.; Weigraber, K. H. *Biochemistry* **2000**, *39*, 11657.

(38) Fuller, W. D.; Verlander, M. S.; Goodman, M. *Biopolymers* **1976**, *15*, 1869.

(39) Klein, H. F.; Karsch, H. H. *Chemische Berichte* **1975**, *108*, 944.

CHAPTER FIVE

Methionine Diblock Copolypeptide Vesicles

5.1 Abstract

This chapter describes the preparation and assembly of block copolypeptides, where the amphiphilicity is obtained by simple modification to poly(L-methionine). In this study, diblock copolypeptides were prepared by ring-opening polymerization of L-methionine N-carboxyanhydride (Met NCA), followed by copolymerization of L-leucine N-carboxyanhydride (Leu NCA) and L-phenylalanine N-carboxyanhydride (Phe NCA) to form the second block, making a fully hydrophobic block copolypeptide, poly(L-methionine)$_x$-*block*-poly(L-leucine$_{0.5}$-*co*-L-phenylalanine$_{0.5}$)$_y$, M$_x$(L$_{0.5}$/F$_{0.5}$)$_y$. The poly(L-methionine), M, segment is then simply modified by either oxidation or alkylation to give poly(L-methionine sulfoxide), M^O, poly(L-methyl-methionine sulfonium chloride), M^M, or poly(L-carboxymethyl-methionine sulfonium chloride), M^C. These modified methionine blocks are hydrophilic and fully disordered in water, imparting solubility of the block copolypeptide under aqueous conditions, while the hydrophobic domain drives self-assembly of vesicular morphologies. This new family of block copolypeptides was tested for cytotoxicity and intracellular delivery, showing promise for drug delivery applications.

5.2 Introduction

The focus of the vesicle project has been to incorporate new polypeptide domains that can lead to enhanced cellular uptake, reduced cytotoxicity and stimuli responsiveness. Previous

results have shown that the use of arginine (homoarginine) domains may enhance cellular uptake, however these cationic polymers show increasing cytotoxicity with increasing polypeptide concentration.[1,2] This cytotoxicity can be reduced with the use of more negatively charged polypeptides (i.e., poly(L-glutamic acid)), but at the cost of reduced cellular uptake due to possible polyion complexation with arginine.[3] Promising results were seen with the use of the neutral charged poly(N_ε-2-(2-(2-methoxyethoxy)ethoxy)acetyl-L-lysine), K^P, masking the cytotoxic effects of poly(L-homoarginine).[3] The disadvantage of using K^P is the α-helical conformation that leads to membrane rigidity preventing extrusion of vesicles below 200 nanometers.[3,4] From these previous results it was determined that the ideal hydrophilic domain would contain a nonionic charged segment with a random coil conformation. If this domain does not provide enhanced cellular uptake, a short domain of homoarginine may be incorporated without polyion complexation due to the overall neutral charge of hydrophilic domain.

Poly(L-methionine) has not been previously incorporated into block copolypeptides due to inability to purify the monomer for living polymerization. Recent developments in the purification of α-amino acid-N-carboxyanhydrides (NCAs) in our lab have broadened the number of monomers that can be readily synthesized and purified for controlled living polymerization. This has allowed the easy production of a L-methionine NCA in high purity.

Poly(L-methionine)$_x$-*block*-poly(L-leucine$_{0.5}$-*co*-L-phenylalanine$_{0.5}$)$_y$, $M_x(L_{0.5}/F_{0.5})_y$, was prepared and the methionine block was modified to yield amphiphilic diblock copolypeptide (**Figure 5.1**). The new polypeptides were processed to test for vesicle self-assembly. Cell studies were conducted to evaluate their cytotoxicity and intracellular uptake.

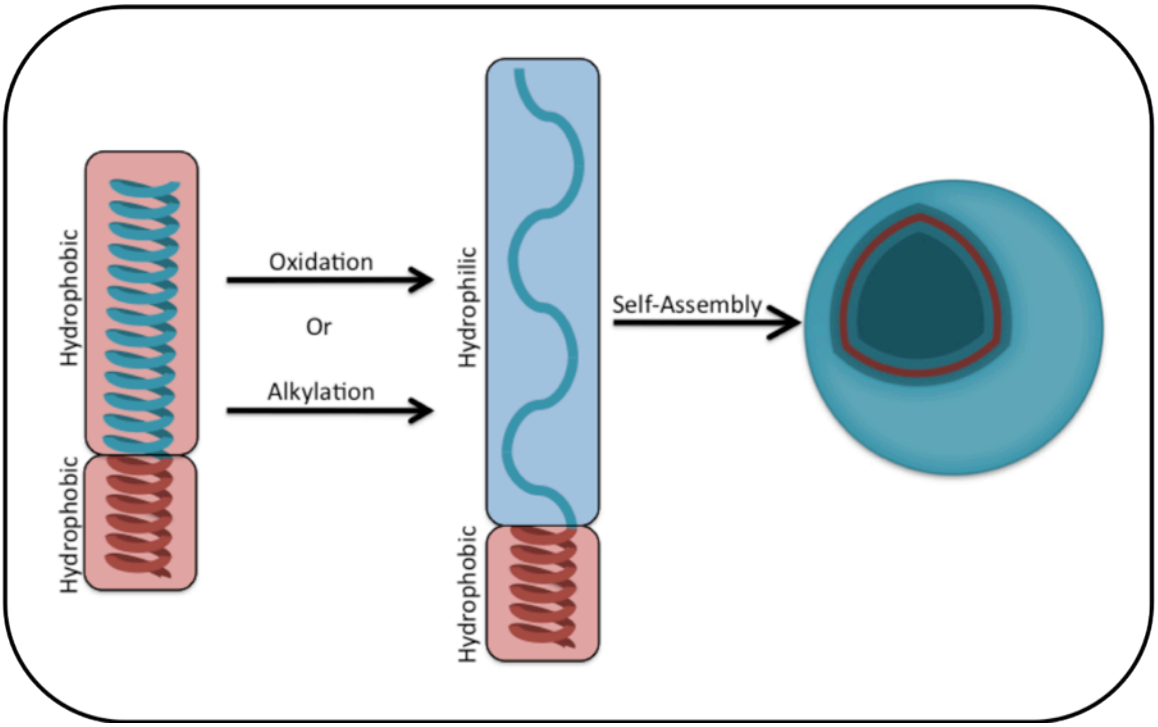

Figure 5.1 Schematic drawing of the modification of the hydrophobic diblock copolypeptides to amphiphilic diblock copolypeptides and proposed self-assembly into vesicles.

5.3 Reactivity of Methionine

Methionine is a sulfur containing amino acid that has a thioether in its side chain. Polymethionine has the tendency to drive the formation of the α-helix and in some cases β-sheet.[6,7] It is considered a very hydrophobic amino acid along with leucine, phenylalanine, valine, tryptophan and isoleucine. The thioether can be oxidized to form sulfoxides and with further oxidation to sulfones in the presence of hydrogen peroxide.[5,8,9] Oxidation of the thioether group of poly(L-methionine) was studied in the 1970s as a means to make water soluble polypeptides. Research has shown that poly(L-methionine sulfoxide) is biocompatible with no toxicity *in vitro* or *in vivo*, which may also help reduce the cytotoxicity of the polypeptide vesicles.[5] The thioether is also readily alkylated to form sulfonium salts.[10-13] The modification of

polymethionine by oxidation and alkylated imparts water solubility. This reactivity leads to an endless amount of materials with different functionality and properties making methionine polymers desirable.[13]

5.4 Modification of Poly(L-Methionine) Leads to Water Solubility

Poly(L-methionine) was polymerized by ring opening polymerization of Met NCA with $(PMe_3)_4Co$. Poly(L-methionine) on it own forms a highly rigid α-helical structure (**Figure 5.2**) that makes the polymer insoluble in most solvents (exception of dichloromethane and trifluoroacetic acid). Following a protocol in the literature, 30 % hydrogen peroxide containing 1% Acetic acid yields mostly methionine sulfoxides versus methionine sulfone. Consideration to reaction times and temperature helps to yield poly(L-methionine sulfoxide) reproducibly. Preliminary data has shown that methionine sulfone begins to lose water solubility. The CD spectra of poly(L-methionine sulfoxide) shows the characteristic structure of a random coil (**Figure 5.3**) were as the poly(L-methionine sulfone) begins to form the α-helix in solution (**Figure 5.4**). Poly(L-methionine sulfoxide) is a non-charged polypeptide that contains a random coil conformation, which may impart flexibility for the vesicle membrane. Alkylation of methionine using commercially available iodomethane and iodoacetic acid gives the poly(L-methionine sulfonium salts), poly(L-methyl-methionine sulfonium chloride), M^M, and poly(L-carboxymethyl-methionine sulfonium chloride), M^C, respectively, which are both water soluble.

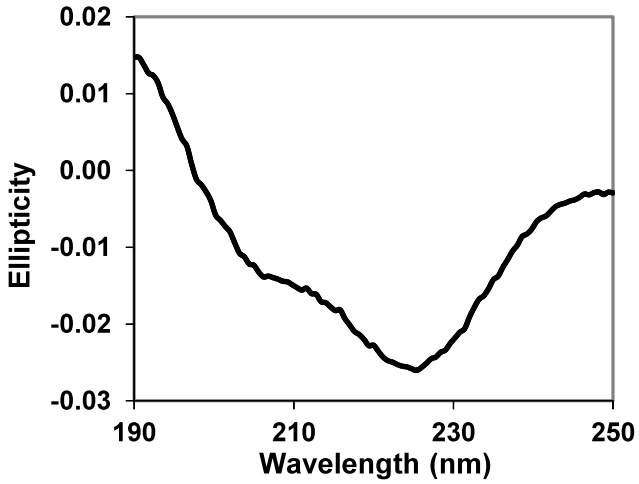

Figure 5.2 Circular dichroism spectra of poly(Met), prepared as a thin film cast from a 0.25 mg/mL solution in THF, 20 ºC. Ellipticity is reported in degrees·cm^2; since sample is a solid film, molar ellipticity could not be calculated.

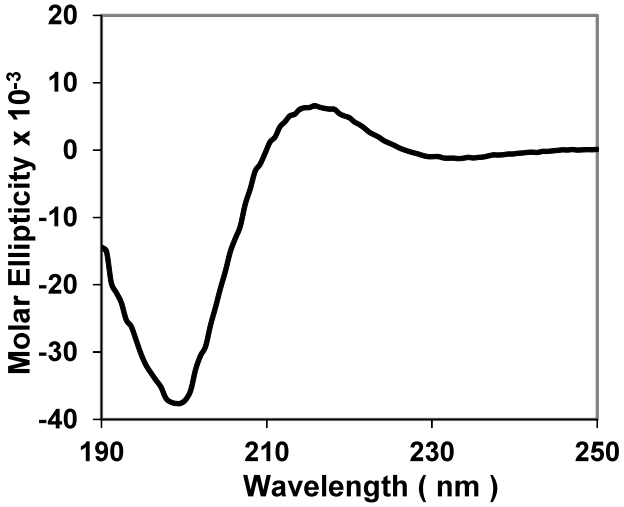

Figure 5.3 Circular dichroism spectra of poly(Met^O), 0.25 mg/mL, 20 ºC.

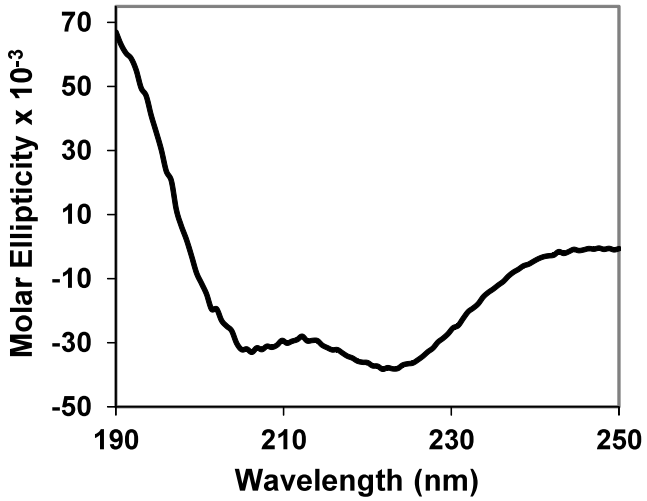

Figure 5.4 Circular dichroism spectra of poly(Met^{O2}), 99% α helical, 0.1 mg/mL, 20 ºC.

5.5 Methionine Diblock Polypeptide Composition for Vesicle Self-Assembly

After determination of the initiator efficiency of $(PMe_3)_4Co$ with methionine N-carboxyanhydrides (Met NCA) a series of block copolymers where synthesized using different M:I ratios (10:1, 20:1, 30:1 and 40:1) (**Figure 5.5**).

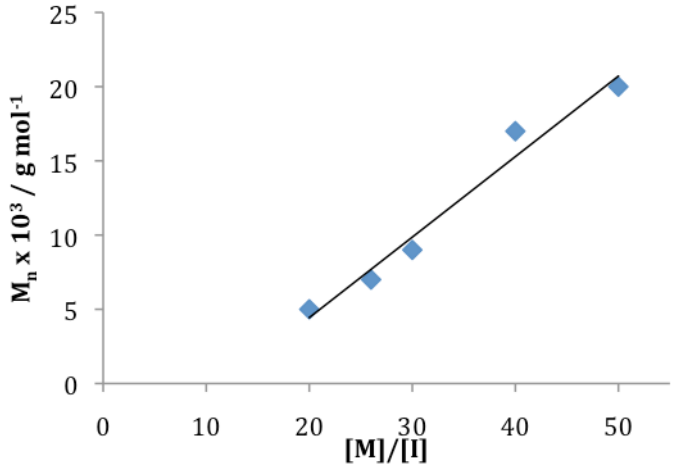

Figure 5.5 Molecular weight (M_n) of Met NCA as function of monomer to initiator ratio ([M]/[I]) using $(PMe_3)_4Co$ in THF at 20 °C.

Based on the amount of Met NCA, the second addition of Leu and Phe NCAs was added to give different lengths of the hydrophobic block by adjusting the mole ratio. It must noted that 5 % of methionine domain is made up of N_{ε}-benzyloxycarbonyl-L-lysine; incorporated for amino side chain functionality. The mole ratio of methionine block to leucine-phenylalanine block was varied to find a composition range that would form vesicles. After the preparation of the block copolypeptides, poly(L-methionine$_{0.95}$-*co*-N_{ε}-benyzloxycarbonyl-L-lysine$_{0.05}$)$_x$-*block*- (L-leucine$_{0.5}$-*co*- L-phenylalanine$_{0.5}$)$_y$ (x = 20 to 80, y = 15 to 25), the methionine was alkylated by iodomethane to give poly(L- methyl-methionine sulfonium chloride$_{0.95}$-*co*-N_{ε}-benyzloxycarbonyl-L-lysine$_{0.05}$)$_x$-*block*- (L-leucine$_{0.5}$-*co*- L-phenylalanine$_{0.5}$)$_y$, $(M^{M}_{0.95}/K^{Z}_{0.05})_x(L_{0.5}/F_{0.5})_y$. The twelve $(M^{M}_{0.95}/K^{Z}_{0.05})_x(L_{0.5}/F_{0.5})_y$ samples were processed using solvent annealing. The results from processing all samples into vesicles showed evidence that vesicles can be self-assembled from the block copolypeptides containing poly(L-methyl-methionine sulfonium chloride), M^{M}. As the hydrophilic segment is increased from 20 to 80 mer the suspensions become more homogenous with vesicles (**Figure 5.6**).

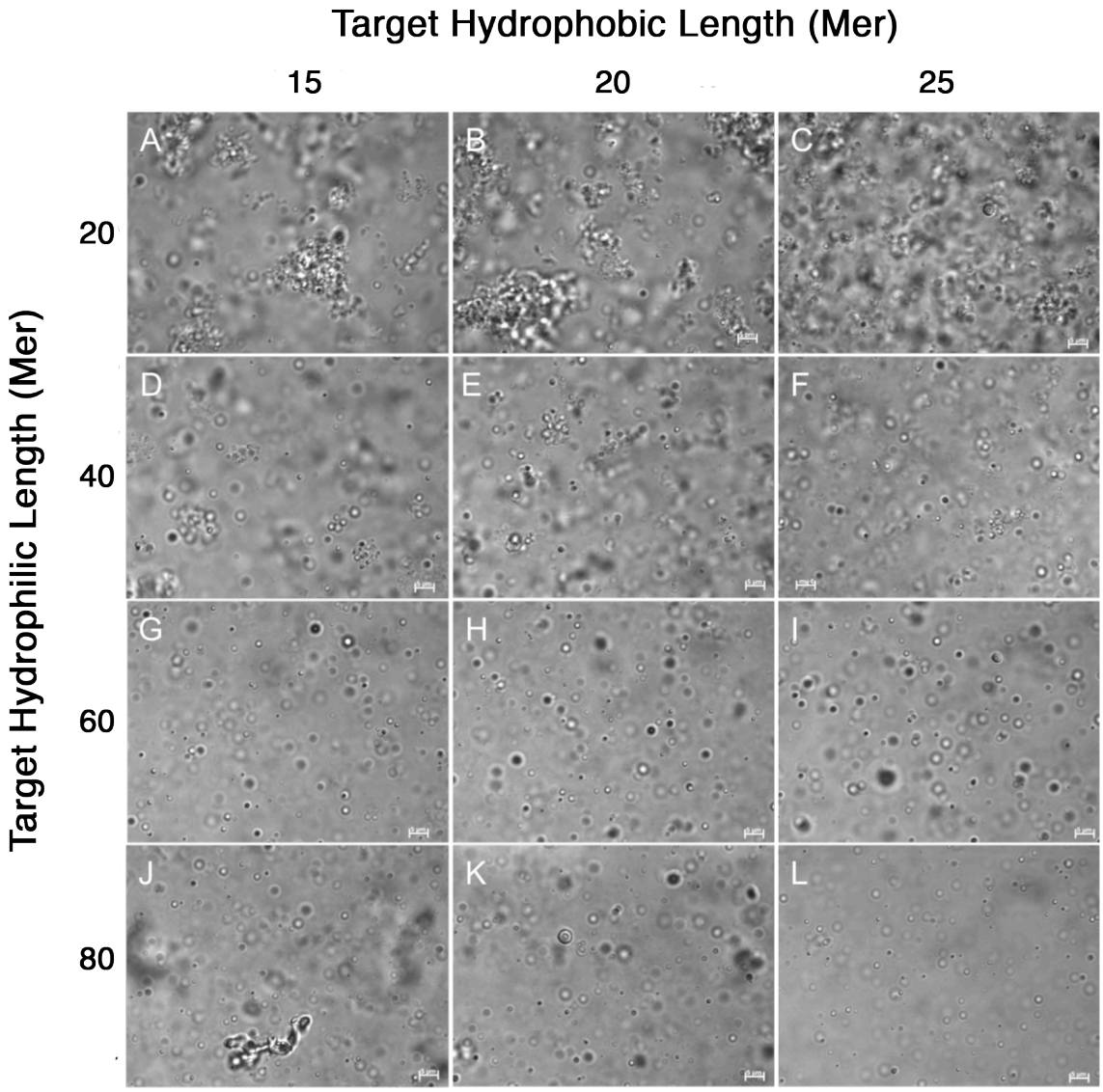

Figure 5.6 Differential interference contrast microscopy (DIC) images of processed $(M^{M}_{0.95}/K^{Z}_{0.05})_x(L_{0.5}/F_{0.5})_y$ block copolypeptides. (A) $(M^{M}_{0.95}/K^{Z}_{0.05})_{20}(L_{0.5}/F_{0.5})_{15}$, (B) $(M^{M}_{0.95}/K^{Z}_{0.05})_{20}(L_{0.5}/F_{0.5})_{20}$, (C) $(M^{M}_{0.95}/K^{Z}_{0.05})_{20}(L_{0.5}/F_{0.5})_{25}$, (D) $(M^{M}_{0.95}/K^{Z}_{0.05})_{40}(L_{0.5}/F_{0.5})_{15}$, (E) $(M^{M}_{0.95}/K^{Z}_{0.05})_{40}(L_{0.5}/F_{0.5})_{20}$, (F) $(M^{M}_{0.95}/K^{Z}_{0.05})_{40}(L_{0.5}/F_{0.5})_{25}$, (G) $(M^{M}_{0.95}/K^{Z}_{0.05})_{60}(L_{0.5}/F_{0.5})_{15}$, (H) $(M^{M}_{0.95}/K^{Z}_{0.05})_{60}(L_{0.5}/F_{0.5})_{20}$, (I) $(M^{M}_{0.95}/K^{Z}_{0.05})_{60}(L_{0.5}/F_{0.5})_{25}$, (J) $(M^{M}_{0.95}/K^{Z}_{0.05})_{80}(L_{0.5}/F_{0.5})_{15}$, (K) $(M^{M}_{0.95}/K^{Z}_{0.05})_{80}(L_{0.5}/F_{0.5})_{20}$, and (L) $(M^{M}_{0.95}/K^{Z}_{0.05})_{80}(L_{0.5}/F_{0.5})_{25}$.

Table 5.1 Poly(L- methyl-methionine sulfonium chloride$_{0.95}$-*co*-N$_{\varepsilon}$-benyzloxycarbonyl-L-lysine$_{0.05}$)$_x$-*block*- (L-leucine$_{0.5}$-*co*- L-phenylalanine$_{0.5}$)$_y$, ($M^M_{0.95}$/$K^Z_{0.05}$)$_x$($L_{0.5}$/$F_{0.5}$)$_y$ compositions and self-assembled structures.

	($M^M_{0.95}$/$K^Z_{0.05}$)$_x$($L_{0.5}$/$F_{0.5}$)$_y$ Constructs		
x	20	20	20
y	15	20	25
mol % y	43	50	56
Structure	S	S	S
x	40	40	40
y	15	20	25
mol % y	27	33	38
Structure	I	I	I
x	60	60	60
y	15	20	25
mol % y	20	25	29
Structure	V	V	V
x	80	80	80
y	15	20	25
mol % y	16	20	24
Structure	I,V	V	V

S = sheets, I = irregular aggregates, and V= vesicular assemblies.

5.6 Preparation of Well-Defined Methionine Diblocks for Vesicle Self-Assembly

After finding proof of vesicle self-assembly with methionine containing polymers, well-defined block copolypeptides were synthesized and characterized to confirm previous results. Poly(L-methionine)$_{65}$-*block*- (L-leucine$_{0.5}$-*co*- L-phenylalanine$_{0.5}$)$_{20}$, $M_{65}(L_{0.5}/F_{0.5})_{20}$, was prepared by Met NCA polymerization with $(PMe_3)_4Co$. Once Met NCA fully polymerized (confirmed by FTIR) and small aliquot (10 mg) was removed and end-capped with poly(ethylene glycol)$_{45}$ monofunctionalized with isocyanate for average molecular weight determination by ^{1}H NMR integration.

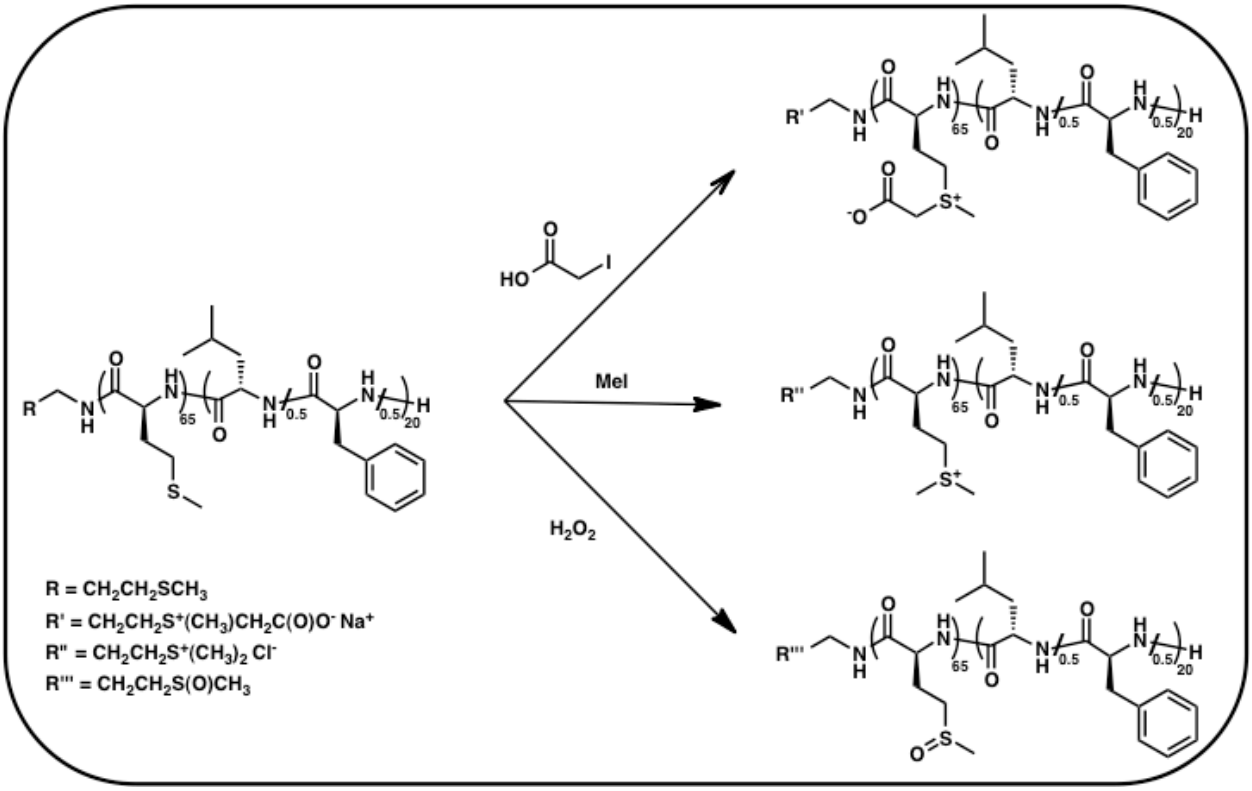

Figure 5.7 Structures of the methionine diblock copolypeptide and its modification by iodoacetic acid, iodomethane and hydrogen peroxide.

This polymer was then modified separately with hydrogen peroxide, iodomethane and iodoacetic acid to yield the three new polypeptides, poly(L-methionine sulfoxide)$_{65}$-*block*- (L-leucine$_{0.5}$-*co*- L-phenylalanine$_{0.5}$)$_{20}$, $M^{O}{}_{65}(L_{0.5}/F_{0.5})_{20}$, poly(L-methyl-methionine sulfonium chloride)$_{65}$-*block*- (L-leucine$_{0.5}$-*co*- L-phenylalanine$_{0.5}$)$_{20}$, $M^{M}{}_{65}(L_{0.5}/F_{0.5})_{20}$, or poly(L-carboxymethyl-methionine sulfonium chloride)$_{65}$-*block*- (L-leucine$_{0.5}$-*co*- L-phenylalanine$_{0.5}$)$_{20}$, $M^{C}{}_{65}(L_{0.5}/F_{0.5})_{20}$, respectively (**Figure 5.7**). These new copolypeptides were processed into vesicles with slight modification to the solvent annealing system.

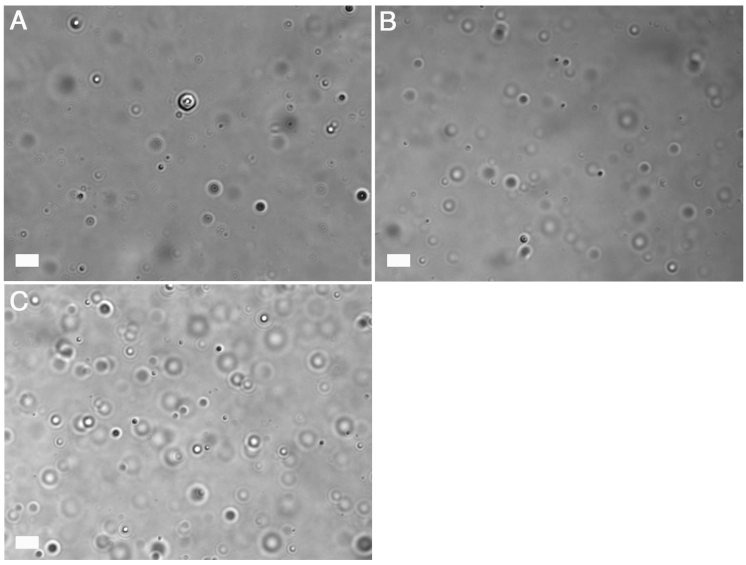

Figure 5.8 Differential interference contrast (DIC) images of 1 % (w/v) aqueous suspensions of (A) $M^{O}_{65}(L_{0.5}/F_{0.5})_{20}$, (B) $M^{M}_{65}(L_{0.5}/F_{0.5})_{20}$ and (C) $M^{C}_{65}(L_{0.5}/F_{0.5})_{20}$. Scale bars = 5 μm.

The results from imaging the suspensions showed that all three modifications of methionine produce amphiphilic block copolypeptides that can self-assemble into vesicular structures (**Figure 5.8**).

5.7 Membrane Extrudability and Surface Charge of Oxidized and Alkylated Methionine Diblock Copolypeptide Vesicles

The self-assembly of methionine vesicles yielded microns size diameters as seen by DIC. For further studies, the vesicles were subsequently serially passed through 1.0, 0.4 and 0.2 μm PC membranes. The suspensions were easily passed through membrane with little to no resistance in comparison to previous $K_{60}L_{20}$ samples. Bradford assay revealed that 80 to 100 % of polypeptide was recovered after passage through membrane filters. Dynamic light scattering

(DLS) results showed that these methionine vesicles could be extruded to average diameters below 200 nm with polydispersities of *ca*. 0.2.

These methionine vesicle suspension, $M^{O}_{65}(L_{0.5}/F_{0.5})_{20}$, $M^{M}_{65}(L_{0.5}/F_{0.5})_{20}$ and $M^{C}_{65}(L_{0.5}/F_{0.5})_{20}$ contain diverse functionality on the vesicle surface of neutral, cationic and zwitterionic charges, respectively. The surface charge of the three samples was determined using zeta potential under various pH conditions. In comparison to poly(L-lysine), (L- methyl-methionine sulfonium chloride) has a permanent positive charge that should not be influenced by pH. Surface charge of $M^{M}_{65}(L_{0.5}/F_{0.5})_{20}$ was consistent at 40 mV from pH 3 to 9. The neutral and zwitterionic suspensions stayed consistently around 0 mV (**Figure 5.9**).

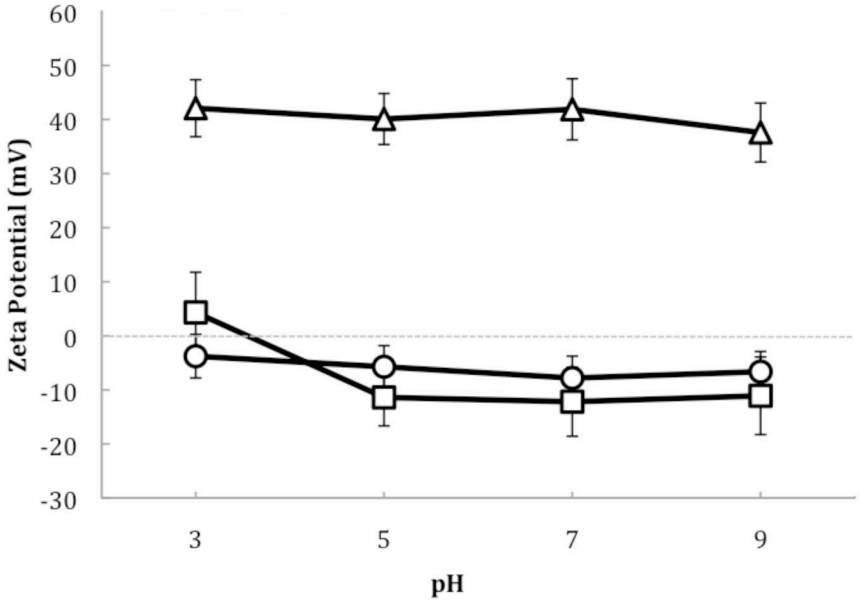

Figure 5.9 Zeta potential versus pH for aqueous suspensions of $M^{O}_{65}(L_{0.5}/F_{0.5})_{20}$ (open circle), $M^{M}_{65}(L_{0.5}/F_{0.5})_{20}$ (open triangle) and $M^{C}_{65}(L_{0.5}/F_{0.5})_{20}$ (open square).

5.8 Cytotoxicity of Oxidized and Alkylated Methionine Diblock Copolypeptide Vesicles

The effect of methionine modified hydrophilic domains on cytotoxicity was investigated. The modification of methionine leads to different functionalities on the surface of the vesicle,

which can drastically change the toxicity. From previous research, we have seen that poly(L-glutamic acid) on the surface of the polypeptide vesicles making it anionic leads to no toxicity *in vitro*. On the other side of the spectrum, poly(L-lysine) on the surface of the polypeptide vesicles making it cationic leads to high toxicity *in vitro*. Polyethylene glycol is a neutral water-soluble polymer that is commonly used in making biomaterials because it shows no cytotoxicity *in vitro* or *in vivo*.

The oxidation of $M_{65}(L_{0.5}/F_{0.5})_{20}$ with hydrogen peroxide leads to the neutral water-soluble hydrophilic domain on the surface $M^{O}_{65}(L_{0.5}/F_{0.5})_{20}$ polypeptide vesicles, and like polyethylene glycol, in vitro studies show no cytotoxicity (tested up to 100 μg/mL) (**Figure 5.10**). This makes a highly biocompatible material for drug delivery. Modification by alkylation using iodomethane yields cationic $M^{M}_{65}(L_{0.5}/F_{0.5})_{20}$ polypeptide vesicles, which is shown to be toxic at concentration as low as 20 μg/mL using MTS assay (**Figure 5.10**). A different functionality is yielded by alkylation of $M_{65}(L_{0.5}/F_{0.5})_{20}$ with iodoacetic acid making the zwitterionic block copolypeptide, $M^{C}_{65}(L_{0.5}/F_{0.5})_{20}$, which contains both a positive and negative charge making the overall net charge neutral. The MTS assay of $M^{C}_{65}(L_{0.5}/F_{0.5})_{20}$ suspension shows no toxicity up to 100 μg/mL (**Figure 5.10**).

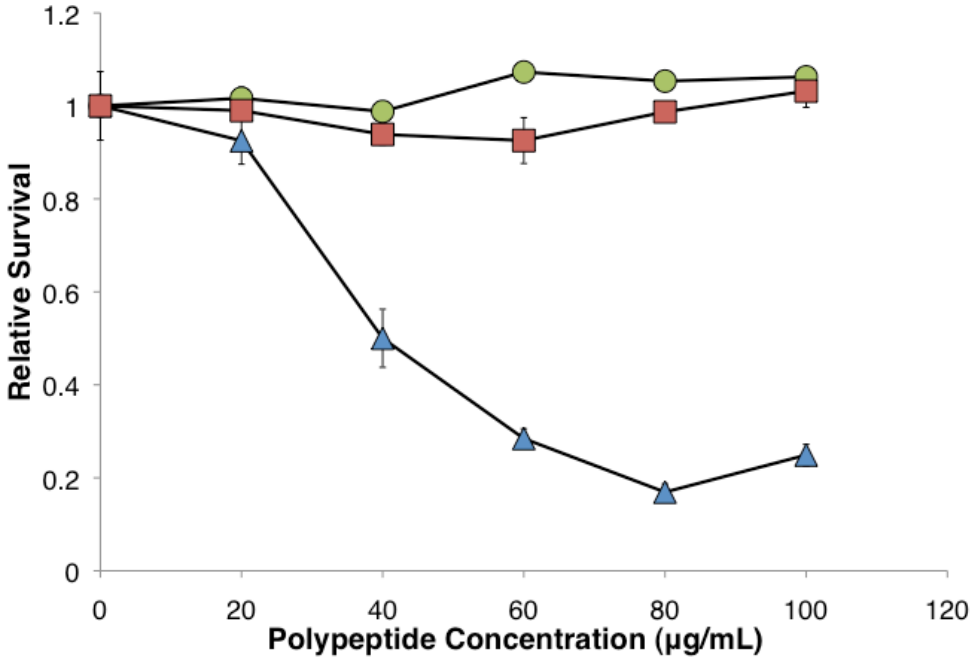

Figure 5.10 MTS cell survival data after 5 hours for HeLa cells separately incubated with medium containing aqueous suspensions of $M^{O}_{65}(L_{0.5}/F_{0.5})_{20}$ (circle), $M^{M}_{65}(L_{0.5}/F_{0.5})_{20}$ (triangle) and $M^{C}_{65}(L_{0.5}/F_{0.5})_{20}$ (square).

5.9 Cellular Uptake of Oxidized and Alkylated Methionine Diblock Copolypeptide Vesicles

The cellular uptake ability of these new methionine modified vesicle suspensions, $M^{O}_{65}(L_{0.5}/F_{0.5})_{20}$, $M^{M}_{65}(L_{0.5}/F_{0.5})_{20}$ and $M^{C}_{65}(L_{0.5}/F_{0.5})_{20}$ were investigated by incubation with HeLa cells (**Figure 5.11**). It was found that the oxidize, $M^{O}_{65}(L_{0.5}/F_{0.5})_{20}$, and zwitterionic, $M^{C}_{65}(L_{0.5}/F_{0.5})_{20}$ vesicles were not taken up by HeLa cells at 10 µg/mL. Cellular uptake was reinvestigated with both suspensions at 100 µg/mL revealing minimal internalization. It was found that the cationic, $M^{M}_{65}(L_{0.5}/F_{0.5})_{20}$, vesicle suspension was taken up with efficiency comparable to the $R^{H}_{55}L_{20}$ samples.

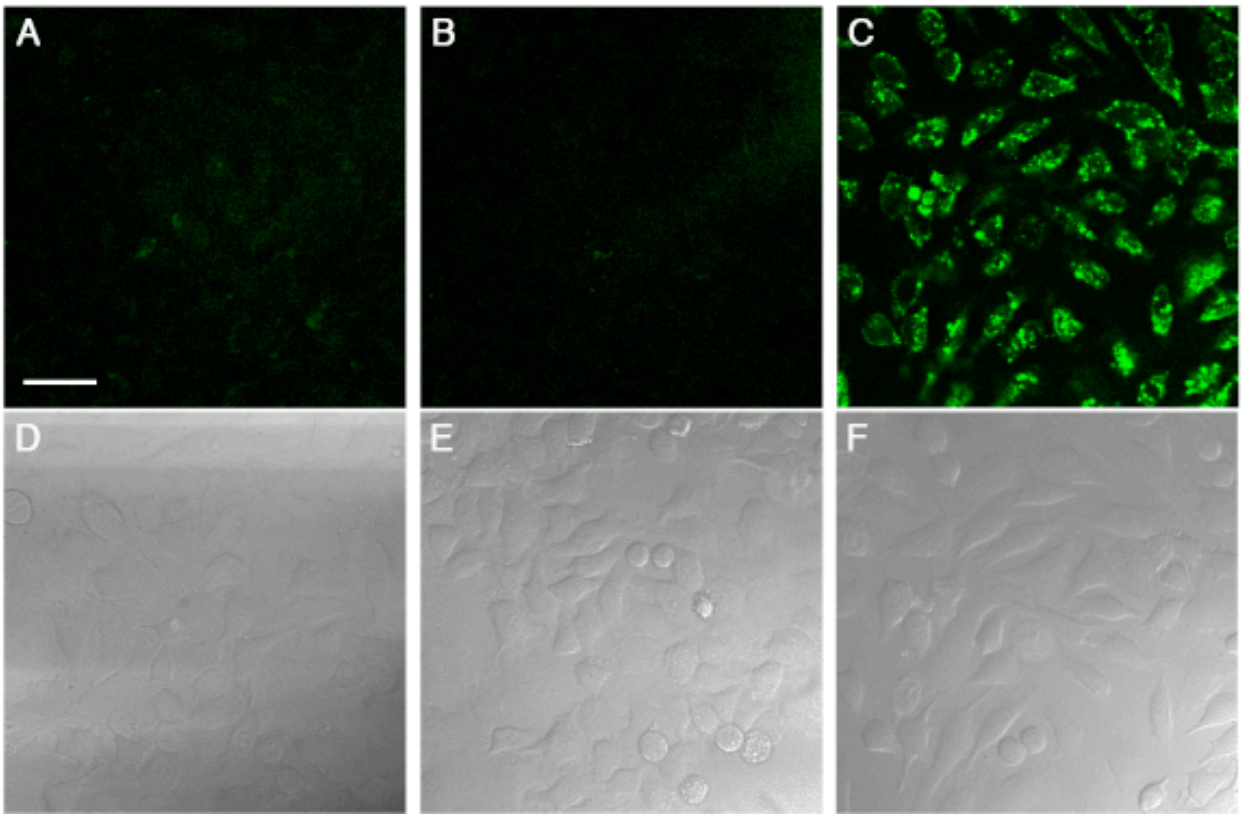

Figure 5.11 LSCM and DIC images of HeLa cells after 5 h incubation at 37 °C with vesicle suspensions (A and D) $M^{O}_{65}(L_{0.5}/F_{0.5})_{20}$, (B and E) $M^{C}_{65}(L_{0.5}/F_{0.5})_{20}$ and (C and F) $M^{M}_{65}(L_{0.5}/F_{0.5})_{20}$ (10 μg/mL). Scale bar = 20 μm.

5.10 Protease Degradation of Polymethionine Derivatives

The degradation of these new polymethionine derivatives, M^{O}, M^{M} and M^{C} was tested using Proteinase K. Proteinase K is a protease with broad specificity that cleaves the peptide backbone adjacent to the carbonyl group of aliphatic and aromatic amino acids. For these studies, homopolypeptide, poly(L-methionine)$_{256}$, M_{256}, was synthesized and end-capped with polyethylene glycol$_{45}$ functionalized with isocyanate, PEG_{45}-NCO. The purpose of end-capping with PEG is to have a segment that will not be degraded by the protease and provide a way for determining the molecular weight of the methionine segment after incubation with Proteinase K.

NMR spectra before and after incubation with the protease revealed almost complete degradation of M^O, M^M and M^C (**Figure 5.12**).

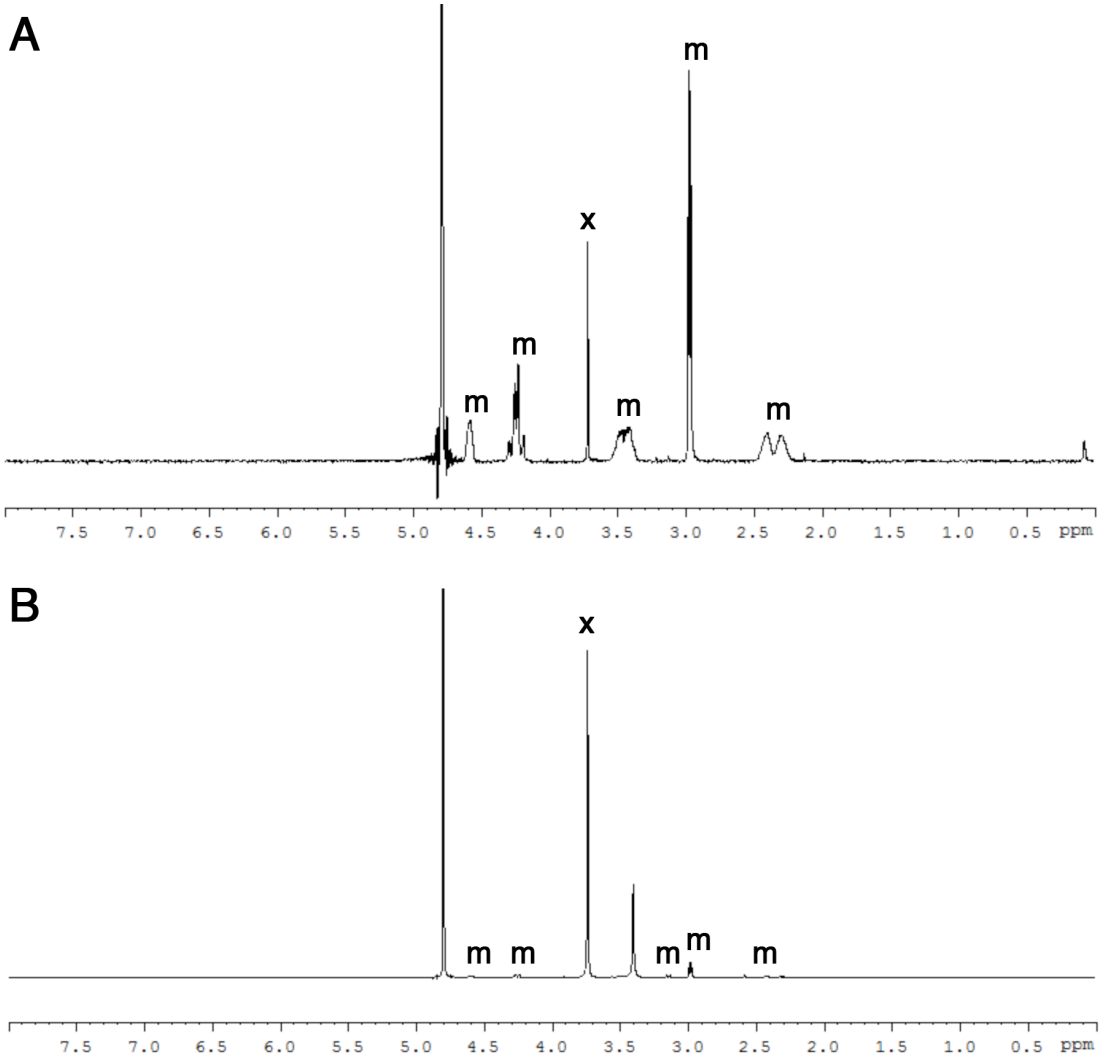

Figure 5.12 ^{1}NMR spectra of M^C_{256}-*block*-PEG_{45} (A) before and (B) after incubation with Proteinase K. x = PEG_{45} peak, m = M^C peaks.

5.11 Conclusion

The use of poly(L-methionine) as a new polypeptide domain for amphiphilic diblock copolypeptides has shown promising results for vesicle self-assembly, extrudability and

cytotoxicity. Poly(L-methionine) has shown versatility by giving access to various functionalities on polypeptide vesicle surfaces that can tune their properties. Vesicle self-assembly of these methionine vesicles have been robust and unaffected by the different hydrophilic side chain functionalities on $M^{O}_{65}(L_{0.5}/F_{0.5})_{20}$, $M^{C}_{65}(L_{0.5}/F_{0.5})_{20}$ and $M^{M}_{65}(L_{0.5}/F_{0.5})_{20}$.

5.12 Experimental

5.12.1 General Methods and Materials:

Dried tetrahydrofuran (THF), hexane and diethyl ether were prepared by passage through alumina columns, and oxygen was removed by purging with nitrogen prior to use.[14] Perkin Elmer RX1 FTIR Spectrophotometer was used for recording infrared spectra. ^{1}H NMR spectra were recorded on a Bruker AVANCE 400 MHz spectrometer. Ultrapure (18 MΩ) water was obtained from a Millipore Milli-Q Biocel A10 purification unit.

5.12.2 Synthesis:

The α-amino acid-N-carboxyanhydride (NCA) monomers, phenylalanine, leucine and lysine were synthesized using previously described protocols.[15,16] Methionine monomer was prepared by a published protocol.[17]

5.12.3 Determining Monomer to Initiator Ratio for L-Methionine-N-carboxyanhydride (Met NCA) With Initiator, $(PMe_3)_4Co$:

L-methionine-N-carboxyanhydride (Met NCA) (60 mg, 0.34 mmol) was dissolved in THF (1.2 mL) and was separated into three vials containing equal volumes (0.11 mmol of NCA). To each vial, an aliquot of $(PMe3)_4Co$ initiator solution (100 μL, 50 μL, and 35 μL of a 20 mg/mL

solution in THF) was added via syringe to give different monomer to initiator (M:I) ratios. The vials were sealed and allowed to stir in the glove box for 1 hour. An aliquot (20 μL) was removed from each polymerization solution and analyzed by FTIR to confirm that all Met NCA was consumed. In the glove box, poly(ethylene glycol)$_{45}$-isocyanate (mPEG$_{45}$-NCO) (65 mg) was dissolved in THF (2.6 mL) in a 20 mL scintillation vial. An aliquot solution of mPEG$_{45}$-NCO (1320 μL, 680 μL, and 480 μL of 25 mg/mL) was added to each polymerization solution containing different amounts of initiator (0.006 mmol, 0.003 mmol, and 0.002 mmol, respectively). The PEG end-capping solution vials were sealed and allowed to react for 24 hours. Outside of the dry box, the PEG end-capped polypeptide (M$_x$-PEG$_{45}$) was isolated by precipitation with H_2O (3 times) to remove excess PEG. M$_x$-PEG$_{2000}$ was placed under high vacuum to remove residue H_2O before NMR analysis. The degree of polymerization of the polymer was determined by NMR integrations of PEG end-capped polymer and was plotted against M:I ratio to determine inflation.

5.12.4 Synthesis of Poly(L-methionine)$_{65}$-*block*-(L-Leucine$_{0.5}$-*co*-L-phenylalanine$_{0.5}$)$_{20}$, M$_{65}$(L$_{0.5}$/F$_{0.5}$)$_{20}$:

L-Methionine-N-carboxyanhydride (Met NCA) (80 mg, 0.4 mmol) was dissolved in THF (1.6 mL) and placed in a 20 mL scintillation vial containing a stir bar. To the vial, Co(PMe$_3$)$_4$ initiator solution (280 μL of a 20 mg/mL solution in THF) was added via syringe. The vial was sealed and allowed to stir in the glove box for 1 hour. An aliquot (20 μL) was removed and analyzed by FTIR to confirm that all the NCA was consumed. In the glove box, PEG$_{45}$-isocyanate (20 mg) was dissolved in THF (1 mL) in a 20 mL scintillation vial. An aliquot (240 μL) of the polymerization solution containing active chain ends was removed and added to the solution of

PEG_{45}-isocyanate. The PEG end-capping solution vial was sealed and allowed to react for 24 hours. L-Leucine NCA (10. 5 mg, 0.07 mmol) and L-phenylalanine NCA (12.8 mg, 0.07 mmol) was dissolved in THF (210 μL and 260 μL, respectively), combined and added to the polymerization solution via syringe. The vial was sealed and allowed to stir in the glove box for 1 hr to give the diblock $M_{65}(L_{0.5}/F_{0.5})_{20}$. Outside of the dry box, the PEG end-capped polypeptide (M_x-PEG_{45}) was isolated by precipitation with H_2O (3 times) to remove excess PEG. M_x-PEG_{45} was placed under high vacuum to remove residue H_2O. Outside the dry box, the block copolypeptide was isolated by evaporating off all volatiles and dispersed in 10 mM HCl (3 times) to remove cobalt. The average composition of the copolymer as determined by ^{1}H NMR integrations of PEG end-capped polymer and diblock copolymer was $M_{66}(L_{0.5}/F_{0.5})_{22}$.

5.12.5 Preparation of Poly(L-methionine sulfoxide)$_{65}$-*block*-(L-leucine$_{0.5}$-*co*-L-phenylalanine$_{0.5}$)$_{20}$, $M^O{}_{65}(L_{0.5}/F_{0.5})_{20}$:

A 20 mL scintillation vial was charged with $M_{65}(L_{0.5}/F_{0.5})_{20}$ (10 mg) and a stir bar. A solution of 1 % AcOH in 30% hydrogen peroxide (1 mL) was added to the scintillation vial and sealed and allowed to react for 20 min total. The sample was diluted with water to twice its original volume. Saturated sodium thiosulfate was added drop wise to quench the peroxide and transferred to a 2000 MWCO dialysis bag and dialyzed against water for 2 days with frequent water changes. The solution was lyophilized to dryness to yield a white solid. Yield 80 %, loss is due to dialysis.

5.12.6 Preparation of Poly(L-methyl-methionine sulfonium chloride)$_{65}$-*block*-(L-leucine$_{0.5}$-*co*-L-phenylalanine$_{0.5}$)$_{20}$, $M^M{}_{65}(L_{0.5}/F_{0.5})_{20}$:

A 20 mL scintillation vial was charged with $M_{65}(L_{0.5}/F_{0.5})_{20}$ (10 mg), H_2O (500 μL) and a stir bar. Methyl iodide (8μL, 2 equivalents to thioether units) was added to the polypeptide solution via

syringe. The reaction was sealed, covered in foil and stirred for 48 hours at room temperature. The solution was transferred to a 2000 MWCO dialysis bag and dialyzed against water containing sodium bisulfite for 24 hours with 3 solution changes. To convert to sulfonium chloride salts, the polymers were dialyzed against NaCl for 24 hours with 3 solution changes and then dialyzed against water with frequent water changes. The polypeptide solution was lyophilized to yield a white solid. Yield 80 %, loss is due to dialysis.

5.12.7 Preparation of Poly(L-sodium carboxymethyl-methionine sulfonium chloride)$_{65}$-*block*-(L-Leucine$_{0.5}$-*co*-L-phenylalanine$_{0.5}$)$_{20}$, $M^{C}_{65}(L_{0.5}/F_{0.5})_{20}$:

A 20 mL scintillation vial was charged with $M_{65}(L_{0.5}/F_{0.5})_{20}$ (10 mg), H_2O (500 μL) and a stir bar. Iodoacetic acid (43 mg, 4 equivalents to thioether units) was dissolved in H_2O (860 μL, 50 mg/mL) added to the polypeptide solution via syringe. The reaction was sealed, covered in foil and stirred for 48 hours at room temperature. The solution was transferred to a 2000 MWCO dialysis bag and dialyzed against water containing sodium bisulfite for 24 hours with 3 solution changes. To convert to sulfonium chloride salts, the polymers were dialyzed against NaCl for 24 hours with 3 solution changes and then dialyzed against water with frequent water changes. The polypeptide solution was lyophilized to yield a white solid. Yield 80 %, loss is due to dialysis.

5.12.8 Fluorescent Probe Modification of Polypeptide Vesicles:

5-(Iodoacetamido)fluorescein was conjugated to the thioether of the methionine side chains using the previous alkylation method. The polypeptide $M_{65}(L_{0.5}/F_{0.5})_{20}$ (10 mg) was dissolved in DMF (1 mL) in a 20 mL scintillation vial. 5-(Iodoacetamido)fluorescein was dissolved in DMF (10 mg/mL) and added to the a 1 % (w/v) polypeptide solution a 5:1 molar ratio to the polypeptide chains. The alkylation was allowed to proceed for 16 hours. After fluorescein

modification, the remaining methionine residues were concentrated to remove DMF for oxidation. For alkylation of remaining methionine residues, iodomethane and iodoacetic acid were added directly to the DMF solution.

5.12.9 Determination of Hydrophilic to Hydrophobic Ratio for Forming Vesicles:

L-methionine-N-carboxyanhydride (Met NCA) (240 mg, 1.4 mmol) and N_{ε}-benzyloxycarbonyl-L-lysine-N-carboxyanhydride (Z-Lys NCA) (20 mg, 0.06 mmol) were dissolved in THF (4.8 mL and 0.4 mL, respectively) and combined to give a solution containing 95% Met NCA and 5% Z-Lys NCA. The solution was separated into four vials containing equal volumes (0.36 mmol of NCA) in order to prepare different samples. To each vial, a different amount $(PMe_3)_4Co$ initiator solution (820 μL, 410 μL, 275 μL and 200 μL of a 20 mg/mL solution in THF) was added via syringe to give different monomer to initiator (M:I) ratios. The vials were sealed and allowed to stir in the glove box for 1 hour. An aliquot (20 μL) was removed from each polymerization solution and analyzed by FTIR to confirm that all NCA was consumed. Each vial was further divided into three vials in order to prepare twelve different samples. L-Leucine-N-carboxyanhydride (Leu NCA) (65 mg, 0.41 mmol) and L-phenylalanine-N-carboxyanhydride (Phe NCA) (80 mg, 0.41 mmol) were dissolved in THF (1.3 mL and 1.6 mL, respectively) and combined to give a solution containing 1:1 moles of Leu NCA to Phe NCA. An aliquot of the Leu/Phe NCA solution was added to each polymerization vial to give different hydrophilic and hydrophobic compositions. Refer to table for amounts of Leu/Phe NCA solution added to each reaction.

Table 5.2 Preparation of $(M_{0.95}/K^{Z}_{0.05})_x(L_{0.5}/F_{0.5})_y$ block copolypeptides for determining composition of vesicle formers.

$(M_{0.95}/K^{Z}_{0.05})_x(L_{0.5}/F_{0.5})_y$ (x:y)	1st Domain NCAs (mmol)	1st Domain: 2nd Domain ratio	2nd Domain NCAs			2nd Domain Amount			volume (0.05 mg NCA/μL)
			Total (mmol)	50% L (mmol)	50% F (mmol)	Total (mg)	L (mg)	F (mg)	
20:15	0.12	1:0.75	0.09	0.045	0.045	7	9	16	320
20:20	0.12	1:1	0.12	0.060	0.060	9	12	21	420
20:25	0.12	1:1.25	0.15	0.075	0.075	12	14	26	520
40:15	0.12	1:0.38	0.045	0.023	0.023	4	5	8	160
40:20	0.12	1:0.5	0.06	0.030	0.030	5	6	11	220
40:25	0.12	1:0.63	0.075	0.038	0.038	6	7	13	260
60:15	0.12	1:0.25	0.03	0.015	0.015	2	3	5	100
60:20	0.12	1:0.33	0.04	0.020	0.020	3	4	7	140
60:25	0.12	1:0.42	0.05	0.025	0.025	4	5	9	180
80:15	0.12	1:0.19	0.023	0.012	0.012	2	3	4	80
80:20	0.12	1:0.25	0.03	0.015	0.015	2	3	5	100
80:25	0.12	1:0.31	0.038	0.019	0.019	3	4	7	140

5.12.10 Preparation of $M^{O}_{65}(L_{0.5}/F_{0.5})_{20}$ Polypeptide Assemblies:

Solid polypeptide powder ($M^{O}_{65}(L_{0.5}/F_{0.5})_{20}$) was dispersed in THF to give a 1 % (w/v) suspension. The suspension was placed in a bath sonicator for 30 minutes to evenly disperse the polypeptide and reduce large particulates. An equivalent amount of Millipore water was then added to give a 0.5 % (w/v) suspension. The suspension becomes clear as the solution is mixed by vortex. The mixture is then dialyzed (2,000 MWCO membrane) against Millipore water overnight with changing the water 3 times. The THF can also be removed by evaporation resulting in vesicular assemblies.

5.12.11 Preparation of $M^{M}_{65}(L_{0.5}/F_{0.5})_{20}$ and $M^{C}_{65}(L_{0.5}/F_{0.5})_{20}$ Polypeptide Assemblies:

Solid polypeptide powder was dispersed in THF to give 4 % (w/v) suspensions, which were then placed in a bath sonicator for 30 minutes until the copolypeptides were evenly dispersed. An

equal volume of Millipore water was added to each suspension, which was then placed in a bath sonicator for 30 minutes. Four equivalent aliquots of THF were then added in succession to the suspension, with vortexing in between each addition, to give final sample concentrations of 1 % (w/v) and a 3:1 ratio of THF to water. The suspensions were then placed in dialysis bags (MWCO = 2000 Da) and dialyzed against Millipore water under sterile conditions for 24 hours. The water was changed every hour for the first 4 hours.

5.12.12 Differential Interference Microscopy (DIC):

Suspensions of the copolypeptides, $M^{O}_{65}(L_{0.5}/F_{0.5})_{20}$, $M^{M}_{65}(L_{0.5}/F_{0.5})_{20}$ or $M^{C}_{65}(L_{0.5}/F_{0.5})_{20}$, (1 % (w/v)) were visualized on glass slides with a spacer between the slide and the cover slip (double-sided tape or Secure Seal Imaging Spacer, *Grace Bio-labs*) allowing the self-assembled structures to be minimally disturbed during focusing. The samples are imaged using a Zeiss Axiovert 200 DIC/Fluorescence Inverted Optical Microscope.

5.12.13 Extrusion of Polypeptide Assemblies:

The aqueous vesicle suspensions, $M^{O}_{65}(L_{0.5}/F_{0.5})_{20}$, $M^{M}_{65}(L_{0.5}/F_{0.5})_{20}$ or $M^{C}_{65}(L_{0.5}/F_{0.5})_{20}$, diluted to 0.2 % (w/v) were extruded using an Avanti Mini-Extruder. Extrusions were performed using different pore size Whatman Nuclepore Track-Etched polycarbonate (PC) membranes, following a protocol of serial extrusions of vesicles through decreasing filter pore sizes: 3 times through a 1.0 μm filter, 3 times through 0.4 μm nm filter, 3 times through 0.2 μm filter, and 3 times through 0.1 μm filter. The PC membranes and filter supports are soaked in Millipore water for 10 minutes prior to extrusion.

5.12.14 Dynamic Light Scattering (DLS) of Extruded Vesicles:

The 0.2 % (w/v) of extruded polypeptide suspensions, $M^{O}_{65}(L_{0.5}/F_{0.5})_{20}$, $M^{M}_{65}(L_{0.5}/F_{0.5})_{20}$ or $M^{C}_{65}(L_{0.5}/F_{0.5})_{20}$, were placed in a disposable cuvette and analyzed with the Malvern Zetasizer Nano ZS model Zen 3600 (Malvern Instruments Inc, Westborough, MA). A total scattering intensity of approximately 1 x 10^5 cps was targeted. The autocorrelation data was fitted using the CONTIN algorithm to determine the diameters of suspended assemblies.

5.12.15 Zeta Potential of Polypeptide Assemblies:

A 0.5 % (w/v) suspensions of copolypeptide vesicles, $M^{O}_{65}(L_{0.5}/F_{0.5})_{20}$, $M^{M}_{65}(L_{0.5}/F_{0.5})_{20}$ or $M^{C}_{65}(L_{0.5}/F_{0.5})_{20}$, was diluted to 0.2 % (w/v) with Millipore water containing NaCl to give a final concentration of 10 mM salt. The pH was then adjusted using NaOH or HCl to give acidic to basic solutions ranging from pH 3 to 8. The solution was added to a disposable capillary cell (Malvern Instruments Inc, Westborough, MA). The zeta potential was analyzed with the Malvern Zetasizer Nano ZS model Zen 3600 (Malvern Instruments Inc, Westborough, MA).

5.12.16 Dye Encapsulation in Polypeptide Vesicles

The diblock copolypeptide, $M^{M}_{65}(L_{0.5}/F_{0.5})_{20}$, sample were dispersed in THF to give 4 % (w/v) suspensions, which were then placed in a bath sonicator for 30 minutes until the copolypeptides were evenly dispersed. An equal volume of Millipore water containing Texas Red labeled dextran (Molecular Probes, MW = 3000, 0.25 mg/mL) was added to the suspension to give final sample concentrations of 2 % (w/v), which was then placed in a bath sonicator for 30 minutes. Four equivalent aliquots of THF were then added in succession to the suspension, with vortexing in between each addition, to give final sample concentrations of 1 % (w/v) and a 3:1 ratio of THF to water. The suspensions were then placed in dialysis bags (MWCO = 2000 Da) and

dialyzed against Millipore water under sterile conditions for 24 hours. The water was changed every hour for the first 4 hours. The THF can be removed by evaporation. After 24 hours, the suspension was transferred to a dialysis bag (MWCO = 8000 Da) to remove all dextran that was not encapsulated by the vesicles. The water was changed every hour for the first 4 hours and dialyzed for a total of 24 hours.

5.12.17 Protease Degradation of Poly(L-methionine sulfoxide), M^O, Poly(L-sodium carboxymethyl-methionine sulfonium chloride), M^C, and Poly(L-methyl-methionine sulfonium chloride), M^M:

A sample of poly(L-methionine sulfoxide)$_{265}$-*block*-poly(ethylene glycol)$_{45}$, M^O-PEG_{45}, poly(L-sodium carboxymethyl-methionine sulfonium chloride)$_{265}$-*block*-poly(ethylene glycol)$_{45}$, M^C-PEG_{45}, or poly(L-methyl-methionine sulfonium chloride)$_{265}$-*block*-poly(ethylene glycol)$_{45}$, M^M-PEG_{45}, (0.1 μmol, 28 μmol M^X) was dissolved in Millipore water containing 50 mM Tris- HCl and 5 mM $CaCl_2$ (1 mL). After the polypeptide was completely soluble, Proteinase K (0.0036 μmol) was added to the solution and placed in a 37 °C water bath and allowed to react for 24 hrs. After 24 hours, EDTA was added to the solution to stop the degradation. The solution was added to a dialysis bag (1000 MWCO) and dialyzed against water to remove EDTA and Calcium from the solution. The sample was freeze-dried to yield a white solid (Poly(ethylene glycol)$_{45}$).

5.12.18 Bradford Assay with Polypeptide Vesicle:

Bradford assay was performed to quantify the final concentration of the polypeptide vesicles after extrusion according to the manufacture supplied instructions, using the pre-dialyzed samples as the standard.

5.12.19 Cell Culture:

The HeLa cell line was grown in Minimal Essential Medium supplemented with 26.2 mM sodium bicarbonate, 1 mM sodium pyruvate, 10% FBS, and 1% penicillin/streptomycin, at a pH of 7.4. The cell line is maintained in a 37°C humidified atmosphere with 5% CO2 and handled with standard sterile tissue culture protocols.

5.12.20 Measurement of Cytotoxicity using the MTS Cell Proliferation Assay:

The MTS cell proliferation assay (CellTiter 96® AQueous Non-Radioactive Cell Proliferation Assay) was performed to assess the cytotoxicity level of the vesicles. The uptake experiments were performed with HeLa cells seeded on 96-well plates with triplicates of each condition. After the 5-hr incubation period, the medium was aspirated and fresh medium containing 20% MTS reagent was added to the cells. The cells were incubated again at 37°C for 1 hr, and the absorbances at 490 nm and 700 nm were measured using the Infinite F200 plate reader (Tecan Systems Incorporated, San Jose, CA). The relative survival of cells compared to control cells (*i.e.*, cells incubated in growth medium without vesicles) was calculated by determining the ratio of the (A490 – A700) values.

5.12.21 Cellular Uptake of Polypeptide Vesicles:

HeLa cells were seeded at a density of $5x10^5$ cells/cm2 and incubated overnight prior to the experiment. The cells were seeded onto 8-well chambered coverglasses for confocal microscopy experiments and 35 mm tissue culture plates for flow cytometry. On the day of the experiment, different fluorescently-labeled vesicles were separately diluted in serum-free media and incubated with HeLa cells for 5 hrs to allow the vesicles to be internalized into the cells. Subsequently, the medium containing the vesicles was aspirated, and the cells were washed three

times with PBS to remove nonspecifically attached peptides on the cell surface. Afterwards, the cells are subjected to either confocal microscopy or flow cytometry to determine the extent of vesicle uptake.

5.12.22 Laser Scanning Confocal Microscopy (LSCM) of Cells:

The LSCM images of the cells were taken on a Leica Inverted TCS-SP MP Spectral Confocal and Multiphoton Microscope (Heidelberg, Germany) equipped with an argon laser (488 nm blue excitation: JDS Uniphase), a diode laser (DPSS; 561 nm yellow-green excitation: Melles Griot), a helium-neon laser (633 nm red excitation), and a two photon laser setup consisting of a Spectra-Physics Millenia X 532 nm green diode pump laser and a Tsunami Ti-Sapphire picosecond pulsed infrared laser tuned at 768 nm for UV excitation.

5.13 Spectral Data:

[1]H-NMR spectra of polypeptides in *d*-TFA

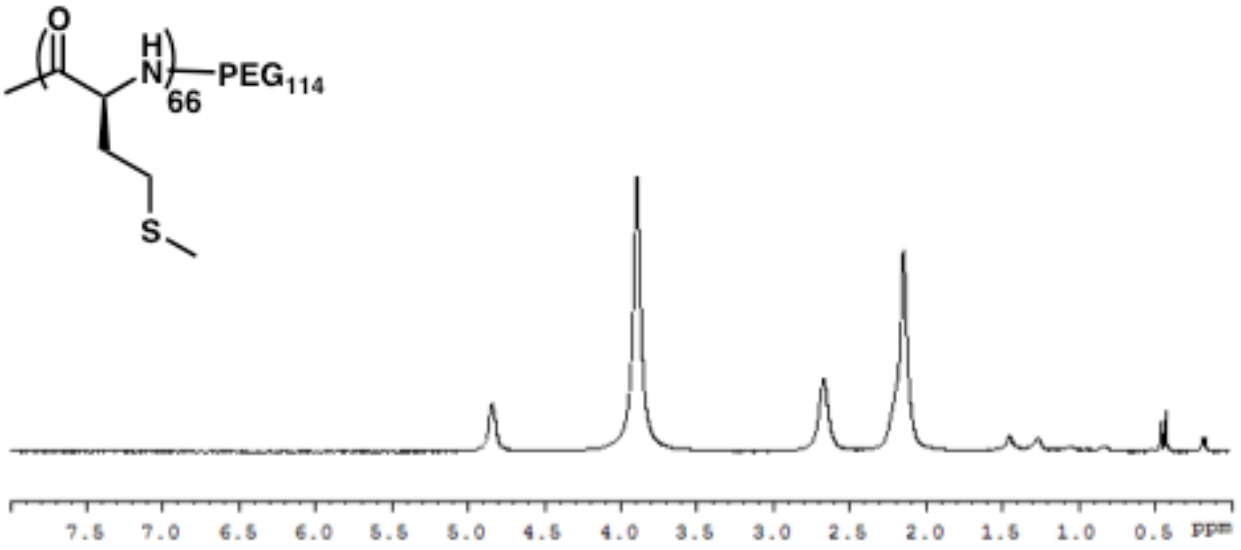

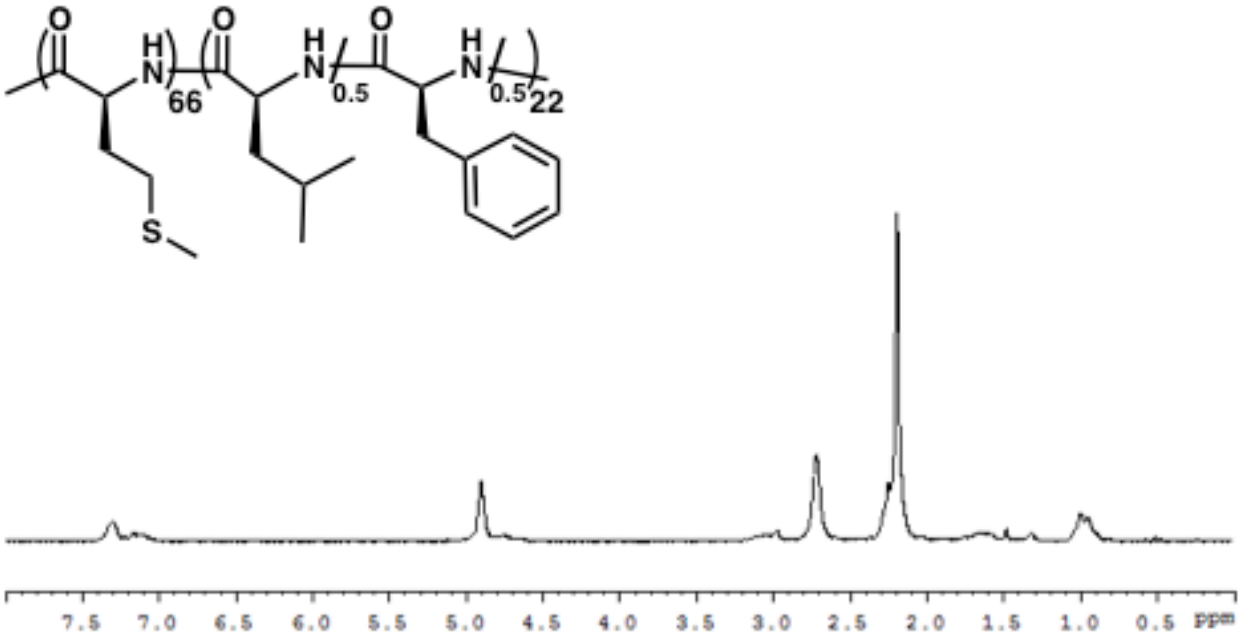

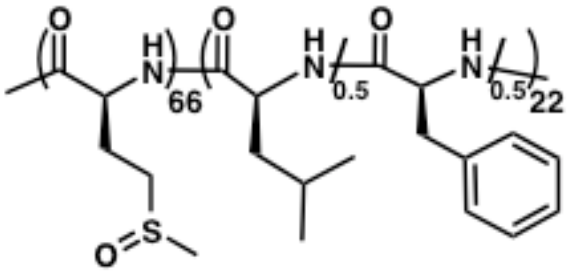
O
H
N
66
O
H
N
0.5
O
H
N
0.5
22
O=S

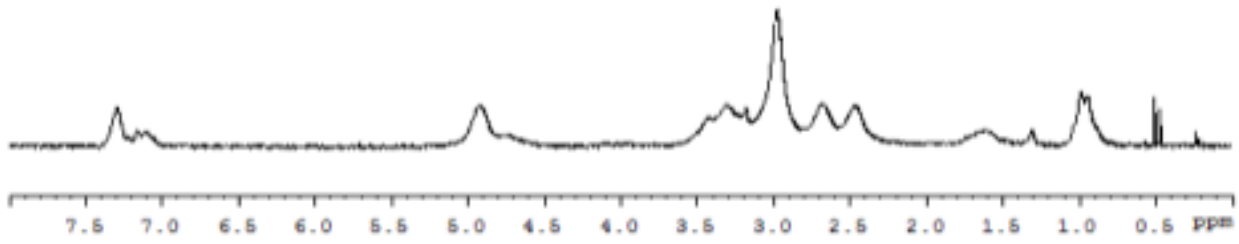
7.5 7.0 6.5 6.0 5.5 5.0 4.5 4.0 3.5 3.0 2.5 2.0 1.5 1.0 0.5 ppm

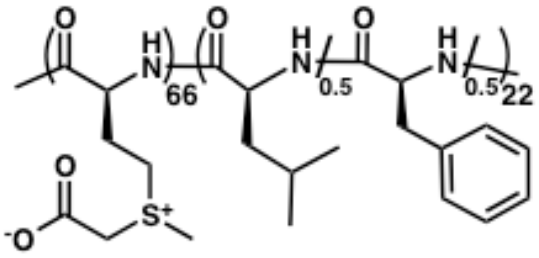
O
H
N
66
O
H
N
0.5
O
H
N
0.5
22
O
-O
S+

7.5 7.0 6.5 6.0 5.5 5.0 4.5 4.0 3.5 3.0 2.5 2.0 1.5 1.0 0.5 ppm

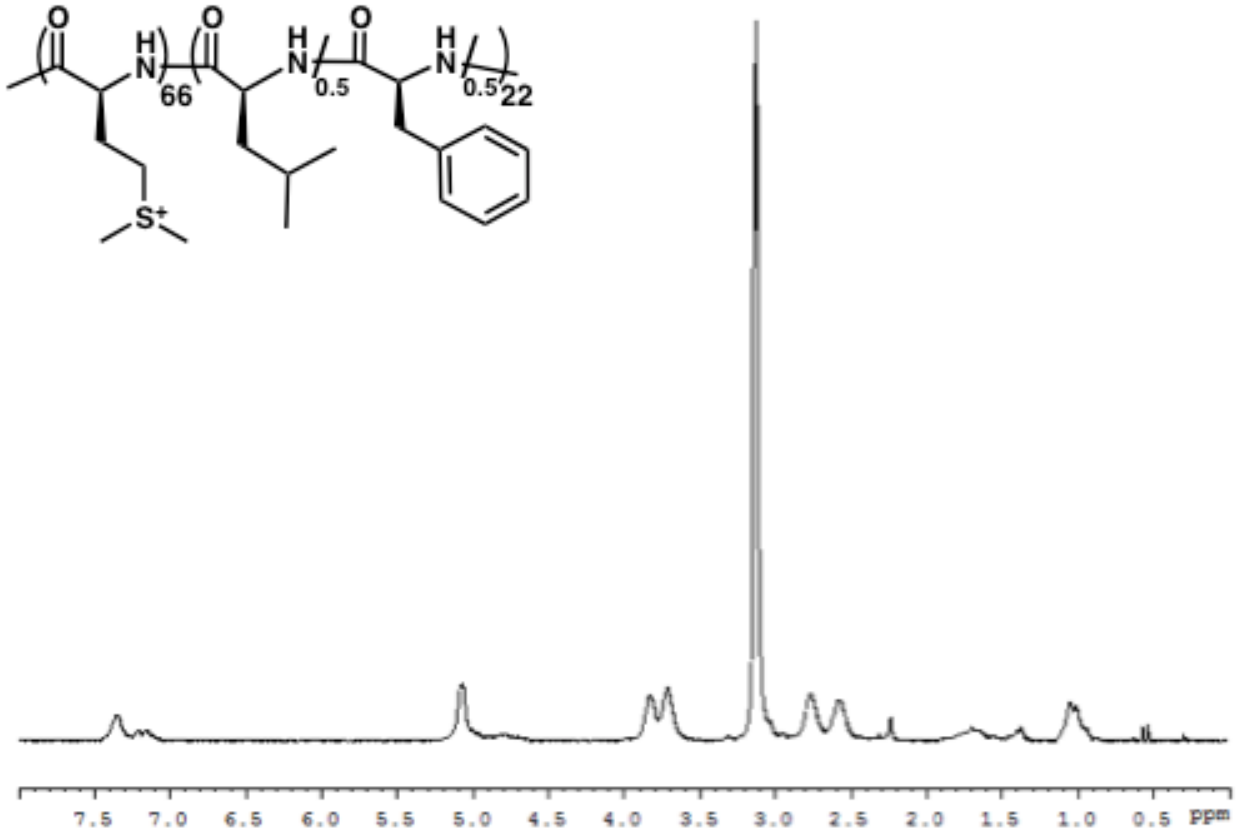

5.14 References

(1) Holowka, E. P.; Sun, V. Z.; Kamei, D. T.; Deming, T. J. *Nat Mater* **2007**, *6*, 52.

(2) Mitchell, D. J.; Steinman, L.; Kim, D. T.; Fathman, C. G.; Rothbard, J. B. *The Journal of Peptide Research* **2000**, *56*, 318.

(3) Rodriguez, A. R.; Choe, U.-J.; Kamei, D. T.; Deming, T. J. *Macromolecular Bioscience* **2012**, *12*, 805.

(4) Bellomo, E. G.; Wyrsta, M. D.; Pakstis, L.; Pochan, D. J.; Deming, T. J. *Nat Mater* **2004**, *3*, 244.

(5) Pitha, J.; Szente, L.; Greenberg, J. *Journal of Pharmaceutical Sciences* **1983**, *72*, 665.

(6) Paskowski, D. J.; Stevens, E. S.; Bonora, G. M.; Toniolo, C. *Biochimica et Biophysica Acta (BBA) - Protein Structure* **1978**, *535*, 188.

(7) Hunt, S. *Comparative Biochemistry and Physiology Part B: Comparative Biochemistry* **1987**, *88*, 1013.

(8) Minoura, N.; Fujiwara, Y.; Nakagawa, T. *Journal of Applied Polymer Science* **1978**, *22*, 1593.

(9) Perlmann, G. E.; Katchalski, E. *Journal of the American Chemical Society* **1962**, *84*, 452.

(10) Bodanszky, M.; Bednarek, M. A. *International Journal of Peptide and Protein Research* **1982**, *20*, 408.

(11) Goverman, J. M.; Pierce, J. G. *Journal of Biological Chemistry* **1981**, *256*, 9431.

(12) Lawson, W. B.; Schramm, H.-J. *Biochemistry* **1965**, *4*, 377.

(13) Kramer, J. R.; Deming, T. J. *Biomacromolecules* **2012**, *13*, 1719.

(14) Pangborn, A. B.; Giardello, M. A.; Grubbs, R. H.; Rosen, R. K.; Timmers, F. J. *Organometallics* **1996**, *15*, 1518.

(15) Breedveld, V.; Nowak, A. P.; Sato, J.; Deming, T. J.; Pine, D. J. *Macromolecules* **2004**, *37*, 3943.

(16) Fuller, W. D.; Verlander, M. S.; Goodman, M. *Biopolymers* **1976**, *15*, 1869.

(17) Kramer, J. R.; Deming, T. J. *Biomacromolecules* **2010**, null.

CHAPTER SIX

Incorporation of Methionine to Reduce Cytotoxicity of Block Copolypeptides Vesicles, While Maintaining Cellular Uptake

6.1 Abstract

This chapter describes the preparation, design and self-assembly of multiblock copolypeptides, of the composition poly(L-homoarginine)$_x$-*block*-poly(L-methionine sulfoxide)$_{55}$-*block*-poly(L-leucine$_{0.5}$-*co*-L-phenylalanine$_{0.5}$)$_{20}$, $R^H{}_xM^O{}_{55}(L_{0.5}/F_{0.5})_{20}$. In this study, triblock copolypeptides were prepared by ring-opening polymerization of N_ε-trifluoroacetyl-L-lysine-N-carboxyanhydride (TFA-Lys NCA), followed by L-methionine N-carboxyanhydride (Met NCA), and by copolymerization of L-leucine N-carboxyanhydride (Leu NCA) and L-phenylalanine N-carboxyanhydride (Phe NCA) to form the third block. These triblock copolypeptides have the ability to self-assemble into vesicles and have enhanced intracellular delivery. The poly(L-methionine sulfoxide) domain has the ability to be reduced back to poly(L-methionine) under reductive conditions and by natural occurring enzymes leading to disruption of vesicle assemblies.

6.2 Introduction

The focus of the vesicle project has been to incorporate new polypeptide domains that can lead to enhanced cellular uptake, reduced cytotoxicity and stimuli responsiveness. The previous chapter has shown the advantages of using poly(L-methionine) as a versatile domain

that may be modified for incorporating multiple side chain functionalities. The diblock copolypeptide poly(L-methionine)$_{65}$-*block*-poly(L-leucine$_{0.5}$-*co*-L-phenylalanine$_{0.5}$)$_{20}$, $M_{65}(L_{0.5}/F_{0.5})_{20}$, was modified by oxidation and alkylation to yield poly(L-methionine sulfoxide)$_{65}$-*block*- (L-leucine$_{0.5}$-*co*- L-phenylalanine$_{0.5}$)$_{20}$, $M^{O}{}_{65}(L_{0.5}/F_{0.5})_{20}$, poly(L-methyl-methionine sulfonium chloride)$_{65}$-*block*- (L-leucine$_{0.5}$-*co*- L-phenylalanine$_{0.5}$)$_{20}$, $M^{M}{}_{65}(L_{0.5}/F_{0.5})_{20}$, and poly(L-carboxymethyl-methionine sulfonium chloride)$_{65}$-*block*- (L-leucine$_{0.5}$-*co*- L-phenylalanine$_{0.5}$)$_{20}$, $M^{C}{}_{65}(L_{0.5}/F_{0.5})_{20}$. All three samples gave vesicles with flexible membranes that could be extruded to diameters below 200 nanometers.

Poly(L-methionine sulfoxide) has shown properties of being biologically inert with no toxicity *in vitro* or *in vivo*,[1] and when incorporated into polypeptide vesicle showed no toxicity up to 100 μg/mL. These results show promise of a new inert material that may be biocompatible and biodegradable. Methionine sulfoxide can be found in biological systems on proteins in the presence of oxidative stress. However, the oxidation of methionine can destabilize the protein structure and cause loss of function.[2] To circumvent methionine oxidation, nature has developed the enzymes methionine sulfoxide reductase A and B (MsrA and MsrB) that are responsible for reducing methionine sulfoxide back to methionine.[3,4] It must be noted that research has shown reduction of methionine-S-sulfoxide by MsrA and methionine-R-sulfoxide by MsrB, however results vary with free methionine sulfoxides versus protein bound methionine sulfoxides.[5,6] Recently, research has shown other Msr activities when MsrA^{-}B^{-} genes are knocked out showing that there are other possible reductase enzymes.[5] Research has shown that many cells contain methionine sulfoxide reductases and can be isolated from mammalian cells, fungus as well as plant cells (i.e. HeLa, spinach, yeast etc).[2,3]

In biological systems reducing environments are typically found intracellularly, while oxidizing environments are found extracellularly.[2,7,8] This can be used as design strategy for the development of intracellular drug delivery vehicles. There is research into developing drug carriers that contain disulfide linkages for reduction-triggered release of therapeutics, once the drug carrier is taken up by the cell.[7] Design of a polypeptide vesicle containing methionine sulfoxide may also utilize the redox environments of biological systems. Polypeptide vesicles containing domains of poly(L-methionine sulfoxide) may be stable extracellularly while circulating the blood stream; once internalized by cells the reductase enzymes and reducing environment may reverse the oxidation to yield methionine. Reduction of the methionine sulfoxide domain may disrupt the amphiphilic ratio; destabilizing the vesicles causing them to fall apart and release their cargo.

This chapter presents the design and synthesis of multiblock copolypeptides that contains dual hydrophilic domains: poly(L-methionine sulfoxide) domain for reduced cytotoxicity and stimuli responsiveness; poly(L-homoarginine) for structure and enhanced intracellular delivery of vesicles. The vesicular assemblies were characterized and cellular studies were conducted for cytotoxicity and cellular uptake. The last part of the chapter focuses on vesicle response to reducing environments.

6.3 Preparation of Methionine Containing Triblock Copolypeptides

The dual hydrophilic triblock copolypeptides were designed with both hydrophilic segments on one side opposite the hydrophobic domain. This leads to vesicle assemblies containing both hydrophilic segments on the same sides of the membrane. As previously

reported in chapter three, other "dual hydrophilic" triblock copolymer vesicles differ from this strategy by having the hydrophobic domain in the middle separating the hydrophilic segments.

As previously described, literature shows that individual polyguanidine segments of ca. 6-9 residues in length are sufficient to promote cellular uptake, allowing the design of triblocks with a shorter homoarginine segment in comparison to the methionine sulfoxide segment. Triblock copolypeptides were designed with the composition poly(L-homoarginine-HCl)$_x$-*block*-poly(L-methionine sulfoxide)$_{55}$-*block*-poly(L-leucine$_{0.5}$-*co*-L-phenylalanine$_{0.5}$)$_{20}$, $R^H_xM^O_{55}(L_{0.5}/F_{0.5})_{20}$ (x = 10 or 20). The oxidized diblock copolypeptide, poly(L-methionine sulfoxide)$_{65}$-*block*-poly(L-leucine$_{0.5}$-*co*-L-phenylalanine$_{0.5}$)$_{20}$, $M^O_{65}(L_{0.5}/F_{0.5})_{20}$, prepared in the previous chapter was used for further experiments along with $R^H_xM^O_{55}(L_{0.5}/F_{0.5})_{20}$ (x = 10 or 20).

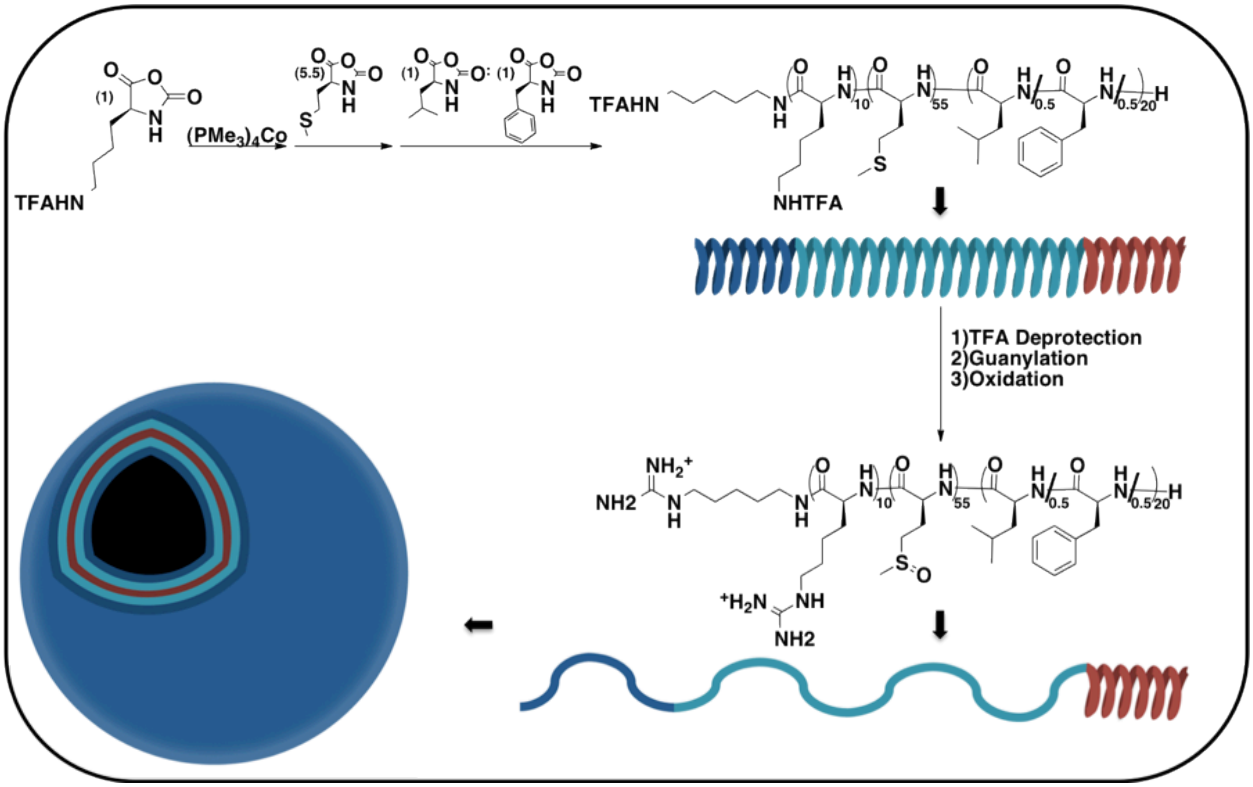

Figure 6.1 Structures and schematic drawings of triblock copolypeptide preparation and modification for vesicle self-assembly.

Table 6.1 Characterization of $M_{60}(L_{0.5}/F_{0.5})_{20}$, $(TFA)K_{10}M_{55}(L_{0.5}/F_{0.5})_{20}$, $(TFA)K_{20}M_{55}(L_{0.5}/F_{0.5})_{20}$ block copolypeptides.

Block Copolypeptide	M^a	Found Composition[b]	Yield (%)[c]
$M_{65}(L_{0.5}/F_{0.5})_{20}$	8,650	$M_{66}(L_{0.5}/F_{0.5})_{22}$	93
$(TFA)K_{10}M_{55}(L_{0.5}/F_{0.5})_{20}$	9,670	$(TFA)K_{11}M_{55}(L_{0.5}/F_{0.5})_{18}$	97
$(TFA)K_{20}M_{55}(L_{0.5}/F_{0.5})_{20}$	11,780	$(TFA)K_{21}M_{54}(L_{0.5}/F_{0.5})_{18}$	90

[a] Hydrophilic segment lengths (average molecular weight, *M*, for M, and (TFA)KM segments) determined using ^{1}H NMR by end-capping analysis of polypeptide. [b] Calculated using ^{1}H NMR. [c] Total isolated yield of block copolypeptide.

6.4 Vesicle Self-Assembly Using Methionine Triblock Copolypeptides

Since short polyguanidine segments of ca. 6-9 residues in length are sufficient to promote cellular uptake, poly(L-homoarginine) segments covering the entire vesicle surface is unnecessary for enhanced intracellular delivery. The cationic charge on the surface of the vesicle may cause increased toxicity with increased polypeptide concentrations. In order to reduce the amount of cationic character on the surface of the vesicle, the triblock copolypeptides, $R^H_{10}M^O_{55}(L_{0.5}/F_{0.5})_{20}$ and $R^H_{20}M^O_{55}(L_{0.5}/F_{0.5})_{20}$, were mixed during vesicle formation with the purely neutral diblock copolypeptide, $M^O_{65}(L_{0.5}/F_{0.5})_{20}$. The triblock:diblock mixtures are prepared by combining the corresponding amounts of polypeptide and following the same protocol. The percentage of triblock was varied from 0 to 100 % of 1 % (w/v) polypeptide during solvent annealing. Briefly, the polypeptide is dispersed in tetrahydrofuran (THF) to give a 1 % (w/v) suspension, which is then placed in a bath sonicator for 30 minutes until the copolypeptide is evenly dispersed. An equal volume of Millipore water is added in one portion to give a 0.5 % (w/v) suspension. The sample is vortexed to fully solubilize the sample and then placed in a

dialysis bag (MWCO = 2000 Da) and dialyzed against Millipore water, with the water changed every hour for the first 4 hours. Vesicles are also self-assembled from the evaporation of THF. Images from DIC confirmed the presence of vesicles for all samples, containing $R^{H}_{10}M^{O}_{55}(L_{0.5}/F_{0.5})_{20}$ or $R^{H}_{20}M^{O}_{55}(L_{0.5}/F_{0.5})_{20}$, processed by solvent annealing with 1:1 ratio of THF to water (**Figure 6.2**).

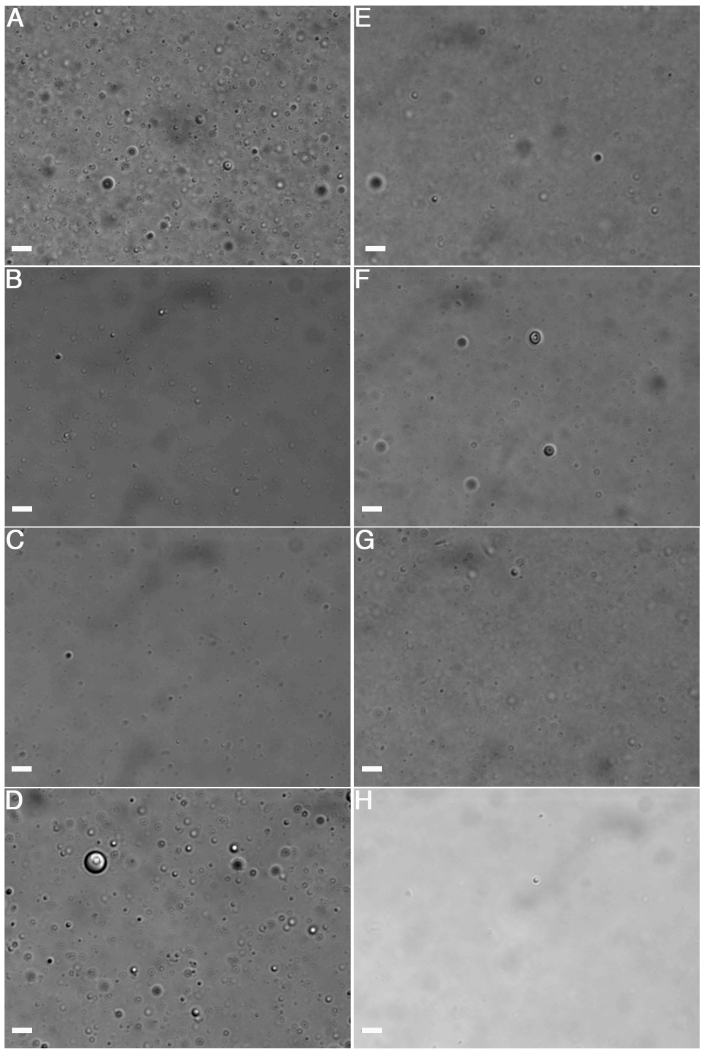

Figure 6.2 Differential interference contrast (DIC) images of 1 % (w/v) aqueous triblock: diblock suspensions of (A) 25 % $R^{H}_{10}M^{O}_{55}(L_{0.5}/F_{0.5})_{20}$: 75 % $M^{O}_{65}(L_{0.5}/F_{0.5})_{20}$, (B) 50 % $R^{H}_{10}M^{O}_{55}(L_{0.5}/F_{0.5})_{20}$: 50 % $M^{O}_{65}(L_{0.5}/F_{0.5})_{20}$, (C) 75 % $R^{H}_{10}M^{O}_{55}(L_{0.5}/F_{0.5})_{20}$: 25 % $M^{O}_{65}(L_{0.5}/F_{0.5})_{20}$, (D) 100 % $R^{H}_{10}M^{O}_{55}(L_{0.5}/F_{0.5})_{20}$, (E) 25 % $R^{H}_{20}M^{O}_{55}(L_{0.5}/F_{0.5})_{20}$: 75 % $M^{O}_{65}(L_{0.5}/F_{0.5})_{20}$, (F) 50 % $R^{H}_{20}M^{O}_{55}(L_{0.5}/F_{0.5})_{20}$: 50 % $M^{O}_{65}(L_{0.5}/F_{0.5})_{20}$, (G) 75 % $R^{H}_{20}M^{O}_{55}(L_{0.5}/F_{0.5})_{20}$: 25 % $M^{O}_{65}(L_{0.5}/F_{0.5})_{20}$, and (H) 100 % $R^{H}_{20}M^{O}_{55}(L_{0.5}/F_{0.5})_{20}$. Scale bars = 5 μm.

These samples contain sulfoxides, which is similar in structure to dimethylsulfoxide (DMSO) solvent. DMSO is a polar aprotic solvent that can solubilize both polar and nonpolar compounds and is commonly used as a solvent for solubilizing drug compounds. For these reasons it was tested as a cosolvent for solvent annealing since it is miscible with water. Images revealed vesicular assemblies of different methionine sulfoxide samples (**Figure 6.3**).

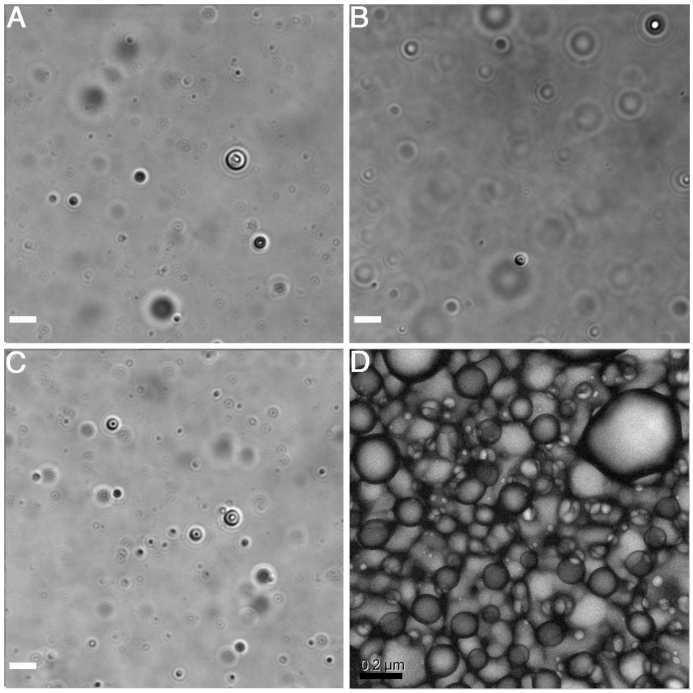

Figure 6.3 Differential interference contrast (DIC) images of 1 % (w/v) aqueous suspensions of (A) $R^{H}_{10}M^{O}_{55}(L_{0.5}/F_{0.5})_{20}$, (B) $R^{H}_{20}M^{O}_{55}(L_{0.5}/F_{0.5})_{20}$, and (C) 25 % $R^{H}_{10}M^{O}_{55}(L_{0.5}/F_{0.5})_{20}$: 75 % $M^{O}_{65}(L_{0.5}/F_{0.5})_{20}$. Transmission electron microscopy of 0.1 % (D) $M^{O}_{65}(L_{0.5}/F_{0.5})_{20}$. White scale bars = 5 μm and black scale bar = 0.2 μm.

The vesicle morphology is confirmed by labeling their hydrophilic domain with a fluorescent molecule and imaging thin slices through the suspension of the sample using laser scanning confocal microscopy (LSCM), which revealed their membrane structure and hydrophilic interior (**Figure 6.4**).

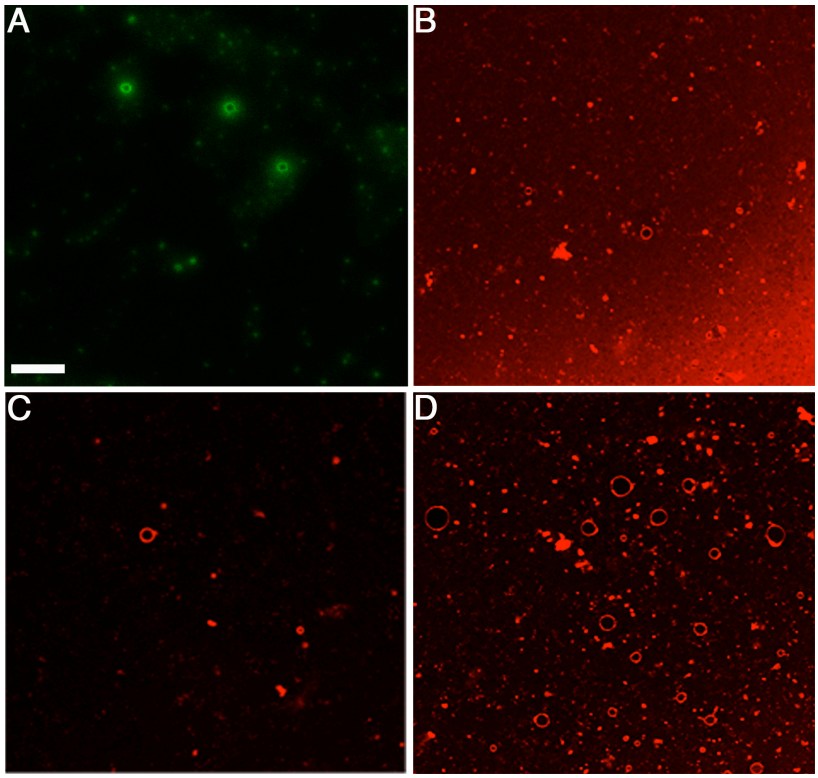

Figure 6.4 LSCM images of 1 % (w/v) aqueous suspensions of (A) FITC labeled $M^{O}_{65}(L_{0.5}/F_{0.5})_{20}$, (B) TRITC labeled $R^{H}_{10}M^{O}_{55}(L_{0.5}/F_{0.5})_{20}$, and (C) TRITC labeled $R^{H}_{20}M^{O}_{55}(L_{0.5}/F_{0.5})_{20}$ (D) 25 % TRITC labeled $R^{H}_{20}M^{O}_{55}(L_{0.5}/F_{0.5})_{20}$: 75 % $M^{O}_{65}(L_{0.5}/F_{0.5})_{20}$. Scale bars = 10 μm.

To test that the triblock copolypeptides are mixing with diblock copolypeptides and not segregating, forming separate vesicular assemblies, each copolypeptide is labeled separately with different fluorescent molecules and imaged using LSCM. The colocalization of the fluorescence will show that both copolypeptides are together forming the same vesicles. The triblock copolypeptide, $R^{H}_{10}M^{O}_{55}(L_{0.5}/F_{0.5})_{20}$, was labeled with tetramethyl rhodamine isothiocyanate (TRITC) and the diblock copolypeptide, $M^{O}_{65}(L_{0.5}/F_{0.5})_{20}$, was labeled fluorescein isothiocyanate (FITC) (**Figure 6.5**). The suspension was imaged in the xy plane at different optical z-slices showing the unilamellar vesicles.

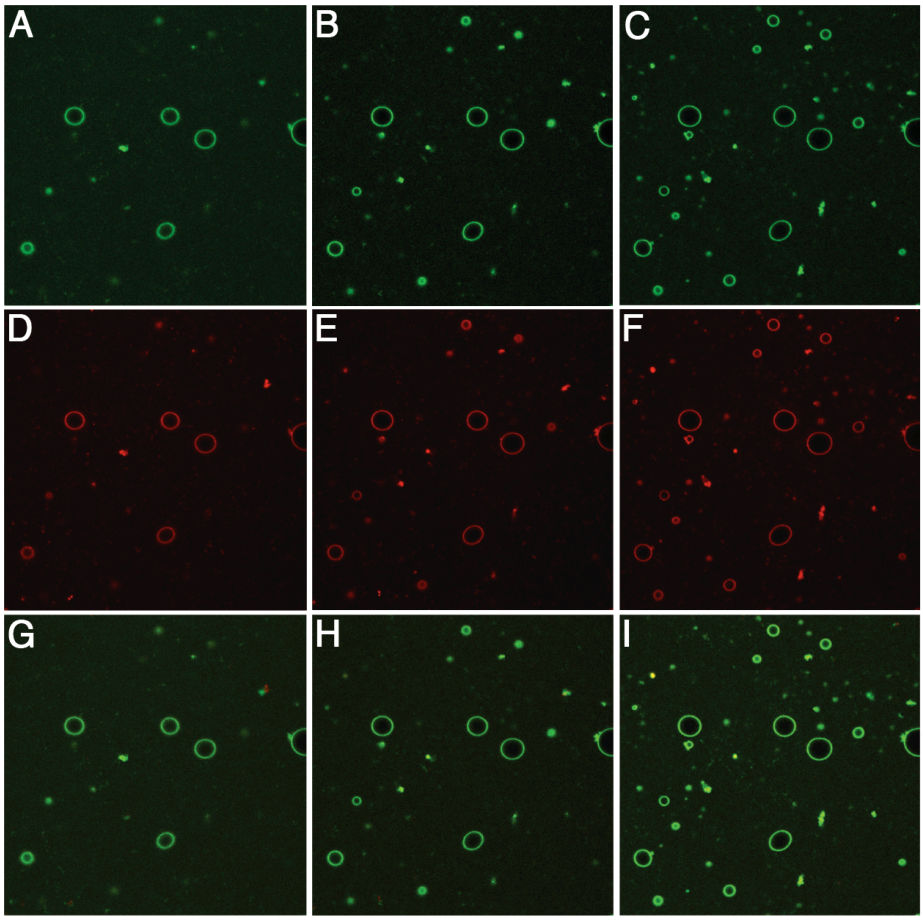

Figure 6.5 LSCM z-series images of 1 % (w/v) aqueous suspensions 25 % TRITC labeled $R^{H}_{10}M^{O}_{55}(L_{0.5}/F_{0.5})_{20}$: 75 % FITC labeled $M^{O}_{65}(L_{0.5}/F_{0.5})_{20}$. (A-C) FITC channel, (D-F) TRITC channel and (G-I) overlay.

Fluorescence spectroscopy of the suspension, 25 % TRITC labeled $R^{H}_{10}M^{O}_{55}(L_{0.5}/F_{0.5})_{20}$: 75 % FITC labeled $M^{O}_{65}(L_{0.5}/F_{0.5})_{20}$, was excited at 495 nm; excitation wavelength of FITC. The fluorescence energy of FITC was transferred to excite TRITC molecules in close proximity showing the emission of TRITC (**Figure 6.6**C).[9]

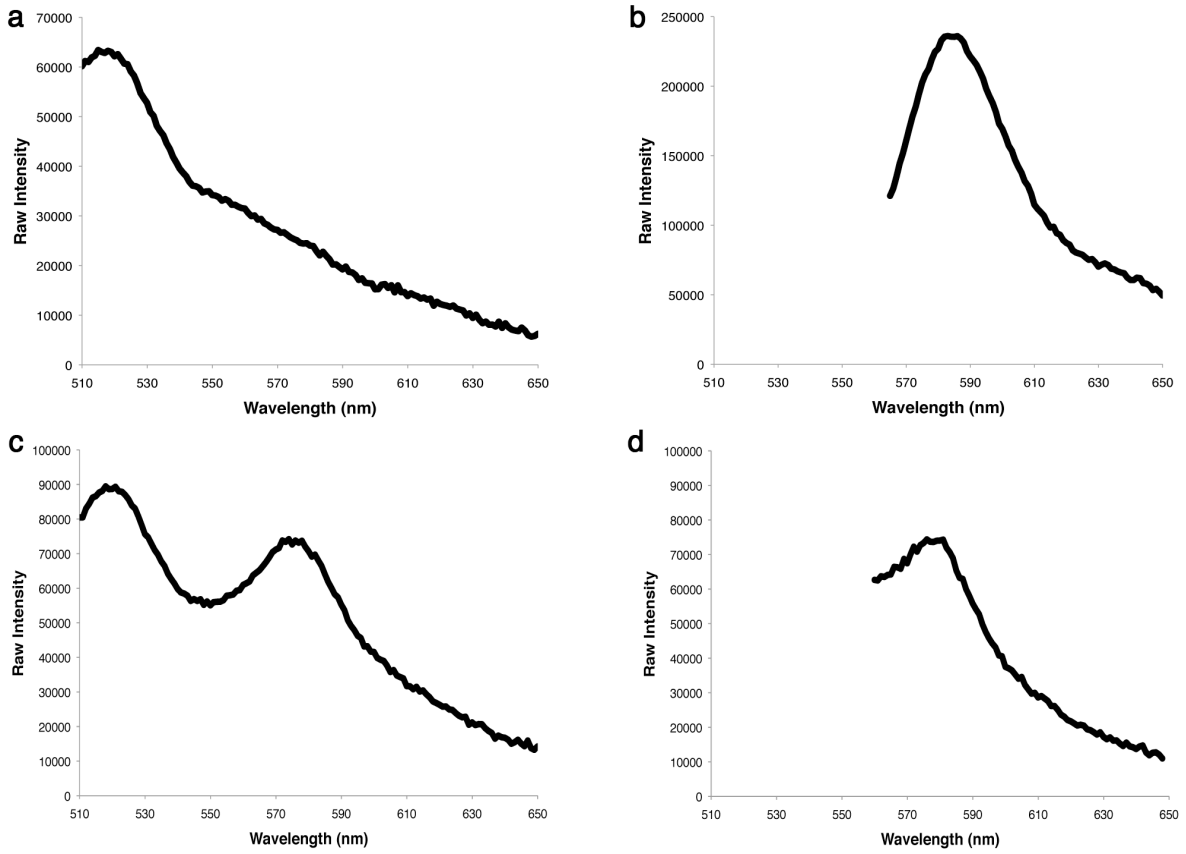

Figure 6.6 Fluorescence emission of vesicle suspensions (a) FITC labeled $M^{O}_{65}(L_{0.5}/F_{0.5})_{20}$ (excitation = 495 nm), (b) TRITC labeled $R^{H}_{20}M^{O}_{55}(L_{0.5}/F_{0.5})_{20}$ (excitation = 555 nm), (c) 25 % TRITC labeled $R^{H}_{20}M^{O}_{55}(L_{0.5}/F_{0.5})_{20}$: 75 % FITC labeled $M^{O}_{65}(L_{0.5}/F_{0.5})_{20}$ (excitation = 495 nm) and (d) 25 % TRITC labeled $R^{H}_{20}M^{O}_{55}(L_{0.5}/F_{0.5})_{20}$: 75 % FITC labeled $M^{O}_{65}(L_{0.5}/F_{0.5})_{20}$ (excitation = 555 nm). Panel c shows transfer of energy from FITC to TRITC showing emission at 575 nm. Panel d shows similar level of fluorescence intensity of TRITC emission excited at 555 nm vs. 495 nm.

6.5 Cytotoxicity of Triblock Containing Polypeptide Vesicles

Previous chapter showed that poly(L-methionine sulfoxide) as a hydrophilic domain on polypeptide vesicles showed no toxicity up to 100 μg/mL. The incorporation of cationic domains on the surface can lead to increased toxicity with increased polypeptide concentration. MTS assay was used to determine the cytotoxicity with increasing polypeptide concentrations of

suspensions containing 0 to 100 % triblock copolypeptides (**Figure 6.7**). The cationic sample, $R^{H}_{55}L_{20}$, was used for comparison with the triblock copolypeptide containing vesicles.

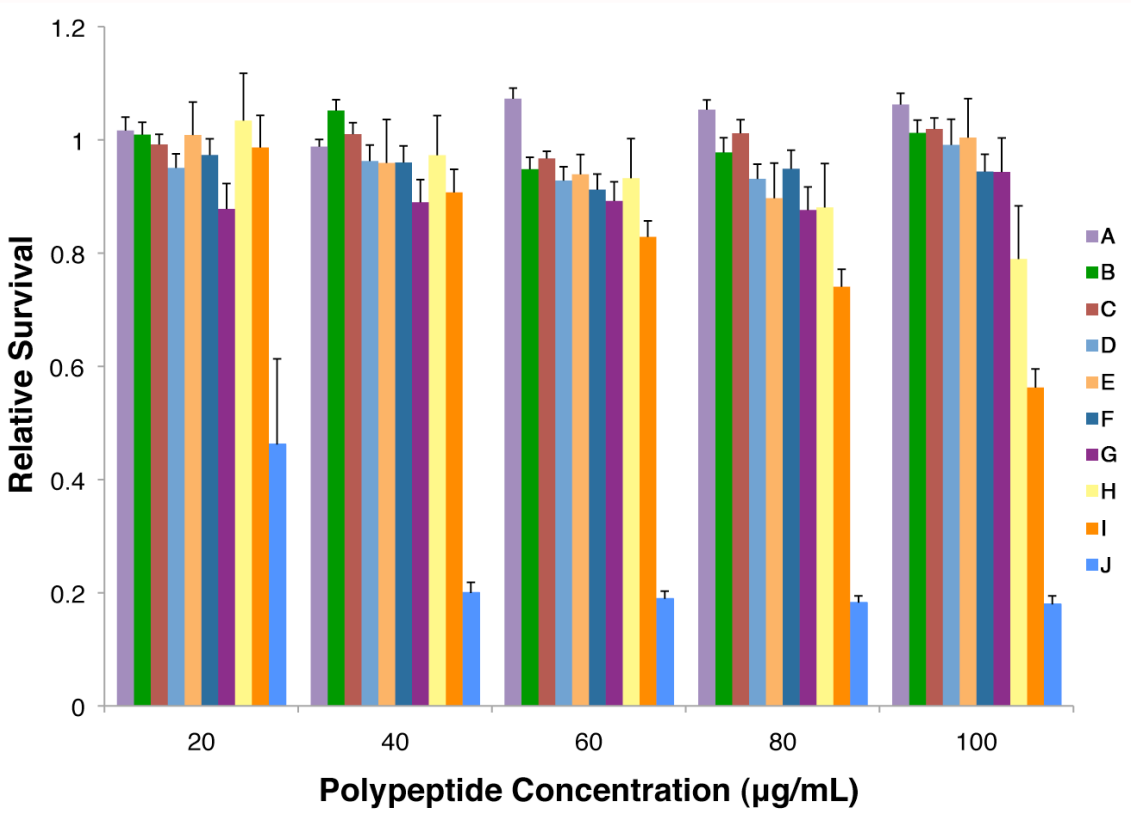

Figure 6.7 MTS cell survival data after 5 hr for HeLa cells separately incubated with aqueous suspensions (A) $M^{O}_{65}(L_{0.5}/F_{0.5})_{20}$, (B) 25 % $R^{H}_{10}M^{O}_{55}(L_{0.5}/F_{0.5})_{20}$: 75 % $M^{O}_{65}(L_{0.5}/F_{0.5})_{20}$, (C) 25 % $R^{H}_{20}M^{O}_{55}(L_{0.5}/F_{0.5})_{20}$: 75 % $M^{O}_{65}(L_{0.5}/F_{0.5})_{20}$, (D) 50 % $R^{H}_{10}M^{O}_{55}(L_{0.5}/F_{0.5})_{20}$: 50 % $M^{O}_{65}(L_{0.5}/F_{0.5})_{20}$, (E) 50 % $R^{H}_{20}M^{O}_{55}(L_{0.5}/F_{0.5})_{20}$: 50 % $M^{O}_{65}(L_{0.5}/F_{0.5})_{20}$, (F) 75 % $R^{H}_{10}M^{O}_{55}(L_{0.5}/F_{0.5})_{20}$: 25 % $M^{O}_{65}(L_{0.5}/F_{0.5})_{20}$, (G) 75 % $R^{H}_{20}M^{O}_{55}(L_{0.5}/F_{0.5})_{20}$: 25 % $M^{O}_{65}(L_{0.5}/F_{0.5})_{20}$, (H) $R^{H}_{10}M^{O}_{55}(L_{0.5}/F_{0.5})_{20}$, (I) $R^{H}_{20}M^{O}_{55}(L_{0.5}/F_{0.5})_{20}$, and (J) $R^{H}_{60}L_{20}$.

Results from MTS do show a slight trend with suspensions containing higher amounts of triblock making the sample more toxic at higher concentrations. Validating the vesicle design, very little cytotoxicity is seen up to 100 µg/mL with suspension containing 75 % or less triblock copolypeptides making up the vesicles.

6.6 Cellular Uptake of Triblock Containing Polypeptide Vesicles

To test if the M^O segment is inhibiting the R^H segments from promoting enhanced cellular uptake, fluorescein labeled polypeptides were self-assembled into vesicles where the fluorescence of each sample was equilibrated. The % of triblock needed for enhanced cellular uptake was investigated by self-assembling vesicle suspension with 25 to 100 % triblock copolypeptides.

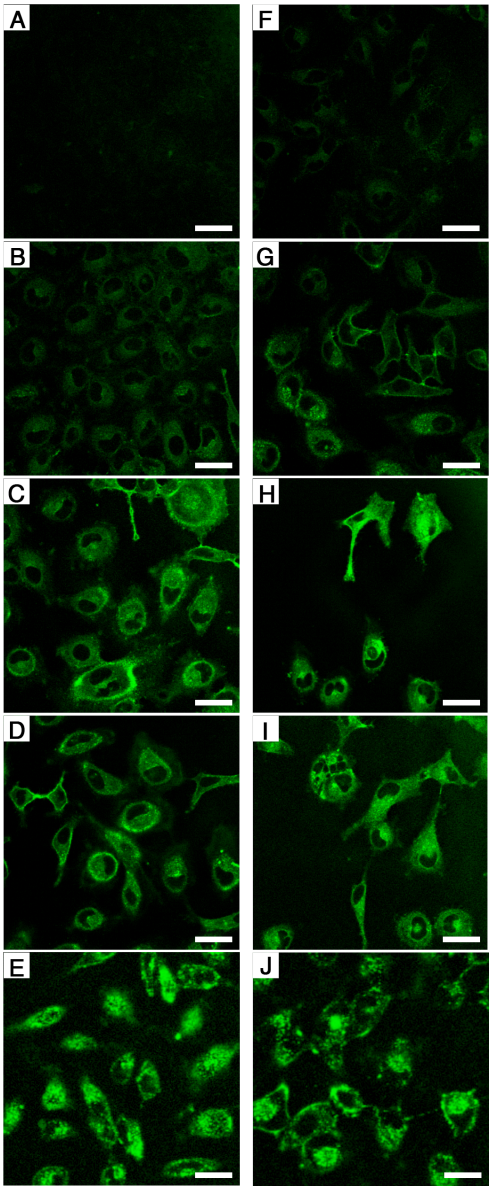

Figure 6.8 Fluorescence microscopy of HeLa cells incubated with vesicle suspensions (10 μg/mL). (A) Cells only, (B) 25 % $R^{H}_{10}M^{O}_{55}(L_{0.5}/F_{0.5})_{20}$: 75 % $M^{O}_{65}(L_{0.5}/F_{0.5})_{20}$, (C) 50 % $R^{H}_{10}M^{O}_{55}(L_{0.5}/F_{0.5})_{20}$: 50 % $M^{O}_{65}(L_{0.5}/F_{0.5})_{20}$, (D) 75 % $R^{H}_{10}M^{O}_{55}(L_{0.5}/F_{0.5})_{20}$: 25 % $M^{O}_{65}(L_{0.5}/F_{0.5})_{20}$, (E) $R^{H}_{10}M^{O}_{55}(L_{0.5}/F_{0.5})_{20}$, (F) $M^{O}_{65}(L_{0.5}/F_{0.5})_{20}$, (G) 25 % $R^{H}_{20}M^{O}_{55}(L_{0.5}/F_{0.5})_{20}$: 75 % $M^{O}_{65}(L_{0.5}/F_{0.5})_{20}$, (H) 50 % $R^{H}_{20}M^{O}_{55}(L_{0.5}/F_{0.5})_{20}$: 50 % $M^{O}_{65}(L_{0.5}/F_{0.5})_{20}$, (I) 75 % $R^{H}_{20}M^{O}_{55}(L_{0.5}/F_{0.5})_{20}$: 25 % $M^{O}_{65}(L_{0.5}/F_{0.5})_{20}$, and (J) $R^{H}_{20}M^{O}_{55}(L_{0.5}/F_{0.5})_{20}$. Scale bars = 10 μm.

It was found that as the percentage of triblock copolypeptide was increased the cellular uptake increased. Above 50 %, both triblock copolypeptides, $R^{H}_{10}M^{O}_{55}(L_{0.5}/F_{0.5})_{20}$ and $R^{H}_{20}M^{O}_{55}(L_{0.5}/F_{0.5})_{20}$, were taken up with efficiency comparable to the $R^{H}_{55}L_{20}$. To accurately

compare the cellular uptake of $R^{H}_{10}M^{O}_{55}(L_{0.5}/F_{0.5})_{20}$ and $R^{H}_{20}M^{O}_{55}(L_{0.5}/F_{0.5})_{20}$ with $R^{H}_{55}L_{20}$, vesicle suspensions were created containing equivalent fluorescence intensity. Flow cytometry analysis was conducted on HeLa cells incubated separately with the same concentration of polypeptide. The average fluorescence intensity represents the degree of vesicle internalization into the cells (10,000 cells per sample) (**Figure 6.9**).

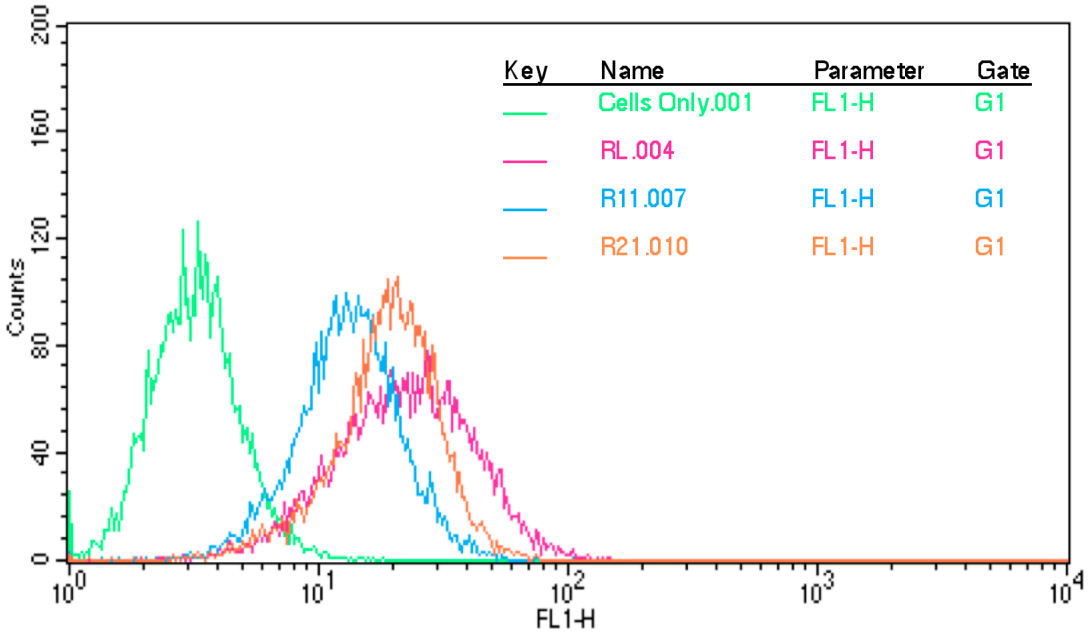

Figure 6.9 FACS cytometry analysis showing cell uptake populations.

Results from FACS cytometry show that the degree of vesicles internalization from fluorescein labeled $R^{H}_{60}L_{20}$ was slightly higher than fluorescein labeled $R^{H}_{10}M^{O}_{55}(L_{0.5}/F_{0.5})_{20}$ and $R^{H}_{20}M^{O}_{55}(L_{0.5}/F_{0.5})_{20}$ at the same concentration (5 μg/mL). When converted to molar concentration of arginine residues, $R^{H}_{60}L_{20}$ sample contains 2 times more arginine than $R^{H}_{20}M^{O}_{55}(L_{0.5}/F_{0.5})_{20}$ and 4 times more arginine than $R^{H}_{10}M^{O}_{55}(L_{0.5}/F_{0.5})_{20}$. However the fluorescence intensity of $R^{H}_{60}L_{20}$ is only 1.2 times greater than $R^{H}_{20}M^{O}_{55}(L_{0.5}/F_{0.5})_{20}$ and 1.8 times greater than greater than $R^{H}_{10}M^{O}_{55}(L_{0.5}/F_{0.5})_{20}$ (**Table 6.2**).

Table 6.2 Flow cytometry results of $M_{65}(L_{0.5}/F_{0.5})_{20}$, $R^{H}_{20}M^{O}_{55}(L_{0.5}/F_{0.5})_{20}$, and $R^{H}_{10}M^{O}_{55}(L_{0.5}/F_{0.5})_{20}$ block copolypeptides.

Block Copolypeptide	M_n	Polypeptide Concentration (μg/mL)	Arginine Concentration (μM)	Fold Increase in Fluorescence
$R^{H}_{60}L_{20}$	14,878	5	20	7.7
$R^{H}_{20}M^{O}_{55}(L_{0.5}/F_{0.5})_{20}$	12,247	5	9	6.2
$R^{H}_{10}M^{O}_{55}(L_{0.5}/F_{0.5})_{20}$	10,340	5	5	4.2
Cells Only				1

6.7 Reduction of Poly(L-methionine sulfoxide)

An interesting property of methionine sulfoxide is its ability to be reduced back to methionine, changing it from a water-soluble material back to a hydrophobic material.[10,11] Methionine amino acids in proteins are susceptible to oxidation when exposed to oxidative stresses.[3,12-14] This oxidation of methionine can lead to disruption of structure and inactivation of proteins. [3,12-14] To circumvent this problem, nature has created methionine sulfoxide reductase enzymes to reduce methionine and restore protein function. These enzymes are found in human, animal and plant cells. [3,12-18]

The reduction of methionine sulfoxide can potentially be used for a stimuli response to release cargo from vesicles. These vesicles may be stable during circulation within the circulatory system, however, when vesicles enter the reducing environment of cells they can potentially be reduced back to methionine disrupting amphiphilic rupturing vesicles. This rupturing of the vesicles maybe lead to the instant release of cargo within the cell.

6.7.1 Chemical Reduction of Poly(L-methionine sulfoxide) and $M^{O}_{65}(L_{0.5}/F_{0.5})_{20}$ Vesicles

To test the reduction of poly(L-methionine sulfoxide), the polypeptide was first incubated with thioglycolic acid for chemical reduction.[19] The homopolypeptide, poly(L-methionine sulfoxide), is completely water soluble and upon incubation with thioglycolic acid at 37 °C the polypeptide begins to lose solubility (**Figure 6.9**A). The polypeptide was isolated to confirm that the methionine sulfoxide was being reduced back to methionine, by the reappearance of methionine NMR peaks (**Figure6.9**B).

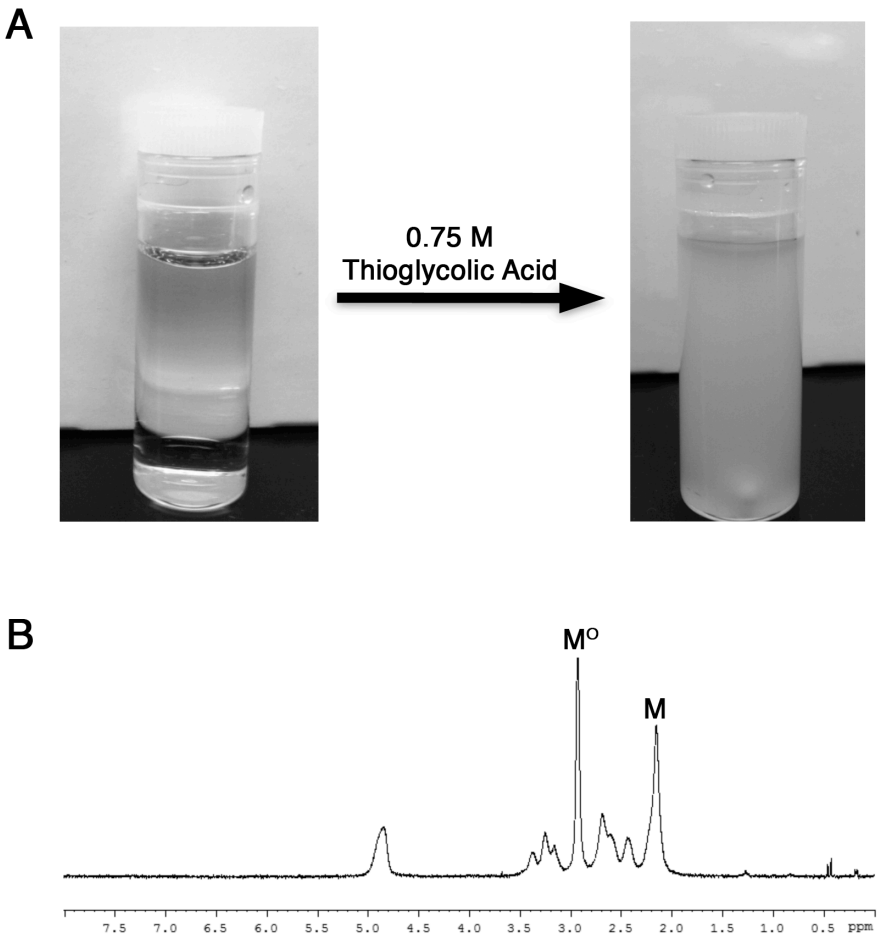

Figure 6.9 (A) Images of homopolypeptide, M^{O}, dissolved in water before and after reduction with thioglycolic acid. (B) ^{1}H NMR of homopolypeptide, M^{O}, after incubation with thioglycolic acid showing reduction back to M.

The chemical reduction of methionine sulfoxide on vesicles was then tested. Thioglycolic acid was incubated with $M^{O}_{65}(L_{0.5}/F_{0.5})_{20}$ vesicles and $K_{60}(L_{0.5}/F_{0.5})_{20}$ vesicles as a control. The vesicles were imaged before and after incubation. It was found by DIC that after 1 hour of incubation the $M^{O}_{65}(L_{0.5}/F_{0.5})_{20}$ vesicles lost solubility and began forming sheets (**Figure 6.10**B). However, $K_{60}(L_{0.5}/F_{0.5})_{20}$ vesicles showed no disruption after 20 hours of incubation (**Figure 6.10**F).

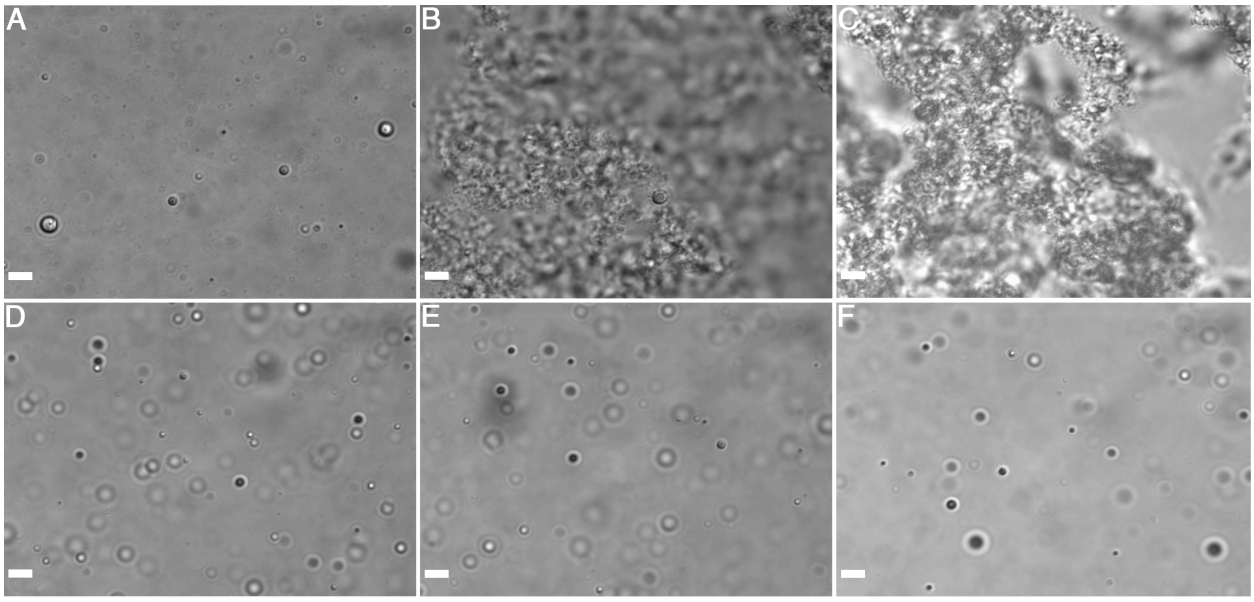

Figure 6.10 Differential interference contrast (DIC) images of 0.5 % (w/v) suspension incubated with 0.75 M Thioglycolic acid at 37 °C. (A) $M^{O}_{65}(L_{0.5}/F_{0.5})_{20}$, (B) $M^{O}_{65}(L_{0.5}/F_{0.5})_{20}$ after 1 hr incubation, (C) $M^{O}_{65}(L_{0.5}/F_{0.5})_{20}$ after 20 hrs incubation, (D) $K_{60}(L_{0.5}/F_{0.5})_{20}$, (E) $K_{60}(L_{0.5}/F_{0.5})_{20}$ after 1 hr incubation and (F) $K_{60}(L_{0.5}/F_{0.5})_{20}$ after 20 hrs incubation. Scale bars = 5 μm.

6.7.2 Enzyme Reduction of $M^{O}_{65}(L_{0.5}/F_{0.5})_{20}$ Vesicles

The vesicle reduction was then tested with methionine sulfoxide reductase A and B (MsrA and MsrB) enzymes. After incubation of $M^{O}_{65}(L_{0.5}/F_{0.5})_{20}$ vesicle suspension with MsrA and MsrB in the presence of the reductant dithiothreitol (DTT), sheet appearance and loss of

vesicle structure was seen using DIC (**Figure 6.11**B). To test that the DTT was not responsible for sheet formation, the vesicles were incubated with the buffer and just DTT. After incubation only vesicle could be seen using DIC (**Figure 6.11**A). The vesicles were then incubation with MsrA and MsrB, minus dithiothreitol to ensure that sheet formation and aggregation was not caused by aggregation with enzymes (**Figure 6.11**C). As a final control, $K_{60}(L_{0.5}/F_{0.5})_{20}$ vesicles were incubated with MsrA and MsrB with reductant DTT and only vesicles were seen (**Figure 6.11**D).

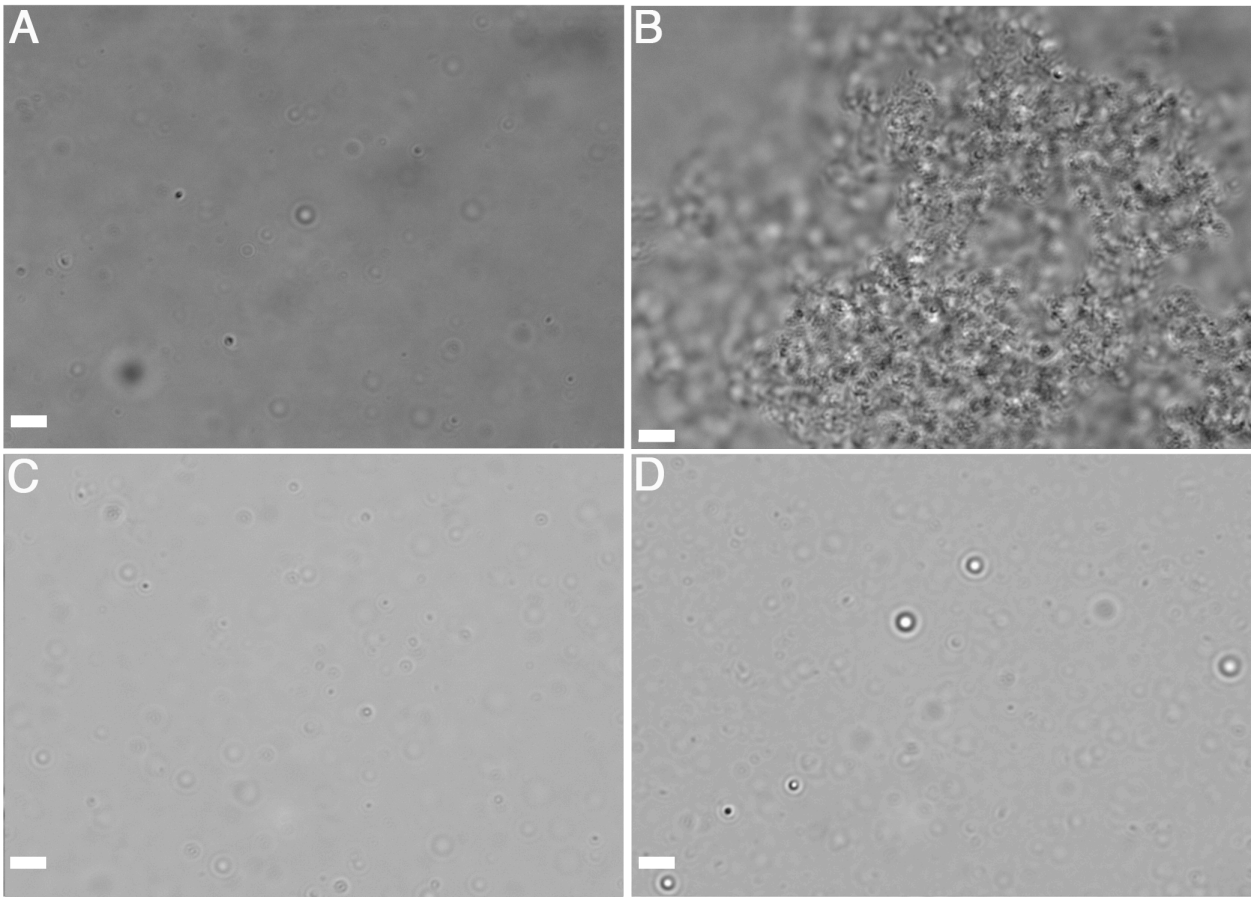

Figure 6.11 Differential interference contrast (DIC) images of 0.5 % (w/v) suspension incubated with MsrA and MsrB 37 °C. (A) $M^{O}_{65}(L_{0.5}/F_{0.5})_{20}$ incubated in buffer and the reducing agent dithiothreitol (DTT), (B) $M^{O}_{65}(L_{0.5}/F_{0.5})_{20}$ incubated with MsrA and MsrB in the presence of DTT, (C) $M^{O}_{65}(L_{0.5}/F_{0.5})_{20}$ incubated with MsrA and MsrB without DTT, and (D) $K_{60}(L_{0.5}/F_{0.5})_{20}$ incubated with MsrA and MsrB in the presence of DTT as a control. Scale bars = 5 μm.

6.8 Dye Release of Reduced Polypeptide Vesicles

The previous section displayed the reducing nature of poly(L-methionine sulfoxide) and poly(L-methionine sulfoxide)$_{65}$-*block*-poly(L-leucine$_{0.5}$-*co*-L-phenylalanine$_{0.5}$)$_{20}$, $M^{O}_{65}(L_{0.5}/F_{0.5})_{20}$, with loss of solubility and loss of vesicle structure, respectively. To determine if the vesicles were rupturing and not aggregating together during reduction, $M^{O}_{65}(L_{0.5}/F_{0.5})_{20}$ vesicles encapsulating Texas Red labeled Dextran (MW = 3000 g/mol) were used. The vesicles were dialyzed in the presence of MsrA and MsrB at 37 °C (**Figure 6.12**). As the poly(L-methionine sulfoxide) is reduced the vesicles should destabilize and the dye should leak out and diffuse out of the bag.

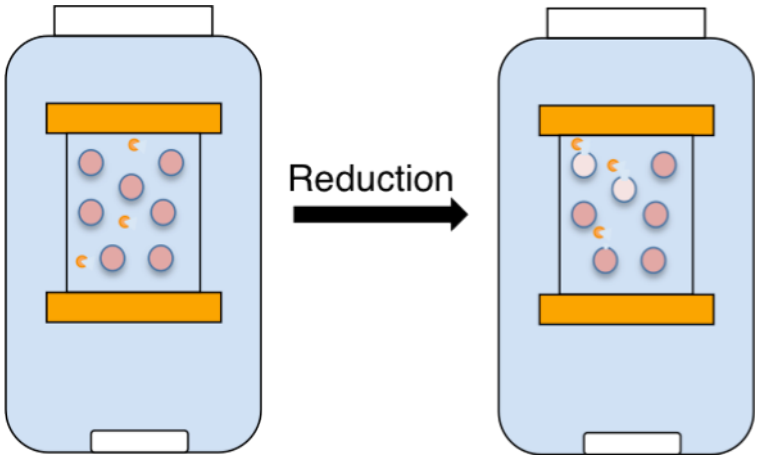

Figure 6.12 Schematic showing the dye releasing from vesicles upon incubation with enzymes. Vesicles are encapsulating Texas Red labeled dextran. Enzymes (MW = 17 to 26 kDa, MsrB and MsrA respectively) are placed in dialysis bag (MWCO = 8000 Da) with vesicle suspension and should be retained.

Dye retained in dialysis bag was checked at different time points by analyzing excitation and emission of Texas Red using a spectrofluorimeter. The data was plotted to determine the release profile of the dye (**Figure 6.13**). Minimal dye leaked from $M^{O}_{65}(L_{0.5}/F_{0.5})_{20}$ not incubated enzymes, where there was a steady release of dye from vesicles incubated with MsrA and MsrB

enzymes validating our design of triggered release of cargo. This data shows that the vesicles are destabilizing and not aggregating to form clumps of vesicles.

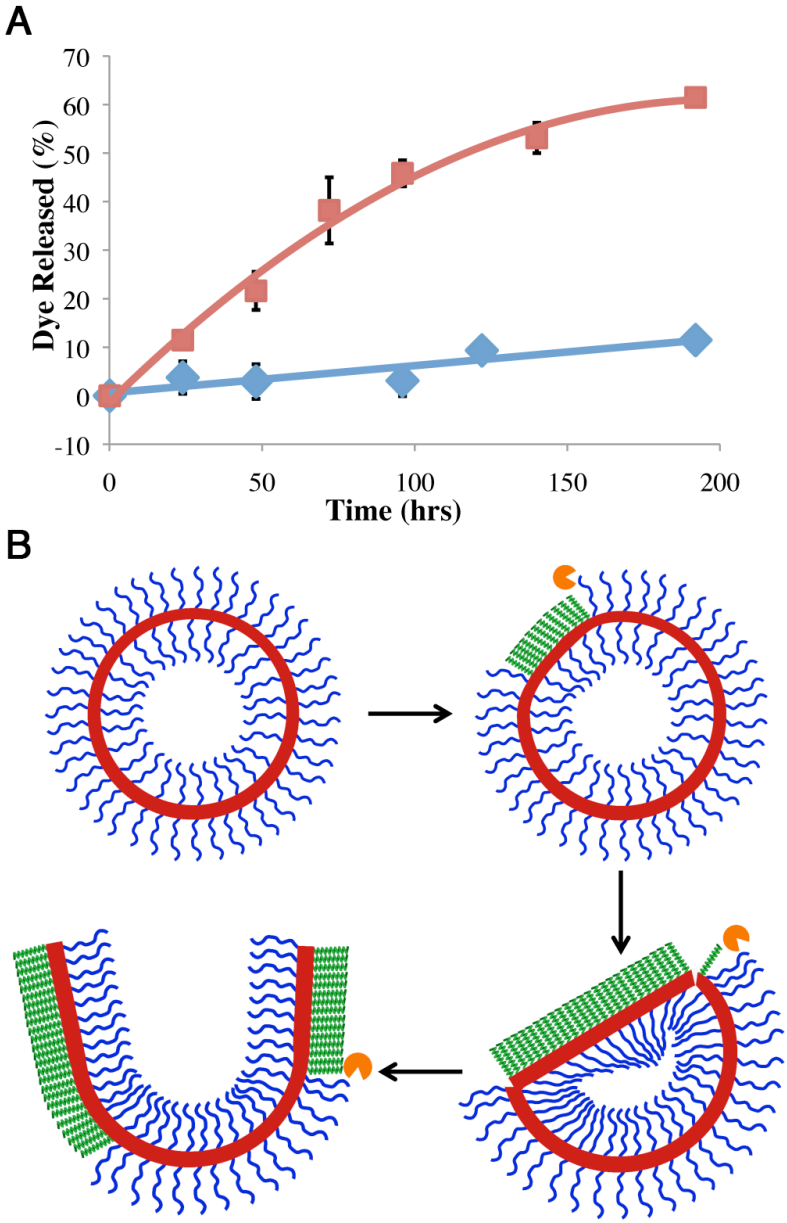

Figure 6.13 (A) Dye release profiles of block copolypeptide suspensions, $M^{O}_{65}(L_{0.5}/F_{0.5})_{20}$, encapsulating Texas Red-labeled dextran incubated with MsrA and MsrB enzymes (red line) and with buffer only (blue line). Dye release determined by measuring absorbance and fluorescence of Texas Red. (B) Schematic showing possible mechanism of dye release in the presence of Msr reductases.

6.9 Conclusion

In conclusion, the incorporation of methionine triblock copolypeptides, containing a short homoarginine segment, into vesicles imparts enhanced cellular uptake. The cytotoxicity of the polypeptide vesicles was reduced by mixing triblock copolypeptides, $R^{H}_{10}M^{O}_{55}(L_{0.5}/F_{0.5})_{20}$ and $R^{H}_{20}M^{O}_{55}(L_{0.5}/F_{0.5})_{20}$, with diblock copolypeptide, $M^{O}_{65}(L_{0.5}/F_{0.5})_{20}$. The mixing of polypeptides reduces the amount of cationic arginine segments on the surface of the vesicle. It was found that 50 % triblock with 50 % diblock was the optimal composition with having enhanced cell uptake and minimal toxicity up to 100 μg/mL.

The ability of methionine sulfoxide to reduce back to methionine under reducing environments has provided a way to release cargo from these polypeptide vesicles. The disruption of vesicle structure can occur upon chemical reduction with thioglycolic acid and more importantly in the presence of methionine sulfoxide reductase enzymes commonly found in human, animal and plant cells. These advances in polypeptide vesicles have provided ideal properties for applications in drug delivery.

6.10 Experimental

6.10.1 General Methods and Materials:

Dried tetrahydrofuran (THF), hexane and diethyl ether were prepared by passage through alumina columns, and oxygen was removed by purging with nitrogen prior to use.[20] Perkin Elmer RX1 FTIR Spectrophotometer was used for recording infrared spectra. ^{1}H NMR spectra were recorded on a Bruker AVANCE 400 MHz spectrometer. Ultrapure (18 MΩ) water was obtained from a Millipore Milli-Q Biocel A10 purification unit.

6.10.2 Synthesis:

The α-amino acid-N-carboxyanhydride (NCA) monomers, phenylalanine, leucine and lysine were synthesized using previously described protocols.[21,22] L-Phenylalanine, L-leucine and N_ε-trifluoroacetyl-L-lysine NCAs were synthesized by phosgenation and purified by recrystallization. Methionine monomer was prepared by a phosgenation and purified by column chromatography within a glovebox.[23] Isocyanate functionalized poly(ethylene glycol)$_{45}$ (mPEG$_{45}$-NCO) was prepared by reacting mPEG-NH_2 with phosgene in THF for 16 hours.[24]

6.10.3 Determining Monomer to Initiator Ratio for N_ε-trifluoroacetyl-L-lysine-*N*-carboxyanhydride (TFA-Lys NCA) with initiator, $(PMe_3)_4Co$:

N_ε-Trifluoroacetyl-L-lysine-*N*-carboxyanhydride (TFA-Lys NCA) (10– 30 mg, 0.04- 0.11 mmol) was measured in three separate vials and dissolved in THF (50 mg NCA/mL THF). To each vial, a different amount of $(PMe_3)_4Co$ initiator solution (20 mg/mL solution in THF) was added via syringe to give different monomer to initiator (M:I) ratios of 5: 1, 10: 1 and 20: 1. The vials were sealed and allowed to stir in the glove box for 1 hour. An aliquot (20 μL) was removed from each polymerization solution and analyzed by FTIR to confirm that all TFA-Lys NCA was consumed. In the glove box, mPEG$_{2000}$-NCO (87 mg) was dissolved in THF (3.5 mL) in a 20 mL scintillation vial. An aliquot solution of mPEG$_{2000}$-NCO (2.2 mL, 920 μL, and 250 μL of 25 mg/mL) was added to each polymerization solution containing different amounts of initiator (9.0 mmol, 4.6 mmol, and 1.2 mmol, respectively). The PEG end-capping solution vials were sealed and allowed to react for 24 hours. Outside of the dry box, the PEG end-capped poly(N_ε-trifluoroacetyl-L-lysine)$_x$-PEG$_{2000}$ (K(TFA)$_x$-PEG$_{2000}$) was isolated by precipitation with H_2O (3 times) to remove excess PEG. K(TFA)$_x$-PEG$_{2000}$ was placed under high vacuum to

remove residue H_2O before NMR analysis. The degree of polymerization of the polymer was determined by NMR integrations of PEG end-capped polymer and was plotted against M:I ratio to determine inflation.

6.10.4 Synthesis of Poly(N_ε-trifluoroacetyl-L-lysine)$_{10}$-*block*-poly(L-methionine)$_{55}$-*block*-poly(L-leucine$_{0.5}$-*co*-L-phenylalanine$_{0.5}$)$_{20}$, (TFA)$K_{10}M_{55}(L_{0.5}/F_{0.5})_{20}$:

N_ε-trifluoroacetyl-L-lysine-*N*-carboxyanhydride (TFA-Lys NCA) (20 mg, 0.076 mmol) was dissolved in THF (410 μL) in a 20 mL scintillation vial. To the vial, $(PMe_3)_4Co$ initiator solution (380 μL of a 20 mg/mL solution in THF) was added via syringe. The vial was sealed and allowed to stir in the glove box for 1 hour. An aliquot (20 μL) was removed and analyzed by FTIR to confirm that all TFA-Lys NCA was consumed. In the glove box, L-methionine-N-carboxyanhydride (Met NCA) was measured in a separate vial (80 mg, 0.46 mmol) and dissolved in THF (1.60 mL). The Met NCA solution was added to the polymerization mixture vial syringe. The vial was sealed and allowed to stir in the glove box for 1 hour. An aliquot (20 μL) was removed and analyzed by FTIR to confirm that all Met NCA was consumed. In the glove box, $mPEG_{45}$-NCO (12 mg) was dissolved in THF (0.5mL) in a 20 mL scintillation vial. An aliquot (240 μL) of the polymerization solution containing active chain ends (0.002 mmol) was removed and added to the solution of $mPEG_{45}$-NCO. The PEG end-capping solution vial was sealed and allowed to react for 24 hours. L-leucine-N-carboxyanhydride (11 mg, 0.07 mmol) and L-phenylalanine-N-carboxyanhydride (13 mg, 0.07 mmol) was dissolved in THF (222 μL and 270 μL, respectively), combined and added to the polymerization solution via syringe. The vial was sealed and allowed to stir in the glove box for 1 hour to give the triblock (TFA)$K_{10}M_{55}(L_{0.5}/F_{0.5})_{20}$. FTIR was used to confirm complete consumption of NCA. Outside of the dry box, the PEG end-

capped polypeptide ((TFA)K_xM_y-PEG_{45}) was isolated by precipitation with H_2O (3 times) to remove excess PEG. (TFA)K_xM_y-PEG_{45} was placed under high vacuum to remove residue H_2O before taking an NMR to determine length of each block. Outside the dry box, the triblock copolypeptide was isolated by evaporating off all volatiles and dispersed in 10 mM HCl (3 times) to remove cobalt. The average composition of the copolymer as determined by ^{1}H NMR integrations of PEG end-capped polymer and diblock copolymer was (TFA)$K_{11}M_{55}(L_{0.5}/F_{0.5})_{18}$.

6.10.5 Synthesis of Poly(N_ε-trifluoroacetyl-L-lysine)$_{20}$-*block*-poly(L-methionine)$_{55}$-*block*-poly(L-leucine$_{0.5}$-*co*-L-phenylalanine$_{0.5}$)$_{20}$, (TFA)$K_{20}M_{55}(L_{0.5}/F_{0.5})_{20}$:

N_ε-Trifluoroacetyl-L-lysine-*N*-carboxyanhydride (TFA-K NCA) (50 mg, 0.185 mmol) was dissolved in THF (1 mL) in a 20 mL scintillation vial. To the vial, $(PMe_3)_4Co$ initiator solution (463 μL of a 20 mg/mL solution in THF) was added via syringe. The vial was sealed and allowed to stir in the glove box for 1 hour. An aliquot (20 μL) was removed and analyzed by FTIR to confirm that all TFA-K NCA was consumed. In the glove box, L-methionine-*N*-carboxyanhydride (Met NCA) was measure in a separate vial (98 mg, 0.556 mmol) and dissolved in THF (1.96 mL). The Met NCA solution was added to the polymerization mixture vial syringe. The vial was sealed and allowed to stir in the glove box for 1 hour. An aliquot (20 μL) was removed and analyzed by FTIR to confirm that all Met NCA was consumed. In the glove box, PEG_{45}-isocyanate (10 mg) was dissolved in THF (0.350 mL) in a 20 mL scintillation vial. An aliquot (230 μL) of the polymerization solution containing active chain ends (0.0017 mmol) was removed and added to the solution of PEG_{45}-isocyanate. The PEG end-capping solution vial was sealed and allowed to react for 24 hours. L-Leucine-N-carboxyanhydride (Leu NCA) (14 mg, 0.09 mmol) and L-phenylalanine-N-carboxyanhydride (Phe NCA) (17 mg, 0.09 mmol) was

dissolved in THF (280 μL and 340 μL, respectively), combined and added to the polymerization solution via syringe. The vial was sealed and allowed to stir in the glove box for 1 hour to give the triblock (TFA)$K_{20}M_{55}(L_{0.5}/F_{0.5})_{20}$. FTIR was used to confirm complete consumption of NCA. Outside of the dry box, the PEG end-capped polypeptide ((TFA)K_xM_y-PEG_{45}) was isolated by precipitation with H_2O (3 times) to remove excess PEG. (TFA)K_xM_y-PEG_{45} was placed under high vacuum to remove residue H_2O before taking an NMR to determine length of each block. Outside the dry box, the triblock copolypeptide was isolated by evaporating off all volatiles and dispersed in 10 mM HCl (3 times) to remove cobalt. The average composition of the copolymer as determined by ^{1}H NMR integrations of PEG end-capped polymer and diblock copolymer was (TFA)$K_{21}M_{54}(L_{0.5}/F_{0.5})_{18}$.

6.10.6 Preparation of Poly(N_ε-trifluoroacetyl-L-lysine)$_x$-*block*-poly(L-methionine sulfoxide)$_{55}$-*block*-poly(L-leucine$_{0.5}$-*co*-L-phenylalanine$_{0.5}$)$_{20}$ (x= 11, 21), (TFA)$K_xM^O_{55}(L_{0.5}/F_{0.5})_{20}$:

A 20 mL scintillation vial was charged with (TFA)$K_xM_{55}(L_{0.5}/F_{0.5})_{20}$ (10 mg) and a stir bar. A solution of 1 % AcOH in 30% hydrogen peroxide (1 mL) was added to the scintillation vial and sealed and allowed to react for 20 min total. The sample was diluted with water to twice its original volume. Saturated sodium thiosulfate was added drop wise to quench the peroxide and transferred to a 2000 MWCO dialysis bag and dialyzed against Millipore water for 2 days with frequent water changes. The solution was lyophilized to dryness to yield a white solid. Yield >80%, loss is due to dialysis.

6.10.7 Deprotection of Trifluoroacetyl Groups:

The protected triblock polypeptides, (TFA)$K_{10}M^{O}_{55}(L_{0.5}/F_{0.5})_{20}$ and (TFA)$K_{20}M^{O}_{55}(L_{0.5}/F_{0.5})_{20}$, were dispersed in a 1:20 (v/v) solution of H_2O to MeOH (5 mg/mL) containing 60 mM K_2CO_3. The suspension was heated to reflux. After 4 hours, the reaction mixture was allowed to cool to room temperature and the solvent was removed under high vacuum. The solid was dispersed in water and transferred to a dialysis bag (2000 MWCO) and dialyzed against 10 mM HCl and NaCl for 24 hours with 3 water changes and then against Millipore water for 24 hours with 3 water changes. The polypeptide solution was lyophilized to yield a white solid. Yield >80 %, loss is due to dialysis.

6.10.8 Guanylation to Poly(L-homoarginine)$_x$-*block*-poly(L-methionine sulfoxide)$_{55}$-*block*-poly(L-leucine$_{0.5}$-*co*-L-phenylalanine$_{0.5}$)$_{20}$, $R^{H}_{x}M^{O}_{55}(L_{0.5}/F_{0.5})_{20}$ (x = 10, 20):

The polypeptide sample, $K_xM^{O}_{55}(L_{0.5}/F_{0.5})_{20}$ (from previous reaction), was dispersed in aqueous NaOH (10 mg/ml, 1 mM) in a plastic 15 mL conical tube. The guanylating reagent, 3,5-dimethylpyrazole-1-carboxamidine nitrate (10 eq per each lysyl amine group), was dissolved in aqueous 1 M NaOH and added to the polypeptide suspension. The reaction mixture was sealed and placed in a bath sonicator for 1 minute and then placed in an oven at 37 °C for 72 hours. After 72 h, the reaction mixture was acidified to pH of 3 with HCl and placed in a dialysis bag (MWCO = 2000 Da) and dialyzed against aqueous NaCl (10 mM, 2 days) and Millipore water (2 days), changing each solution 3 times/day. The polypeptide was isolated by freeze-drying the solution. The typical guanylation efficiency is *ca*. 90 %, and isolated yields ranged from 85 to 95%.

6.10.9 Circular Dichroism of Polypeptides:

Circular Dichroism spectra (190–250 nm) were recorded in a quartz cuvette of 0.1 cm path length with samples prepared at concentrations of 0.10 to 0.25 mg/mL using Millipore deionized water. All spectra were recorded as an average of 3 scans. The spectra are reported in units of molar ellipticity $[\theta]$ ($deg \cdot cm^2 \cdot dmol^{-1}$). The formula used for calculating molar ellipticity, $[\theta]$, was $[\theta] = (\theta \times 100 \times M_W)/(c \times l)$ where θ is the experimental ellipticity in millidegrees, M_W is the average molecular weight of a residue in g/mol, c is the peptide concentration in mg/mL; and l is the cuvette pathlength in cm. The percent α-helical content of the peptides was estimated using the formula % α-helix = $100x(-[\theta]_{222nm} +3000)/39000)$ where $[\theta]_{222nm}$ is the measured molar ellipticity at 222 nm.[8] Using this estimation, poly$(Met^{O2})_{80}$ is 99% α-helical in deionized water, 20 ºC.

6.10.10 Fluorescent Probe Modification of Diblock Polypeptide:

5-(Iodoacetamido)fluorescein was conjugated to the thioether of the methionine side chains using the previous alkylation method. The polypeptide $M_{60}(L_{0.5}/F_{0.5})_{20}$ (10 mg) was dissolved in DMF (1 mL) in a 20 mL scintillation vial. 5-(Iodoacetamido)fluorescein was dissolved in DMF (10 mg/mL) and added to the a 1 % (w/v) polypeptide solution a 5:1 molar ratio to the polypeptide chains. The alkylation was allowed to proceed for 16 hours. After fluorescein modification, the remaining methionine residues were concentrated to remove DMF for oxidation.

6.10.11 Fluorescent Probe Modification of Triblock Polypeptide:

Fluorescein isothiocyanate (FITC) or rhodamine isothiocyanate (TRITC) was conjugated to the amino group of the lysine side chains in triblock copolypeptides and to the amino end group of

the backbone of diblock copolypeptides. The polypeptide $K_xM_{60}(L_{0.5}/F_{0.5})_{20}$ (x = 10, 20, 10 mg) was dispersed in sodium carbonate buffer at pH 8.0 (1 mL) in a 15 mL conical tube. FITC or TRITC (0.2 equivalence to 1 equivalence of polypeptide) was dissolved in dry DMSO (10 mg/mL) and was added to the polymer solution. The conjugation was allowed to proceed overnight. The resulting copolypeptide solution was dialyzed (8,000 MWCO membrane) against Millipore water for 2 days, changing the water 3 times/day. The purified polypeptide was isolated by lyophilization to yield 1 fluorescent molecule per 5 chains of polypeptide.

6.10.12 Preparation of Polypeptide Assemblies:

Solid polypeptide powder ($M^{O}_{60}(L_{0.5}/F_{0.5})_{20}$, $R^{H}_{10}M^{O}_{55}(L_{0.5}/F_{0.5})_{20}$, $R^{H}_{20}M^{O}_{55}(L_{0.5}/F_{0.5})_{20}$) was dispersed in THF to give a 1 % (w/v) suspension. The suspension was placed in a bath sonicator for 30 minutes to evenly disperse the polypeptide and reduce large particulates. An equivalent amount of Millipore water was then added to give a 0.5 % (w/v) suspension. The suspension becomes clear as the solution is mixed by vortex. The mixture is then dialyzed (2,000 MWCO membrane) against Millipore water overnight with changing the water 3 times. The THF can also be removed by evaporation resulting in vesicular assemblies.

6.10.13 Self-assembly of Polypeptide Vesicles Containing Both Diblock and Triblock Polypeptides:

Solid diblock polypeptide powder ($M^{O}_{60}(L_{0.5}/F_{0.5})_{20}$) and triblock polypeptide powder ($R^{H}_{10}M^{O}_{55}(L_{0.5}/F_{0.5})_{20}$ or $R^{H}_{20}M^{O}_{55}(L_{0.5}/F_{0.5})_{20}$) are dispersed separately in THF to give a 1 % (w/v) suspensions. The suspensions are placed in a bath sonicator for 30 minutes to evenly disperse the polypeptides and reduce large particulates. An equivalent amount of Millipore water was then added to give 0.5 % (w/v) suspensions. The suspensions become clear as the solution is mixed by

vortex. Aliquots of triblock and diblock (25:75, 50:50 and 75:25 (w/w) triblock to diblock) are mixed and then placed in bath sonicator for 30 min to evenly distribute. The mixture is then dialyzed (2,000 MWCO membrane) against Millipore water overnight with changing the water 3 times. The THF can also be removed by evaporation resulting in vesicular assemblies.

6.10.14 Differential Interference Microscopy (DIC):

Suspensions of the copolypeptides, $M^{O}_{60}(L_{0.5}/F_{0.5})_{20}$, $R^{H}_{10}M^{O}_{55}(L_{0.5}/F_{0.5})_{20}$ or $R^{H}_{20}M^{O}_{55}(L_{0.5}/F_{0.5})_{20}$, (0.5 % (w/v)) were visualized on glass slides with a spacer between the slide and the coverslip (double-sided tape or Secure Seal Imaging Spacer, *Grace Bio-labs*) allowing the self-assembled structures to be minimally disturbed during focusing. The samples are imaged using a Zeiss Axiovert 200 DIC/Fluorescence Inverted Optical Microscope.

6.10.15 Extrusion of Polypeptide Assemblies:

The aqueous vesicle suspensions, $M^{O}_{60}(L_{0.5}/F_{0.5})_{20}$, $R^{H}_{10}M^{O}_{55}(L_{0.5}/F_{0.5})_{20}$ or $R^{H}_{20}M^{O}_{55}(L_{0.5}/F_{0.5})_{20}$, diluted to 0.2 % (w/v) were extruded using an Avanti Mini-Extruder. Extrusions were performed using different pore size Whatman Nuclepore Track-Etched polycarbonate (PC) membranes, following a protocol of serial extrusions of vesicles through decreasing filter pore sizes: 3 times through a 1.0 μm filter, 3 times through 0.4 μm filter, 3 times through 0.2 μm filter, and 3 times through 0.1 μm filter. The PC membranes and filter supports are soaked in Millipore water for 10 minutes prior to extrusion.

6.10.16 Dynamic Light Scattering (DLS) of Extruded Vesicles:

The 0.2 % (w/v) of extruded polypeptide suspensions, $M^{O}_{60}(L_{0.5}/F_{0.5})_{20}$, $R^{H}_{10}M^{O}_{55}(L_{0.5}/F_{0.5})_{20}$ or $R^{H}_{20}M^{O}_{55}(L_{0.5}/F_{0.5})_{20}$, were placed in a disposable cuvette and analyzed with the Malvern Zetasizer

Nano ZS model Zen 3600 (Malvern Instruments Inc, Westborough, MA). A total scattering intensity of approximately 1 x 10^5 cps was targeted. The autocorrelation data was fitted using the CONTIN algorithm to determine the diameters of suspended assemblies.

6.10.17 Zeta Potential of Polypeptide Assemblies:

A 0.5 % (w/v) suspension of copolypeptide vesicles, $M^O_{60}(L_{0.5}/F_{0.5})_{20}$ was diluted to 0.2 % (w/v) with Millipore water containing NaCl to give a final concentration of 10 mM salt. The pH was then adjusted using NaOH or HCl to give acidic to basic solutions ranging from pH 3 to 8. The solution was added to a disposable capillary cell (Malvern Instruments Inc, Westborough, MA). The zeta potential was analyzed with the Malvern Zetasizer Nano ZS model Zen 3600 (Malvern Instruments Inc, Westborough, MA).

6.10.18 Laser Scanning Confocal Microscopy (LSCM) of Fluorescently Labeled Vesicles:

LSCM images of the vesicles were taken on a Leica Inverted TCS-SP1 MP-Inverted Confocal and Multiphoton Microscope equipped with an argon laser (476 and 488 nm blue lines), a diode (DPSS) laser (561 nm yellow-green line), and a helium-neon laser (633 nm far red line). Suspensions of the fluorescently labeled copolypeptides (0.5 % (w/v)) were visualized on glass slides with a spacer between the slide and the cover slip (Secure Seal Imaging Spacer, *Grace Bio-labs*) allowing the self-assembled structures to be minimally disturbed during focusing. Imaging of an xy plane with an optical z-slice showed that the assemblies were water filled, unilamellar vesicles.

6.10.19 Transmission Electron Microscopy (TEM) of Extruded Vesicles:

The extruded aqueous copolypeptide suspensions were diluted to give 0.1 % (w/v). The sample (4 μL) was placed on a 300 mesh Formvar/carbon coated copper grid (Ted Pella) and allowed to remain on the grid for 60 seconds. Filter paper was used to remove the residual sample. One drop of 2 % (w/v) uranyl acetate (negative stain) was then placed on the grid for 90 seconds, and subsequently removed by washing with drops of Millipore water and removing the excess liquid with filter paper. The grids containing sample were allowed to dry before imaging with JEM 1200-EX (JEOL) transmission electron microscope at 80 kV.

6.10.20 Cryogenic Electron Microscopy of Extruded Vesicles:

A drop of 0.2 % (w/v) extruded aqueous copolypeptide suspension was placed on a 300 mesh copper grid containing a Quantifoil holey carbon film (SPI Supplies, West Chester, PA). The sample was allowed to remain on the grid for 30 seconds and was blotted with filter paper and quickly placed in a cryogenic bath containing liquid ethane. The grid was stored under liquid nitrogen and then placed, using a cold stage, in a TF20 (FEI Tecnai G2) electron microscope and imaged with an accelerating voltage of 200 kV. Sample preparation and imaging was performed at the Electron Imaging Center for Nanomachines (EICN) established at the California NanoSystems Institute (CNSI).

6.9.21 Bradford Assay with Polypeptide Vesicle:

Bradford assay was performed to quantify the final concentration of the polypeptide vesicles after extrusion according to the manufacture supplied instructions, using the pre-dialyzed samples as the standard.

6.10.22 Cell Culture:

The HeLa cell line was grown in Minimal Essential Medium supplemented with 26.2 mM sodium bicarbonate, 1 mM sodium pyruvate, 10% FBS, and 1% penicillin/streptomycin, at a pH of 7.4. The cell line is maintained in a 37°C humidified atmosphere with 5% CO2 and handled with standard sterile tissue culture protocols.

6.10.23 Vesicle Uptake:

HeLa cells were seeded at a density of $5x10^5$ cells/cm2 and incubated overnight prior to the experiment. The cells were seeded onto 8-well chambered coverglasses for confocal microscopy experiments and 35 mm tissue culture plates for flow cytometry. On the day of the experiment, different fluorescently-labeled vesicles were separately diluted in serum-free media and incubated with HeLa cells for 5 hrs to allow the vesicles to be internalized into the cells. Subsequently, the medium containing the vesicles was aspirated, and the cells were washed three times with PBS to remove nonspecifically attached peptides on the cell surface. Afterwards, the cells are subjected to either confocal microscopy or flow cytometry to determine the extent of vesicle uptake.

6.10.24 Laser Scanning Confocal Microscopy (LSCM) of Cells:

The LSCM images of the cells were taken on a Leica Inverted TCS-SP MP Spectral Confocal and Multiphoton Microscope (Heidelberg, Germany) equipped with an argon laser (488 nm blue excitation: JDS Uniphase), a diode laser (DPSS; 561 nm yellow-green excitation: Melles Griot), a helium-neon laser (633 nm red excitation), and a two photon laser setup consisting of a

Spectra-Physics Millenia X 532 nm green diode pump laser and a Tsunami Ti-Sapphire picosecond pulsed infrared laser tuned at 768 nm for UV excitation.

6.10.25 Flow Cytometry:

Flow cytometry analysis of HeLa cells incubated with the vesicles were performed on a BD FACScan™ (BD Bioscience, San Jose, CA) system equipped with an argon laser (488 nm blue excitation) and two filters: a green filter (530 ± 30 nm) and an orange filter (585 ± 42 nm). A total of 10,000 cells per sample were used for the analysis. The mean fluorescence intensity was used as a metric to represent the degree of vesicle internalization into the cells.

6.10.26 Measurement of Cytotoxicity using the MTS Cell Proliferation Assay:

The MTS cell proliferation assay (CellTiter 96® AQueous Non-Radioactive Cell Proliferation Assay) was performed to assess the cytotoxicity level of the vesicles. The uptake experiments were performed with HeLa cells seeded on 96-well plates with triplicates of each condition. After the 5-hr incubation period, the medium was aspirated and fresh medium containing 20% MTS reagent was added to the cells. The cells were incubated again at 37°C for 1 hr, and the absorbances at 490 nm and 700 nm were measured using the Infinite F200 plate reader (Tecan Systems Incorporated, San Jose, CA). The relative survival of cells compared to control cells (*i.e.*, cells incubated in growth medium without vesicles) was calculated by determining the ratio of the (A490 – A700) values.

6.10.27 Chemical Reduction of Poly(L-methionine sulfoxide):

Homopolypeptide, poly(L-methionine sulfoxide), was dissolved in Millipore water containing thioglycolic acid (750 mM) to give a 0.1 % (w/v) solution. The solution was allowed to react for

20 hours at 37 °C. The solution was dialyzed (2,000 MWCO membrane) for 3 days against Millipore water, changing the water 3 times/day. The dialyzed polymer was isolated by lyophilization to yield a white powder. Yield >80 %, loss is due to dialysis.

6.10.28 Chemical Reduction of Polypeptide Vesicles:

Thioglycolic acid (0.05 mmol) was added to a 0.5 % (w/v) suspension of $M^{O}_{60}(L_{0.5}/F_{0.5})_{20}$ (20 μL) to give a concentration 750 mM. The solution was allowed to react at 37 °C for 40 min. The solution was imaged using DIC before and after the reduction to monitor the vesicular morphology. A 0.5 % (w/v) suspension of $K_{60}L_{20}$ (20 μL) was used as a control for reduction with thioglycolic acid.

6.10.29 Enzyme Reduction of Polypeptide Vesicles:

A 1 % (w/v) suspension of copolypeptide vesicles, $M^{O}_{60}(L_{0.5}/F_{0.5})_{20}$ was diluted to 0.1 % (w/v) with Millipore water containing 20 mM Tris-HCl, 10 mM $MgCl_2$, 30 mM KCl, 20 mM DTT and 1 μg of each Methionine sulfoxide reductase A and Methionine sulfoxide reductase B (Prospec-Tany TechnoGene Ltd. Ness Ziona, Israel). A control sample was prepared as above without the addition of enzymes. The suspensions were placed in a 37 °C water bath for 16 hrs. The suspensions were then visualized by differential interference contrast microscopy (DIC).

6.10.30 Dye Encapsulation in Polypeptide Vesicles:

The diblock copolypeptide, $M^{O}_{60}(L_{0.5}/F_{0.5})_{20}$, sample were dispersed in THF to give 1 % (w/v) suspensions, which were then placed in a bath sonicator for 30 minutes until the copolypeptides were evenly dispersed. An equal volume of Millipore water containing Texas Red labeled dextran (Molecular Probes, MW = 3000, 0.25 mg/mL) was added to the suspension to give final

sample concentrations of 0.5 % (w/v), which was then placed in a bath sonicator for 30 minutes. The THF was removed by evaporation. After 24 hours, the suspension was transferred to a dialysis bag (MWCO = 8000 Da) to remove all dextran that was not encapsulated by the vesicles. The water was changed every hour for the first 4 hours. For enzyme reduction studies the sample was dialyzed against a buffered solution (20 mM Tris-HCl, 10 mM $MgCl_2$, 30 mM KCl) prior to dye release studies.

6.10.31 Dye Leakage of Enzymatically Reduced Polypeptide Vesicles:

A 1 % (w/v) suspension of copolypeptide vesicles, $M^{O}_{60}(L_{0.5}/F_{0.5})_{20}$ with encapsulated Texas Red labeled dextran, was diluted to 0.1 % (w/v) with Millipore water containing 20 mM Tris-HCl, 10 mM $MgCl_2$, 30 mM KCl, 20 mM DTT and 1 μg of each Methionine sulfoxide reductase A and Methionine sulfoxide reductase B (Prospec-Tany TechnoGene Ltd. Ness Ziona, Israel). The diluted suspension (1mL) was added to an 8000 MWCO dialysis bag and dialyzed against 20 mM Tris-HCl, 10 mM $MgCl_2$, 30 mM KCl, 20 mM DTT (250 mL). An aliquot (20 μL) was removed from the dialysis bag at different time points. DMSO (180 μL) was added to each aliquot and the suspension was sonicated before the excitation and emission was read on a QuantaMaster 40 UV Vis spectrofluorometer (Photon Technology International Inc., Birmingham, NJ).

6.11 References

(1) Pitha, J.; Szente, L.; Greenberg, J. *Journal of Pharmaceutical Sciences* **1983**, *72*, 665.

(2) Davies, M. J. *Biochimica et Biophysica Acta (BBA) - Proteins and Proteomics* **2005**, *1703*, 93.

(3) Moskovitz, J.; Bar-Noy, S.; Williams, W. M.; Requena, J.; Berlett, B. S.; Stadtman, E. R. *Proceedings of the National Academy of Sciences* **2001**, *98*, 12920.

(4) Moskovitz, J.; Berlett, B. S.; Poston, J. M.; Stadtman, E. R. In *Methods in Enzymology*; Lester, P., Ed.; Academic Press: 1999; Vol. Volume 300, p 239.

(5) Lin, Z.; Johnson, L. C.; Weissbach, H.; Brot, N.; Lively, M. O.; Lowther, W. T. *Proceedings of the National Academy of Sciences of the United States of America* **2007**, *104*, 9597.

(6) Le, D. T.; Lee, B. C.; Marino, S. M.; Zhang, Y.; Fomenko, D. E.; Kaya, A.; Hacioglu, E.; Kwak, G.-H.; Koc, A.; Kim, H.-Y.; Gladyshev, V. N. *Journal of Biological Chemistry* **2009**, *284*, 4354.

(7) Saito, G.; Swanson, J. A.; Lee, K.-D. *Advanced Drug Delivery Reviews* **2003**, *55*, 199.

(8) Rubartelli, A.; Lotze, M. T. *Trends in Immunology* **2007**, *28*, 429.

(9) Grant, S. A.; Xu, J.; Bergeron, E. J.; Mroz, J. *Biosensors and Bioelectronics* **2001**, *16*, 231.

(10) Schenck, H. L.; Dado, G. P.; Gellman, S. H. *Journal of the American Chemical Society* **1996**, 118, 12487.

(11) Dado, G. P.; Gellman, S. H. *Journal of the American Chemical Society* **1993**, 115, 12609.

(12) Grimaud, R.; Ezraty, B.; Mitchell, J. K.; Lafitte, D.; Briand, C.; Derrick, P. J.; Barras, F. *Journal of Biological Chemistry* **2001**, 276, 48915.

(13) Tarrago, L.; Kaya, A.; Weerapana, E.; Marino, S. M.; Gladyshev, V. N. *Journal of Biological Chemistry* **2012**, 287, 24448.

(14) Lowther, W. T.; Brot, N.; Weissbach, H.; Honek, J. F.; Matthews, B. W. *Proceedings of the National Academy of Sciences* **2000**, 97, 6463.

(15) Misiti, F.; Clementi, M. E.; Giardina, B. *Neurochemistry International* **2010**, 56, 597.

(16) Brot, N.; Weissbach, L.; Werth, J.; Weissbach, H. *Proceedings of the National Academy of Sciences* **1981**, 78, 2155.

(17) Boschi-Muller, S.; Olry, A.; Antoine, M.; Branlant, G. *Biochimica et Biophysica Acta* **2005**, 1703, 231.

(18) Ezraty, B.; Bos, J.; Barras, F.; Aussel, L. *Journal of Bacteriology* **2005**, 187, 231.

(19) Houghten, R. A.; Li, C. H. *Analytical Biochemistry* **1979**, 98, 36.

(20) Pangborn, A. B.; Giardello, M. A.; Grubbs, R. H.; Rosen, R. K.; Timmers, F. J. *Organometallics* **1996**, *15*, 1518.

(21) Breedveld, V.; Nowak, A. P.; Sato, J.; Deming, T. J.; Pine, D. J. *Macromolecules* **2004**, *37*, 3943.

(22) Fuller, W. D.; Verlander, M. S.; Goodman, M. *Biopolymers* **1976**, *15*, 1869.

(23) Kramer, J. R.; Deming, T. J. *Biomacromolecules* **2010**, null.

(24) Brzezinska, K. R.; Curtin, S. A.; Deming, T. J. *Macromolecules* **2002**, *35*, 2970.

CHAPTER SEVEN

pH Sensitive Diblock Copolypeptides for Endosomal Release of Vesicles

7.1 Abstract

Previously we have shown that $R^h_{60}L_{20}$ vesicles enter cells more efficiently than $K_{60}L_{20}$.[1] Detailed studies have been done to determine the intracellular trafficking pathway and shown our vesicles enter by macropinocytosis.[2] In these trafficking studies, fluorescently labeled vesicles were colocalized with an immunofluorescent tag for the early endosome antigen-1 (EEA-1), but were not colocalized with the fluorescent tag for the lysosomal-associated membrane protein-1 (LAMP-1). This showed that the vesicles were internalized and carried within endosomes but did not reach lysosomes. Consequently the vesicles may be recycled back to the surface before releasing their cargos. This issue may be overcome by creating vehicles that have the ability to escape from endosomes.

7.2 Introduction

Detailed studies were conducted to determine the intracellular trafficking pathway of $R_{60}L_{20}$ vesicles. In these studies they were able to inhibit certain pathways of endocytosis while monitoring the cellular uptake and it was shown that vesicles enter by macropinocytosis in HeLa cells.[2] After determining pathway of endocytosis the next set of experiments were conducted to determine the fate of the vesicle after cellular uptake. The fate of the vesicles is important in determining where the delivery of therapeutics will occur. For example, it is necessary for some therapeutics to enter the nucleus, especially when delivering genes to cells. In these trafficking

studies, fluorescently labeled vesicles were colocalized with an immunofluorescent tag for the early endosome antigen-1 (EEA-1), but were not colocalized with the fluorescent tag for the lysosomal-associated membrane protein-1 (LAMP-1). This showed that the vesicles were internalized and carried within endosomes but did not reach lysosomes. Consequently the vesicles may be recycled back to the surface before releasing their cargos. This issue may be overcome by creating vehicles that have the ability to escape from endosomes.

Research is being done to create delivery systems with the capacity of escaping endosomes before degradation of the drug cargos. Many groups have looked at carriers that possess a buffering capacity at endosomal pH for efficient gene delivery. Behr et al. studied the properties of these buffering vectors (i.e., lipopolyamines and polyamidoamine polymers) and studied the gene delivery potential of polyethylenimine (PEI).[3] The transfection efficiency of PEI, as compared to the previously studied lipopolyamines, was believed to be the result of its amine groups that become protonated at endosomal pH of 5-6. This property gives PEI the ability to act as a proton acceptor, which led to the concept of the "proton sponge effect" for endosomal escape.[3,4]

The endosome is a vesicle that forms from endocytosis of extracellular material through the plasma membrane. The pH of the endosome becomes more acidic than physiological pH (pH 7.4), which is controlled by ATPase.[4] This enzyme pumps protons into the endosome to lower the pH, which is also coupled with the entry of chloride anions.

A proton sponge will absorb protons, causing an influx of more protons and chloride ions as ATPase tries to lower the pH, leading to an increase in osmotic pressure within the endosome, which will in turn cause endosomal swelling and possibly rupture. In order to act as a proton sponge, the drug carrier must contain functional groups that can be protonated at the pH within

endosomes. This usually involves functional groups (e.g., secondary, tertiary amines) that have a pKa within the range of 5 to 6. If the pKa is too high (e.g., primary amines) the molecule will not act as a proton sponge because it is already protonated at physiological pH.

Meyer et al. reported the use of pH-labile amides called maleamic acids to mask the membrane-active antimicrobial agent Melittin.[5,6] Their idea was to mask the amino groups of Melittin and reduce its extracellular toxicity. When the vector (containing Melittin) reached the endosome, the pH-labile amides of the maleamic acid were removed and the disruptive membrane properties of Melittin were restored.

Conversion of amines into maleamic acids can be applied to our $K_{60}L_{20}$ polypeptides. The primary amines on the side chains of lysine have an average pKa of 10.5 and thus cannot act as a proton sponge at the desired pH because they are already protonated. Maleic anhydride derivatives can react with primary amines to form the maleamic acid groups. $K_{60}L_{20}$ modified in this way should also have low cytotoxicity, similar to $E_{60}L_{20}$ vesicles. Anionic polypeptide vesicles (i.e., $E_{60}L_{20}$) have shown little to no toxicity when incubated with HeLa cells. When these vesicles enter the endosome, the pH-labile maleamic acids will be cleaved off and the amino groups on the side chain will be protonated, acting as a proton sponge (**Figure 7.1**). In order to be effective, most of the amines in the polylysine domain should be converted to maleamic acids (**Figure 7.2**).

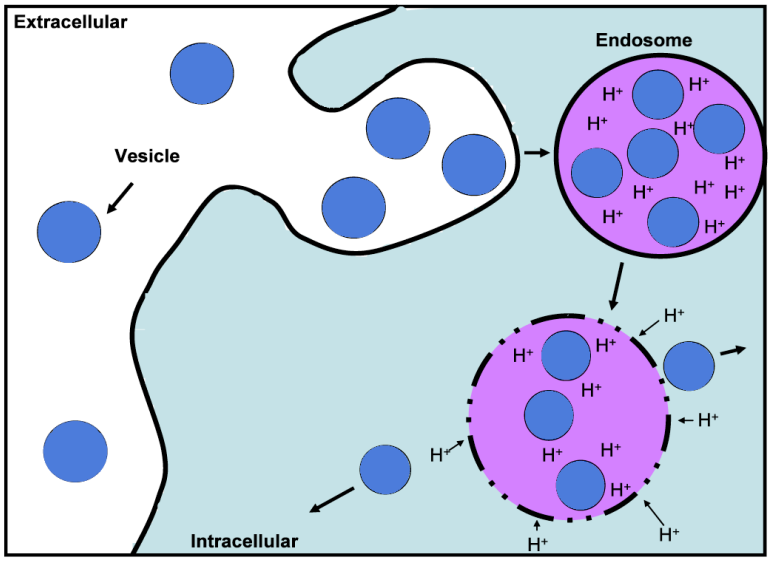

Figure 7.1 Illustration of vesicles uptaken by endocytosis. Acidification within the endosome removes acid labile compound, allowing free amine groups to become protonated. Proton sponge effect should result in rupture of endosome releasing vesicles into the cytosol.

In these studies, both K_{60} and $K_{60}L_{20}$ were prepared for modification with maleic anhydride derivatives. The polypeptide K_{60} was used to optimize the reaction with different maleic anhydrides for efficient modification of the amino groups. Succinic anhydride was used as a control because it forms an amide bond that is not pH-labile. Based on the research of Meyer et al. and Rozema et al., 2,3-dimethylmaleic anhydride and 2-propionic-3-methylmaleic anhydride were used for the pH-labile maleamic acids.[5,7]

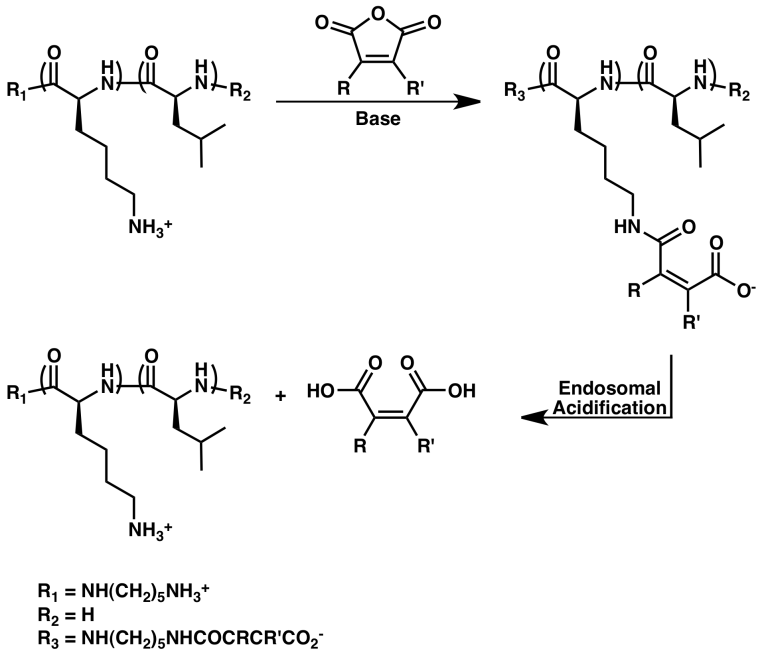

Figure 7.2 Example of acid-cleavable linkage to block copolypeptide, $K_{60}L_{20}$.

7.3 Endosome Introduction

Endosomes are compartments found in eukaryotic cells that participate in the endocytic membrane transport pathway. These compartments carry molecules that have been transferred from the extracellular environment to the intracellular environment by endocytic vesicles. There are three types of endosomes: the early endosome, late endosome and recycling endosome. These endosomes function as sorting compartments and determine whether the cargo will continue on to the lysosome or be recycled back to the cell surface. The process begins with endocytic vesicles forming at the plasma membrane of eukaryotic cells with the budding of the membrane to form these compartments and trap the molecules from the extracellular environment to isolate from the cell interior. After budding away from the membrane, this vesicles fuses with early endosomes that will begin to mature. They mature by becoming more acidic through the activity of V-ATPase. At this stage recycling endosomes will form and return

molecules back to the cell surface or the endosome will continue to mature to a late endosome, while losing certain membrane proteins and gaining others to prepare for lysosome fusion. The late endosome will then fuse with a lysosome to form a hybrid, the material will then be digested by digestive enzymes that are non-specific and function at a pH as low as 4.5.

7.4 Optimization of Anhydride Conjugation to Polypeptides

In order to optimize the conjugation protocol, succinic anhydride was reacted with the ε-amino groups of poly(L-lysine-HCl)$_{60}$, K_{60}, or poly(L-lysine-HCl)$_{70}$, K_{70}, and poly(L-lysine-HCl)$_{55}$-*block*-poly(L-leucine)$_{20}$, $K_{55}L_{20}$, or poly(L-lysine-HCl)$_{50}$-*block*-poly(L-leucine)$_{20}$, $K_{50}L_{20}$, to give poly(N_ε-4-oxobutanoic acid-L-lysine)$_x$, K^S_x (x = 60 or 70), and poly(N_ε-4-oxobutanoic acid-L-lysine)$_x$-*block*-poly(L-leucine)$_{20}$, $K^S_xL_{20}$ (x = 55 or 50), respectively. Characterization of synthesized K_{60}, K_{70}, $K_{55}L_{20}$, and $K_{50}L_{20}$ polypeptides is found in **Table 7.1**. This conjugation forms a stable, non-pH sensitive, amide linkage as a control for ease of synthesis and handling that allows for manipulation and purification of the polypeptide. Multiple reaction protocols from the literature were tested. The modified polypeptides were then purified by dialysis and characterize with NMR and GC to determine conjugation efficiency.

Table 7.1 Characterization of K_{70}, K_{60} polypeptides and $K_{55}L_{20}$, $K_{50}L_{20}$ diblock copolypeptides.

Block Copolypeptide	M_n[a]	M_w/M_n[a]	Found Composition[b]	Yield (%)[c]
K_{70}	17,950	1.166	K_{68}	48
K_{60}	14,890	1.190	K_{57}	85
$K_{55}L_{20}$	14,040	1.143	$K_{54}L_{18}$	90
$K_{50}L_{20}$	13,280	1.134	$K_{50}L_{23}$	95

[a]Hydrophilic segment lengths (number average molecular weight, M_n, for (Z)K segment) and polydispersities (M_w/M_n) determined using gel permeation chromatography. [b]Calculated using ^{1}H NMR. [c]Total isolated yield after deprotection of polypeptides.

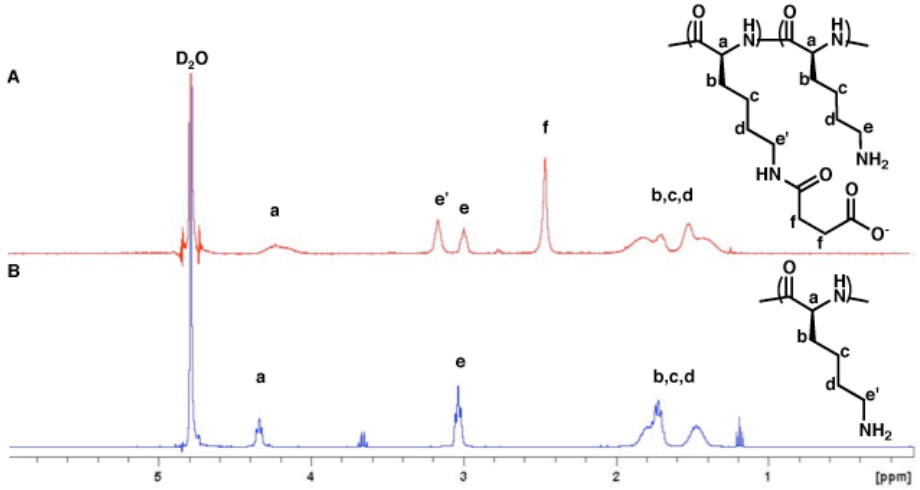

Figure 7.3 NMR Spectra of (A) poly(L-lysine)$_{60}$ reacted with succinic anhydride and (B) poly(L-lysine)$_{60}$ in D_2O.

The ^{1}H NMR spectra of the products showed new methylene peaks from the succinate groups (2.50 ppm) and a shift in the methylene peaks next to the ε-amino groups after amide bond formation from 3.00 to 3.20 ppm (**Figure 7.3**). Using calibrated GC data from hydrolyzed polypeptides, the concentrations of lysine and succinic acid could be independently determined in each sample (**Table 7.2**). The results showed that 0.1 M Na_2CO_3 in water gave the highest conjugation efficiency for the homopolypeptide (99.7 % conjugation).

Table 7.2 Protocols used for succinic anhydride conjugation and the conjugation efficiency to homopolypeptides.

Homopolypeptide	Protocol	Lysine[a] (mM)	Succinic[a] (mM)	%[b] Conjugation
K_{70}	0.1 M TEA in DMF	17.34	16.62	95.80
K_{70}	0.1 M Na_2CO_3	12.61	12.58	99.70
K_{70}	0.1 M NaOH/ 0.1 M HEPES	17.96	12.56	69.90
K_{60}	0.1 M $NaHCO_3$	18.43	14.42	78.20

[a]Concentration of lysine amino acid and succinic acid determined by GC analysis of hydrolyzed polypeptide; [b]% Conjugation calculated based on the ratio of succinic acid to lysine amino acid concentrations.

Once the conditions for the homopolypeptides showed high conversion, the optimization with amphiphilic diblock copolypeptides, $K_{60}L_{20}$, was attempted. Some conditions were modified due to reduced solubility under aqueous conditions (**Table 7.3**). The results showed that 0.1 M Na_2CO_3 in water gave the highest conjugation efficiency for the diblock copolypeptide (84.4 % conjugation). The conjugation efficiency for the diblock copolypeptide was lower, likely due to the reduced solubility of this material in 0.1 M Na_2CO_3.

Table 7.3 Protocols used for succinic anhydride conjugation and the conjugation efficiency to diblock copolypeptides.

Diblock Copolypeptide	Protocol	Lysine[a] (mM)	Succinic[a] (mM)	%[b] Conjugation
$K_{55}L_{20}$	0.1 M NaOH/ 0.1 M HEPES	9.59	8.07	84.20
$K_{55}L_{20}$	0.1 M Na_2CO_3	14.01	11.83	84.40
$K_{55}L_{20}$	0.6 M TEA in MeOH/H_2O (3:1 ratio)	13.72	8.75	63.80
$K_{55}L_{20}$	0.1 M $NaHCO_3$ in THF/H_2O (1:1 ratio)	14.65	11.32	77.30

[a]Concentration of lysine amino acid and succinic acid determined by GC analysis of hydrolyzed polypeptide; [b]% Conjugation calculated based on the ratio of succinic acid to lysine amino acid concentrations.

7.5 Vesicle Self-Assembly of Succinylated $K_{55}L_{20}$, $K^{S}_{55}L_{20}$

Once the conjugation of succinic anhydride was optimized for the amphiphilic block copolypeptide, $K_{55}L_{20}$, the next step was to test the vesicle self-assembly. The conjugation efficiency was ~ 85 % leaving free amino groups in the presence of carboxylic acids. This may lead to polyion complexes that disrupt vesicle assembly and water insolubility. The sample was processed using a THF to water ratio of 3:1, a solvent annealing system that works for charged diblock copolyeptides.[1,8,9] Vesicle self-assembly of the modified $K_{55}L_{20}$ samples was checked using differential interference contrast microscopy (DIC) (**Figure 7.4**). Only vesicles were seen from DIC imaging, and no polyion complexes or insoluble aggregates were seen.

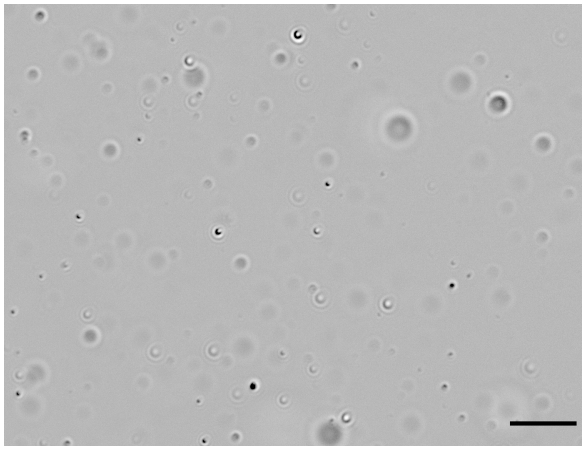

Figure 7.4 DIC image of 0.5 % (w/v) aqueous suspension of $K^{S}_{55}L_{20}$ (Scale bar = 10 μm).

7.6 Cytotoxicity of Succinylated Polypeptides

The cytotoxicity of the modified copolypeptides poly(N_{ε}-4-oxobutanoic acid-L-lysine)$_{55}$-*block*-poly(L-leucine)$_{20}$, $K^{S}_{55}L_{20}$ and poly(N_{ε}-4-oxobutanoic acid-L-lysine)$_{60}$, K^{S}_{60} were tested in HeLa cells to see how efficient the conjugation was at masking the cationic ε-amino groups. The MTS data (**Figure 7.5**A and B) shows the cytotoxicity of $K^{S}_{55}L_{20}$ vesicles and K^{S}_{60} polypeptide.

These vesicles show cell viabilities similar to poly(sodium-L-glutamate)$_{60}$-*block*-poly(L-leucine)$_{20}$, $E_{60}L_{20}$, vesicles.

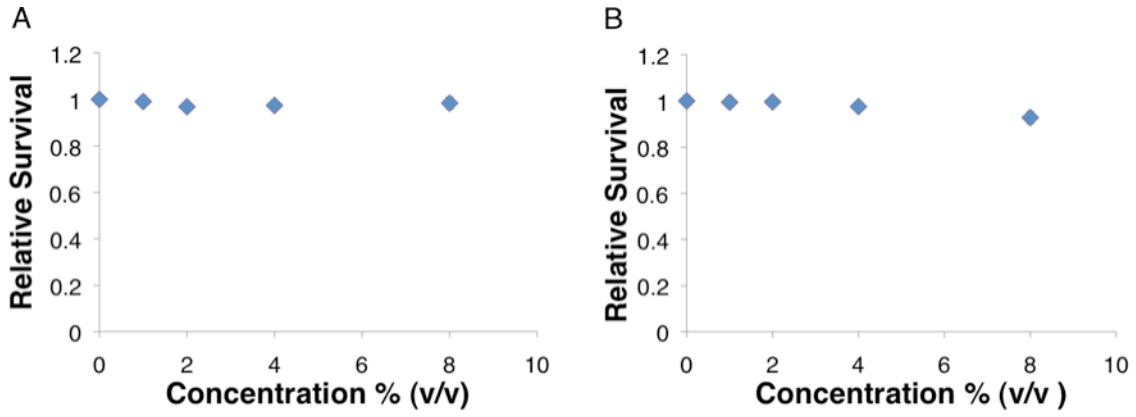

Figure 7.5 MTS assay of HeLa Cells incubated with (A) $K^{S}_{55}L_{20}$ vesicles and (B) K^{S}_{60} polypeptide.

7.7 Conjugation of pH-Label Maleamic Acid to Polypeptides

The choice of maleic anhydride derivatives is dependent on pH at which the maleamic acid will hydrolyze. For drug delivery applications, the maleamic acid must be stable at a pH of 7.4, physiological pH, so that it may circulate the blood until it reaches its desired location. Once the vesicle enters the cell through macropinocytosis it buds off into the cytosol as an endocytic vesicle, which proceeds to early endosome. The early endosome has a reduced pH of 6.0, the desired pH for the maleamic acid to begin hydrolyzing. This could active the proton sponge effect and disrupt the endosome releasing the vesicle into the cytosol before recycling back to the surface. The anhydrides were chosen based on the pH that cleaves the amide bond removing the maleamic acid and on the research of Meyer et al. and Rozema et al., 2,3-dimethylmaleic anhydride and 2-propionic-3-methylmaleic anhydride were used for the pH-labile maleamic acids (**Figure 7.6**).

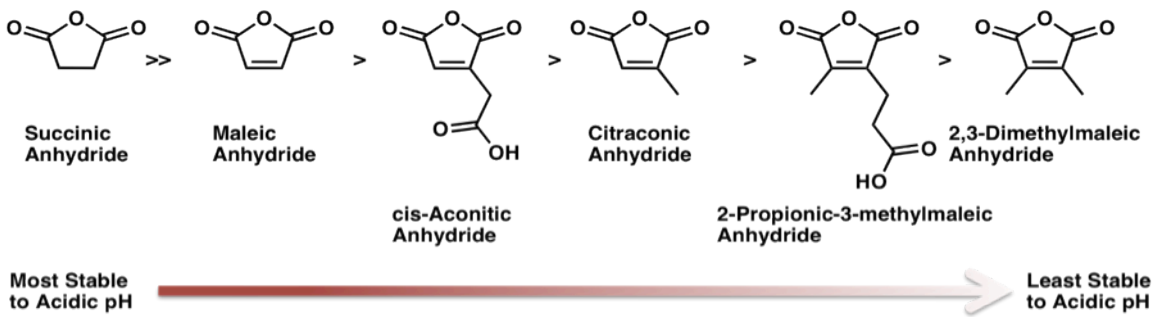

Figure 7.6 Maleic anhydride derivatives in order of most stable to least stable in under acidic conditions.

After previous optimization of the conjugation protocol, additional lysine modifications were performed using 2,3-dimethylmaleic anhydride (DMMA). Poly(L-lysine)$_{60}$ was reacted with 2,3-dimethylmaleic anhydride to form poly(N_{ε}-2,3-dimethyl-4-oxobut-2-enoic acid-L-lysine)$_{60}$ or $K^{DMMA}{}_{60}$. It was important to maintain a basic pH with these samples to ensure the stability of the maleamic acid bond. The samples were purified by dialyzing against water with a pH of 8, maintained by addition of NaOH. The ^{1}H NMR spectra of the modified polymer showed a single sharp peak, which was not expected for the two methyl groups that are non equivalent. The sample was purified once more and dialyzed against basic water with 0.1 M NaCl to displace any 2,3-dimethylmaleic acid complexed as a counterion with amino groups of the lysine. The sharp singlet disappeared after this purification, showing that the 2,3-dimethylmaleic acid was not covalently bonded to the polypeptide but just a counterion (**Figure 7.7**). This result also explains why the NMR was a sharp singlet instead of two peaks. Since the dialysis against basic water gave no conjugated product this led us to believe this maleamic acid bond was too unstable.

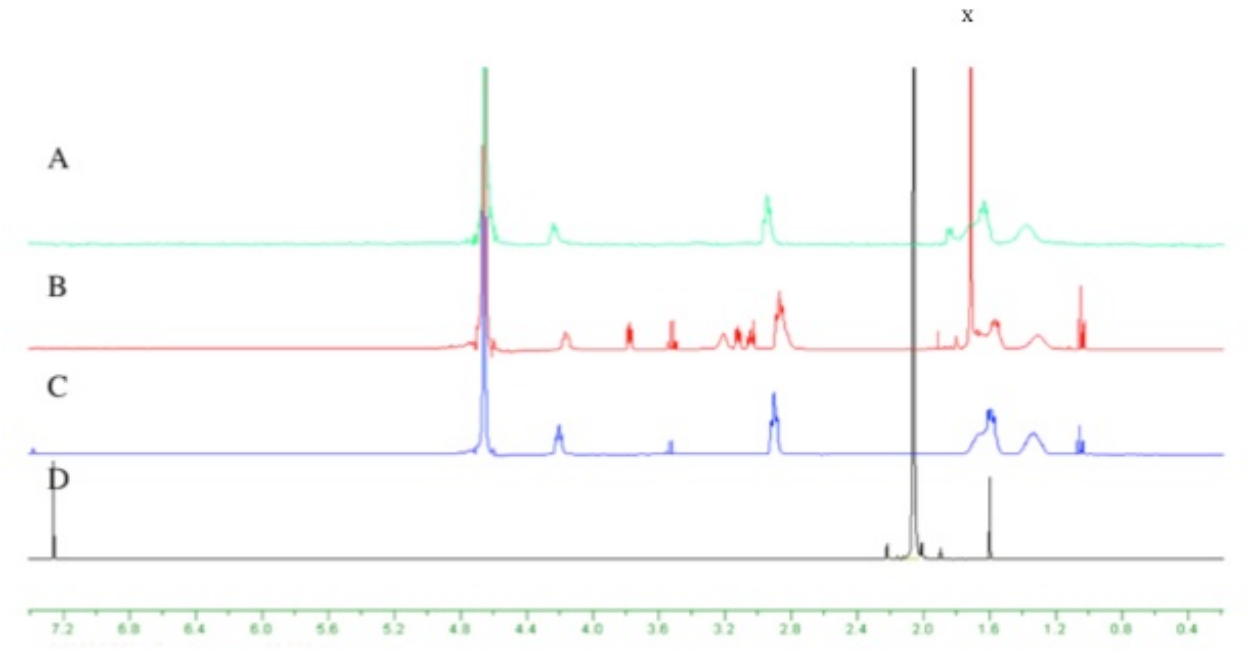

Figure 7.7 ^{1}H NMR Spectra of (A) K^{DMMA}_{60} after 0.1 M NaCl dialysis shows disappearance of peak at 1.70 ppm, (B) K^{DMMA}_{60} after dialysis shows sharp peak at 1.70 ppm, (C) K_{60} before reaction with DMMA and (D) DMMA. (A-C) in D_2O and (D) in $CDCl_3$.

Stanic et al. reported the modification of mugwort pollen allergen using citraconic anhydride, *cis*-aconitic anhydride and 2,3-dimethylmaleic anhydride and found that 2,3-dimethylmaleyl group was easily hydrolyzed at neutral pH.[10] After taking a closer look at the maleamic acids and their pH sensitivity it was determined that 2-propionic-3-methylmaleic anhydride (CDM) might be a better candidate (**Figure 7.6**).

Following the synthesis reported by Rozema et al. in **Figure 7.8**, CDM was synthesized and purified by column chromatography and then conjugated to polypeptides K_{60} and $K_{60}L_{20}$.

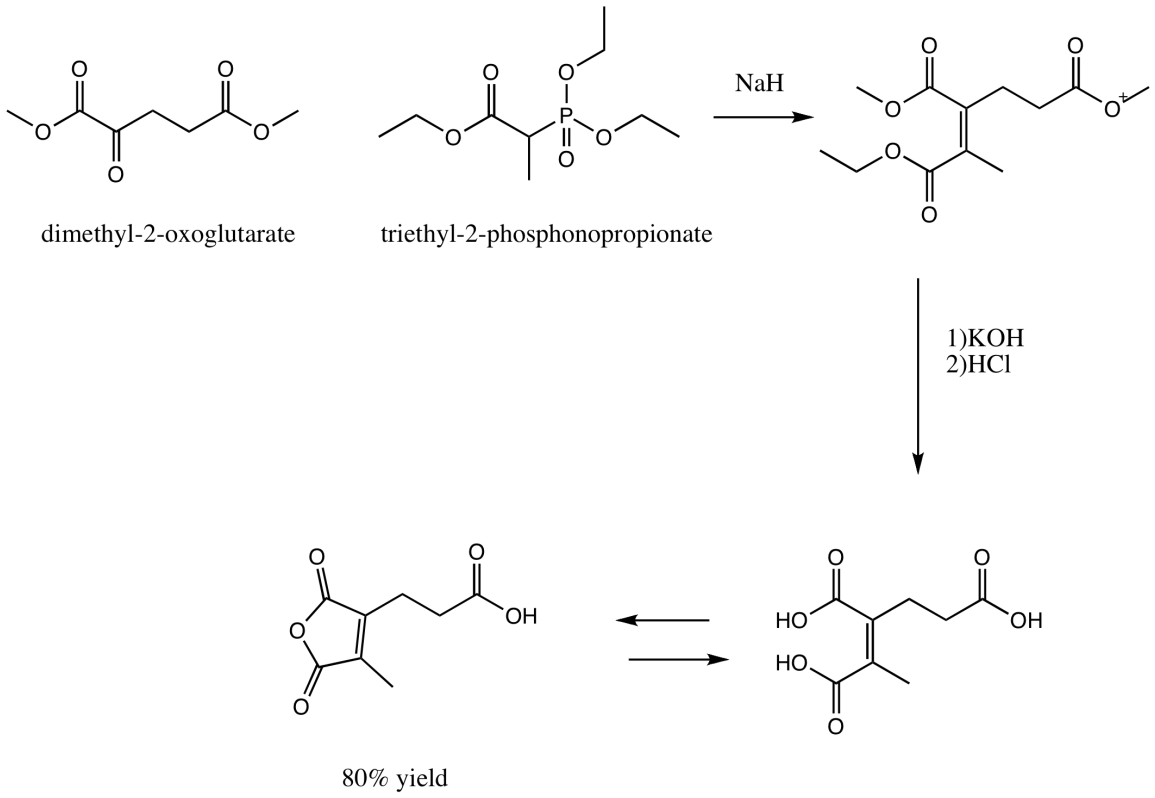

dimethyl-2-oxoglutarate triethyl-2-phosphonopropionate

80% yield

Figure 7.8 Synthesis of 2-propionic-3-methylmaleic anhydride (CDM).

The purification of the CDM modified polypeptides was optimized using NaCl to remove any acid complexed as counterions before NMR analysis. The NMR spectra showed efficient conjugation of CDM to K_{60} (60 % yield) (**Figure 7.9**). The sample poly(N_{ε}-2-propionic-3-methylmaleamic acid-L-lysine)$_{60}$-*block*-poly(L-leucine)$_{20}$ has not yet been tested for endosomal release.

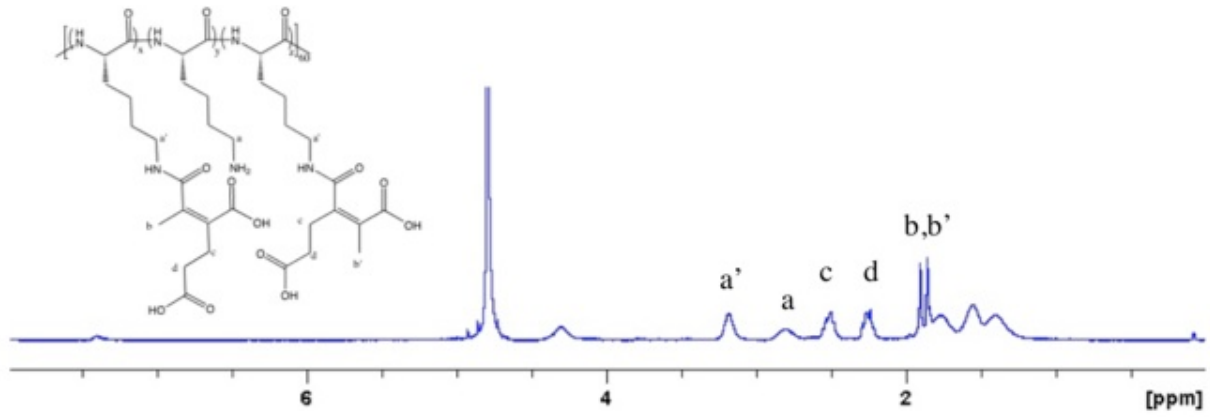

Figure 7.9 NMR Spectrum of K_{60} reacted with 2-propionic-3-methylmaleic anhydride (CDM) in D_2O.

7.8 Experimental

7.8.1 Synthesis of Poly(N_ε-benzyloxycarbonyl-L-lysine)$_x$, (Z)K_x (x = 60, 70):

Under nitrogen atmosphere, N_ε-benzyloxycarbonyl-L-lysine-N-carboxyanhydride (Z-Lys NCA) (370 mg, 1.2 mmol) was dissolved in THF (7.4 mL) in a 20 mL scintillation with a stir bar. A $(PMe_3)_4Co$ initiator solution (1 mL of a 20 mg/mL solution in THF) was then added to the flask via syringe. The flask was sealed and allowed to stir in for 45 minutes at 25 °C. After 45 minutes, an aliquot (50 μL) was removed and analyzed by FTIR to confirm that all the Z-lys NCA was consumed. The aliquot was diluted to a concentration of 5 mg/mL in DMF containing 0.1 M LiBr for GPC/LS analysis (M_n = 14,890; M_w/M_n = 1.19). The actual composition determined by GPC/LS is K_{57}. Same protocol used for synthesis of K_{68}.

7.8.2 Preparation of Poly(L-lysine-HCl)$_x$, K_x (x = 60, 70):

A 20 mL scintillation was charged with (Z)K_{60} and TFA (12 mL) and a stir bar. The flask was placed in an ice bath and allowed to stir until polymer was completely dissolved and the flask

was cooled to 0 °C. At this point, HBr (1mL of 33 % solution in HOAc, 5 equivalents to (Z)-Lysine) was added to the solution and was allowed to stir in the ice bath for 1 hour. Diethyl ether (30 mL) was added to precipitate the polymer. The product was isolated by centrifugation and was washed with ether twice more before resuspending in water. The solution was placed in a dialysis bag (MWCO = 2000 Da) and dialyzed against aqueous disodium EDTA (3 mM, 2 days), then aqueous HCl and NaCl (10 mM, 10 mM, 2 days), followed by water (2 days) before lyophilization to give a fluffy white powder. Yield 85 %, probably due to loss during dialysis.

7.8.3 Synthesis of Poly(N_ε-benzyloxycarbonyl-L-lysine)$_x$-*block*-Poly(L-leucine)$_{20}$, (Z)K_xL_{20} (x = 55, 50):

Under nitrogen atmosphere, N_ε-benzyloxycarbonyl-L-lysine-N-carboxyanhydride (Z-Lys NCA) (800 mg, 2.6 mmol) was dissolved in THF (16 mL) in a 100 mL round bottom flask with a stir bar. A $(PMe_3)_4Co$ initiator solution (2.4 mL of a 55 mM solution in THF) was then added to the flask via syringe. The flask was sealed and allowed to stir in for 45 minutes at 25 °C. After 45 minutes, an aliquot (50 μL) was removed and analyzed by FTIR to confirm that all the Z-lys NCA was consumed. The aliquot was diluted to a concentration of 5 mg/mL in DMF containing 0.1 M LiBr for GPC/LS analysis (M_n =13,280; M_w/M_n = 1.134). To the polymerization solution L-Leucine-carboxyanhydrides (Leu-NCA) (3.2 mL of 320 mM solution in THF) was added to give the desired diblock copolypeptide amphiphile $K_{50}L_{20}$. The number of the leucine residues was checked using ^{1}H NMR to give the actual composition, $K_{50}L_{23}$. Same protocol used for synthesis $K_{54}L_{18}$.

7.8.4 Poly(L-lysine-HCl)$_x$-*block*-Poly(L-leucine)$_{20}$, K_xL_{20} (x = 50, 55):

A 100 mL round-bottom flask was charged with (Z)K_xL_{20} (x = 50, 55) and TFA (20 mL) and a stir bar. The flask was placed in an ice bath and allowed to stir until polymer was completely dissolved and the flask was cooled to 0 °C. At this point, HBr (2.3 mL of 33 % solution in HOAc, 5 equivalents to (Z)-Lysine) was added to the solution and was allowed to stir in the ice bath for 1 hour. Diethyl ether (40 mL) was added to precipitate the polymer. The product was isolated by centrifugation and was washed with ether twice more before resuspending in water. The solution was placed in a dialysis bag (MWCO = 2000 Da) and dialyzed against aqueous disodium EDTA (3 mM, 2 days), then aqueous HCl and NaCl (10 mM, 10 mM, 2 days), followed by water (2 days) before lyophilization to give a fluffy white powder.

7.8.5 Conjugation of Anhydride:

The polypeptides were dissolved in 0.1M Na_2CO_3 aqueous solution. The anhydride was dissolved in DMSO. The anhydride was then added 5eq at a time to the polypeptide until 20 equivalents was added to the reaction. The reaction was place in the refrigerator overnight. After the polypeptide was placed in a dialysis bag (MWCO = 2000 Da) and dialyzed against basic water to remove unreacted anhydride. The polypeptide was isolated by lyophilization to give a fluffy white powder.

7.8.6 Preparation of Diblock Copolypeptide Assemblies in Water:

Solid copolypeptide powder ($K^S_{55}L_{20}$) was dispersed in THF to give a 4 % (w/v) suspension, which was then placed in a bath sonicator for 30 minutes until the copolypeptides was evenly dispersed. An equal volume of Millipore water was added to the suspension and place in a bath sonicator for 30 minutes. An equal volume of THF was then added to the suspension in four

equivalent aliquots with vortexing in between each addition to give a final concentration of 1 % (w/v) copolypeptides suspension in 3:1 ratio of THF to water. The suspension was placed in a dialysis bag (MWCO = 2000 Da) and dialyzed against Millipore water for 24 hours. The water was changed every hour for the first 4 hours.

7.8.7 Synthesis of 2-Propionic-3-Methylmaleic Anhydride (CDM):

In a 250 mL, 580 mg of 95% NaH (25 mmol) was weighed and charged with a stir bar and sealed with a rubber septum. Under N_2 50 mL of anhydrous tetrahydrofuran (THF) was added via cannulation. 7.1 g of triethyl-2-phosphonopropionate (30 mmol, d=1.111 g/mL, 6.39 mL) was added to the NaH suspension via syringe. Mixture was allowed to react until the evolution of H_2 could no longer be seen. A solution of 3.5 g of dimethyl-2-oxoglutarate (20 mmol, d=1.203 g/mL, 2.91 mL) in 10 mL of anhydrous THF was added to the reaction mixture via syringe and reacted for 30 minutes. An orange color change was observed in the solution. A TLC (thin-layer chromatography) was taken to verify the consumption of starting material. 10 mL of water (10 mL) was added to the reaction mixture, and the THF was removed by rotary evaporation. The solid and water mixture was then extracted with diethyl ether (3 x 50 mL) and dried with magnesium sulfate. The filtered solution was then placed under rotary evaporation to remove diethyl ether leaving a yellow oil. The oil was purified by silica gel chromatography elution with 2:1 ether:hexane to yield 3.4 g of the triester (65% yield). The triester was then dissolved with 1:1 (v/v) of water and ethanol (50 mL) containing potassium hydroxide (5 eq.,4.5 g) and heated to reflux for 1 hour. After 1 hour, the ethanol was removed by rotary evaporation and the solution was acidified using HCl (pH 2). The product was isolated by extraction with ethyl

acetate, dried with magnesium sulfate, and concentrated down to a white solid. Recrystallized from DCM and hexane to yield a pure product.

7.8.8 Cytotoxicity Assay:

MTS cell proliferation assay was performed according to the manufacture-supplied instructions. Briefly, HeLa cells were seeded onto a 48-well tissue culture plate at 40,000 cells/cm^{-2} and incubated overnight in a 37 ºC humidified atmosphere with 5 % Co_2. The next day the media was aspirated off for each well, and the cells were incubated with 250 μL of fresh media containing different concentrations of vesicles for 5 hours. Afterwards, the media was aspirated, followed by an addition of 250 μL of media and 50 μL of MTS reagent to each well. The cells were then place a 37 °C air incubator for 1 hour and absorbance of each well was measured at 490 nm (A_{490}). The background absorbance was also read at 700 nm (A_{700}) and subtracted from A_{490}. The relative survival of cells relative to the control was calculated by taking the ratio of the ($A_{490}B - A_{700}$) values.

7.9 References

(1) Holowka, E. P.; Sun, V. Z.; Kamei, D. T.; Deming, T. J. *Nature Materials* **2007**, *6*, 52.

(2) Sun, V. Z., University of California Los Angeles, 2009.

(3) Boussif, O.; Lezoualc'h, F.; Zanta, M. A.; Mergny, M. D.; Scherman, D.; Demeneix, B.; Behr, J. P. *Proceedings of the National Academy of Sciences of the United States of America* **1995**, *92*, 7297.

(4) Behr, J.-P. *CHIMIA International Journal for Chemistry* **1997**, *51*, 34.

(5) Meyer, M.; Philipp, A.; Oskuee, R.; Schmidt, C.; Wagner, E. *Journal of the American Chemical Society* **2008**, *130*, 3272.

(6) Meyer, M.; Zintchenko, A.; Ogris, M.; Wagner, E. *The Journal of Gene Medicine* **2007**, *9*, 797.

(7) Rozema, D. B.; Ekena, K.; Lewis, D. L.; Loomis, A. G.; Wolff, J. A. *Bioconjugate Chemistry* **2002**, *14*, 51.

(8) Holowka, E. P.; Pochan, D. J.; Deming, T. J. *Journal of the American Chemical Society* **2005**, *127*, 12423.

(9) Rodriguez, A. R.; Choe, U.-J.; Kamei, D. T.; Deming, T. J. *Macromolecular Bioscience* **2012**, *12*, 805.

(10) Stanic, D.; Burazer, L.; Gavrovic-Jankulovi, M.; Jankov, R. M.; Velickovic, T. C. *Journal of the Serbian Chemical Society* **2009**, *74*, 359.